UNIVERSITY OF KWAZULU-NATAL

SYNTHESIS AND BIOLOGICAL ACTIVITIES OF 2-HYDROXYPHENYLACYL AZOLES AND THEIR OXIME DERIVATIVES

2012

ADELE CHEDDIE

UNIVERSITY OF KWAZULU-NATAL

SYNTHESIS AND BIOLOGICAL ACTIVITIES OF 2-HYDROXYPHENYLACYL AZOLES AND THEIR OXIME DERIVATIVES

A THESIS

SUBMITTED

in the partial fulfillment of the requirements

for the award of the degree of

MASTER OF SCIENCE

in

School of Chemistry and Physics

Collage of Science and Agriculture,

by

ADELE CHEDDIE

2012

Supervisor: Dr N.A. Koorbanally

Preface

This study represents original work by the author and has not been submitted in any other form to another university. Where use was made of work of others it has been duly acknowledged in the text.

Candidate:

Signed:_____Name:_____Date:_____

As the Candidate's supervisor, I have approved this thesis for submission.

Supervisor:

Signed:_____Name:_____Date:_____

ABSTRACT

Fourteen phenylacyl and 2-hydroxyphenylacyl azoles and their oxime derivatives of which three were new, 2-(2-methyl-1*H*-imidazol-1-yl)-1-phenylethanone oxime **7**; 1-(2-hydroxyphenyl)-2-(2-methyl-1*H*-imidazol-1-yl)ethanone oxime **13** and 1-(2-hydroxyphenyl)-2-(1*H*-1,2,4 traizol-1-yl)ethanone oxime **14**. The yields obtained for the ketone derivatives were between 50 and 60%, and between 80 and 95% for the oxime derivatives. All compounds were characterized using NMR, IR, UV and GCMS, and were tested for their antifungal and antibacterial activity. These compounds possessed moderate antifungal and weak antibacterial activity, with compound **12**, 1-(2-hydroxyphenyl)-2-(1H-imidazol-1-yl)ethanone oxime showing the highest antifungal activity with a MIC value of 1 $\mu g\ mL^{-1}$. In general, the 2'-hydroxy substituted compounds were shown to have better antifungal and antibacterial activity than the unsubstituted compounds.

STRUCTURES OF COMPOUNDS

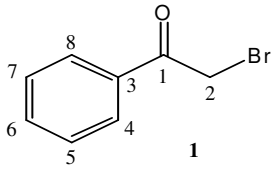

1

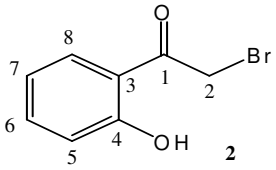

2

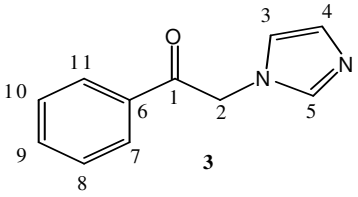

3

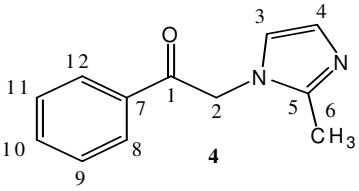

4

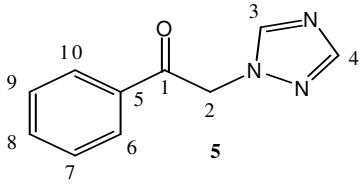

5

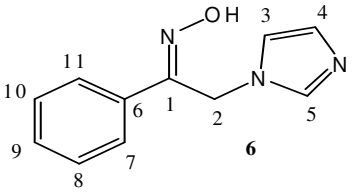

6

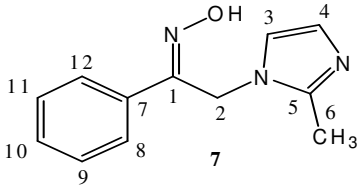

7

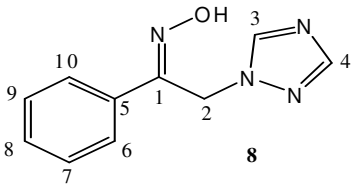

8

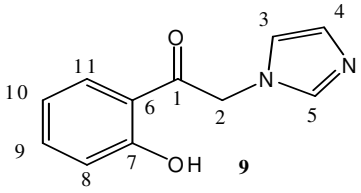

9

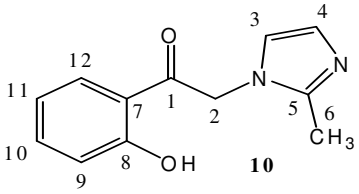

10

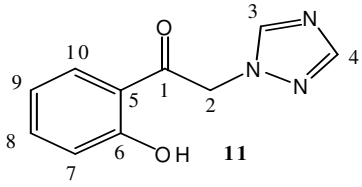

11

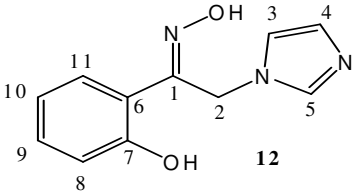

12

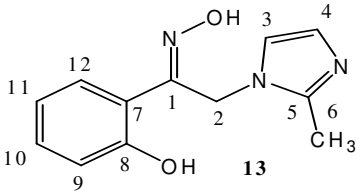

13

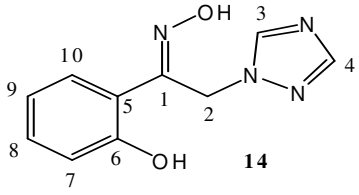

14

ABBREVIATIONS

^{1}H NMR	proton nuclear magnetic resonance spectroscopy
^{13}C NMR	C-13 nuclear magnetic resonance spectroscopy
$CDCl_3$	deuterated chloroform
COSY	correlated spectroscopy
DMSO-d_6	deuterated dimethyl sulfoxide
DCM	Dichloromethane
EIMS	electron impact mass spectroscopy
EtOH	ethanol
HMBC	heteronuclear multiple bond coherence
HREIMS	high resolution electron impact mass spectroscopy
HSQC	heteronuclear single quantum coherence
MeOH	methanol
MIC	minimum inhibitory concentration
NOESY	nuclear overhauser effect spectroscopy
TLC	thin layer chromatography
UV	ultraviolet
d	doublet
dd	double doublet
Hz	hertz
IR	infrared
Mp	melting point

m	multiplet
Rf	Retention factor
s	singlet
t	triplet
td	triplet of doublets

DECLARATION

DECLARATION 1 – PLAGIARISM

I, **ADELE CHEDDIE** declare that

1. The research reported in this thesis is my original research, except where otherwise indicated.
2. This thesis has not been submitted for any degree or examination at any other university.
3. This thesis does not contain other persons' data, pictures, graphs or other information, unless specifically acknowledged as being sourced from other persons.
4. This thesis does not contain other persons' writing, unless specifically acknowledged as being sourced from other researchers. Where other written sources have been quoted, then:
    a. Their words have been re-written but the general information attributed to them have been referenced
    b. Where their exact words have been used, then their writing has been placed in italics and inside quotation marks, and referenced.
5. This thesis does not contain text, graphics or tables copied and pasted from the Internet, unless specifically acknowledged, and the source being detailed in the thesis and in the References sections.

Signed ……

ACKNOWLEDGEMENTS

I would like to thank my supervisor, Dr Neil Anthony Koorbanally. Thank you for your guidance, support and patience throughout this project. Your dedication and humility are sincerely appreciated.

Thank you also goes to Dr Naidu and Dr Patrick Govender, from the Department of Biochemistry at the University of KwaZulu-Natal, for conducting the antifungal and antibacterial assays. The technical staff of the schoolof Chemistry and Physics for their help, and special thanks to Mr Dilip Jagjivan for his assistance with my NMR experiments.

I would like to thank my colleagues in the Natural Products Research Group (NPRG). Dr Mahidhansha (Nizam) Shaikh, for your unfailing help and support in the lab, you have taught me everything I needed to know, I am truly grateful for all you have done for me. To the rest of my colleagues, Dr James Habila, Dr Joyce Kiplimo, Dr Dev Reddy, Abubakar, Asif, Dorothy, Hamisu, Kaalin, Lunga, Nomfundo, Roshila, Samuel, Sunayna, Thrineshen and Victoria thank you all for providing a supportive and encouraging relationship in the lab. I am blessed to have met each and every one of you.

To my family, I would like to say thank you for all your love and support, I could not have done this without of you. To my parents, you have dedicated your lives to your children, your selflessness, love and dedication I will always be grateful for. To my brother, Ryan, thank you for all your support and encouragement.

I would like to thank the National Research Foundation, for funding my studies.

TABLE OF CONTENTS

LIST OF TABLES

LIST OF FIGURES

LIST OF SCHEMES

Chapter 1. Introduction

The search for new compounds that could have useful practical applications is an ongoing process. Compounds containing an azole ring possess properties which make them valuable in medicinal applications. Azoles are five-membered heterocyclic rings which contain nitrogen and at least one other heteroatom (Figure 1-1). They are known to have a wide range of applications, such as antimicrobial, antitumor, anti-tubercular, and most commonly, antifungal activities. We intend to evaluate the antifungal activity of compounds containing a phenyl ethanone backbone bonded to five membered heterocycles such as those below (Figure 1-1).

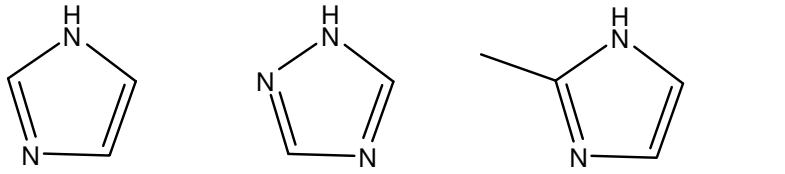

1*H*-imidazole 1*H*-1,2,4-triazole 2-methyl-1*H*-imidazole

Figure 1-1 Structure of azole rings, imidazole, triazole and 2-methylimidazole

Most antifungal drugs are highly toxic, and ineffective against new or re-emerging fungi due to the appearance of resistant strains. In spite of ongoing research on antifungal agents, azoles are still the drug of choice against invasive fungal infections. This is due to their low toxicity, fungistatic, and broad-spectrum properties (Aher *et al*., 2009). The discovery of new and potent antifungal azoles is the best way forward in overcoming resistance and developing effective therapies.

There is a vast amount of literature reported on the synthesis of structurally modified analogues of azoles. In this study we have chosen to focus our attention on phenylacyl and hydroxyphenylacyl azoles and their oxime compounds (Figure 1-2). Emami and co-workers (2008) developed an efficient protocol for the synthesis of 2-hydroxyphenylacyl azoles and its oxime derivative, where the azole and azolium compounds synthesized showed significant inhibition of fungal growth *in vitro* when compared to the reference drug fluconazole. The study also indicated that the hydroxyl group and 4'- substitution on the phenyl ring increased the antifungal activity of the compound. This was also shown by Chai *et al.* (2011), where they used molecular docking to show that substitution at the 2' and 4' positions on phenylacyl azoles form hydrophobic and van der Waals interactions with hydrophobic regions on lanesterol. These substitutions increase the binding of these phenylacyl azole compounds to the active site; as shown by their antifungal activity at concentrations less than 1μg mL^{-1} (Chai *et al.*, 2011). Therefore, 2-hydroxyphenylacyl azoles may be considered as promising new antifungal agents.

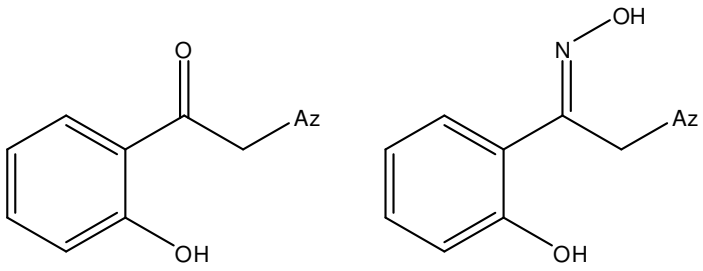

Az: 1H-imidazole, 1H-1,2,4-triazole, 2-methyl-1H-imidazole

Figure 1-2 Structure of 2-hydroxyphenylacyl azole and its oxime derivative

1.1 Azole antifungals

Fungi are eukaryotic microorganisms such as yeast and molds. Many fungi have pathogenic potential and pose a continuous threat to human health and life. Healthy individuals are susceptible to a host of superficial mycoses (mycoses of skin, nails and hair), as well as severe life-threatening diseases such as histoplasmosis (Pfaller and Diekema, 2010; Kathiravan *et al*., 2012). Invasive fungal infections are a significant cause of morbidity and mortality in individuals with increased vulnerability. These are patients receiving immunosuppressive therapy, organ transplant patients and those infected with the human immunodeficiency virus (HIV) (Ranganathan, 2012).

The development of polyene antifungals was the first major milestone in medical mycology and Amphotericin B quickly became the 'Gold standard' treatment for serious infections. Due to its numerous side effects and high toxicity a continued search for new drugs led to the discovery of azoles as potent antifungals (Maertens, 2004).

These azoles were first reported to show antifungal activity by Woolley in 1944. Interest in the antifungal activity of azole compounds only began to increase in the late 1960's with the discovery of miconazole, econazole and ketoconazole, by Janssen pharmaceutica (Beerse, Belgium) (Maertens, 2004). It wasn't until the late 1980's that the most useful alternative emerged through the development of triazole derivatives, fluconazole and itraconazole (Figure 1-3).

The most active antifungals contain an imidazole or triazole ring, which share the same mechanism of action. The imidazoles are used to treat superficial mycoses, whereas the triazoles are more active in treating both superficial and systemic invasive fungal infections (Sheehan *et al*., 1999).

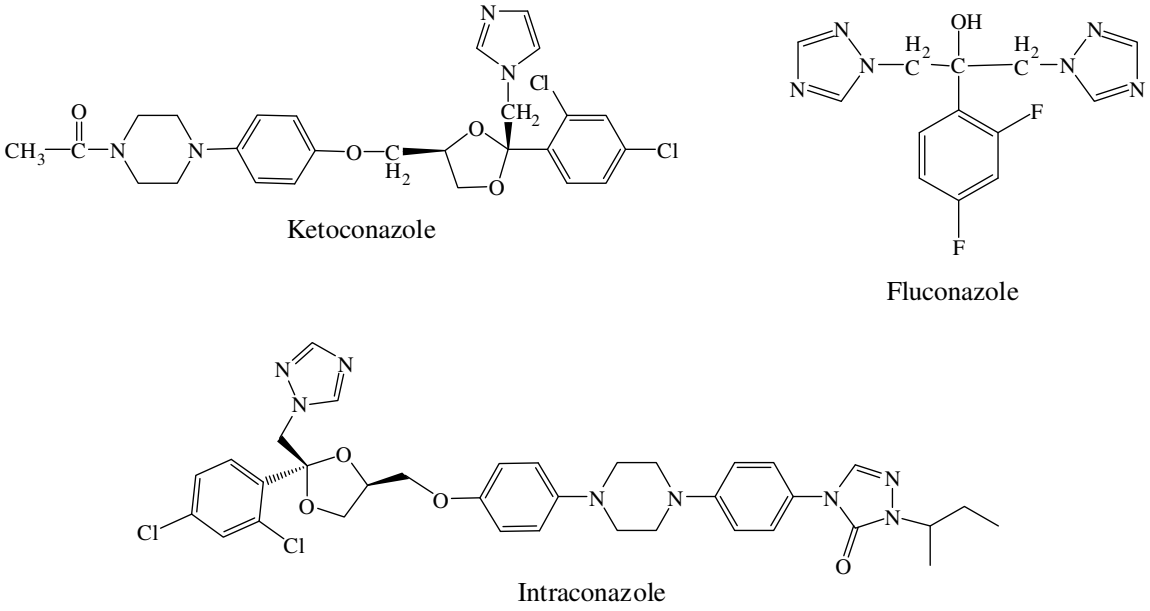

Figure 1-3 Structures of some antifungal agents

1.1.1 Mechanism of Action

The mode of action of all azole antifungals is to inhibit the synthesis of ergosterol from lanosterol in fungal cell membranes. Ergosterol is an essential component of fungal cell membranes, regulating its fluidity, asymmetry and integrity. Azoles target the 14α-demethylase enzyme, which catalyze the synthesis of lanesterol to ergosterol, which results in

a decrease in ergosterol and an accumulation of methyl steroids leading to the inhibition of fungal growth and replication (Maertens, 2004; Lass-Flörl, 2011; Kathiravan *et al*., 2012). Different targets for antifungal drugs are shown in Figure 1-4 (Kathiravan *et al*. 2012).

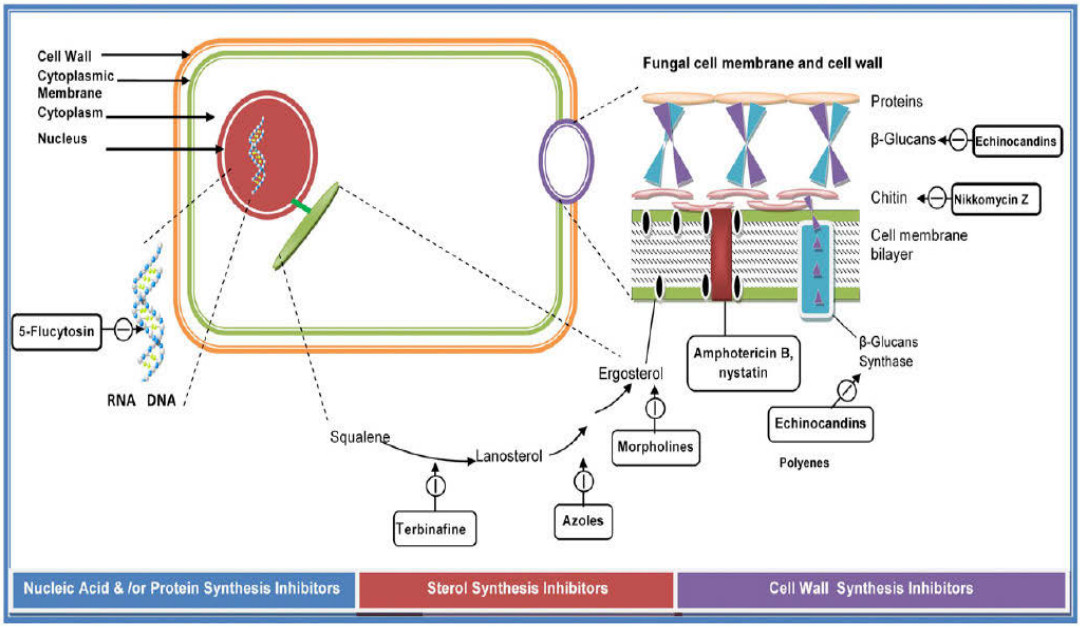

Figure 1-4 Target sites for different antifungal drugs (Kathiravan *et al*., 2012)

1.1.2 Prevalence of fungal infections

The frequency of invasive fungal infections has clearly increased in recent years. This was reported in a study of the epidemiology of sepsis in the United States, where the results showed that the annual number of cases of sepsis caused by fungal organisms increased by more than two-fold between 1979 and 2000 (Martin *et al*., 2003). Data collected from 49 hospitals over a 7-year period (1995-2002) revealed that *Candida* species had become the fourth most common cause of nosocomial blood stream infections (Wisplinghoff, 2004).

Candida and *Aspergillus* remain the most well-known cause of opportunistic pathogens, with an annual incidence of 72 – 290 infections per million people for *Candida* and 12-34 infections per million people for *Aspergillus* (Rees *et al*., 1998). Although there have been significant advances in antifungal drug development, the available drugs do not meet all the requirements of managing infections in the complex patient populations. The development of more antifungal drugs is urgently needed.

1.1.3 Antifungal resistance to azoles

The development of resistance of fungal species to therapeutic drugs has become increasingly apparent, and is a dominant factor for the concomitant rise in invasive fungal infections. Resistance is defined as the inability of an antifungal agent to inhibit the growth of the organism at concentrations that are achieved with normal dosing (Pfaller, 2012). Clinical resistance is defined as the inability to eradicate a fungal infection despite the use of antifungal agents at normal dosage (Pfaller, 2012).

The four mechanisms for azole resistance was described by Kanafani (2008); the first is the regulation of efflux pumps, which decreases the concentration of the drug at the target site, the second is point mutations which alter the target site, the third is over expression of the altered site inhibiting binding, and fourth is the development of pathways that bypass the disruptive effects of the drugs (Casalinuovo *et al*., 2004; Kanafani and Perfect, 2008).

The epidemiology of invasive fungal infections has been reported extensively. The increase in resistance by *Candida* species to fluconazole, as well as cross resistance to other azoles have been reported in a study by Pfaller *et al.* (2009). The results showed a rise in

fluconazole resistance from 9% to 14% during the period 2001 to 2007. A recent study conducted by the SENTRY antimicrobial surveillance program in 2008 to 2009, reported on the frequency of fungal infections and its associated resistance to azole antifungal agents (Pfaller *et al.*, 2010). These results showed a total of 1239 infections of *Candida* species with the highest resistance rates to fluconazole (16.7%), voriconazole (11%) and posaconazole (5%) (Pfellar, 2010).

The emergence of multidrug resistant species of fungi is a real concern since neither the azole nor polyene antifungals are effective against them. The discovery of new and potent antifungal azoles is the best way forward in overcoming resistance and developing effective therapies.

1.2 Other Uses of Azoles

1.2.1 Anti-malarial

Rodrigues *et al.* (2011) and Tien Huy *et al.* (2002) reported known azole mycotics, such as ketoconazole and fluconazole, to be active against malaria causing *Plasmodium* spp. Havaldar and Patil (2008), synthesized and screened a series of triazole derivatives for anti-malarial activity. Among these derivatives, 3-{4-[4-(4-fluorophenyl)-4*H*-[1,2,4]-triazol-3-ylmethoxy]-phenyl}-2-phenyl-3*H*-quinazolin-4-one (Figure 1-5) was found to be most active against *Plasmodium falciparum* strains.

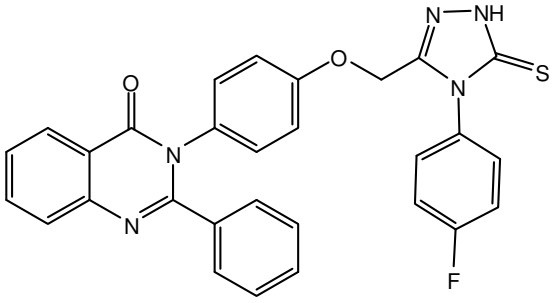

Figure 1-5 Structure of 3-{4-[4-(4-fluorophenyl)-4*H*-[1,2,4]-triazol-3-ylmethoxy]-phenyl}-2-phenyl-3*H*-quinazolin-4-one (Havaldar and Patil, 2008)

1.2.2 Anti-tubercular

Banfi *et al.* (2006) reported the imidazole derivative (Figure 1-6) as well as miconazole to have good anti-tubercular activity when tested against different strains of *Mycobacterium tuberculosis* (MTB) with MICs in the range of 4 to 64 µg mL^{-1}. Guardiola-Diaz *et al.* (2001) also showed imidazole containing antimycotics, ketoconazole and econazole to inhibit growth in mycobacterial strains at 100 µM and 1 µM respectively.

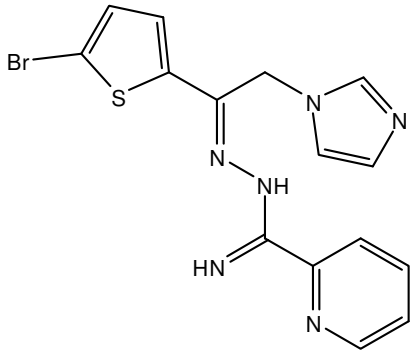

Figure 1-6 Structure of bromo-thienyl imidazole derivative (Banfi *et al.*, 2006)

1.2.3 Anticancer

Compounds having triazole moieties such as vorozole, letrozole and anastrozole are reported to be good inhibitors for preventing breast cancer (Clemons *et al.*, 2004). Demirbas *et al.* (2004) showed the therapeutic activity of the triazole derivative 4-amino-3-phenyl-5-oxo-4,5-dihydro-[1,2,4]-triazol-1-yl acetic acid 2,4-dichlorobenzylidene hydrazide (Figure 1-7) for the treatment of breast cancer, with an activity range of 24 to 50 μM against breast cancer cells.

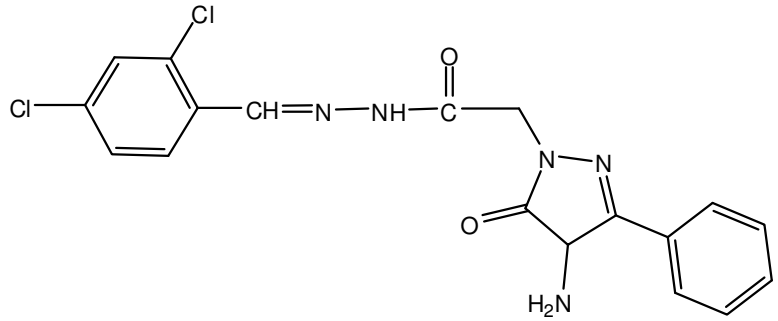

Figure 1-7 Structure of 4-amino-3-phenyl-5-oxo-4,5-dihydro-[1,2,4]-triazol-1-yl acetic acid 2,4-dichlorobenzylidene hydrazide (Demirbas *et al.*, 2004)

1.3 Synthesis of Azoles and its derivatives:

The general phenylacyl azole moiety (Figure 1-8), seen in many well know azole derivatives, is thought to be largely responsible for imparting antifungal activity.

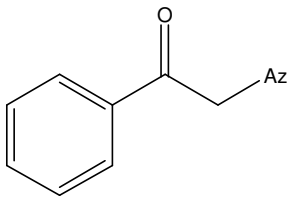

Az: Azole ring

Figure 1-8 General structure of the phenylacyl azole moiety

Azole derivatives have been synthesized using a variety of synthetic methodologies. Conventional methods using polar aprotic solvents, methods using transition metal salts as catalysts and microwave assisted methods have been reported.

1.3.1 Conventional method

The conventional synthetic approach reported for phenylacyl azoles is a two-step reaction which involves a nucleophilic substitution reaction of the azole with 2-bromoacetophenone in the presence of a polar aprotic solvent (Scheme 1-1) since protic solvents would protonate the nitrogen of the azoles.

Güven *et al.* (2007) reported yields of 60% with the use of dioxane-ether as a solvent whilst stirring for 18 hours under ambient conditions. Mamolo *et al.* (2004) and Clader *et al.* (1995) reported very good yields of 83 and 70% respectively using tetrahydrofuran (THF) as a

solvent. Although the reaction time used by Mamolo *et al.* (2004) was considerably longer (12 hours) as opposed to the short 1.5 hour reaction time used by Clader *et al.* (2005). The method proposed by Emami *et al.* (2008) had proved to be most efficient obtaining yields of 60%. This method employed the use of dimethylformamide (DMF), while refluxing at 40-45 °C for 4 to 8 hours.

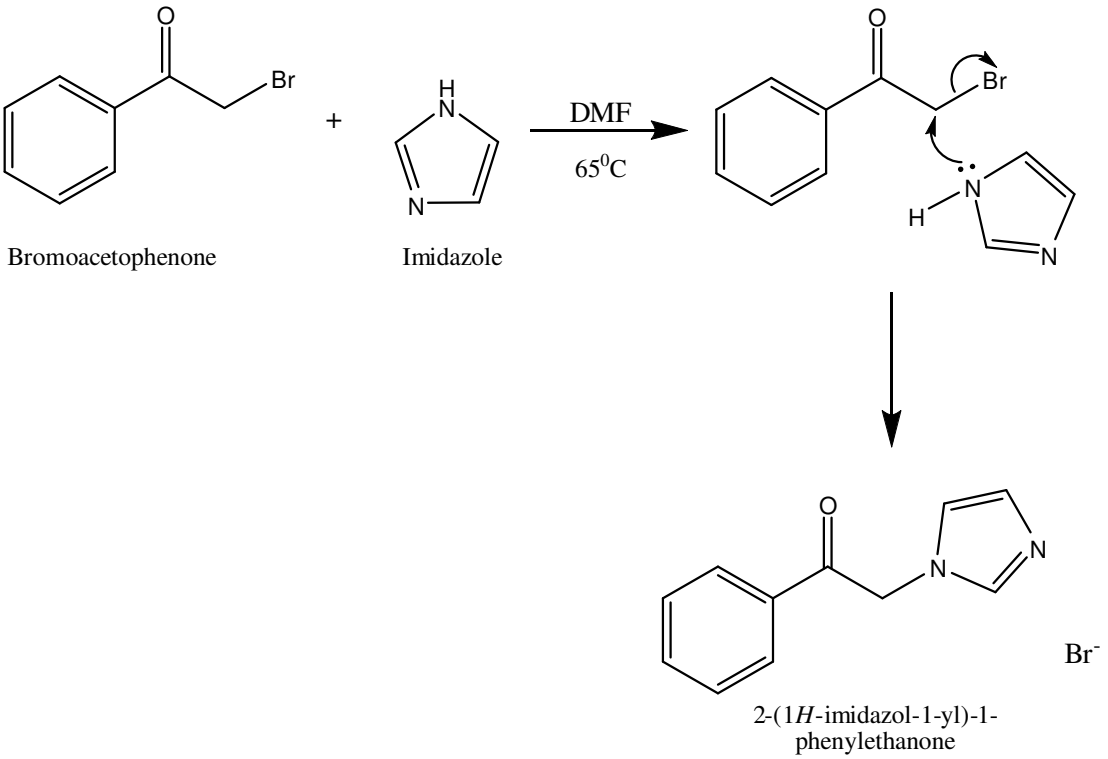

Scheme 1-1 Mechanism for N-alkylation of an azole with bromoacetophenone

1.3.1.1 Bromoacetophenones as intermediates for azole substitution

Various bromination methods of carbonyl compounds have previously been reported, the most common being the use of Br_2 (Siddiqui and Ahsan, 2010). Copper-bromide ($CuBr_2$) (King and Ostrum, 1964) and N-bromosuccinimide (NBS) (Heasley *et al*., 1988; Tanemura, *et al*., 2004) have also been used as milder reagents for bromination (Scheme 1-2). The advantage of using $CuBr_2$ and NBS is that they are less toxic and easier to handle. The use of these milder agents did not affect the overall result of the reaction; in fact they were reported to have excellent yields of 100 % by King and Ostrum (1964) and 80 % by Tanemura *et al*. (2004).

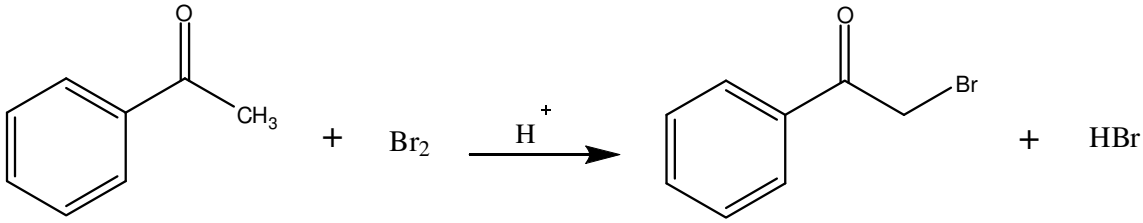

Scheme 1-2 Bromination of carbonyl compounds

The reactivity of bromoacetophenone is due to the inductive effect of the carbonyl group which withdraws electrons toward the oxygen of the carbonyl group resulting in a more electrophilic α carbon atom and a weaker C-Br bond (Erian *et al.*, 2003). The interaction between the carbonyl group and the heteroatom is mainly electrostatic and the reaction is thought to proceed through an alkoxide intermediate resulting from the nucleophilic azole attacking the carbonyl group first due to the polarization interaction caused by the smaller

steric requirement of the ketone group as compared to a carbon of the alkyl bromide moiety (Erian *et al*., 2003) (Scheme 1-3). This is followed by an intramolecular S_N2 reaction where the azole group is substituted for the weaker bromide base. The absence of protons to form a hydroxy group further promotes this and therefore non-protic solvents are ideal for this reaction.

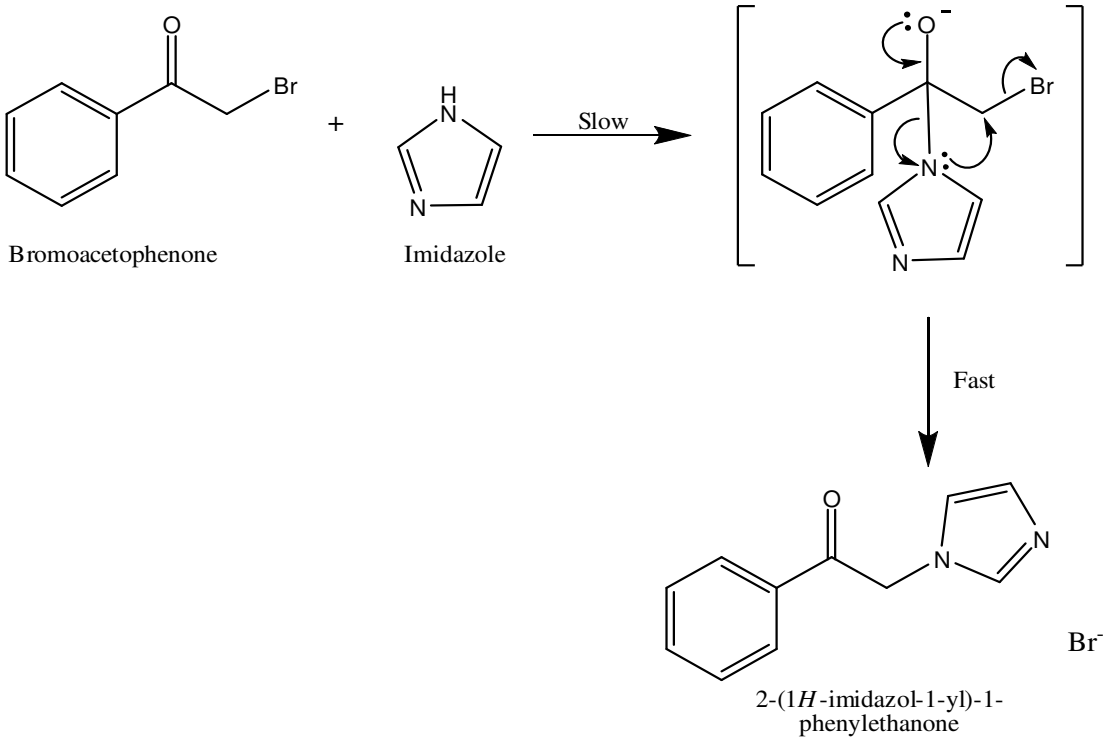

Bromoacetophenone Imidazole

2-(1*H*-imidazol-1-yl)-1-phenylethanone

Scheme 1-3 Mechanism for the S_N2 reaction of an azole with bromoacetophenone (Erian *et al*., 2003)

1.3.1.2 Formation of oxime derivatives

The oxime functional group is incorporated into many medicinal agents, including the antifungal agent, Oxiconazole. Oximes are formed by nucleophillic attack of hydroxylamine with the carbonyl carbon of a ketone to form an unstable carbinolamine intermediate (Emami *et al*., 2002). The carbinolamine intermediate is then broken down to an oxime by an acid catalyzed reaction (Emami *et al*., 2002) (Scheme 1-4).

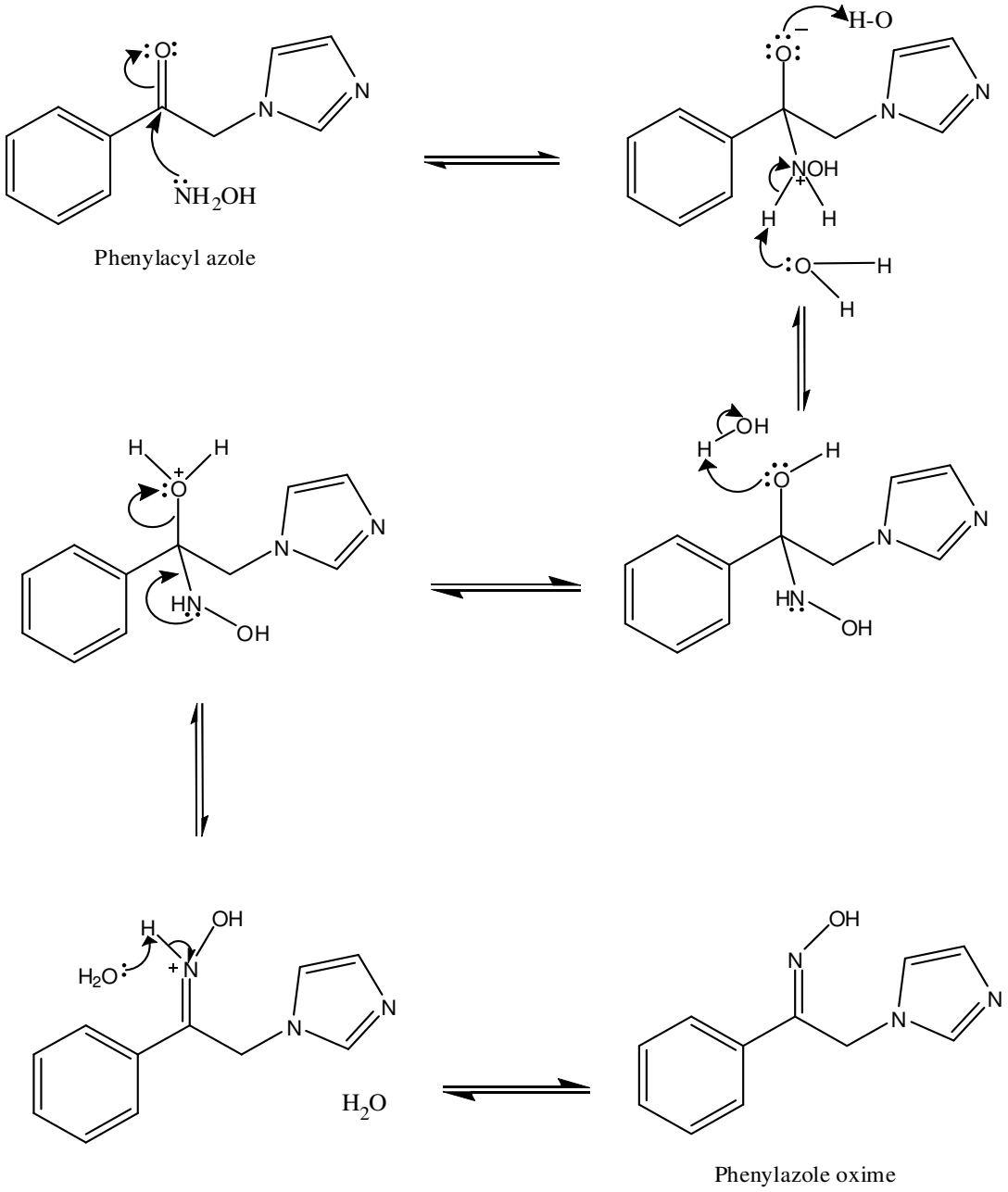

Scheme 1-4 Mechanism for formation of the oxime derivatives

1.3.2 Microwave assisted methods

There are many heterocyclic reactions that can be used for automated medicinal chemistry in drug synthesis. These reactions have traditionally been carried out using solvents and with long reaction times. Microwave synthesis is a technique that has been shown to enhance the speed and reproducibility of the reaction (Bougrin *et al.*, 2005). This was demonstrated by Kidwai *et al.* (2000), who synthesized oxazoles using microwave irradiation by reacting reagents on basic alumina in a microwave. Results showed a dramatic increase in yield and reduction of the reaction time as compared to the conventional method.

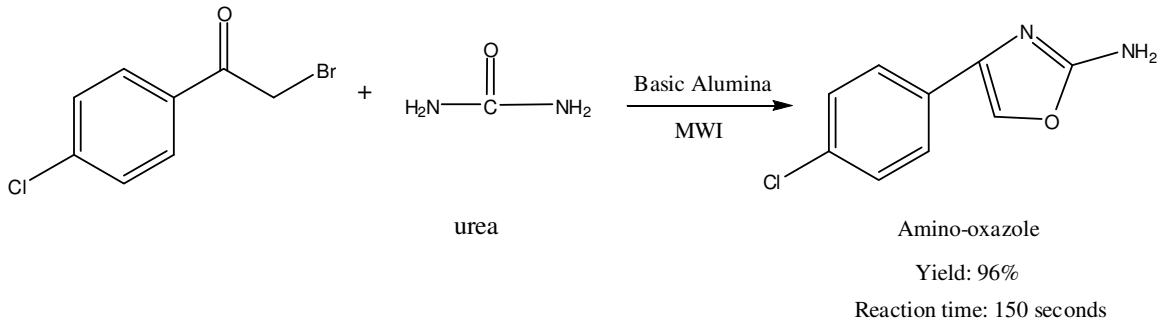

urea

Amino-oxazole

Yield: 96%

Reaction time: 150 seconds

Scheme 1-5 The condensation reaction of urea with 1-(4-chlorophenyl)-2-bromoethanone producing an amino-oxazole, via microwave irradiation (MWI) (Kidwai et al., 2000)

1.3.3 Methods using transition metals

Limitations such as low yields, long reaction times, difficult work-up and occurrence of side reactions warranted the need for better catalysts for the synthesis of azole derivatives. Palladium, copper and platinum are the preferred transition metal catalysts used in these reactions (Aromi *et al*., 2011). Huang *et al.* (2008), showed the amination of aryl halides using imidazole to give higher yields in a shorter reaction time under milder reaction conditions, when using copper (II) acetate ($Cu(OAc)_2$) as a catalyst (Scheme 1-6).

Scheme 1-6 Mechanism for the Cross-Coupling of Aryl Halides with imidazole (Huang *et al.*, 2008)

The copper (II) acetate forms a four-coordination complex with the imidazole and 1,8-diazabicycloundec-7-ene (DBU), which then undergoes oxidative addition with the aryl halides to form a five-coordination copper complex, which is then reduced to produce the phenyl-1*H*-imidazole (Huang *et al*., 2008) (Scheme 1-7).

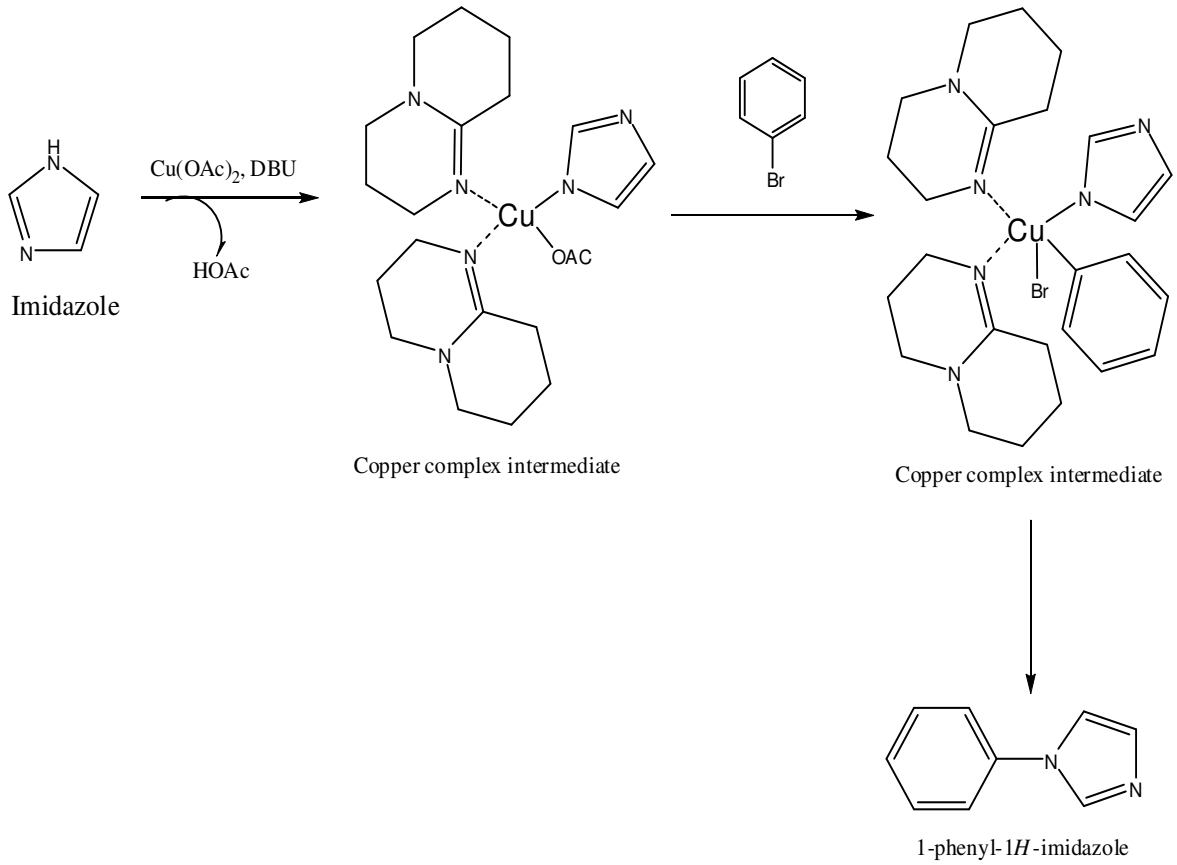

Scheme 1-7 Possible mechanism of N-arylation promoted by copper (II) acetate (Huang *et al.*, 2008)

1.4 Aims and objectives:

Since the azole functional group is present in many antibacterials and antifungals such as miconazole, econazole and ketoconazole, it was hypothesised that this functional group present in other carbon backbones could also possess antifungal and antibacterial activity. Hence we decided to explore the phenylacyl and 2-hydroxyphenylacyl azoles and their oxime derivatives.

The specific aim of the project was to synthesise a small library of phenylacyl and 2-hydroxyphenylacyl azoles and their oxime derivatives and to assess the synthesized compounds for their antimicrobial activity against different strains of fungi and bacteria.

Objectives of the study

1. To synthesize substituted phenylacyl and 2-hydroxyphenylacyl azoles and their oxime derivatives in a three step reaction from acetophenone and 2-hydroxyacetophenone.
2. To investigate and compare the effect that the oxime group and hydroxy substitution at the 2□ postion has on antifungal activity.
3. To conduct primary screening for antifungal and antibacterial activity of the synthesized compounds.

Chapter 2. Experimental

2.1 General

Nuclear magnetic resonance (NMR) spectra were recorded on Bruker AVANCE III 400 MHz spectrophotometer. ^{1}H and ^{13}C NMR spectra were recorded at 400 MHz and 100 MHz respectively, at 30 °C with chemical shifts (δ) recorded against the internal standard, tetramethylsilane (TMS). Melting points were recorded on an Ernst LeitzWetziar micro-hot stage melting point apparatus and are uncorrected. Thin layer chromatography (TLC) was performed using Merck Kieselgel 60 F_{254} plates. Column chromatography was carried out using silica gel 60. Infrared (IR) spectra were recorded neat from the Perkin Elmer spectrum100 instrument with a universal ATR attachment. Ultra Violet (UV) spectra were obtained on a Varian Cary UV-VIS Spectrophotometer in methanol. For Gas chromatography Mass spectrometry (GCMS) analyses, the samples were analysed on an Agilent GC–MSD apparatus equipped with DB-5SIL MS (30 m x 0.25 mm i.d., 0.25 µm film thickness) fused-silica capillary column. Helium (at 2 mL min^{-1}) was used as a carrier gas. The MS was operated in the EI mode at 70 eV.

2.2 Synthetic procedures

2.2.1 Synthesis of 2-bromo-1(2-hydroxyphenyl) ethanone intermediate.

Bromine (0.044 mol, 10 mL) was dissolved in chloroform (50.0 mL) and added drop wise to a cold solution of substituted acetophenone (0.040 mol, 5 g) in chloroform (50.0 mL). The reaction mixture was stirred for an additional two hours at room temperature. The solvent was removed *in vacuo* to yield brominated acetophenones **1** (85% yield) and **2** (70% yield).

2-Bromo-1-phenyl ethanone (**1**);

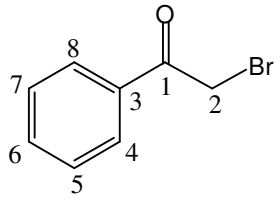

C_8H_7BrO (199.04 g mol^{-1});

85 % yield;

White crystals;

Mp: 47 - 49 °C;

R_f = 0.7 (Ethyl acetate/Hexane 10:90); **UV λ_{max} nm (log ε):** 250 (6.40), 210 (6.32); **IR ν_{max} (cm^{-1}):** 3058, 3030, 2942, 1679 (C=O), 1595, 1447, 1277, 1193; **^{1}H NMR (400 MHz, $CDCl_3$) δ:** 7.96 (d, 2H, *J* = 7.36 Hz, H-4/8), 7.59 (t, 1H, *J* = 7.44 Hz, H-6), 7.47 (t, 2H, *J* = 8.00 Hz, H-5/7), 4.43 (s, 2H, CH_2); **^{13}C NMR (100 MHz, $CDCl_3$) δ:** 191.49 (C-1), 134.16 (C-3), 129.13 and 129.06 (C4 –C-8), 31.11 (C-2); **EIMS *m/z* (rel.int.):** 202 [M^+, Br^{81}] (7), 199 [M^+, Br^{79}] (8), 91 (18), 44 (25), 32 (100).

2-Bromo-1-(2-hydroxy-phenyl) ethanone (**2**);

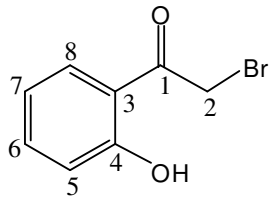

$C_8H_7BrO_2$ (215.04 g mol^{-1});

70% yield;

White crystals;

Mp: 50 - 52 °C;

R_f = 0.7 (Ethyl acetate/Hexane 10:90); **UV λ_{max} nm (log ε):** 330 (6.56), 257 (6.46), 210 (6.38); **IR ν_{max} (cm^{-1}):** 3054, 3008, 2950, 1640 (C=O), 1458, 1448, 1221, 1156, 690 (C-Br); **^{1}H NMR (400 MHz, $CDCl_3$) δ:** 11.70 (s, 1H, OH), 7.72 (dd, 1H, *J* = 8.08, 1.48 Hz, H-8), 7.50 (td, 1H, *J* = 8.60, 1.48 Hz, H-7), 6.99 (dd, 1H, *J* = 8.50, 0.68 Hz, H-5), 6.91 (td, 1H, *J* = 7.16, 0.84 Hz, H-7), 4.42 (S, 2H, CH_2); **^{13}C NMR (100 MHz, $CDCl_3$) δ:** 197.19 (C-1), 163.37 (C-4), 137.62 and 130.52 (C-6/8), 119.47 (C-5), 119.11 (C-7), 117.22 (C-3), 30.14 (C-2); EI**MS *m/z* (rel.int.):** 214 [M^+, Br^{79}] (30), 201 (26), 134 (21), 121 (43), 105 (24), 32 (100).

2.2.2 Synthesis of 2-hydroxyphenylacyl azoles

The desired azole (0.015 mol, 1.0 g) was added to a solution of β-bromoketone (**1** – **2**, 0.005 mol, 1.0 g) in DMF (5.0 mL). The reaction mixture was refluxed with stirring at 65 °C for 4-8 hours; thereafter it was poured into water and extracted with ethyl acetate. The organic phase was concentrated *in vacuo* and further purified by column chromatography using dichloromethane (DCM): methanol (MeOH) (98:2). The appropriate fractions were evaporated to yield crystalline products (**3** – **5, 9 – 11**). The reaction is given in Scheme 2-1.

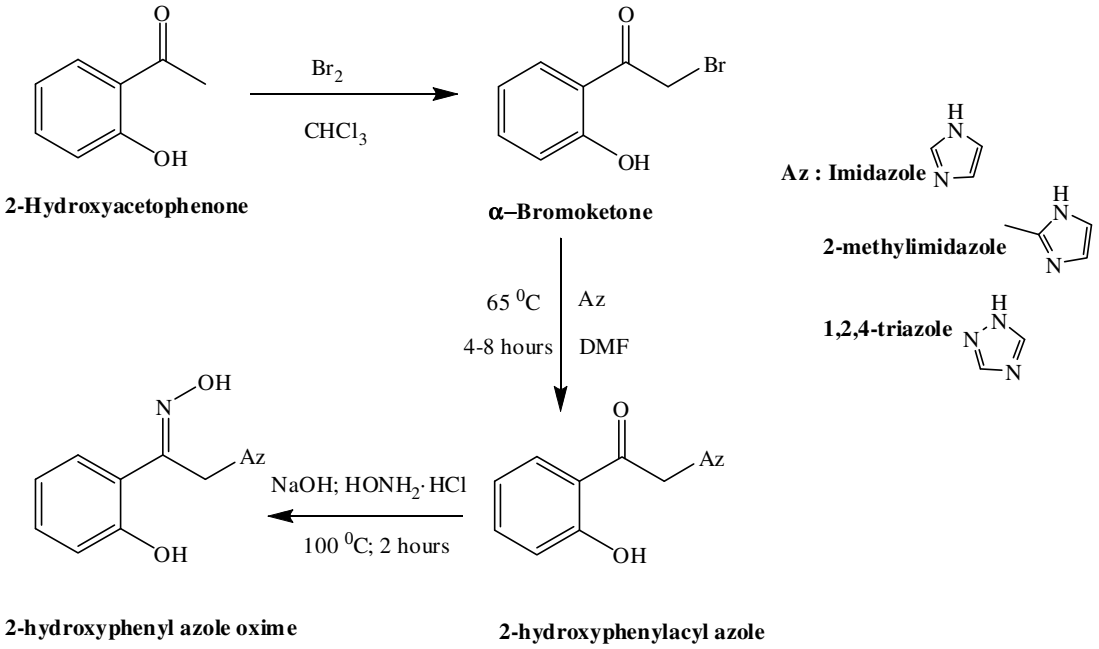

Scheme 2-1 Synthesis of 2-hydroxyphenylacyl azole and its oxime derivatives

2.2.3 Synthesis of oxime derivatives of 2-hydroxyphenylacyl azoles

A 6.0 mL solution of ethanol and water (1:1) containing the desired phenylacyl azole (0.005 mol, 1.0 g) (**3** – **5, 9 – 11**), sodium hydroxide (0.015 mol, 0.6 g) and hydroxylammonium chloride (0.015 mol, 1.1 g) was refluxed with stirring for two hours at 100 ^{0}C. The reaction mixture was cooled and the resulting precipitate was vacuum filtered, washed with cold water (20.0 mL) and dried to give the oxime derivatives (**6 – 8, 12** – **14**). The reaction is given in Scheme 2-1.

2.3 Physical characteristics, UV, IR and NMR data for phenylacyl azoles and their oxime derivatives

2-Imidazol-1-yl-1-phenyl ethanone (**3**)

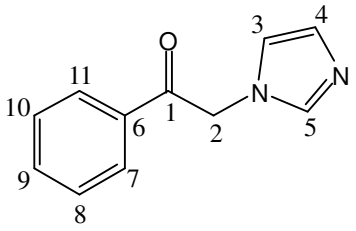

$C_{11}H_{10}N_2O$ (186.21 g mol^{-1});

60% yield;

Yellow crystals;

Mp: 115 - 117 °C;

R_f = 0.5 (DCM/MeOH 95:5); **UV λ_{max} nm (log ε):** 244 (6.26), 208 (6.19); **IR ν_{max} (cm^{-1}):** 3380, 3133, 2935,1691 (C=O), 1560, 1595 (C=N), 1516, 1226 (CH_2 -N), 1058; **^{1}H NMR (400 MHz, $CDCl_3$) δ:** 7.93 (d, 2H, *J* = 7.80 Hz, H-7/11), 7.63 (t, 1H, *J* = 7.48 Hz, H-9), 7.50 (t, 2H, *J* = 7.92 Hz, H-8/10), 7.48 (s, 1H, H-5), 7.10 (s, 1H, H-4), 6.92 (s, 1H, H-3) 5.37 (s, 2H, CH_2); **^{13}C NMR (100 MHz, $CDCl_3$) δ:** 191.60 (C-1), 138.15 (C-5), 134.41 (C-9), 134.18 (C-6), 129.57 (C-4), 129.13 (C-8/10), 127.97(C-7/11), 120.30 (C-3), 52.47(C-2); **EIMS *m/z* (rel. int.):** 186 [M^+] (15), 105 (100), 77 (61), 51 (18).

2-(5-Methyl-1H-imidazol-1-yl)-1-phenylethanone (4)

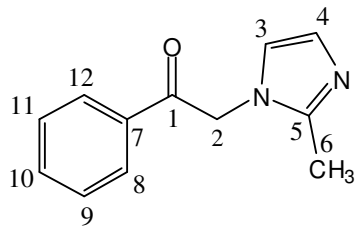

$C_{12}H_{12}N_2O_2$, (200.23 g mol^{-1});

59% yield;

Yellow crystals;

Mp: 134 - 136 °C;

R_f = 0.5 (DCM/MeOH 95:5); **UV λ_{max} nm (log ε):** 244 (6.39), 205 (6.31); **IR ν_{max} (cm^{-1}):** 3362, 3135, 2939, 1686 (C=O), 1597 (C=N), 1432, 1228 (CH_2-N); **^{1}H NMR (400 MHz, $CDCl_3$) δ:** 7.95 (d, 2H, *J* = 7.28 Hz, H-8/12), 7.63 (t, 1H, *J* = 7.44 Hz, H-10), 7.51 (t, 2H, *J* = 7.65 Hz, H-9/11), 6.97 (d, 1H, *J* = 1.28 Hz, H-4), 6.79 (d, 1H, *J* = 1.20 Hz, H-3), 5.27 (s, 2H, CH_2), 2.29 (s, 3H, CH_3); **^{13}C NMR (100 MHz, $CDCl_3$) δ:** 191.75 (C1), 145.72 (C-5), 134.58 (C-10), 134.51 (C-7), 129.35 (C-9/11), 128.19 (C-8/12), 127.68 (C-4), 120.57 (C-3), 52.21 (C-2), 13.07 (C-6); **EIMS *m/z* (rel. int.):** 200 [M^+] (23), 105 (100), 95 (7), 77 (42), 51 (12).

1-Phenyl-2-[1,2,4]triazol-1-yl ethanone (**5**)

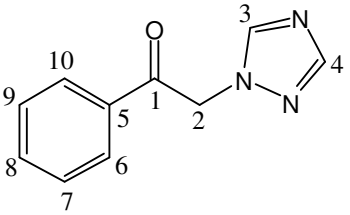

$C_{10}H_9N_3O$ (187.20 g mol^{-1});

65% yield;

Pale yellow crystals;

Mp: 114 - 116 °C;

R_f = 0.6 (DCM/MeOH 95:5); **UV λ_{max} nm (log ε):** 246 (6.36), 206 (6.28); **IR ν_{max} (cm^{-1}):** 3114, 2993, 2955, 1697 (C=O), 1597 (C=N), 1505, 1346 (C-N, aromatic), 1226 (CH_2-N); **^{1}H NMR (400 MHz, $CDCl_3$) δ:** 8.22 (s, 1H, H-3), 7.98 (s, 1H, H-4), 7.96 (d, 1H, *J* = 7.32 Hz H-6/10), 7.64 (t, 1H, *J* = 7.44 Hz, H-8), 7.51 (t, 2H, *J* = 7.66 Hz, H-7/9), 5.65 (s, 2H, CH_2); **^{13}C NMR (100 MHz, $CDCl_3$) δ:** 190.74 (C-1), 152.10 (C-4), 145.06 (C-3), 134.76 (C-8), 134.20 (C-5), 129.36 (C-6/10), 128.30 (C-7/9), 55.20 (C-2); **EIMS *m/z* (rel. int.):** M^+ not detected, 105 (100), 77.1 (50), 51 (14).

2-(1H-Imidazol-1-yl)-1-phenylethaone oxime (6)

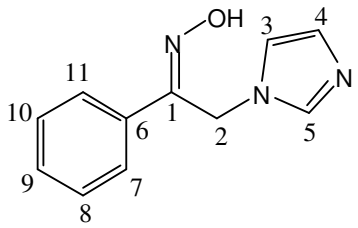

$C_{11}H_{11}N_3O$ (201.22 g mol^{-1}).

98% yield;

Pale yellow crystals;

Mp: 154 - 164 °C;

R_f = 0.5 (DCM/MeOH 95:5); **UV λ_{max} nm (log ε):** 246 (6.39), 206 (6.31); **IR ν_{max} (cm^{-1}):** 3121, 3003, 2817, 2681 (N-OH), 1238 (CH_2-N), 1515, 1499, 1471, 1439, 1287, 957, 938, 924, 913; **^{1}H NMR (400 MHz, DMSO-d_6) δ:** 12.06 (s, OH), 7.66-7.68 (m, 2H, H-7 /11) 7.65 (s, 1H, H-5), 7.36-7.38 (m, 3H, H-8/9/10), 7.04 (s, 1H, H-3), 6.81 (s, 1H, H-4), 5.32 (s, 2H, CH_2); **^{13}C NMR (100 MHz, DMSO-d_6) δ:** 151.90 (C-1), 137.58 (C-5), 133.99 (C-6), 128.33 (C-4), 128.52 (C-8/10), 129.15 (C-9), 126.00 (C-7 & C-11), 119.53 (C-3), 38.94 (C-2); **EIMS *m/z* (rel. int.):** 201 [M^+] (77), 103 (65), 91 (23), 81 (100), 77 (57), 69 (45).

2-(2-Methyl-1H-imidazol-1-yl)-1-phenyl ethanone oxime (7)

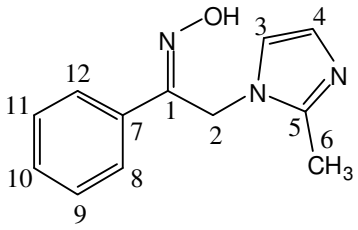

$C_{12}H_{13}N_3O$ (215.25 g mol^{-1})

98% yield;

White crystals;

Mp: 170 - 185 °C;

R_f = 0.5 (DCM/MeOH 95:5); **UV λ_{max} nm (log ε):** 240 (6.38), 204 (6.30); **IR ν_{max}(cm^{-1}):** 2995, 2586 (N-OH), 1497, 1422, 1277 (CH_2-N), 974, 731, 692; **^{1}H NMR (400 MHz, DMSO-d_6) δ:** 12.08 (s, OH), 7.50-7.52 (m, 2H, H-8/12), 7.32-7.34 (m, 3H, H-9/10/11), 6.89

(s, 1H, H-3), 6.60 (s, 1H, H-4), 5.22 (s, 2H, CH_2), 2.19 (s, 3H, CH_3); **^{13}C NMR (100 MHz, DMSO-d$_6$) δ:** 152.82 (C-1), 144.67 (C-5), 134.38 (C-7), 129.62 (C-10), 128.91(C-9/11), 126.88 (C-8/12), 126.27 (C-4), 120.68 (C-3), 39.60 (C-2), 12.71 (C-3); **EIMS *m/z* (rel. int.):** 215 [M^+] (92), 198 (26), 103 (70), 95 (100), 77 (53); **HRMS [M^+ + H]** 216.1136, calculated for $C_{12}H_{14}N_3O$ [M^+ + H] 216.1137.

1-phenyl-2-[1,2,4]triazol-1-yl-ethanone oxime (8)

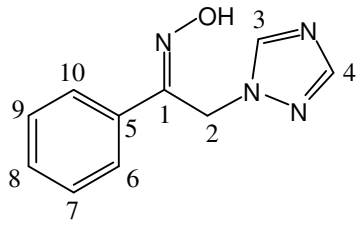

$C_{10}H_{10}N_4O$ (202.21 g mol^{-1}).

98% yield;

White crystals;

Mp: 145 - 155 °C;

R_f = 0.6 (DCM/MeOH 95:5); **UV λ_{max} nm (log ε):** 247 (6.39), 205 (6.31); **IR ν_{max} (cm^{-1}):** 3415, 3103, 3010, 2824, 2764, 1515, 1473, 1444, 1279, 1136, 927; **^{1}H NMR (400 MHz, DMSO-d$_6$) δ:** 7.68 (s, 1H, H-3), 7.01 (s, 1H, H-4), 6.81-6.84 (m, 2H, H-6 /10), 6.50-6.52 (m, 3H, H-7/8/9), 4.65 (s, 2H, CH_2); **^{13}C NMR (100 MHz, DMSO-d$_6$) δ:** 151.12 (C-1), 150.36 (C-4), 145.02 (C-3), 134.35 (C-5), 129.02 (C-8), 128.40 (C-7/9), 126.25 (C-6 /10), 42.43 (C-2); **EIMS *m/z* (rel. int.):** 202 [M^+] (19), 103 (100), 77 (30), 70 (45).

2.4 Physical characteristics, UV, IR and NMR data for 2-hydroxyphenylacyl azoles and their oxime derivatives

1-(2-Hydroxy-phenyl)-2-imidazol-1-yl ethanone (9)

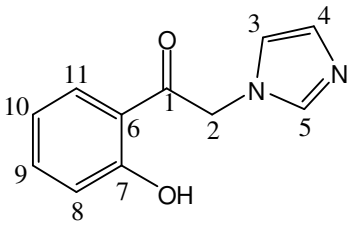

$C_{11}H_{10}N_2O_2$ (202.21 g mol^{-1});

58% yield;

Pale yellow crystals;

Mp: 175 - 177 °C;

R_f = 0.4 (DCM/MeOH 95:5); **UV λ_{max} nm (log ε):** 325 (6.42), 251(6.30), 215(6.24); **IR ν_{max} (cm^{-1}):** 3123, 2934, 2427 (Ph-OH), 1667 (C=O), 1594 (C=N), 1452, 1231 (CH_2- N); **^{1}H NMR (400 MHz, $CDCl_3$) δ:** 7.70 (d, 1H, *J* = 8.00 Hz, H-11), 7.54 – 7.61 (m, 2H, H-5/9), 7.16 (s, 1H, H-4), 7.04 (d, 1H, *J* = 8.40 Hz, H-8), 6.94-6.96 (m, 2H, H-3/10), 5.44 (s, 1H, CH_2); **^{13}C NMR (100 MHz, $CDCl_3$) δ:** 196.88 (C-1), 162.82 (C-7), 140.35 (C-5), 137.82 (C-9), 131.07 (C-4), 128.64 (C-11), 121.31 (C-6), 119.79 (C-10), 119.38 (C-8), 117.49 (C-4), 52.12 (C-2); **EIMS *m/z* (rel. int.):** 202 [M^+] (23), 121 (100), 93 (23), 82 (80).

1-(2-Hydroxyphenyl)-2-(5-methyl-1H-imidazol-1-yl)ethanone (10)

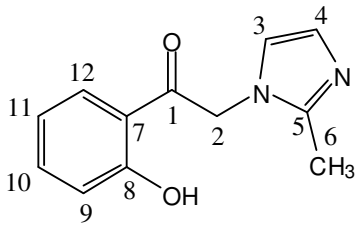

$C_{12}H_{12}N_2O_2$, (216.23 g mol^{-1});

62% yield;

Yellow crystals;

Mp: 164 - 166 °C;

R_f = 0.4 (DCM/MeOH 95:5); **UV λ_{max} nm (log ε):** 328 (6.52), 250 (6.40), 216 (6.33); **IR ν_{max} (cm^{-1}):** 1651 (C=O), 1577 (C=N), 1194 (CH_2-N); **^{1}H NMR (400 MHz, $CDCl_3$) δ:** 7.72 (dd, 1H, *J* = 8.08, 1.4 Hz, H-12), 7.55 (td, 1H, *J* = 7.41, 1.56 Hz, H-10), 7.04 (d, 1H, *J* = 8.52 Hz, H-9), 6.97 (td, 1H, *J* = 8.04, 0.84 Hz, H-11), 6.99 (d, 1H, *J* = 1.2 Hz, H-4), 6.80 (d, 1H, *J* = 1.32 Hz, H-3), 5.32 (s, 2H, CH_2), 2.30 (s, 3H, CH_3); **^{13}C NMR (100 MHz, $CDCl_3$) δ:** 197.07 (C-1), 162.82 (C-8), 145.88 (C-5), 137.78 (C-10), 128.62 (C-12), 127.88 (C-4), 120.60 (C-3), 119.74 (C-11), 119.40 (C-9), 117.57 (C-7), 51.51 (C-2), 13.07 (C-6); **EIMS *m/z* (rel.int.):** 216 [M^+] (30), 121 (100), 96 (84), 65 (30).

1-(2-Hydroxyphenyl)-2-(1H-1,2,4-triazol-1-yl)ethanone (11)

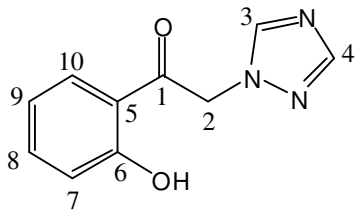

$C_{10}H_9N_3O_2$ (203.19 g mol^{-1});

62% yield;

Pale yellow crystals;

Mp: 135 - 137 °C;

R_f = 0.5 (DCM/MeOH 95:5); **UV λ Max^{nm} (log ε)** 322 (6.50), 251 (6.40), 212 (6.33); **IR ν_{max} (cm^{-1})** 3126, 2924, 1663 (C=O), 1597 (C=N), 1453, 1229 (CH_2-N); **^{1}H NMR (400 MHz, $CDCl_3$) δ:** 11.41 (s, 1H, OH), 8.21 (s, 1H, H-3), 8.00 (s, 1H, H-4), 7.70 (d, 1H, *J* = 7.88 Hz, H-10), 7.54 (t, 1H, *J* = 8.12 Hz, H-8), 7.02 (d, 1H, *J* = 8.48 Hz, H-7), 6.96 (t, 1H, *J* = 7.40 Hz, H-9), 5.68 (s, 2H, CH_2); **^{13}C NMR (100 MHz, $CDCl_3$) δ:** 195.77 (C-1), 162.79 (C-6), 152.29 (C-4), 145.25 (C-3), 137.96 (C-8), 128.80 (C-10), 119.86 (C-9), 119.29 (C-7), 117.36 (C-5), 54.44 (C2); **EIMS *m/z* (rel. int.):** 203 [M^+] (7), 121 (100), 93 (15), 65 (22).

1-(2-Hydroxyphenyl)-2-(1H-imidazol-1-yl) ethanone oxime (12)

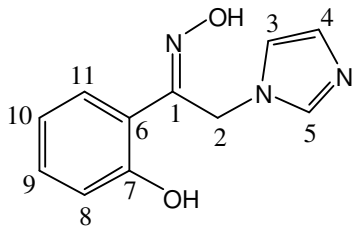

$C_{11}H_{11}N_3O_2$ (217.22 g mol^{-1})

97% yield;

Pale yellow crystals;

Mp: 165 - 177 °C;

R_f = 0.4 (DCM/MeOH 95:5); **UV λ_{max} nm (log ε):** 318 (6.34), 258 (6.23), 221 (6.32); **IR ν_{max} (cm^{-1}):** 3124, 2577 (N-OH), 1579 (C=N), 1510, 1478, 1281, 1242 (CH_2-N), 1068; **^{1}H NMR (400 MHz, DMSO-d_6) δ:** 12.06 (s, 1H, OH), 10.58 (s, 1H, OH), 7.60 (s, 1H, H-5), 7.35 (dd, 1H, *J* = 7.52 , 1.56 Hz, H-11), 7.21 (td, 1H, *J* = 8.48, 1.48 Hz , H-9), 7.02 (s, 1H, H-3), 6.85 (d, 1H, *J* = 8.28 Hz, H-8), 6.80 (t, 2H, *J* = 7.96 Hz, H-4/10), 5.30 (s, 2H, CH_2); **^{13}C NMR (100 MHz, DMSO-d_6) δ:** 156.27 (C-7), 154.29 (C-1), 137.70 (C-5), 130.44 (C-9), 128.95 (C-11), 128.07 (C-3), 119.64 (C-4), 119.29 (C-6), 118.98 (C-10), 116.19 (C-8), 40.69 (C-2); **EIMS *m/z* (rel. int.):** 199 [M^+-H_2O], 172 (11), 132 (23), 81(90), 32 (100).

1-(2-Hydroxyphenyl)-2-(2-methyl-1H-imidazol-1-yl) ethanone oxime (13)

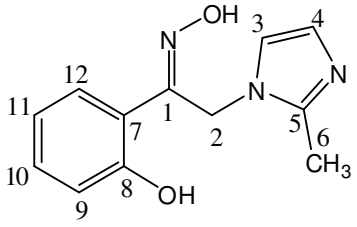

$C_{12}H_{13}N_3O_2$ (231.25 g mol^{-1})

95% yield;

Cream crystals;

Mp: 176 - 188 °C;

R_f = 0.4 (DCM/MeOH 95:5); **UV λ_{max} nm (log ε):** 312 (6.49), 259 (6.41), 225 (6.35); **IR ν_{max} (cm^{-1}):** 2463 (N-OH), 1820, 1586 (C=N), 1447, 1424, 1298, 1272, 1254 (CH_2-N),

1064, 989, 749, 728; **^{1}H NMR (400 MHz, DMSO) δ:** 11.72 (s, 1H, OH), 10.15 (s, 1H, OH), 7.02 -7.07 (m, 2H, H-10/12), 6.71 (d, 1H, *J* = 8.12 Hz, H-9), 6.69 (d, 1H, *J* = 0.64 Hz, H-3), 6.63 (t, 1H, *J* = 7.24 Hz, H-11), 6.46 (d, 1H, *J* = 0.60 Hz H-4), 5.08 (s, 2H, CH_2), 2.06 (s, 3H, CH_3); **^{13}C NMR (100 MHz, DMSO) δ:** 155.75 (C-8), 153.79 (C-1), 143.96 (C-5), 130.26 (C-10), 129.40 (C-12), 125.99 (C-4), 120.33 (C-7), 119.87 (C-3), 118.90 (C-11), 115.79 (C-9), 39.48 (C-2), 12.39 (C-6); **EIMS *m/z* (rel.int.):** 213 [M^+] (100), 133 (80), 132 (78), 105 (26), 95 (88), 77 (38); **HRMS [M^+ + H]** 232.1081, calculated for $C_{12}H_{14}N_3O_2$ (M^+ + H) 232.1086.

1-(2-Hydroxyphenyl)-2-(1 H- 1,2,4 triazol-1-yl) ethanone oxime (14)

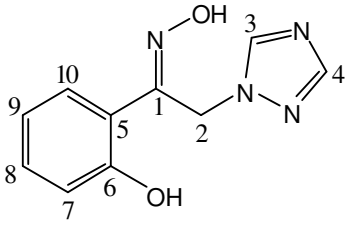

$C_{10}H_{10}N_4O_2$ (218.21 g mol^{-1}).

97% yield;

White crystals;

Mp: 230 - 241 °C;

R_f = 0.5 (DCM/MeOH 95:5); **UV λ_{max} nm (log ε):** 308 (6.49), 255(6.40), 216 (6.33); **IR ν_{max} (cm^{-1}):** 2650.56 (N-OH), 1577.55 (C=N), 1277.60 CH_2-N; **^{1}H NMR (400 MHz, DMSO-d_6) δ:** 8.44 (s, 2 × H-3), 7.84 (s, H-4), 7.82 (s, H-4), 7.38 (d, *J* = 2.28 Hz, H-10), 7.32 (t, *J* = 7.68 Hz, H-8), 7.30 (d, *J* = 2.32 Hz, H-10), 7.18 (td, *J* = 7.12, 0.92 Hz, H-8), 6.80 (t, *J* = 8.64 Hz, 2 × H-9), 6.76 (d, *J* = 8.72 Hz, 2 × H-7), 5.50 (s, H-2) and 5.48 (s, H-2); **^{13}C NMR (100 MHz, DMSO-d_6) δ:** 155.93 (C-6), 155.15 (C-6), 153.13 (C-1), 151.88 (C-1), 151.21 (C-4), 151.10 (C-4), 145.01 (C-3), 144.88 (C-3), 132.69 (C-10), 131.55 (C-10), 130.30 (C-8),

129.30 (C-8), 122.62 (C-5), 119.76 (C-5), 118.89 (C-7), 118.01 (C-7), 115.94 (C-9), 43.58 (C-2), 43.20 (C-2). **EIMS *m/z* (rel. int.):** 200 [M^+ -H_2O] (64), 82 (68), 55 (100); **HRMS [M^+-H]** 217.0732, calculated for $C_{10}H_9N_4O_2$ (M^+-H) 217.0726.

Chapter 3. Results and discussion

This chapter contains the chemistry involved in synthesising six phenylacyl azoles and their oxime derivatives. A full structural elucidation is given for some of the compounds and the ^{1}H and ^{13}C NMR data compared to these compounds for complete assignment of the resonances.

3.1 Chemistry

The synthesis of 2-azolyl-2-hydroxyphenyl ethanone derivatives involves two steps (Scheme 3-1). The first step involves the bromination of acetophenone using Br_2 and chloroform to form the α-bromoketones **1** – **2** and the second step entails reacting the α-bromoketone with an excess of azole in dimethylformamide (DMF) at 65 °C under reflux to produce the corresponding azole derivatives (**3 – 5** and **9 – 11**). The ketones were converted into their oxime derivatives by reacting them with an excess of $HONH_2.HCl$ in ethanol and water at 100 °C.

The first step of this synthesis involves the use of one equivalent of bromine to displace one hydrogen atom. It is important that only one equivalent of bromine is used as excess bromine results in the removal of both hydrogen atoms from the methyl group of acetophenone, and a mixture of di-bromoketone and mono-bromoketone is formed. The use of copper (II) bromide ($CuBr_2$) and NBS was also investigated since these are milder and less toxic reagents

than elemental bromine. The yields obtained with these reagents were however much lower (45 - 60%) (Table 3-1).

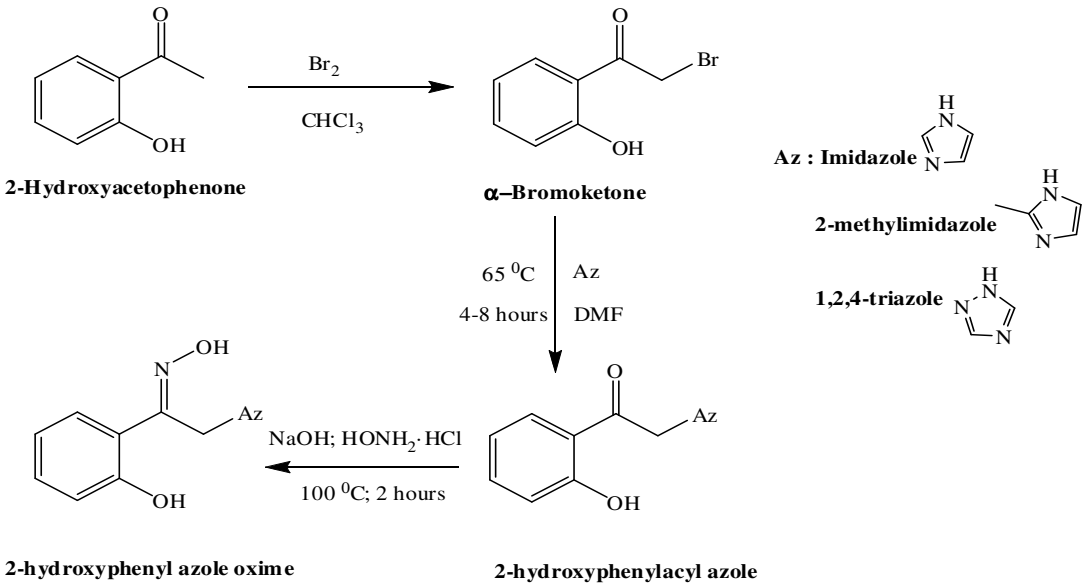

Scheme 3-1 Synthesis of 2-azolyl-2-hydroxyphenyl ethanone and its oxime derivatives

Table 3-1 Yields obtained for α-bromoketones using different brominating agents

Reagent	Reaction time (Hours)	Yield (%)	Literature yields (%)
Br_2	2	80-90	88-96[a]
$CuBr_2$	6-8	58	100[b]
NBS	12	47	71[c]

a-(Cowper and Davidson, 1943), b-(King and Ostrum, 1964), c - (Tanemura *et al*., 2004)

The synthetic approach reported for phenylacyl azoles involves nucleophilic substitution of the desired azole with an α-bromoketone in the presence of an aprotic solvent. The use of different solvents and reaction times were investigated to determine optimum yields for phenylacyl azoles. Emmai et al., (2008) used DMF in a 4 – 8 hour reaction which produced 58% yields. Güven *et al*. (2007) used dioxane-ether as the solvent for the reaction, which took 18 hours at ambient conditions and produced yields of 60%. Clader *et al*. (1995) reported yields of 70% with THF for the same reaction. The use of both THF and dioxane was also investigated in this work, where the reactions took between 12 – 20 hours at 65 °C and produced between 25 – 40 % of the desired product. The use of DMF had been the most efficient, obtaining yields of 60% with reaction times of 4 – 8 hours (Table 3-2). The azole derivatives (**3** – **5** and **9** – **11**) were obtained as white or yellow crystals, after further purification by column chromatography with DCM: MeOH (95:5).

Table 3-2 Yields obtained for phenylacyl azoles using different solvents

Solvent	Reaction time (Hours)	Yield (%)	Literature yields (%)
DMF	4-8	60	58[a]
THF	12-20	25	70[b]
Dioxane-ether	12-20	30-40	60[c]

a-(Emmai et al., 2008), b- (Clader et al., 1995), c- (Güven et al., 2007)

The ketone group in compounds (**3** – **5** and **9** – **11**) was converted into their oxime derivatives by the addition of excess sodium hydroxide and hydroxyaluminium chloride. The reaction was refluxed at 100 °C for two hours, and yields of greater than 95% were obtained. The high temperature was needed since a mixture of water and ethanol was used as the solvent. All the oxime derivatives (**6** – **8** and **12** – **14**) had precipitated out of solution once the reaction was complete. They were then washed with ethyl acetate and then cold water to remove unconverted ketone derivatives.

The yields and melting points of all 14 synthesized compounds are shown in Table 3-3. The melting points of the α-bromoketones was 47 - 49 °C for **1** and 50 - 52 °C for **2**. Upon substitution with an azole moiety the melting points had increased and were greater than 100°C. The 2-hydroxy substituted compounds had much greater melting points than the unsubstituted compounds. The melting points of the 2-azolyl-2-hydroxyphenyl ethanone oxime derivatives showed an increase compared to their corresponding ketone derivatives. The oxime derivatives showed a broad melting point range with a difference of up to 15˚C, this could be due to the racemic mixtures of the *E* and *Z* isomers.

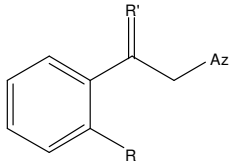

R = H, OH
R' = C, N-OH
Az = Imidazole,
2-methylimidazole,
1,2,4, Triazole, H

Table 3-3 Melting points and yields for the 14 synthesized compounds

Compound	R	R'	Az	Physical Characteristic	Yield (%)	Melting point (°C)
1	H	C	H	White	85	47 - 49
2	OH	C	H	White	70	50 - 52
3	H	C	Imidazole	Yellow	60	115 - 117
4	H	C	2-methylimidazole	Yellow	59	134 - 136
5	H	C	1,2,4-triazole	Yellow	65	114 - 116
6	H	N-OH	Imidazole	Yellow	98	154 - 164
7	H	N-OH	2-methylimidazole	White	98	170 - 185
8	H	N-OH	1,2,4-triazole	White	98	145 - 155
9	OH	C	Imidazole	Yellow	58	175 - 177
10	OH	C	2-methylimidazole	Yellow	62	164 - 166
11	OH	C	1,2,4-triazole	Yellow	62	135 - 137
12	OH	N-OH	Imidazole	Yellow	97	165 - 177
13	OH	N-OH	2-methylimidazole	White	95	176 - 188
14	OH	N-OH	1,2,4-triazole	White	91	230 - 241

3.2 Characterization

All the synthesised compounds were characterized using ^{1}H and ^{13}C NMR, infrared (IR) and ultra violet (UV) spectroscopy and gas-chromatography mass spectrometry (GC-MS). The three novel compounds (**7**, **13** and **14**) were also elucidated using 2D – NMR and high resolution mass spectroscopy (HRMS).

3.2.1 Structural elucidation of phenylacyl azoles and their oxime derivatives

The IR spectrum of **1** showed a carbonyl absorption at 1679 cm^{-1} indicating the presence of the carbonyl group. The mass spectrum showed molecular ion peaks typical for that of the brominated compound with the Br^{81} and Br^{79} molecular ion isotopes at *m/z* 201 and 199 respectively. The peak at *m/z* 91 is typical of the tropylium cation. The ^{1}H NMR spectrum showed the aromatic proton resonances at δ_H 7.96, a doublet assigned to H-4/8, δ_H 7.47, a triplet ascribed to H-5/7 and another triplet at δ_H 7.59 which is that of H-6. The coupling constants of the three resonances were between 7.36 and 7.56 Hz, characteristic of *ortho* coupling. The methylene resonance, H-2 appears as a singlet resonance at δ_H 4.43 and is deshielded because of the electronegative bromine atom. The ^{13}C NMR spectrum shows the presence of the carbonyl group resonance at δ_C 191.49, together with the methylene resonance at δ_C 31.11 and the aromatic resonances at δ_C 129.13 and 129.06 (C-4 – C-8), and δ_C 134.16 (C-3). The ^{1}H and ^{13}C NMR resonances matched those from the literature (Steiner, *et al*., 2005).

Upon replacing the bromine in **1** with an imidazole ring in **3**, the carbonyl peak in the IR spectrum showed a slight shift in wavelength from 1979 to 1691 cm^{-1}. The imidazole aromatic bands were observed at 642-682 cm^{-1} in the IR spectrum. The structure was also verified by the molecular ion peak at *m/z* 186 in the mass spectrum. There was no change to the aromatic resonances in the ^{1}H NMR spectrum as compared to **1**, however as expected there was a downfield shift in the methylene resonance H-2 from δ_H 4.43 in **1** to δ_H 5.37 in **3** due to the electronegative nitrogen atom of the imidazole group. The H-3, H-4 and H-5 proton resonances of the imidazole moiety were present at δ_H 6.92, δ_H 7.10 and δ_H 7.48 respectively, the H-5 resonance overlapping with the H-8/10 resonance. The ^{13}C NMR spectrum showed changes in the chemical shifts with respect to the aromatic carbon resonances and although these are in the same chemical shift region, the C-9, C-8/10, C-7/11 can be clearly distinguished at δ_C134.41, 129.13 and 127.97 respectively. The remaining aromatic resonance C-6 appears at δ_C134.18 and the imidazole carbon resonances appear at δ_C120.30, δ_C 129.57 and δ_C 138.15. The carbonyl resonance is present at δ_C 191.60 and C-2 at δ_C 52.47, much more deshielded than its corresponding resonance in **1** due to being bonded to the imidazole ring. The proton and carbon resonance assignments were made in comparison to **7** below, which were elucidated using HSQC and HMBC data.

The IR spectrum of **4** showed a carbonyl stretching band at 1686 cm^{-1}, which was similar to compound **3** at 1691 cm^{-1}. The aromatic stretching bands of the 2-methylimidazole ring was observed in the region of 624-688 cm^{-1}. The mass spectrum of **4** showed the molecular ion peak at *m/z* 200, and the base peak at *m/z* 105, which was indicative of the phenacyl

fragment. In **4** all the aromatic proton and carbon resonances as well as that for methylene resonance and the carbonyl resonance had similar chemical shifts and splitting patterns to that of **1** and **3**. However in **4**, there were only two imidazole proton resonances as opposed to three in **3**. The H-5 resonance that overlapped with H-8/10 at δ_H 7.48 was absent as indicated by the resonance only integrating to two protons in **4** as opposed to three in **3**. This occurred with a concurrent appearance of an olefinic methyl resonance at δ_H 2.29 and a corresponding methyl carbon resonance at δ_C 13.07. This was assigned to the methyl group at C-5 on the imidazole ring.

The H-2 methylene proton resonance showed HMBC correlations to the carbon resonances at δ_C 120.57, 145.72 and the carbonyl resonance at δ_C 191.75. Since the resonance at δ_C 120.57 was protonated, this was attributed to C-3 with a corresponding doublet proton resonance at δ_H 6.79 (J = 1.28 Hz). It was now able to assign the remaining olefinic resonance at δ_H 6.97 to H-4. The other resonance showing a HMBC correlation to H-2 at δ_C 145.72 was accordingly ascribed to C-5 as this was a non-protonated carbon resonance, which was distinguished from the other non-protonated resonance at δ_C 134.51 because of HMBC correlations to H-3 and H-4. This resonance (δ_C 134.51) was thus assigned to C-7. There was also a weak HMBC correlation to H-2 which supported this assignment.

The triazole substitution in **5**, afforded a slight shift in the carbonyl stretching band in the IR spectrum which was observed at 1697 cm^{-1}. The azole aromatic bands were observed in the same region as **4** at 635 - 688 cm^{-1}. The molecular ion peak in the mass spectrum for **5** was

observed at *m/z* 187. The fragmentation pattern was the same as that in compounds **3** and **4**, showing the phenacyl fragment as the base peak at *m/z* 105, and the phenyl ring fragment at *m/z* 77.

In the ^{1}H NMR spectrum of **5**, most of the resonances were similar to that of **3** with the exception of the azole proton resonances and the methylene proton resonance H-2. The azole proton resonances now occurred at δ_H 8.22 for H-3 and δ_H 7.98 for H-4. These assignments were made in accordance with the assignments made for **12** using HMBC correlations (discussed below). The methylene resonance was more deshielded being present at δ_H 5.65 as opposed to 5.37 in **3**. This could probably be due to hydrogen bonding with the additional nitrogen atom in the azole ring. As expected there were now only two imidazole carbon resonances which were much more deshielded at δ_C 145.06 (C-3) and δ_C 152.10 (C-4) than their corresponding resonances in **3**.

The formation of the imidazole oxime derivative **6** was verified by IR and mass spectroscopy. The disappearance of the carbonyl stretching band at 1691cm^{-1} was observed in the IR spectrum of **3** and a broad N-OH band at 2681 cm^{-1} appeared in **6.** This is indicative that formation of the oxime had occurred. The mass spectrum for compound **6** showed the molecular ion peak at *m/z* 201. The base peak was observed at *m/z* 81 which correlates to the imidazole moiety; the other major peak was the benzonitrile cation at *m/z* 103 (Scheme 3-2).

The H-7/11 resonance in **6** appeared as a multiplet at δ_H 7.66, slightly more shielded than H-7/11 in **3**. The H-8, H-9 and H-10 resonances overlap as a multiplet at δ_H 7.36, also slightly more shielded than their corresponding resonances in **3**. The H-5 resonance however is more deshielded than that in **3**, appearing at δ_H 7.65 in **6**. The methylene resonance H-2 and the H-3 and H-4 resonances of the imidazole ring did not differ much from **3**. There was also the presence of the extra oxime hydroxy resonance at δ_H 12.06 in the ^{1}H NMR spectrum further indicating that the oxime had formed. It must be noted however that the ^{1}H NMR data was acquired in DMSO whereas that for **3** was acquired in $CDCl_3$ and therefore solvent effects could also account for the differences in the ^{1}H NMR chemical shifts. In the ^{13}C NMR spectrum, there was only a difference in the oxime carbon, which occurred at δ_C 151.90 as opposed to the carbonyl resonance at δ_C 191.60 in **3**. This was accompanied by an upfield shift of the C-2 carbon, which occurred together with the solvent peak at δ_C 38.94, determined by HSQC correlations. The ^{1}H and ^{13}C NMR resonances of **6** matched those in the literature (Rad, *et al*., 2009).

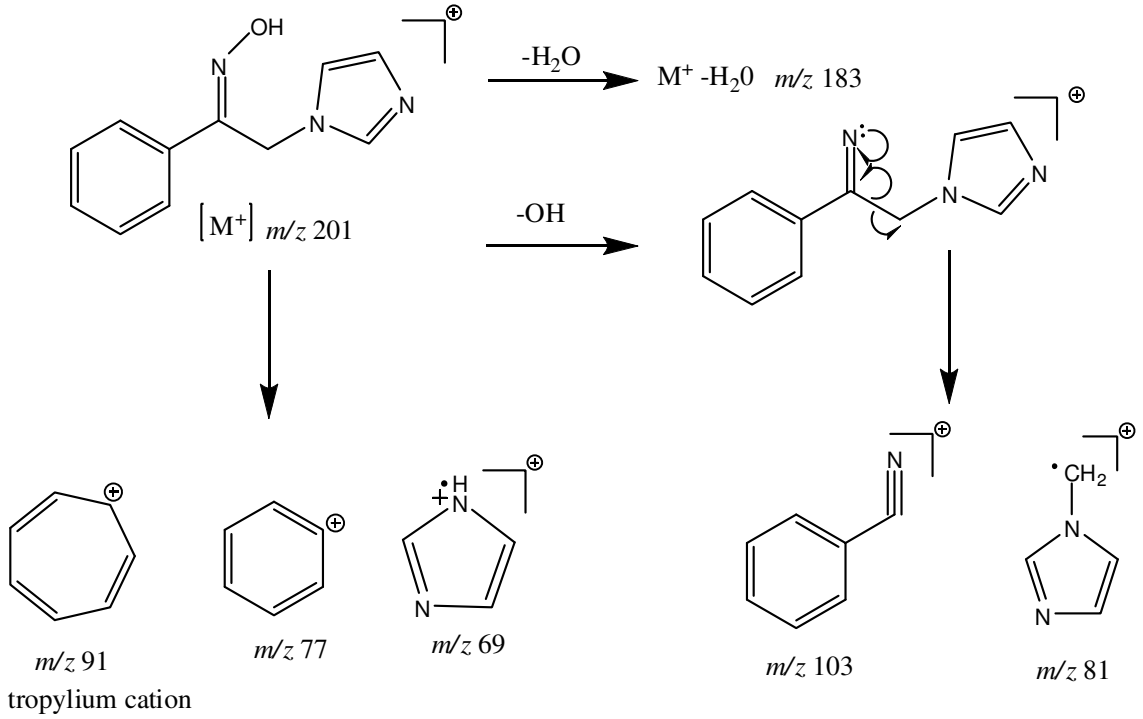

Scheme 3-2 Fragmentation pattern of the oxime derivative 6

In the other two oxime compounds with an unsubstituted phenyl ring (**7** and **8**), a similar splitting pattern was observed for the phenyl ring having two multiplets with similar chemical shifts. These occurred at δ_H 7.33 and δ_H 7.50 in **7** and δ_H 6.50 and δ_H 6.81 in **8**. Similar to **6**, the H-2 resonance did not shift much for **7**; however there was a noticeable difference in chemical shift for H-2 in **8** at δ_H 4.65 as opposed to 5.66 in **5**, the carbonyl derivative. For the triazole oxime derivative **8**, the H-3 and H-4 resonances were seen to be shifted to δ_H 7.68 and 7.01 in comparison to δ_H 8.22 and 7.97 in **5**. In the 2-methylimidazole oxime derivative **7**, the H-3 and H-4 resonances appeared at δ_H 6.89 and δ_H 6.60 compared to δ_H 6.97 and δ_H 6.79 in **4**. We speculate that this could be either due to a lower local magnetic field produced

by the *pi* electrons or this could be due to interaction with the solvent since both these compounds were also acquired in DMSO. The 2-methyl resonance did not change much from **4** to **7**.

In the ^{13}C NMR spectrum of **8**, there was the expected shift of the carbonyl resonance from δ_C 190.74 in **5** to δ_C 151.12 in **8** and a shift of C-2 from δ_C 55.21 in **5** to δ_C 42.43 in **8**, similar to that observed in compound **6**. There was also an additional shift of the C-8 resonance from δ_C 134.76 in **5** to 129.02 in **8**. The same trend was observed in **7** with the oxime carbon resonance being present at δ_C 152.82, C-2 at δ_C 39.60 and C-10 at δ_C 129.62.

The IR spectrum for the oxime derivatives **7** and **8** were similar to **6**, showing respective broad N-OH stretching bands at 2586 and 2764 cm^{-1}. The mass spectrum for **7** and **8** showed the same trend as **6** by the presence of the benzonitrile ion at *m/z* 103 for **7** and **8**, and the 2-methylimidazole moiety at *m/z* 95 for **7**. The molecular ion peaks were observed at *m/z* 215 for **7** and *m/z* 202 for **8**.

3.2.2 Structural elucidation of 2-hydroxyphenylacyl azoles and their oxime derivatives

The IR spectrum of **2** showed a carbonyl absorption at 1640 cm^{-1} which had more single bond character compared to 1679 cm^{-1} in **1**. The mass spectrum showed a molecular ion peak for Br^{79} at *m/z* 214. The base peak at *m/z* 121 indicated a 2-hydroxyphenacyl cation, due to α-cleavage on the side of the azole ring.

With the 2-hydroxy substituted bromo compound, **2**, the splitting patterns of H-5 and H-8 were each double doublets and occurred at δ_H 6.99 (J = 8.50; 0.68 Hz) and δ_H 7.72 (J = 8.08; 1.48 Hz). The H-6 and H-7 resonances appeared as two triplets of doublets at δ_H 7.50 (J = 8.60 and 1.48 Hz) and δ_H 6.91 (J = 7.16 and 0.84 Hz). The H-8 and H-5 resonances as well as the H-6 and H-7 resonances were distinguished based on their electronic effects due to the hydroxy group at C-4 where the *ortho* and *para* proton resonances are more shielded than the *meta* resonances. The shielding is due to electron donation by resonance to the oxygen of the hydroxy group. The phenolic hydroxyl resonance was also observed at δ_H 11.70 due to hydrogen bonding with the carbonyl group. The H-2 proton resonance did not change much as compared to **1**, appearing at δ_H 4.42 as a singlet resonance. In the ^{13}C NMR spectrum of **2**, the carbonyl resonance was present at δ_C 197.19 and the C-2 resonance at δ_C 30.14. The six aromatic resonances were present at δ_C 163.37 for (C-4), δ_C 117.22 (C-3), 119.48 and 119.11 (C-5 and C-7 and could be interchangeable), δ_C 130.52 (C-8) and δ_C137.62 (C-6).

On formation of the imidazole derivative **9**, there were no differences in terms of chemical shifts with regard to the aromatic protons, H-8 to H-11, however due to overlap with the imidazole protons as indicated by the integration of the spectrum, H-3 with H-10 and H-5 with H-9 the splitting pattern of the H-9 and H-10 proton resonances could not clearly be seen and therefore were recorded as multiplets. The ^{1}H NMR resonances of **9** occurred at δ_H 6.95 (m, H-3/10), δ_H 7.04 (d, J = 8.40, H-8), δ_H 7.16 (s, H-4), δ_H 7.54-7.61 (m, H-5/9), δ_H 7.70 (d, J = 8.00 Hz, H-11) and δ_H 5.44 (s, H-2). The change in chemical shift for H-2 as

well as the appearance of the imidazole proton resonances in **9** was evidence that the imidazole ring had successfully substituted the bromide. With reference to the ^{13}C NMR spectrum of **9**, the only resonance that shifted was understandably the C-2 resonance which appeared at δ_C 52.12 because of the imidazole being substituted for the bromide. All the other resonances of the phenyl ring were similar to that of **2**.

The IR spectrum of **9** shows the carbonyl stretching band shift from 1640 cm^{-1} in **2** to 1667 cm^{-1} in **9**. The substitution of the imidazole moiety was also validated by the presence of imidazole aromatic stretching bands which occurred at 619-657 cm^{-1}. The molecular ion peak of **9** was shown at *m/z* 202. The two other major peaks in the mass spectrum of **9** were the 2-hydroxyphenyacyl cation at *m/z* 121, a product of α-cleavage, and the imidazole cation at *m/z* 82.

The 2-methylimidazole **10** and the triazole **11** derivatives of the substituted 2-hydroxy compounds were subsequently compared to **2** to determine if there were any changes to the phenyl ring. The azole rings were also compared to the corresponding un-substituted compounds **4** and **5** to determine if there were changes to the azoles protons in formation of the 2-hydroxy derivatives. The resonances of these two moieties were similar to those they were being compared to and therefore a discussion of these compounds is not included here.

The mass spectra of **10** and **11** showed the same fragmentation pattern as **9** with the base peak being present at *m/z* 121 (2-hydroxyphenacyl cation) for both **10** and **11**. The molecular ion peak was detected at *m/z* 216 for **10** and *m/z* 203 for **11**. The IR spectra were also similar to **9**. The carbonyl stretching bands were visible at 1651 cm^{-1} and 1663 cm^{-1} for **10** and **11** respectively.

The oxime derivatives of the 2-hyrdoxy substituted ketones (**12** – **14**) were acquired in DMSO and the chemical shifts in the ^{1}H and ^{13}C NMR spectra were different to that of the other compounds therefore a discussion on these three compounds are given below.

The ^{1}H NMR spectrum of **12** showed the characteristic splitting pattern for the 2-hydroxy substituted phenyl ring having a double doublet at δ_H 7.35 (J = 7.52, 1.56 Hz) for H-11, a triplet of doublets at δ_H 7.20 (J = 8.48, 1.48 Hz) for H-9, a doublet at δ_H 6.84 (J = 8.28 Hz) for H-8 and a triplet at δ_H 6.80 (J = 7.96 Hz) attributed to H-10. The H-4 resonance overlapped with the triplet at δ_H 6.80, the H-3 resonance occurred at δ_H 7.02 and the H-5 resonance occurred at δ_H 7.60 as broad singlets. The C-5 carbon resonance was indicated by a HMBC correlation between C-5 and H-3. The two hydroxy group proton resonances were present at δ_H 12.07 and 10.58. The H-2 resonance was present at δ_H 5.31 as a singlet. The corresponding carbon resonances were assigned using the HSQC spectrum and the assignments confirmed by HMBC correlations; 2H-2 with C-3, C-5 and C-1; C-7 with H-11, H-9 and H-8. The oxime carbon resonance was present at δ_C 154.29 and the C-7 oxygenated

carbon resonance present at δ_C 156.27. The ^{1}H and ^{13}C NMR resonances of **12** matched those from the literature (Emami, *et al*., 2008).

For the 2-methylimidazole oxime derivative **13**, proton resonances *ortho* and *para* to the hydroxy group (H-9 and H-11) retained the splitting pattern but were more shielded at δ_H 6.71 (d, J = 8.12 Hz) and δ_H 6.63 (t, J = 7.24 Hz). The *meta* protons H-10 and H-12 both overlapped at δ_H 7.02 – δ_H 7.07 and was recorded as a multiplet. The C-3 and C-5 carbon resonance of the 2-methyimidazole ring was determined by HMBC correlations to H-2, which allowed H-3 to be identified by the HSQC spectrum and the remaining H-4 resonance was then determined by elimination. Thus, H-3 occurred at δ_H 6.69 (d, J = 0.64 Hz) and H-4 occurred at δ_H 6.46 (d, J = 0.60 Hz). The carbon resonances of C-3, C-4 and C-5 occurred at δ_C 119.87, 125.99 and 143.97 respectively.

Compound **14**, the oxime derivative of the 2-hydroxyphenyl triazole ketone was synthesised as a mixture of *E* and *Z* isomers (Figure 3-1). This was evident by the twin resonances for H-2, H-4, H-8 and H-10. The two H-8 and two H-10 resonances were most notably separated from each other and upon adding the integration of the resonances, it is evident that the two isomers are present in a racemic mixture. Various attempts at separating the mixture failed and therefore, these are reported as a mixture of isomers.

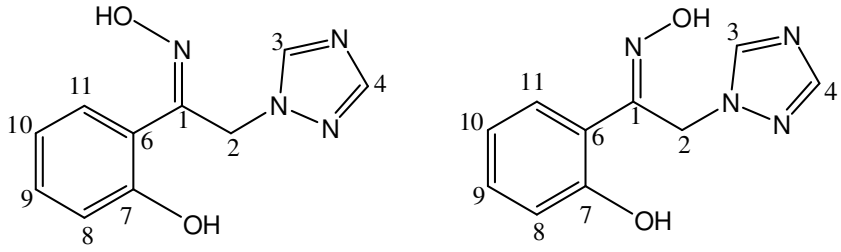

E - isomer of oxime derivative *Z* - isomer of oxime derivative

Figure 3-1 Structures of geometric *E* and *Z* isomers of the oxime derivative (14)

The two H-2 resonances appeared at δ_H 5.50 and 5.48. This resonance was used in the HMBC spectrum to identify the two C-5 resonances at δ_C 122.62 and 119.76, the two C-3 resonances at δ_C 145.01 and 144.88 and the two C-1 resonances at δ_C 153.13 and 151.88. Using the HSQC spectrum, H-3 was identified at δ_H 8.44. The H-3 resonances for both isomers overlapped at this resonance. This H-3 resonance was then used to identify the C-4 resonances due to a HMBC correlation between H-3 and the two C-4 resonances at δ_C 151.21 and 151.10.

The two C-6 resonances were then identified at δ_C 155.93 and 155.15 since these resonances are in the aromatic C-O region of the spectrum. Due to electronic effects by the 2-hydroxy group, the *ortho* (2 × H-7) and *para* (2 × H-9) resonances were identified more upfield at δ_H 6.76 (d, J = 8.72 Hz) and δ_H 6.80 (t, J = 8.64 Hz) respectively to the two *meta* protons of H-8 at δ_H 7.32 (t, J = 7.68 Hz) and δ_H 7.18 (td, J = 7.12, 0.92 Hz) and H-10 at δ_H 7.38 (d, J = 2.28 Hz) and δ_H 7.30 (d, J = 2.32 Hz). We recognize that the coupling constant for the H-10 resonances are rather small (approximately 2.30 Hz) and should be approximately 8.0 Hz, but are unable to explain why this occurs. The only postulated explanation could be that rapid

conversion between the *E* and *Z* isomers affect the coupling constant of H-10 as this proton is in the vicinity of the oxime but could not find any literature on this phenomenon. There are two corresponding carbon resonances for each of C-7 (δ_C 118.89 and 118.01), C-8 (δ_C 130.30 and 129.30) and C-10 (δ_C 132.69 and 131.55), but only one for C-9 at δ_C 115.94. The two C-9 resonances for each of the isomers may overlap.

The molecular ion peaks for the 2-hydroxy substituted oxime derivatives (**12 – 14**) could not be detected in the mass spectra, but a $M^+ - H_2O$ peak was observed in each of the mass spectra (*m/z* 199 for **12**; *m/z* 213 for **13** and *m/z* 200 for **14**). The fragmentation patterns were similar to the corresponding ketones. The base peak for **12** at *m/z* 81, was shown to be the imidazole moiety which was cleaved at C-1. The 1,2-dimethyl-1H-imidazole fragment was detected at *m/z* 95 for **13**. The IR spectrum for compounds (**12 – 14**) all showed the absence of the carbonyl peak, indicating the formation of the oxime group. All oxime derivatives showed broad stretching at 2577 cm^{-1} for **12**, 2463 cm^{-1} for **13** and 2650 cm^{-1} for **14**, indicative of the N-OH group.

The UV spectra for all 14 compounds are in the range of 200 – 260 nm. The $\pi \rightarrow \pi^*$ transitions of the phenyl ring was detected at 200 – 220 nm in all 14 compounds. The 2-hydroxy substituted compounds showed three absorption peaks, as compared to two in the unsubstituted compounds.

Chapter 4. Antifungal and antibacterial activity

4.1 Introduction

Antimicrobial susceptibility testing is an essential technique in many different disciplines, from pathology through to drug development (Powers, 2004). These tests are used to determine the efficacy of novel antimicrobials against a number of different microbial species (Powers, 2004).

In vitro susceptibility tests for measuring antifungal activity have been available since the 1950s. The methods used currently include broth dilution, agar dilution and disc diffusion. Each method has its own advantages and disadvantages, including the type of organism that may be accurately tested by the method. Susceptibility testing with antifungal agents (especially with azoles) against yeasts is markedly influenced by medium composition, length and temperature of incubation, as well as inoculum size (Pfaller, *et al*., 1990).

The broth dilution method determines whether a compound has microbicidal or microbiostatic action at a particular concentration. This procedure involves preparing two-fold dilutions of drugs in a liquid growth medium dispensed in 96 well plates. The plates are then inoculated with a standardized bacterial suspension. The lowest concentration of the drug that prevents microbial growth represents the minimal inhibitory concentration (MIC). Currently, the broth dilution method is recommended for testing commercial antifungal drugs targeting yeasts using either the National Committee for Clinical Laboratory Standards (NCCLS) reference procedure M27-A2 or EUCAST (European Committee on Antibiotic

Susceptibility, 2002). The advantages of the broth dilution procedure include the generation of reproducible MICs, and assistance in generating computerized reports if an automated 96 well plate reader is used (Jorgensen and Ferraro, 2009).

The disk diffusion susceptibility method is widely used since it is cost effective and simple to use. The test is performed by applying absorbent discs containing various concentrations of the drug on agar growth medium inoculated with bacteria. The diameter of the clear zone around the disc is measured at the end of the incubation period and compared with standard drugs (Scorzoni, *et al*., 2007). One other advantage of the disk diffusion method is that it does not require any specialized equipment and the results can be easily interpreted (Jorgensen and Ferraro, 2009). The disadvantage of using this test method is the lack of automation of the test; it is also limiting in that not all bacteria and fungi can be accurately tested (Jorgensen and Ferraro, 2009).

The current study was conducted to investigate the antifungal activity of the 12 synthesized compounds since azole derivatives are known as potent antifungal agents. The susceptibility testing was evaluated by the broth micro-dilution method in accordance with the standardized protocol developed by the NCCLS.

4.2 Experimental

4.2.1 Microbial strains

The antimicrobial activities of the synthesized compounds **3 – 14** were investigated against several representative pathogenic organisms, yeast (*Candida albicans* ATCC 90028, *Candida albicans* ATCC 10231, *Candida krusei* ATCC 6258, and *Candida parapsilosis* ATCC 22019), two gram positive bacteria (*Staphylococcus aureus* ATCC 43300 and *Enterococcus faecalis* ATCC 5129) and three gram negative bacteria (*Escherichia coli* ATCC 35218, *Klebsiella pneumoniae* ATCC 700603 and *Pseudomonas aeruginosa* ATCC 27853).

Fungal test organisms were grown on sabouraud dextrose agar (30 g L^{-1}), and bacterial test organisms on Muller-Hinton agar (21 g L^{-1}) at 35-37 °C in a CO_2 incubator for 24 hours. Organisms were suspended in saline and the turbidity was adjusted to 0.5 McFarland standard. This suspension was further diluted with saline to give a final suspension of 1-5 x 10^3 colony forming units (CFU) mL^{-1}.

4.2.2 Reagents

For susceptibility testing procedures a synthetic medium Roswell Park Memorial Institute (RPMI) 1640 medium was used. This was supplemented with glucose and buffered with 0.165 M morpholine propane sulfonic acid (MOPS, Sigma-Aldrich) to pH 7.0. Sabouraud dextrose agar (Merck) and Muller-Hinton agar were reconstituted according to the manufacturer's instructions and 25 mL aliquots were poured into petri dishes. The 3-(4, 5-

dimethylthiazol-2-yl)-5-(3-carboxymethoxyphenyl)-2-(4-sulfophenyl)-2H-tetrazolium salt (MTS, Promega Corporation, Madison, USA) was prepared by dissolving the MTS salt in phosphate buffered saline. Iodonitrotetrazolium chloride (INT) solution was freshly prepared in phosphate buffered saline to a final concentration of 200 μg mL^{-1}. Each microplate well was measured after 24 hours of incubation with a 96-well microplate spectrophotometer (Mindray MR-96A) set at a wavelength of 490 nm.

4.2.3 Preparation of antimicrobial agents

Stock solutions (10 μg mL^{-1}) of the synthesized compounds **3-14** and reference drugs, Amphotericin B and Neomycin (Sigma Aldrich) were freshly prepared in dimethyl sulfoxide (DMSO). The final concentration of test compounds ranged from 0.0012 to 200 μg mL^{-1} and Amphotericin-B ranged from 0.0015 to 100 μg mL^{-1} and Neomycin from 0.0076 to 500 μg mL^{-1}. All drug dilutions were carried out in 96-well flat bottom microtitre plates; each well contained 100 μL of two fold serial dilutions of the drugs tested and were stored at -70 °C until the day of testing.

4.2.4 Antifungal susceptibility testing

Evaluation of the susceptibility of *Candida albicans* and non- *Candida albicans* species was performed using the broth microdilution method according to the NCCLS reference procedure M27-A2. Yeast strains were grown aerobically overnight at 35 °C on Sabouraud dextrose agar plates. Yeasts were harvested and suspended in 1% sterile saline and the

turbidity of the supernatants measured spectrophotometrically at 625 nm with an absorbance of 0.08-0.1 equivalents to the No. 0.5 Mc Farland standard according to the NCCLS M27-A2 guidelines. The working suspension was diluted to 1:20 in RPMI 1640. The working suspension was further diluted with the medium (1:50) to obtain the final test inocula (1.0 - 1.5 $x10^3$ CFU mL^{-1}). The microtitre plates containing different concentrations of test compounds were allowed to thaw and equilibrate to room temperature under aseptic conditions. Aliquots of 100 µL of working inoculum suspensions were dispensed into each well and the plates incubated in an aerobic environment at 35 °C for 24 hours. After incubation, 20 µL of MTS salt was added directly to each well and incubated at 37 °C for 4 hours. The formation of formazan crystals was quantified by measuring the absorbance at 490 nm on a 96-well plate reader. All analyses were performed in triplicate and data are reported as the mean ± standard error of the mean of ≤ 5.

4.2.5 Antibacterial susceptibility test:

Bacterial susceptibility testing was carried out using the micro broth dilution method (Eloff, 1998; NCCLS M7-A5, 2000; Schwalbe *et al*., 2007). The 16 – 18 hour overnight cultures, which were incubated at 37 °C, were adjusted to turbidity comparable to a No. 0.5 McFarland standard. The inoculum was adjusted to an absorbance between 0.08-0.1 at 625 nm to yield a stock suspension of 0.4 - 0.5 x 10^8 CFU mL^{-1} which was diluted one hundred fold to obtain a working suspension of 1.0 x 10^6 CFU mL^{-1}. Microtitre plates were placed in the laminar flow unit to equilibrate to room temperature under aseptic conditions. Aliquots (100 µL) of

bacterial inoculum were added to the microtiter plates containing appropriately diluted test compounds. Plates were incubated aerobically for 16 - 18 hours at 37 °C. Following incubation, 40 µL of freshly prepared iodonitrotetrazolium chloride solution was added to each well and the plate was further incubated for 45 minutes at 37 °C in the dark. The reduced iodonitrotetrazolium formazan (INTF) was measured after extraction with *N*,*N*-dimethyl formamide (DMF). Persistent growth of bacteria is indicated by a red colour change, while no colour change denotes the lack of bacterial growth. Neomycin was used as the control drug in this study. All analyses were performed in triplicate, and the data is reported as the mean ± standard error of the mean of ≤ 5.

4.3 Results and Discussion

4.3.1 Antifungal activity:

The *in vitro* antifungal activities of the synthesized compounds **3 - 14** were investigated against four pathogenic strains of *Candida* species (Table 4-1) using the broth-dilution method. The Minimum Inhibitory Concentration (MIC) values were determined by comparison to Amphotericin B (Amp-B) as the reference drug. The results indicate that compounds (**9** - **14**) with a 2'-hydroxy substitution on the phenyl ring showed better antifungal activity than the other test compounds, especially against *Candida albicans* (ATCC 90228) and *Candida parapsilosis*.

The 1-(2-hydroxyphenyl)-2-(1H-imidazol-1-yl) ethanone oxime derivative **12** was the most potent against *C. albicans* (ATCC 10231), with a MIC value of 1 µg mL^{-1}, and was comparable to that of the reference drug Amphotericin B (MIC 1.2 µg mL^{-1}). Among the compounds tested, 2-(5-methyl-1H-imidazol-1-yl)-1-phenylethanone **4** and 1-(2-hydroxyphenyl)-2-(5-methyl-1H-imidazol-1-yl)ethanone **10** showed much higher activity than the rest of the test compounds against *C. albicans* (ATCC 90228) with MIC values of 12.5 and 25 µg mL^{-1} respectively.

In general, the compounds containing a triazole or 2-methylimidazole moiety showed better activity than its imidazole counterparts. The oxime derivatives of compounds containing imidazole **6** and triazole **8** and **14**, showed better antifungal activity against *C. albicans* (ATCC 90028) than their ketone derivatives, whereas the oxime compounds containing 2-

methylimidazole (**7** and **12**) had no activity. *C krusei* ATCC-5129 was resistant to all the test compounds (**3** – **14**).

Table 4-1 Minimum Inhibitory Concentration (MIC µg mL^{-1}) of test compounds on *Candida* species

Compound	*C. albicans* ATCC 90028	*C. albicans* ATCC 10231	*C. krusei* ATCC 6258	*C. parapsilosis* ATCC 22019
3	-	-	-	100
4	12.5	-	-	-
5	-	-	-	200
6	200	-	-	-
7	-	-	-	-
8	200	-	-	-
9	-	12.5	-	-
10	25	-	-	12.5
11	200	-	-	12.5
12	-	1	-	-
13	-	25	-	50
14	200	-	-	-
Amp-B	1.2	1.2	5	1.2

-: indicates no activity at 200 µg mL^{-1}. Data reported as the mean ± standard error of the mean ≤ 5.

4.3.2 Antibacterial activity

The antibacterial activity of compounds **3 – 14** were evaluated by the *in vitro* broth dilution assay and the results are presented in Table 4-2. Two Gram-positive (*S. aureus and E. faecalis*) and three Gram negative (*E. coli, K. pneumoniae* and *P. aeruginosa*) bacterial

strains were employed in the present study and Neomycin (Sigma Aldrich) was used as the reference drug. In general the antibacterial activity was not as good as the antifungal activity with moderate activity being exhibited by **6** against *S. aureus* (MIC of 200 µg mL^{-1}) and *K. pneumonia* (100 µg mL^{-1}), **9** against *E. coli* (MIC of 100 µg mL^{-1}) and **5** against *P. aeruginosa* (200 µg mL^{-1}). Both compounds **6** and **9** contain an imidazole moiety. All compounds were inactive against *E. faecalis*.

Compounds containing an oxime group (**6 – 8**, **12 – 14**) as well as **10** containing a 2-methylimidazole group showed inhibitory activity against *K. pneumonia*, although all showed moderate *in vitro* antibacterial activity compared to the reference drug Neomycin.

Table 4-2 Minimum inhibitory concentration of the test compounds (MIC µg mL^{-1}) on gram positive and gram negative bacteria

Compound	***S.aureus*** ATCC-43300	***E.faecalis*** ATCC-5129	***E.coli*** ATCC-35218	***K. pneumonia*** ATCC-700603	***P. aeruginosa*** ATCC-27853
5	-	-	-	-	200
6	200	-	-	100	-
8	-	-	-	200	-
9	-	-	100	-	-
10	-	-	-	200	-
12	-	-	-	200	-
13	-	-	-	200	-
Neomycin	10	20	5	10	5

-: indicates no activity at 200 µg mL^{-1}. Data reported as the mean sd ± ≤5.

* compounds **3**, **4**, **7**, **11** and **14** showed no antibacterial activity to the strains tested

4.4 Conclusion

The antifungal and antibacterial results indicate that the synthesized compounds (**3** - **14**) possess moderate antifungal activity and weak antibacterial activity. These results are in agreement with the literature on antimicrobial activity for azole compounds, which show them to have antifungal properties.

In this study, we found the most active compound to be 1-(2-hydroxyphenyl)-2-(1*H*-imidazol-1-yl)ethanone oxime **12**, at 1 μg mL^{-1} against *C. albicans* (ATCC 10231). In general, the 2-hydroxy substituted compounds are shown to be more active against the different *Candida* species, as compared to their unsubstituted counterparts. The compounds containing a triazole or 2-methylimidazole moiety showed higher activity as compared to compounds containing an imidazole moiety.

The antibacterial results also indicated that in general, the 2-hydroxy substituted compounds showed better activity.

These results are only a preliminary screening for the antifungal activity of these compounds. Further antifungal testing is needed on non-candida species of yeasts, as well as molds and dermatophytes. From this study it is concluded that 2-hydroxyphenylacyl azole compounds have the potential to be antifungal agents and further studies on their structure-activity relationships and mode of action may provide us with a better understanding of their antifungal activities.

Chapter 5. Conclusion

The synthesis of the target compounds **1** – **14**, were synthesised fairly easily in three steps with the only problem being that **14** was not separated into the *E* and *Z* isomers. The yields of the reactions were all between 58 and 98%, with almost half of the compounds having yields of greater than 90%.

The use of DMF proved to be the best solvent for the reaction with yields of 60%. The conversion of the ketones to their oxime derivatives was successfully accomplished with 95% of the ketone derivatives being converted. The oxime derivatives that formed were either *E* or *Z* stereoisomers and could not be separated.

Further work is needed in order to prepare pure isomers of this compound, or to further purify the racemic mixtures. This could lead to further testing of the purified isomers to investigate if the *E* or *Z* configuration of the oxime group has an effect on the antifungal activity of the compound.

Three novel compounds, 2-(2-methyl-1H-imidazol-1-yl)-1-phenyl ethanone oxime **7**; 1-(2-hydroxyphenyl)-2-(2-methyl-1H-imidazol-1-yl) ethanone oxime **13**; and 1-(2-hydroxyphenyl)-2-(1H-1,2,4 triazol-1-yl) ethanone oxime **14**, were synthesized and their structures determined by NMR and confirmed by high resolution mass spectroscopy (HRMS).

Target compounds possessed moderate antifungal activity and weak antibacterial activity against several pathogenic fungi and bacteria. The most active antifungal compound was **10**

with a MIC value of 1µg mL^{-1} against *C. albicans*. The triazole and 2-methylimidazole derivatives showed better antifungal activity with MIC values in the range of 12.5 to 50 µg mL^{-1}. In general, the 2-hydroxy substituted derivatives showed better antifungal and antibacterial activity when compared to their corresponding unsubstituted derivatives.

The present study shows that 2'-methyl substitution on the azole ring and 2'-hydroxyl substitution on the aryl ring lead to enhanced inhibitory activity of the target compounds. Further optimization and antifungal screening against a wider range of pathogenic fungi is needed to assess the extent of the antifungal activity. Cytotoxicity screening is also needed to validate the results.

References

Aher, N.G., Pore, V.S., Mishra, N.N., Kumar, A., Shukla, A.S., Sharma, A. and Bhat, M.K. 2009. Synthesis and antifungal activity of 1,2,3-triazole containing fluconazole analogues. *Bioorganic and Medicinal Chemistry Letters*. **19**: 759-763.

Aromi, G., Barrios, L.A., Roubeau, O. and Gamez, P. 2011. Triazoles and tetrazoles: Prime ligands to generate remarkable coordination materials. *Coordination Chemistry Reviews*. **255**: 485-546.

Banfi, E., Scialino, G., Zampieri, D., Mamolo, M.G., Vio, L., Ferrone, M., Fermeglia, M., Paneni, M.S. and Pricl, S. 2006. Antifungal and antimycobacterial activity of new imidazole and triazole derivatives. A combined experimental and computational approach. *Journal of Antimicrobial Chemotherapy*. **58**: 76-84.

Bougrin, K., Loupy, A. and Soufiaoui, M. 2005. Microwave-assisted solvent-free heterocyclic synthesis. *Journal of Photochemistry and Photobiology C: Photochemistry Reviews*. **6**: 139-167.

Casalinuovo, I.A., Francesco, P.D.I. and Garaci, E. 2004. Fluconazle resistance in *Candida albicans*: A review of mechanisms. *European Review for Medical and Pharmacological Sciences*. **8**: 69-77.

Chai, X., Zhang, J., Cao, Y., Zou, Y., Wu, Q., Zhang, D., Jiang, Y. and Sun, Q. 2011. New azoles with antifungal activity: Design, synthesis, and molecular docking. *Bioorganic and Medicinal Chemistry Letters.* **21**: 686-689.

Clader, J.W., Berger, J. G., Burrier, R.E., Davis, H.R., Domalski, M., Dugar, S., Kogan, T.P., Salisbury, B. and Vaccaro, W. 1995. Substituted (1,2-Diarylethyl) amide acyl-CoA:cholesterol acyltransferase inhibitors: Effect of polar groups on *in vitro* and *in vivo* activity. *Journal of Medicinal Chemistry*. **38**: 1600-1607.

Clemons, M., Coleman, R.E. and Verma, S. 2004. Aromatase inhibitors in the adjuvant setting: bringing the gold to a standard. *Cancer Treatment Reviews*. **30**: 325-332.

CLSI Document. Clinical and Laboratory Standards Institute, Villanova, PA. 2002. 22.

Schwalbe, R., Steele-Moore. L. and Goodwin, A.C. 2007. Antimicrobial susceptibility testing protocols, Vol. 1, CRC Press.

Cowper, R.M. and Davidson, L.H. 1943. Phenylacyl bromide. *Organic Syntheses*. **CV 2**: 480.

Demirbas, N., Karaoglu, S.A., Demirbas, A. and Sancak, K. 2004. Synthesis and antimicrobial activities of some new 1-(5-phenylamino-[1,3,4]-thiadiazol-2-yl)-methyl-5-oxo-[1,2,4]-triazole and 1-(4-phenyl-5-thioxo-[1,2,4]-triazol-3-yl)-methyl-5-oxo-[1,2,4]-triazole derivatives. *European Journal of Medicinal Chemistry*. **39**: 793–804.

Eloff, J.N. 1998. A sensitive and quick microplate method to determine the minimal inhibitory concentration of plant extracts for bacteria. *Planta Medica*. **64**: 711-713.

Emami, S., Falahati, M., Banifatemi, A., Moshiri, K. and Shafiee, A. 2002. Stereoselective synthesis and *in vitro* antifungal evaluation of (*E*) - and (*Z*) - imidazolylchromanone oxime ethers. *Archiv der Pharmazie: Pharmaceutical and Medicinal Chemistry*. **7**: 318-324.

Emami, S., Foroumadi, A., Falahati, M., Lotfali, E., Rajabalian, S., Ebrahimi, S.A., Farahyar, S. and Shafiee, A. 2008. 2-Hydroxyphenacyl azoles and related azolium derivatives as antifungal agents. *Bioorganic and Medicinal Chemistry Letters*. **18:** 141–146.

Erian, A.W., Sherif, S.M. and Gaber, H.M. 2003. The chemistry of α-haloketones and their utility in heterocyclic synthesis. *Molecules*. **8**: 793-865.

Founder, C., Casper, A., Boillot, F. and Villard, J. 1995. Evaluation of a broth microdilution antifungal susceptibility test with a pH indicator: comparison with the broth macrodilution procedures. *Journal of Antimicrobial Chemotherapy*. **35**: 373-380.

Guardiola-Diaz, H.M., Foster, L.A., Mushrush, D. and Vaz, A.D.N. 2001. Azole-antifungal binding to novel cytochrome P450 from *Mycobacterium tuberculosis*: implications for treatment of tuberculosis. *Biochemical Pharmacology*. **61**: 1463-1470.

Güven, O.O., Erdoğan, T., Göker, H. and Yildiz, S. 2007. Synthesis and antimicrobial activity of some novel phenyl and benzimidazole substituted benzyl ethers. *Bioorganic and Medicinal Chemistry letters*. **17**: 2233-2236.

Havaldar, F.H. and Patil, A.R. 2008. Synthesis of 1,2,4 triazole derivatives and their biological activity. *European Journal of Chemistry*. **5**: 347-354.

Heasley, V.L., Louie, T.J., Luttrull, D.K., Millar, M.D., Moore, H.B., Nogales, D.F., Sauerbrey, A.M., Shevel, A.B., Shibuya, T.Y., Stanley, M.S. and Shellhamer, D.F. 1988. Effect of *N*-bromosuccinimide (NBS) and other *N*-brominating agents on the bromination of α, β-unsaturated ketones in methanol. *Organic Chemistry*. **53**: 2199-2204.

Huang, H., Yan, X., Zhu, W., Liu, H., Jiang, H. and Chen, K. 2008. Efficient copper-promoted *N*-arylations of aryl halides with amines. *Journal of Combinatorial Chemistry*. **10**: 617-619.

Jin, S., Guo, M., Wang, D. and Cui, H. 2011. Salt and co-crystal formation from 2-(imidazol-1-yl)-1-phenylethanone and different acidic components. *Journal of Molecular Structure*. **1006**: 128-135.

Jorgensen, J.H. and Ferraro, M.J. 2009. Antimicrobial susceptibility testing: A review of general principles and contemporary practices. *Clinical Infectious Diseases*. **49**: 1749-1755.

Kanafani, Z.A. and Perfect, J.R. 2008. Antimicrobial resistance: resistance to antifungal agents: mechanisms and clinical impact. *Clinical Infectious Diseases*. **46**: 120-128.

Kathiravan, M.K., Salake, A.B., Chothe, A.S., Dudhe, P.B., Watode, R.P., Mukta, M.S. and Gadhwe, S. 2012. The biology and chemistry of antifungal agents: A review. *Bioorganic and Medicinal Chemistry*. **20**: 5678-5698.

Kidwai, M., Dave, B. and Bhushan, K.R. 2000. Alumina-supported synthesis of aminoazoles using microwaves. *Chemistry Papers*. **54**: 231-234.

King, L.C. and Ostrum, G.K. 1964. Selective bromination with copper (II) bromide. *Journal of Organic Chemistry*. **69**: 3459-3461**.**

Lass-Flörl, C. 2011. Triazole antifungal agents in invasive fungal infections: A comparative review. *Drugs*. **71**: 2405-2419.

Maertens, J.A. 2004. History of the development of azole derivatives. *Clinical Microbiology and Infection*. **10**: 1-10.

Mamolo, M.G., Zampieri, D., Falagiani, V., Vio, L., Fermeglia, M., Ferrone, M., Pricl, S., Banfi, E. and Scialino, G. 2004. Antifungal and antimycobacterial activity of new *N*-1-[1-aryl-2-(1*H*-imidazol-1-yl and 1*H*-1,2,4-triazol-1-yl)-ethylidene]-pyridine-2-carboxamidrazone derivatives: a combined experimental and computational approach. *Arkivoc*. **5**: 231-250.

Martin, G.S., Mannino, D.M., Eaton, S. and Moss, M. 2003. The epidemiology of sepsis in the United States from 1979 through 2000. *New England Journal of Medicine*. **348**: 1546-1554.

Nadeem, S. and Waquar A. 2010. Triazole incorporated thiazoles as a new class of anticonvulsants: Design, synthesis and in vivo screening. *European Journal of Medicinal Chemistry*. **45**: 1536–1543.

National Committee for Clinical Laboratory Standards. 2000. Methods for dilution antimicrobial susceptibility tests for bacteria that grow aerobically. Approved Standard. 5th ed. M7-A5. National Committee for Clinical Laboratory Standard. Villanova, PA.

National Committee for Clinical Laboratory Standards. 2002. Reference method for Broth dilution antifungal susceptibility testing of yeasts approved standard. Approved standard. 2nd ed. M27-A2. National Committee for Clinical Laboratory Standard. Wayne, P.A.

Pfaller, M.A. 2012. Antifungal drug resistance: Mechanisms, epidemiology and consequences for treatment. *The American Journal of Medicine*. **125** (1A): S3-S13.

Pfaller, M.A., Castanheira, M., Messer, S.A., Moet, G.A. and Jones, R.N. 2010. Variation in *Candida* species. Distribution and antifungal resistance rates among bloodstream infection isolates by patient age: report from the SENTRY Antimicrobial Surveillance Program (2008-2009). *Diagnostic Microbiology and Infectious Diseases*. **66**: 278-283.

Pfaller, M.A. and Diekema, D.J. 2010. Epidemiology of invasive mycoses in North America. *Critical Reviews in Microbiology*. **36**: 1-53.

Pfaller, M.A., Messer, S.A., Hollis, R.J., Boyken, L., Tendolkar, S., Kroeger, J. and Diekema, D.J. 2009. Variation in susceptibility of bloodstream isolates of *Candida glabrata* to fluconazole according to patient age and geographic location in the United States in 2001 to 2007. *Journal of Clinical Microbiology*. **47**: 3185-3190.

Pfaller, M.A., Rinaldi, M.G., Galgiani, J.N., Bartlett, M.S., Body, B.A., Espinel-Ingroff, A., Fromtling, R.A., Hall, G.S., Huges, C.E., Odds, F.C. and Sugar, A.M. 1990. Collaborative investigation of variables in susceptibility testing of yeasts. *Antimicrobial Agents and Chemotherapy*. **34**: 1648-1654.

Powers, J.H. 2004. Antimicrobial drug development-the past, the present, and the future. *Clinical Microbiology and Infection*. **10**: 23-31.

Ranganathan, D.R. 2012. An overview of changing trends in systemic fungal infections. *WebmedCentral Microbiology*. **3** (5): WMC003386.

Rees, J.R., Pinner, R.W., Hajjeh, R.A., Brandt, M.E. and Reingold, A.L. 1998. The epidemiological features of invasive mycotic infections in the San Francisco Bay area, 1992-1993: Results of population-based laboratory active surveillance. *Clinical Infectious Diseases*. **27**: 1138-1147.

Rodrigues, J.R., Lourenco, D. and Gamboa, N. 2011. Disturbance in hemoglobin metabolism and *in vivo* antimalarial activity of azole antimycotics. *Revista do Instituto de Medicina Tropical de São Paulo (Journal of the Institute of Tropical Medicine of São Paulo).* **53**: 25-29.

Scorzoni, L., Benaducci, T., Almeida, A.M.F., Silva, D.H.S., Bolzani, V.S. and Mendes-Giannini, M.J.S. 2007. Comparative study of disk diffusion and microdilution methods for evaluation of antifungal activity of natural compounds against medical yeasts *Candida spp* and *Cryptococcus sp*. *Revista de Ciencias Farmaceuticas Basica*. **28**: 25-34.

Sheehan, D.J., Hitchcock, C.A. and Sibley, C.M. 1999. Current and emerging azole antifungal agents. *Clinical Microbiology Reviews*. **12**: 40-79.

Siddiqui, N. and Ahsan, W. 2010. Triazole incorporated thiazoles as a new class of anticonvulsants: Design, synthesis and *in vivo* screening. *European Journal of Medicinal Chemistry*. **45**: 1536-1543.

Soltani Rad, M.N., Khalafi-Nezhad, A. and Somayeh Behrouz, S. 2009. Design and Synthesis of Some Novel Oxiconazole-Like Carboacyclic Nucleoside Analogues, as Potential Chemotherapeutic Agents. *Helvetica Chimica Acta*. **92**: 1760-1774.

Steiner, G., Kopacka, H., Ongania, K., Wurst, K., Preishuber-Pflugl, P. and Bildstein, B. 2005. Heteroditopic imino *N*-heterocyclic carbenes and their sulfur, selenium, and tungsten tetracarbonyl derivatives. *European Journal of Inorganic Chemistry*. 1325-1333.

Tanemura, K., Suzuki, T., Nishida, Y., Satsumabayashi, K. and Horaguchi, T. 2004. A mild and efficient procedure for α-bromination of ketones using *N*-bromosuccinimide catalysed by ammonium acetate. *Chemical Communication*. 470-471. DOI: 10.1039/b315340a.

Tien Huy, N., Kamei, E., Kondo, Y., Serada, S., Kanaori, K., Takano, R., Tajima, K. and Hara, S. 2002. Effect of antifungal azoles on the heme detoxification system of malaria parasite. *Journal of Biochemistry*. **131**: 437-444.

Wisplinghoff, H., Bischoff, T., Tallent, S.M., Seifert, H., Wenzel, R.P. and Edmond, M.B. 2004. Nosocomial bloodstream infections in US Hospitals: Analysis of 24,179 cases from a prospective nationwide surveillance study. *Clinical Infectious Diseases*. **39**: 309-317.

APPENDIX A

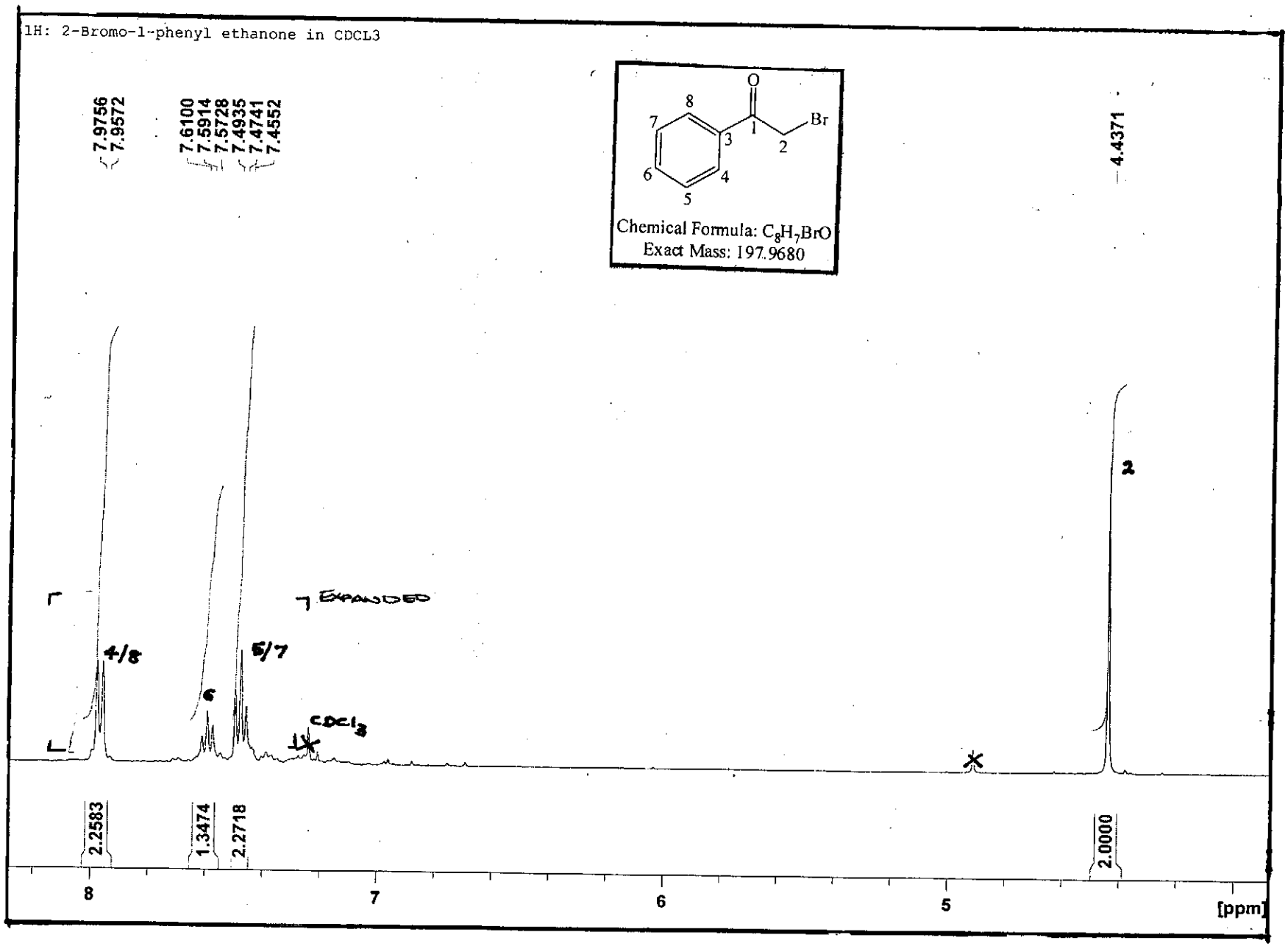

^{1}H NMR spectrum of compound 1, 2-bromo-1-phenylethanone

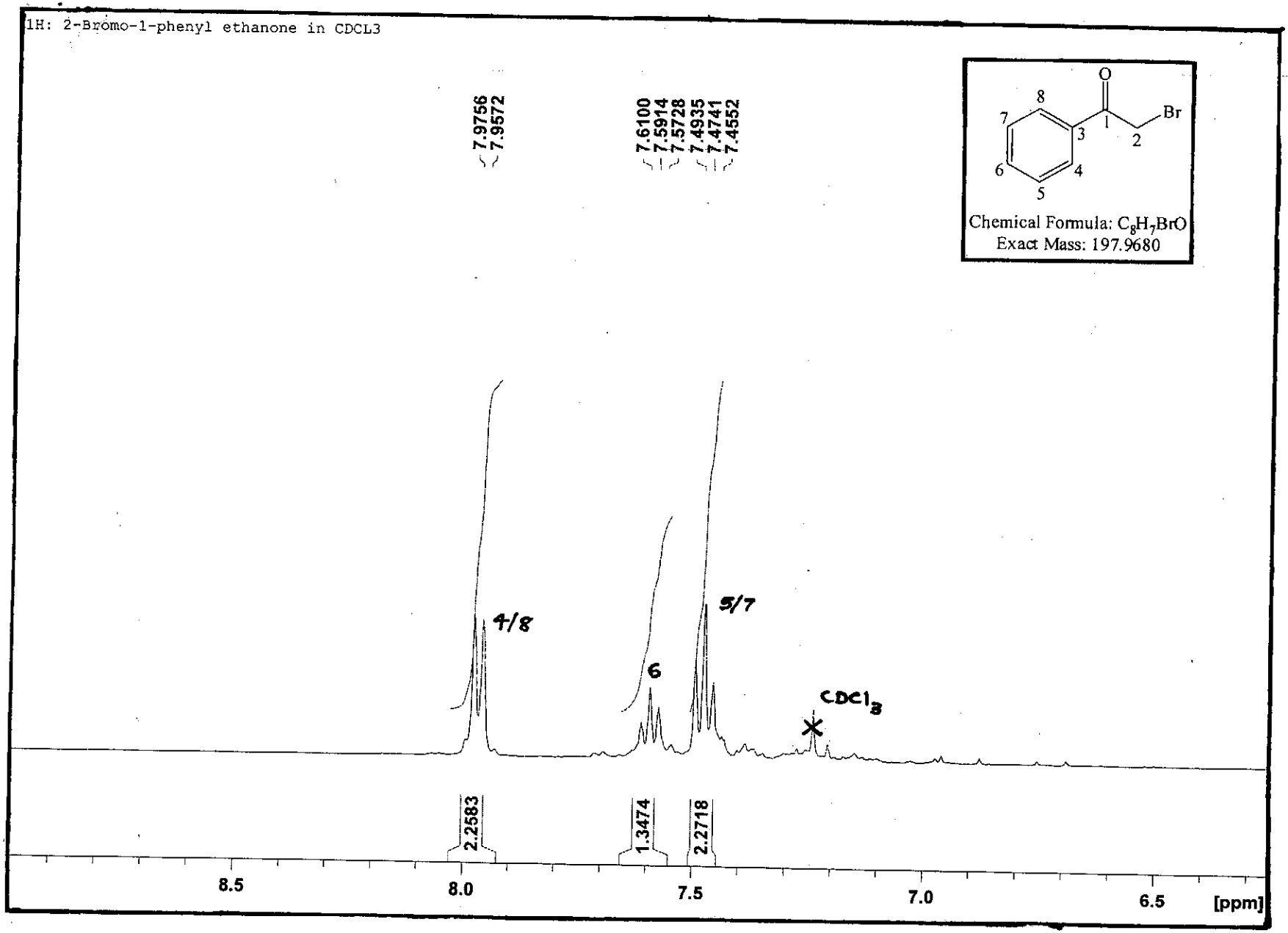

^{1}H NMR spectrum of compound 1, 2-bromo-1-phenylethanone

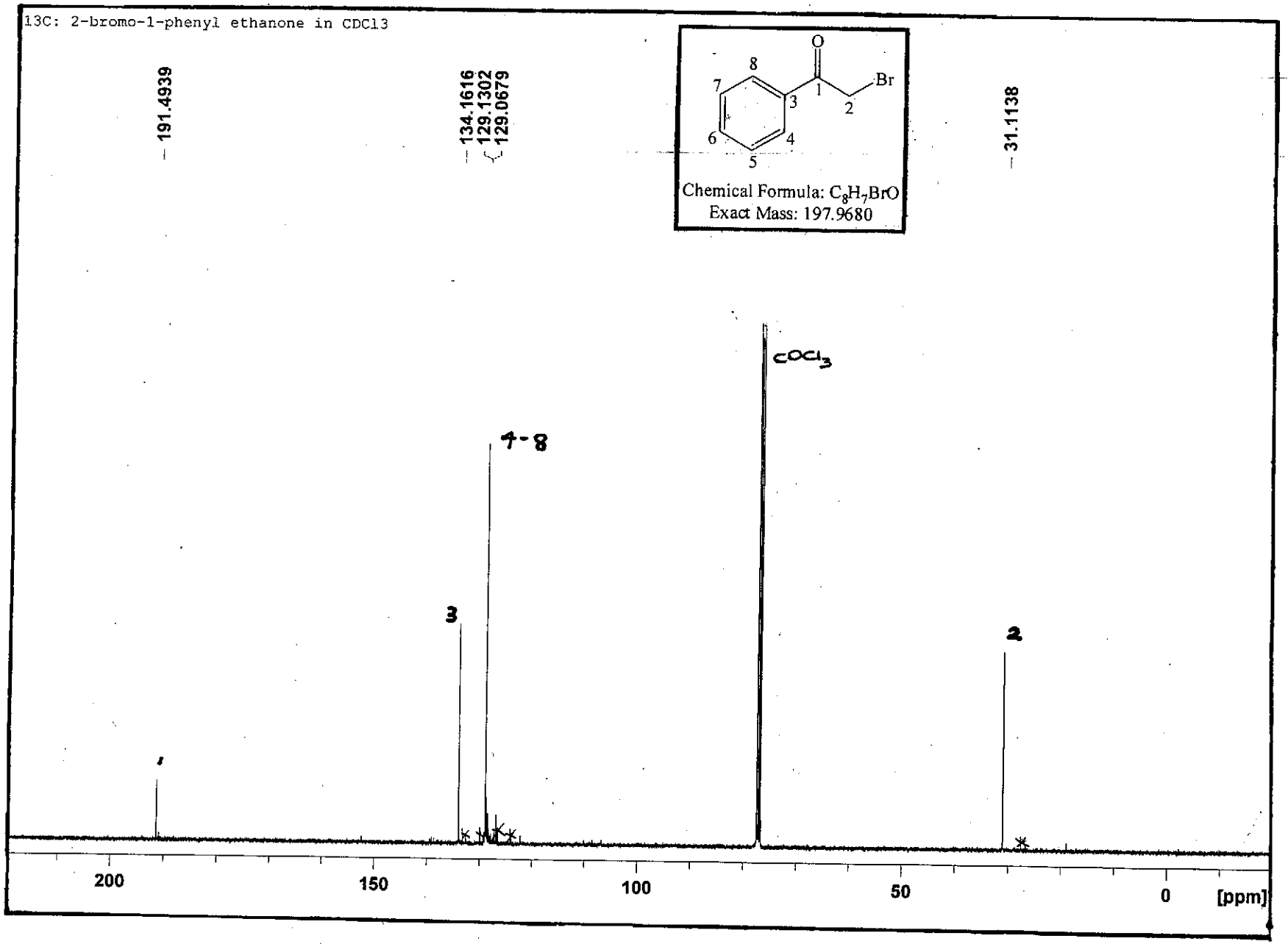

^{13}C NMR of compound 1, 2-bromo-1-phenylethanone

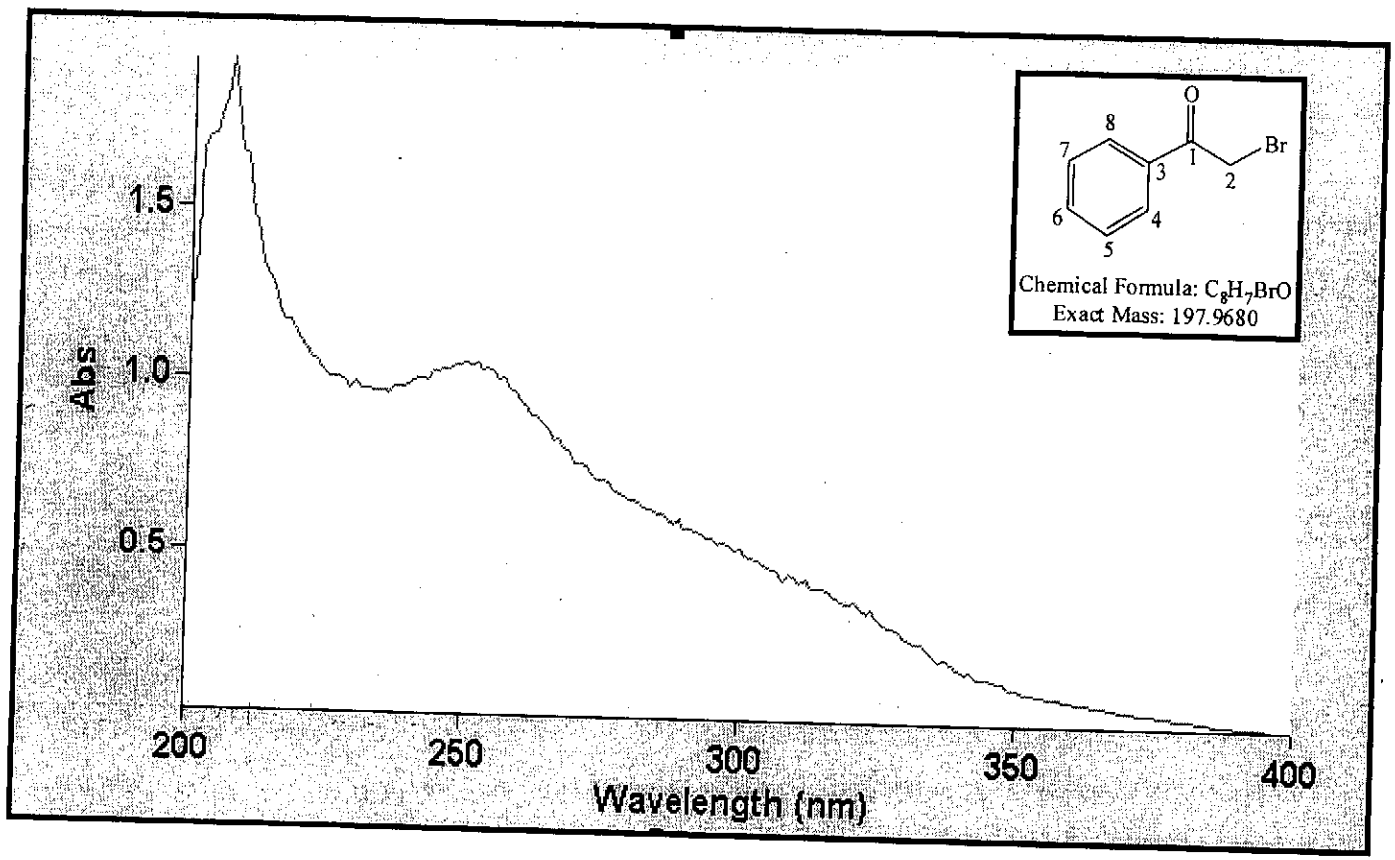

Ultra Violet spectrum of compound 1, 2-bromo-1-phenylethanone

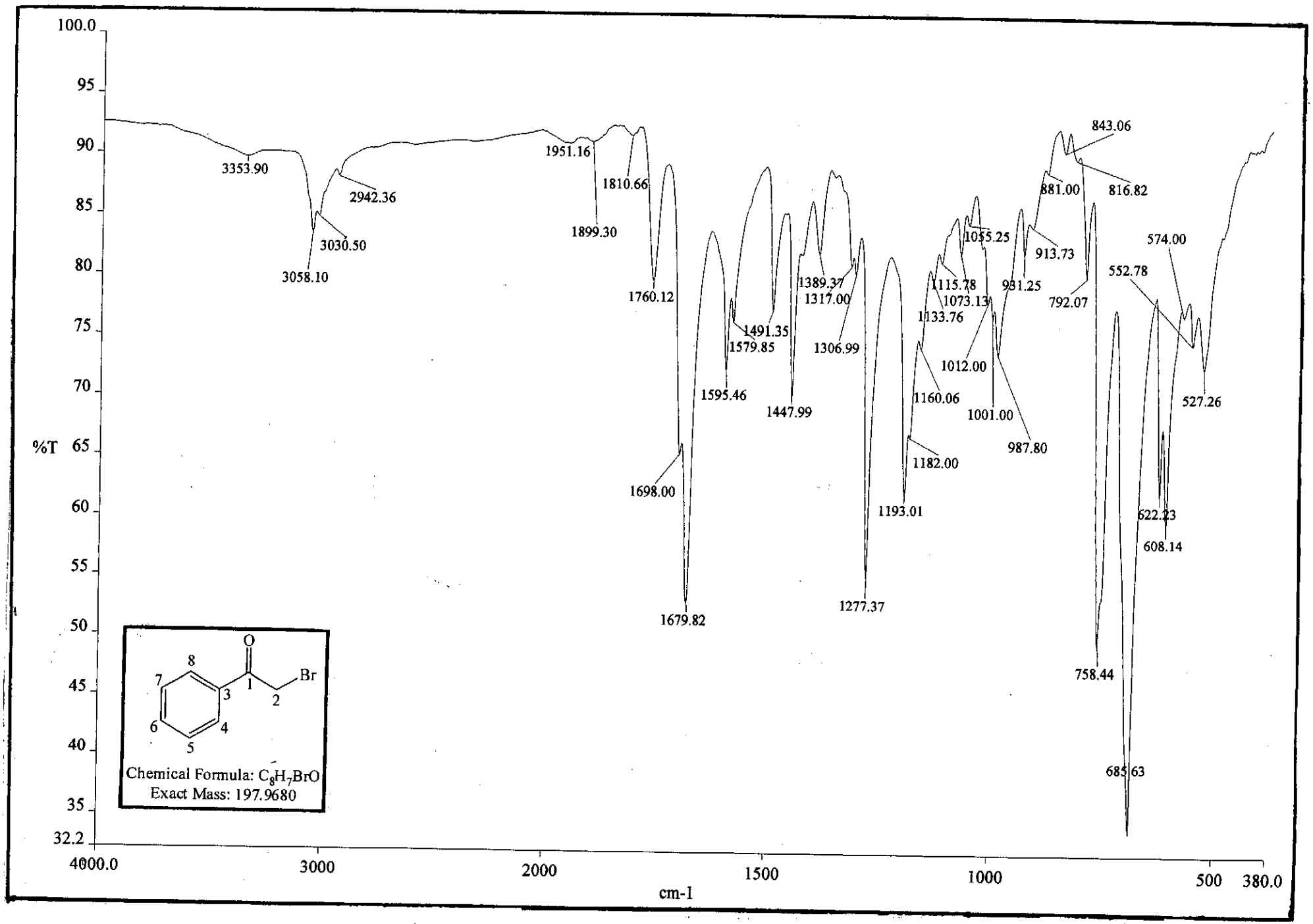

Infrared spectrum of compound 1, 2-bromo-1-phenylethanone

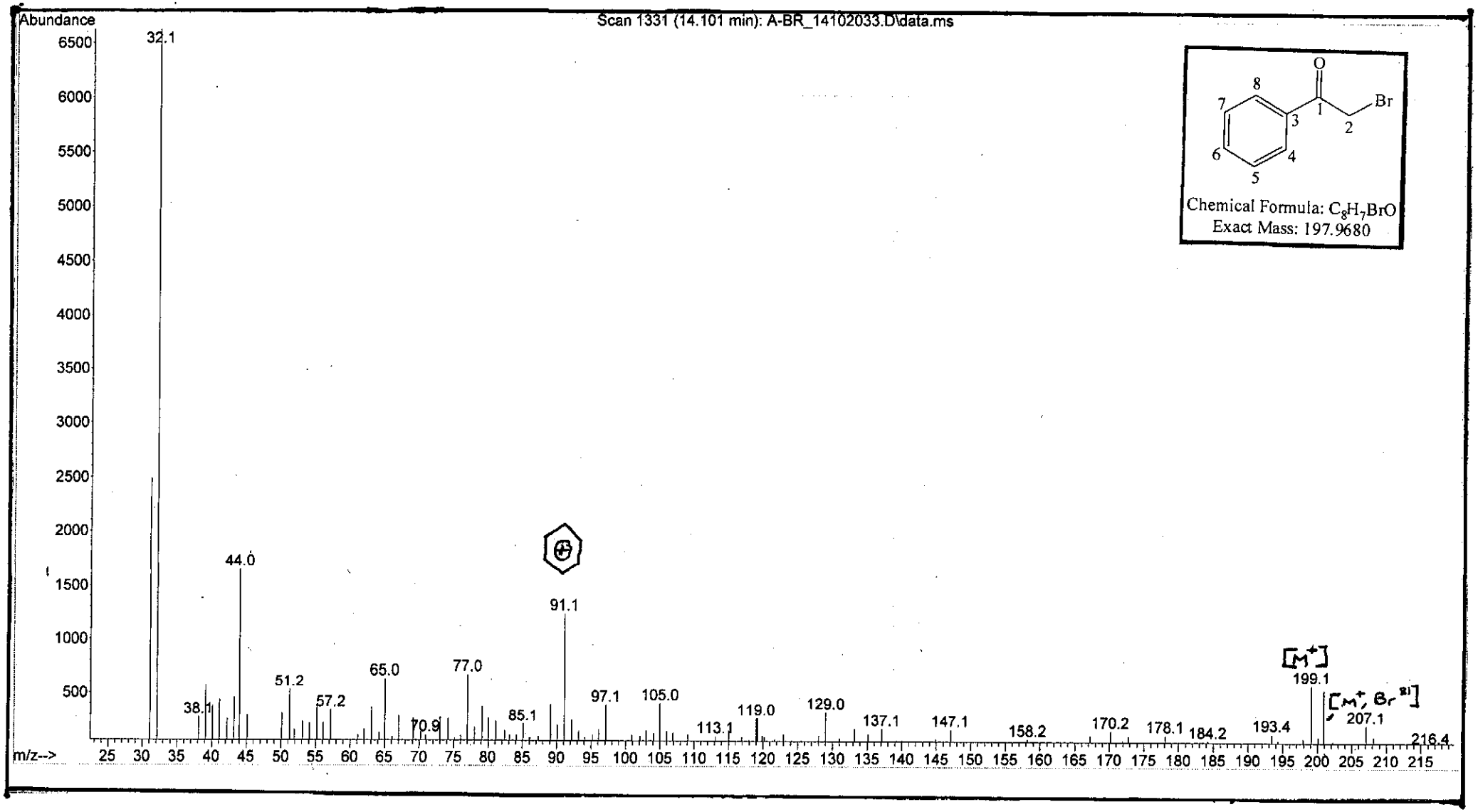

Mass spectrum of compound 1, 2-bromo-1-phenylethanone

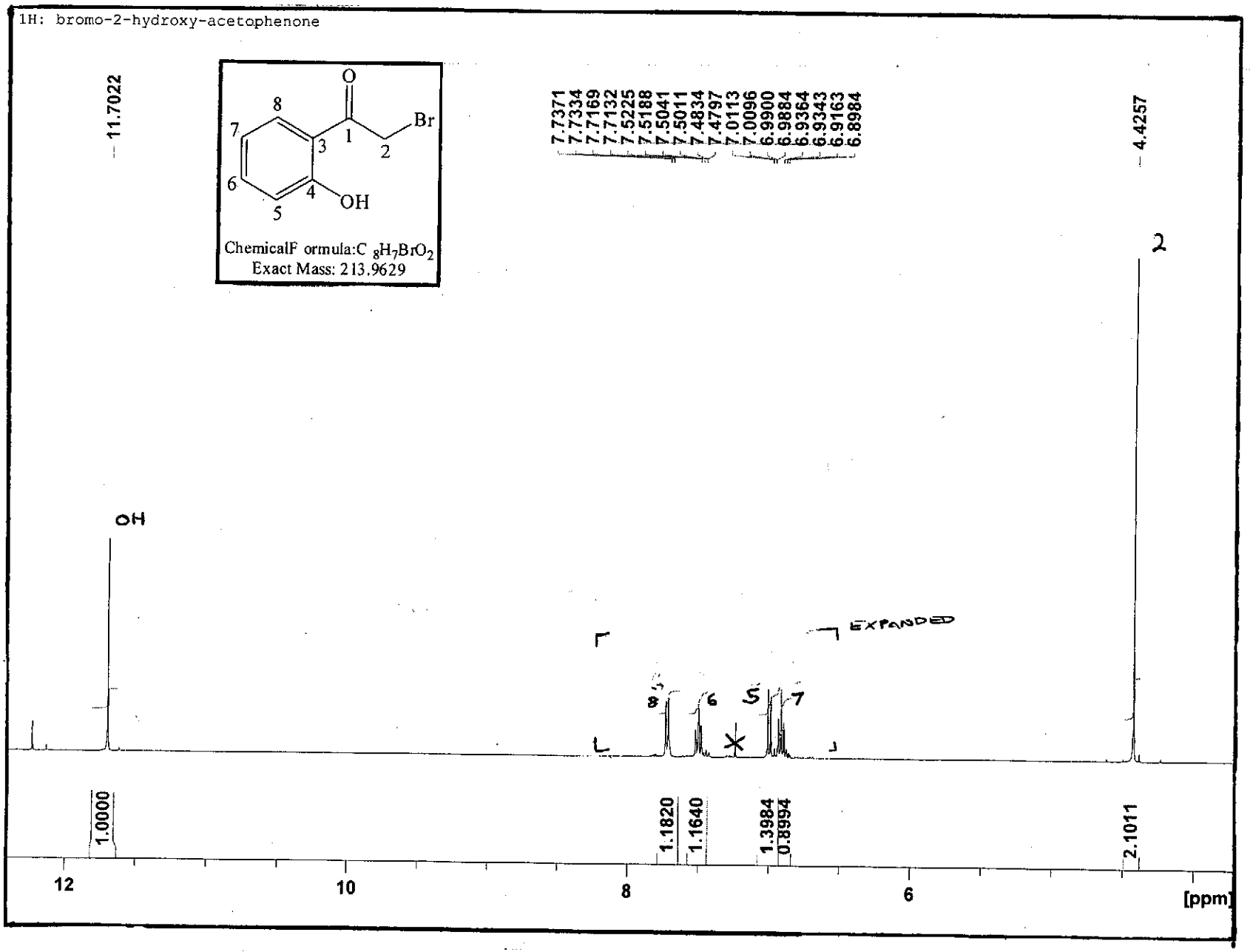

^{1}H NMR spectrum of compound 2, 2-bromo-1-(2-hydroxy-phenyl) ethanone

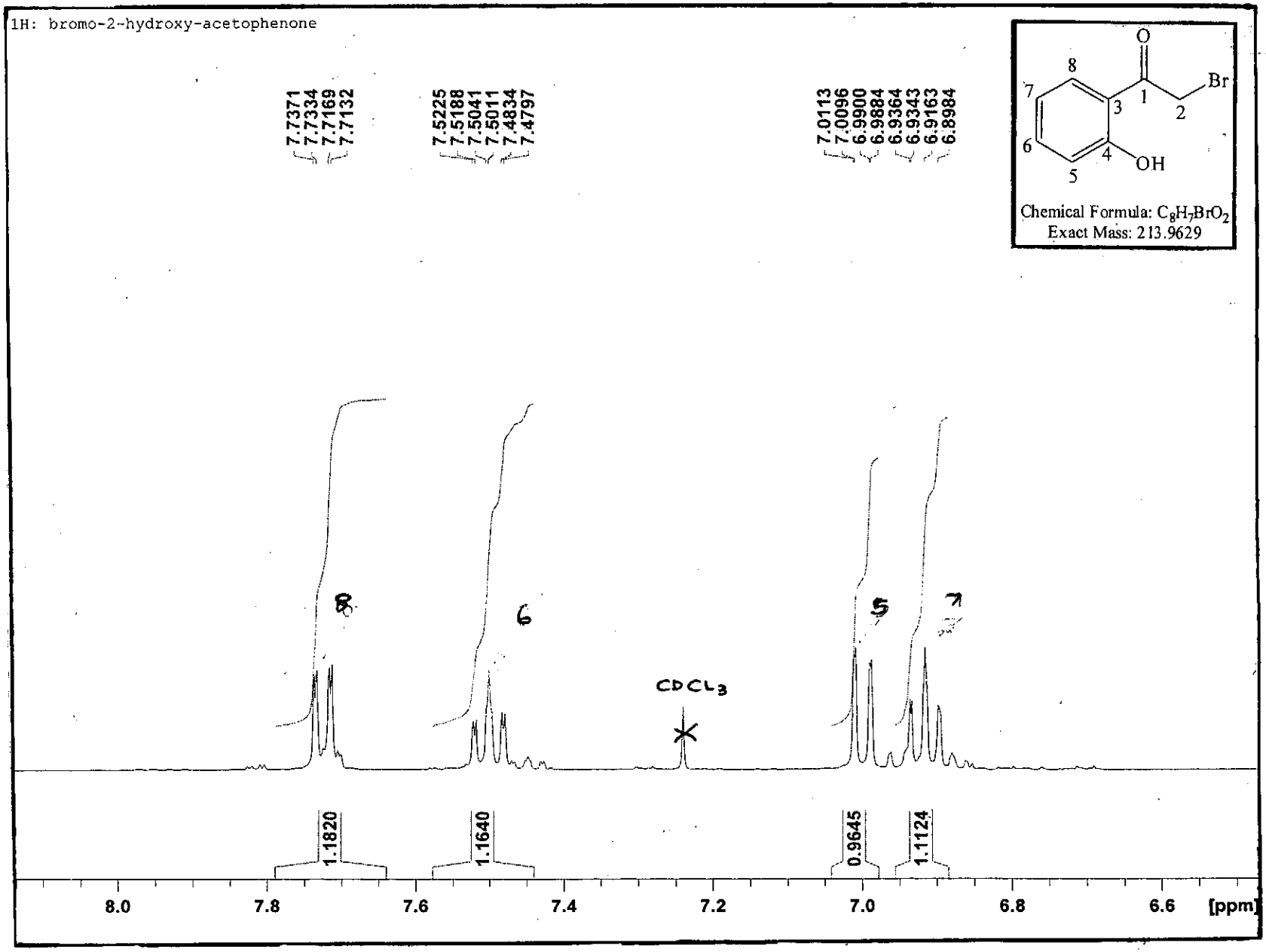

^{1}H NMR spectrum of compound 2, 2-bromo-1-(2-hydroxy-phenyl) ethanone

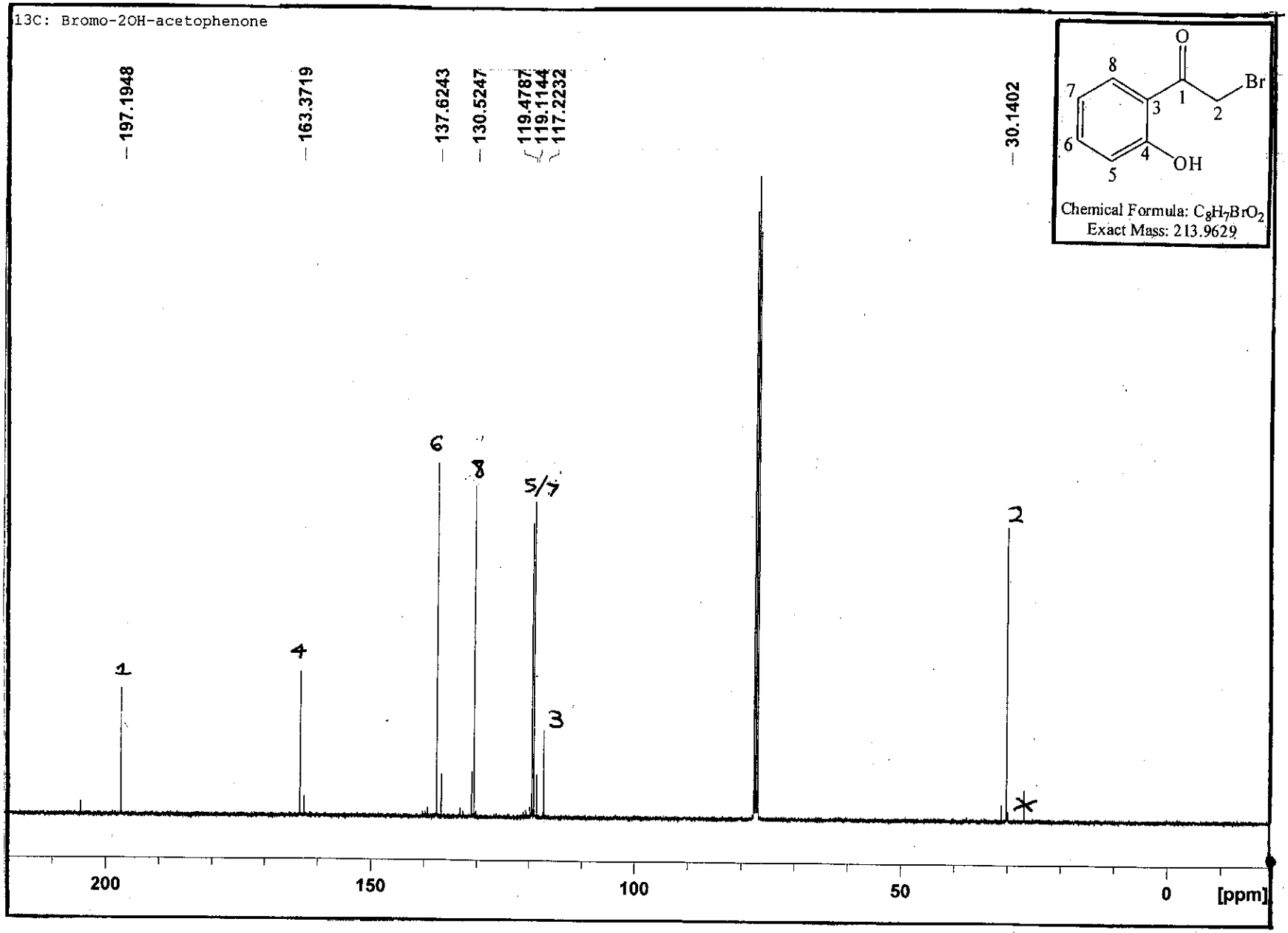

^{13}C NMR of compound 2, 2-bromo-1-(2-hydroxy-phenyl) ethanone

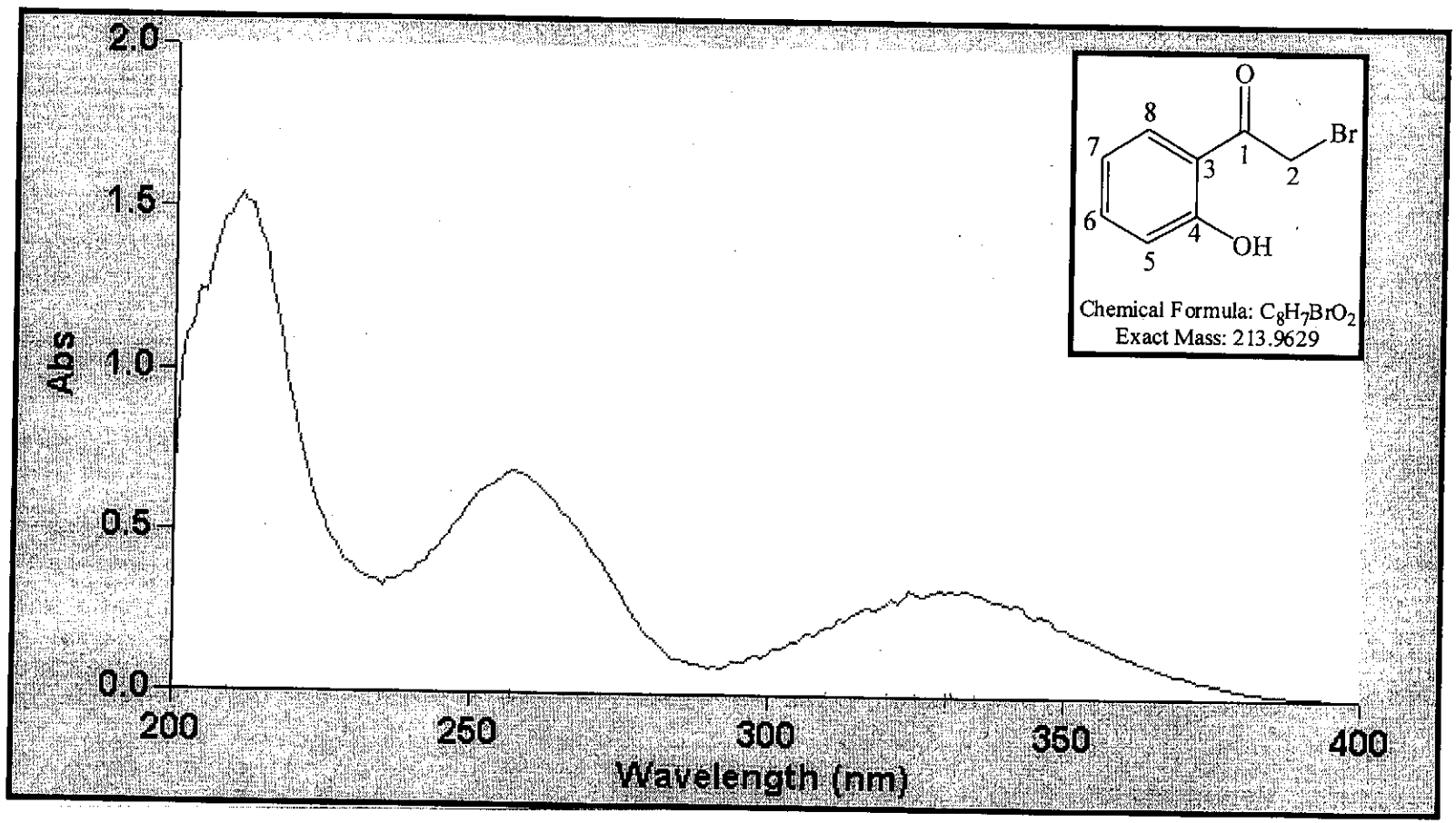

Ultra Violet spectrum of compound 2, 2-bromo-1-(2-hydroxyphenyl)ethanone

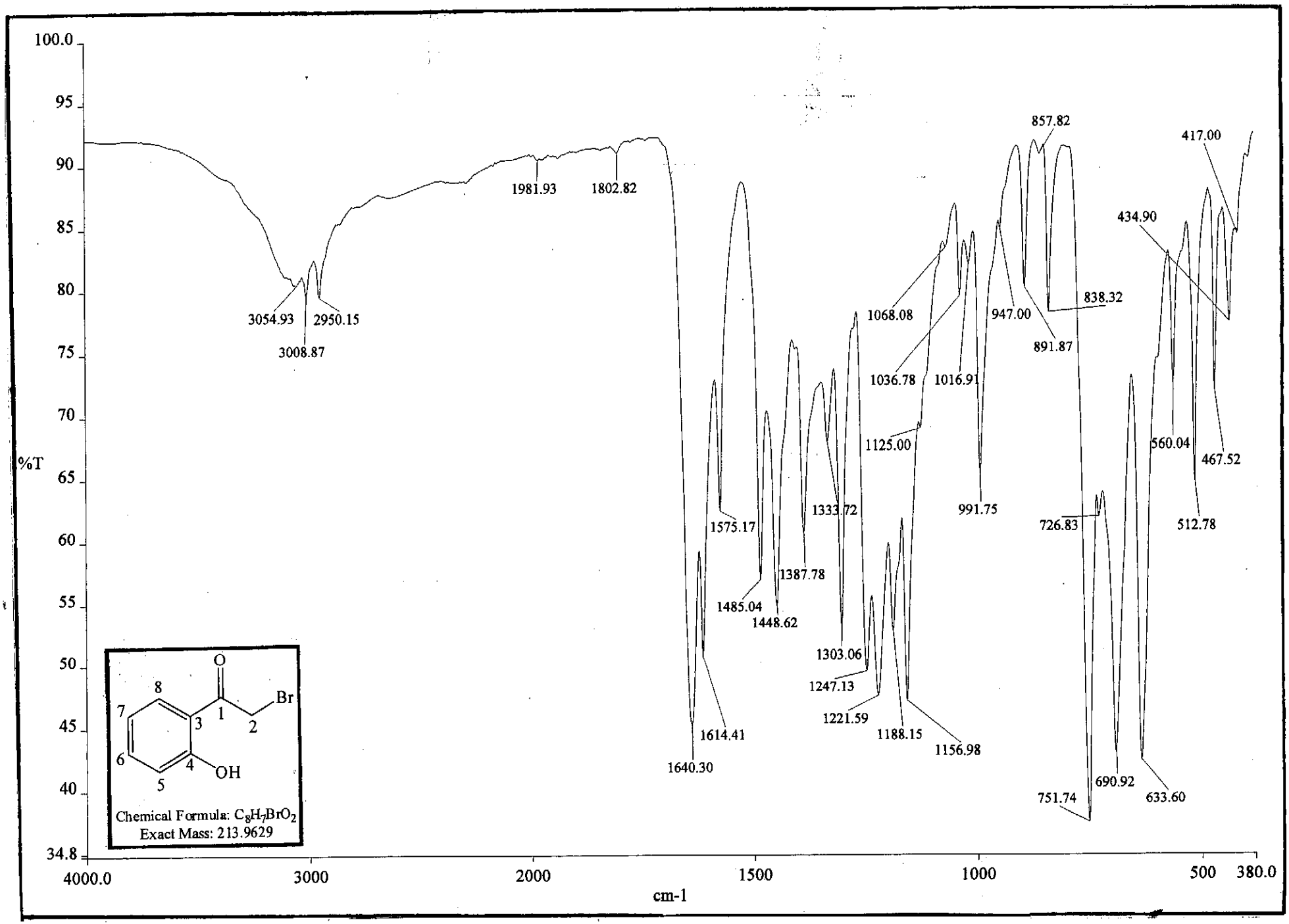

Infrared spectrum of compound 2, 2-bromo-1-(2-hydroxy-phenyl) ethanone

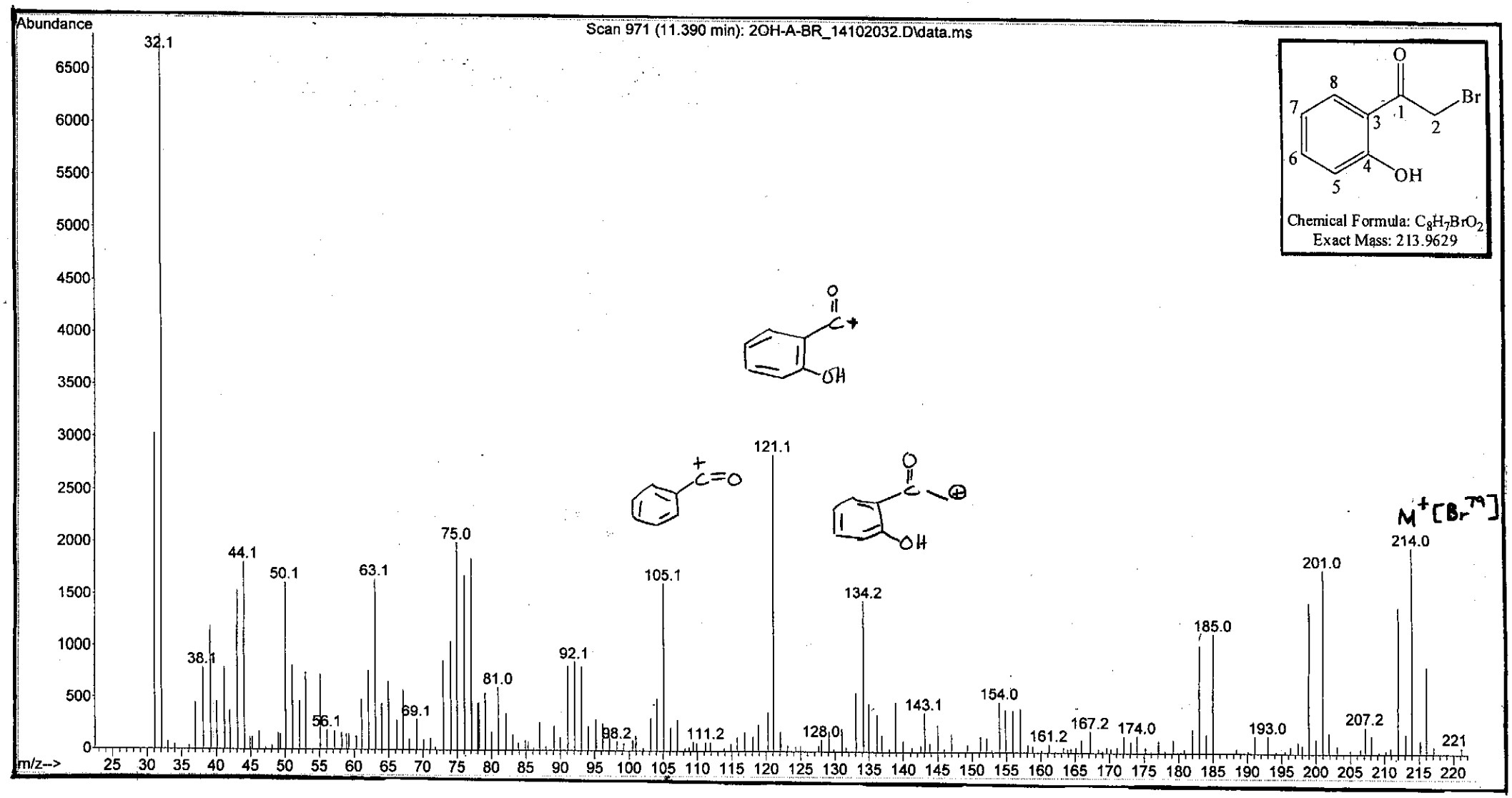

Mass spectrum of compound 2, 2-bromo-1-(2-hydroxy-phenyl) ethanone

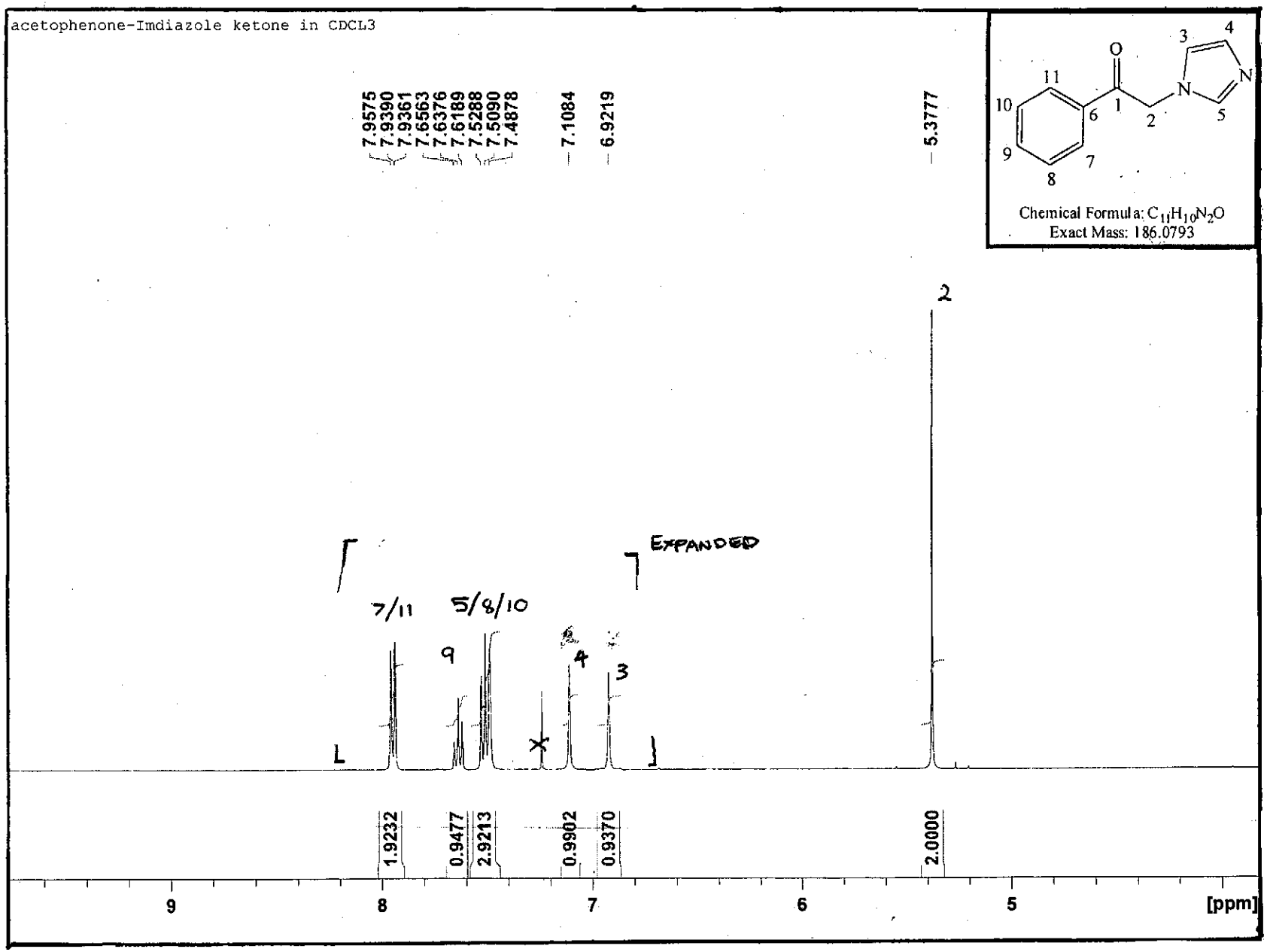

^{1}H NMR spectrum of compound 3, 2-Imidazol-1-yl-1-phenyl ethanone

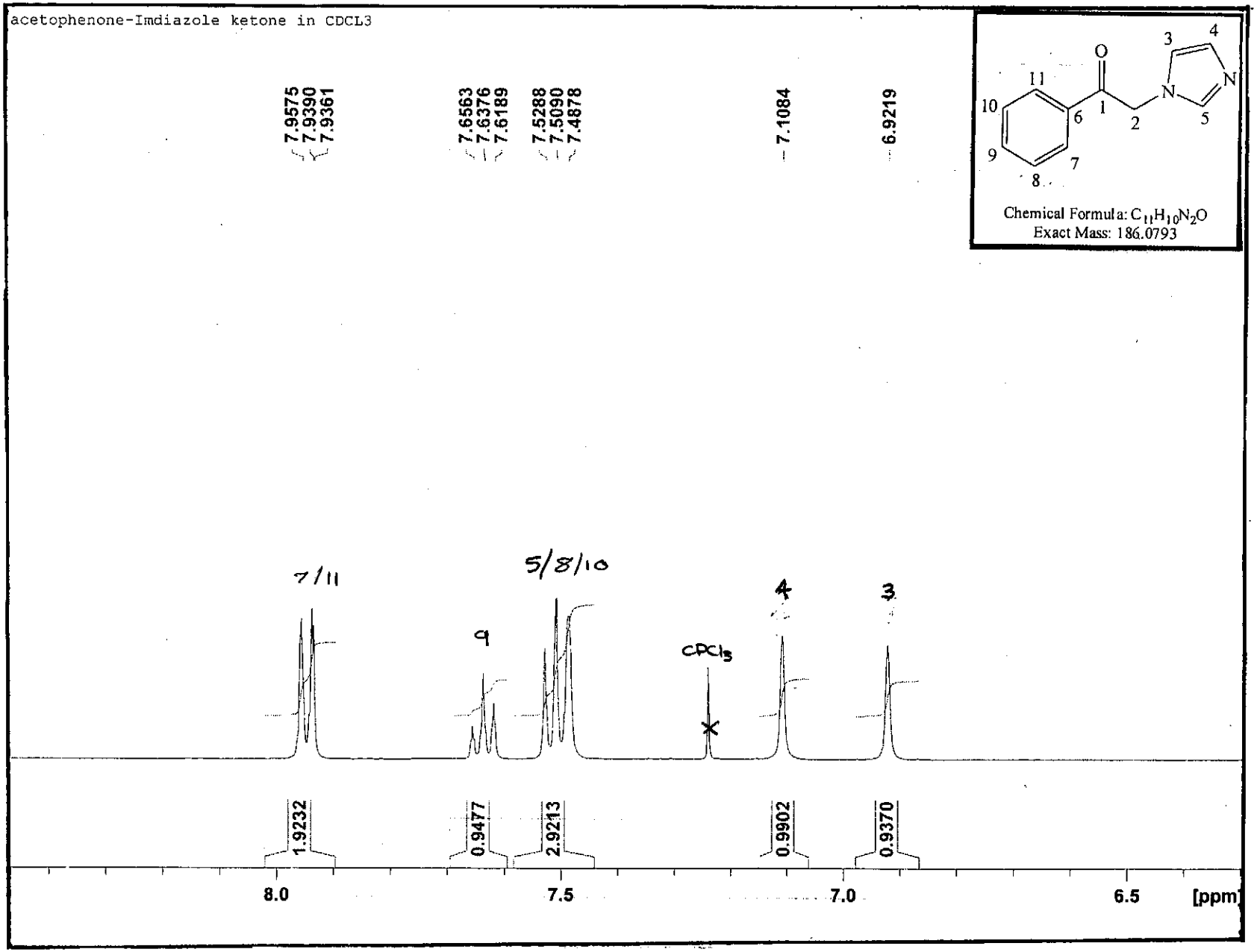

^{1}H NMR spectrum of compound 3, 2-Imidazol-1-yl-1-phenyl ethanone

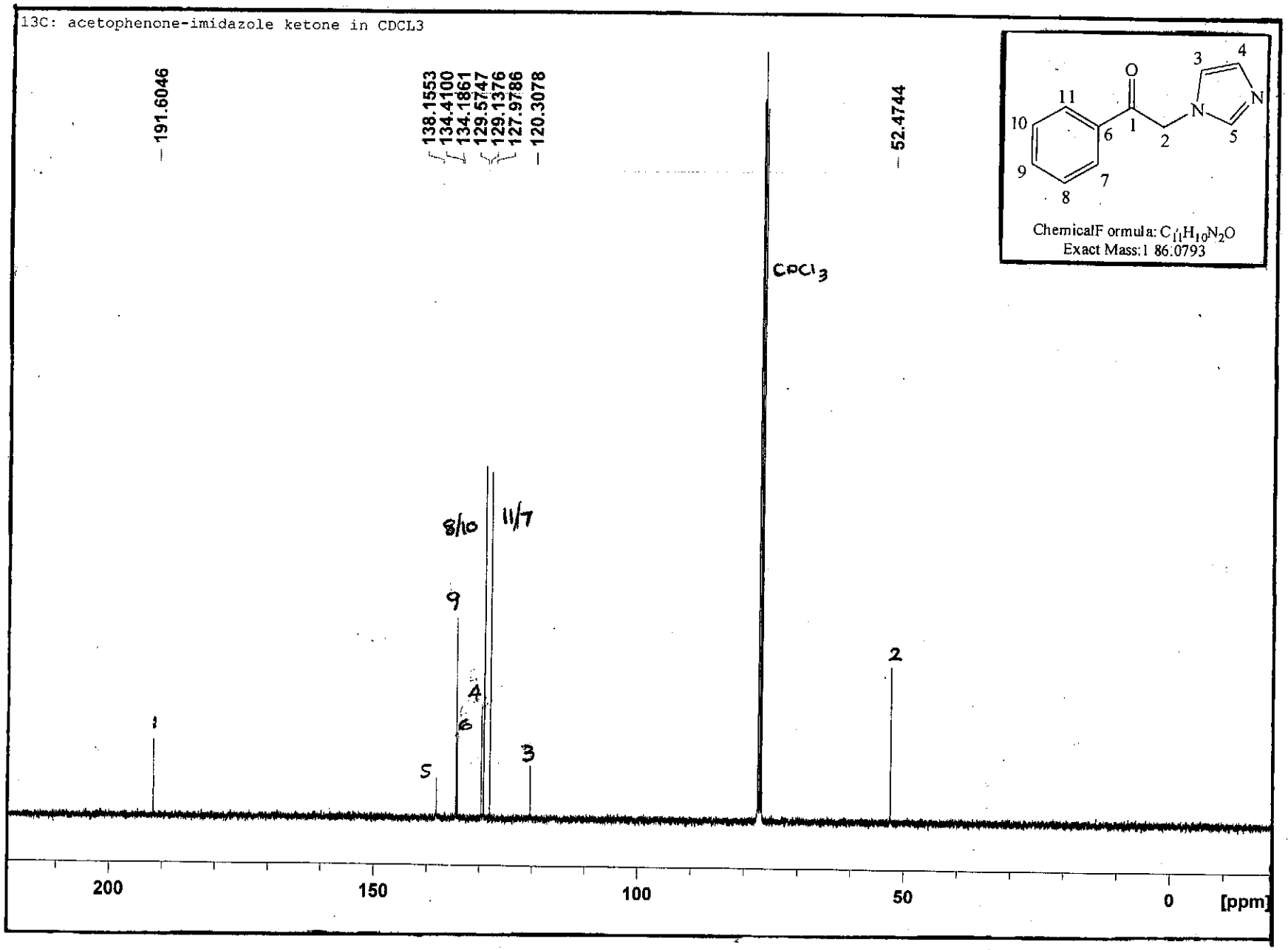

^{13}C NMR of compound 3, 2-Imidazol-1-yl-1-phenyl ethanone

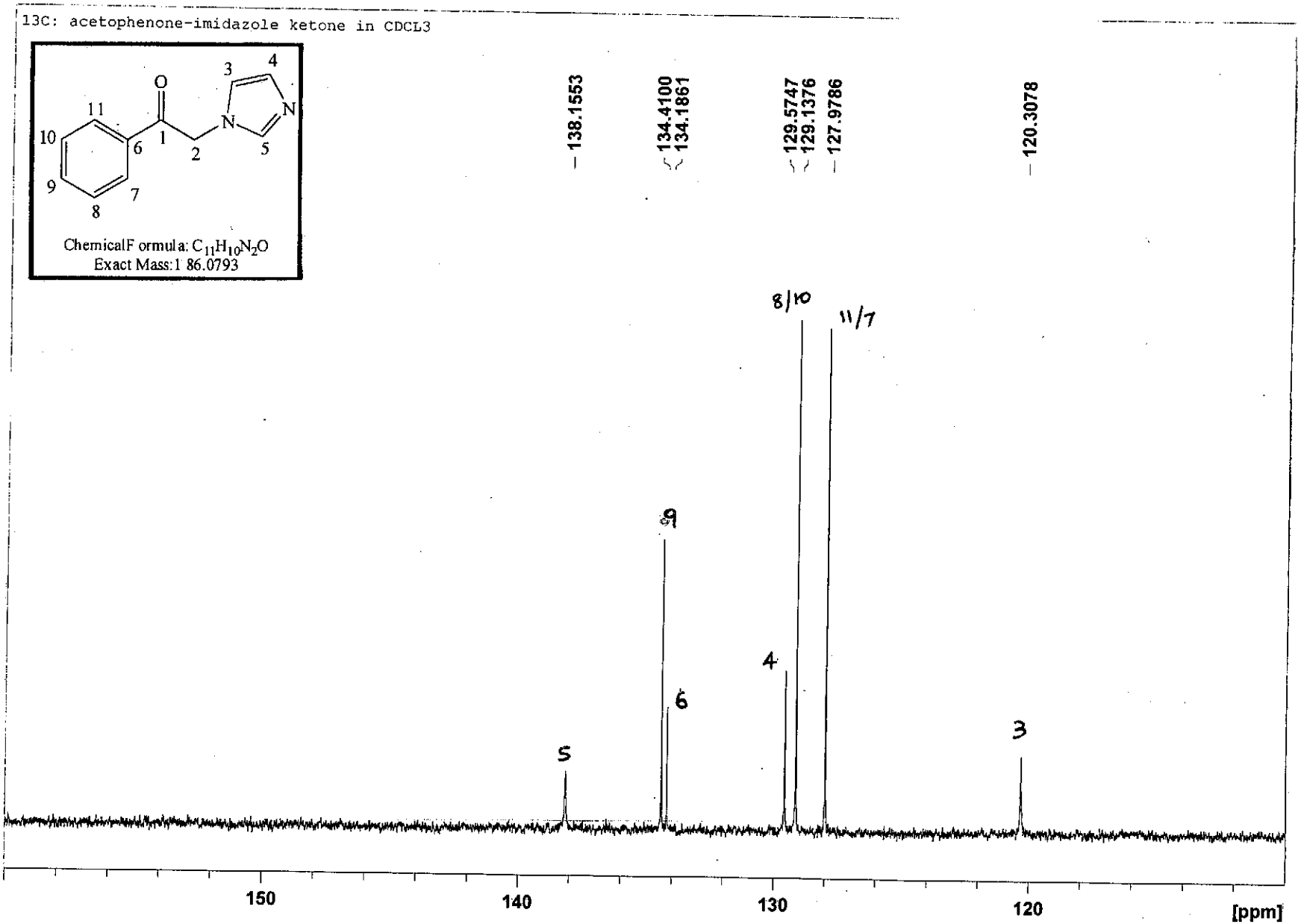

^{13}C NMR of compound 3, 2-Imidazol-1-yl-1-phenyl ethanone

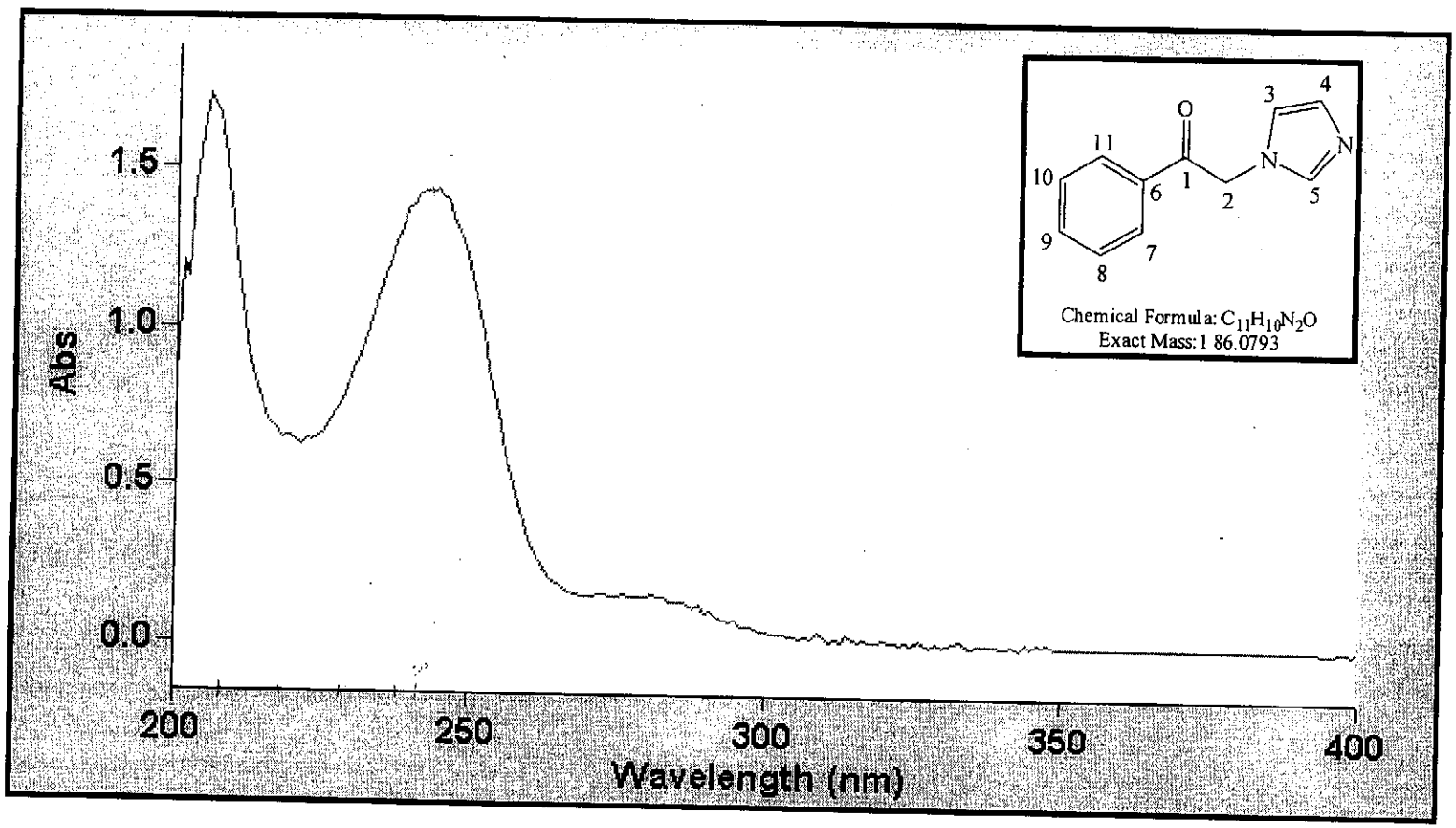

Ultra Violet spectrum of compound 3, 2-(1H-imidazol-1-yl)-1-phenylethanone

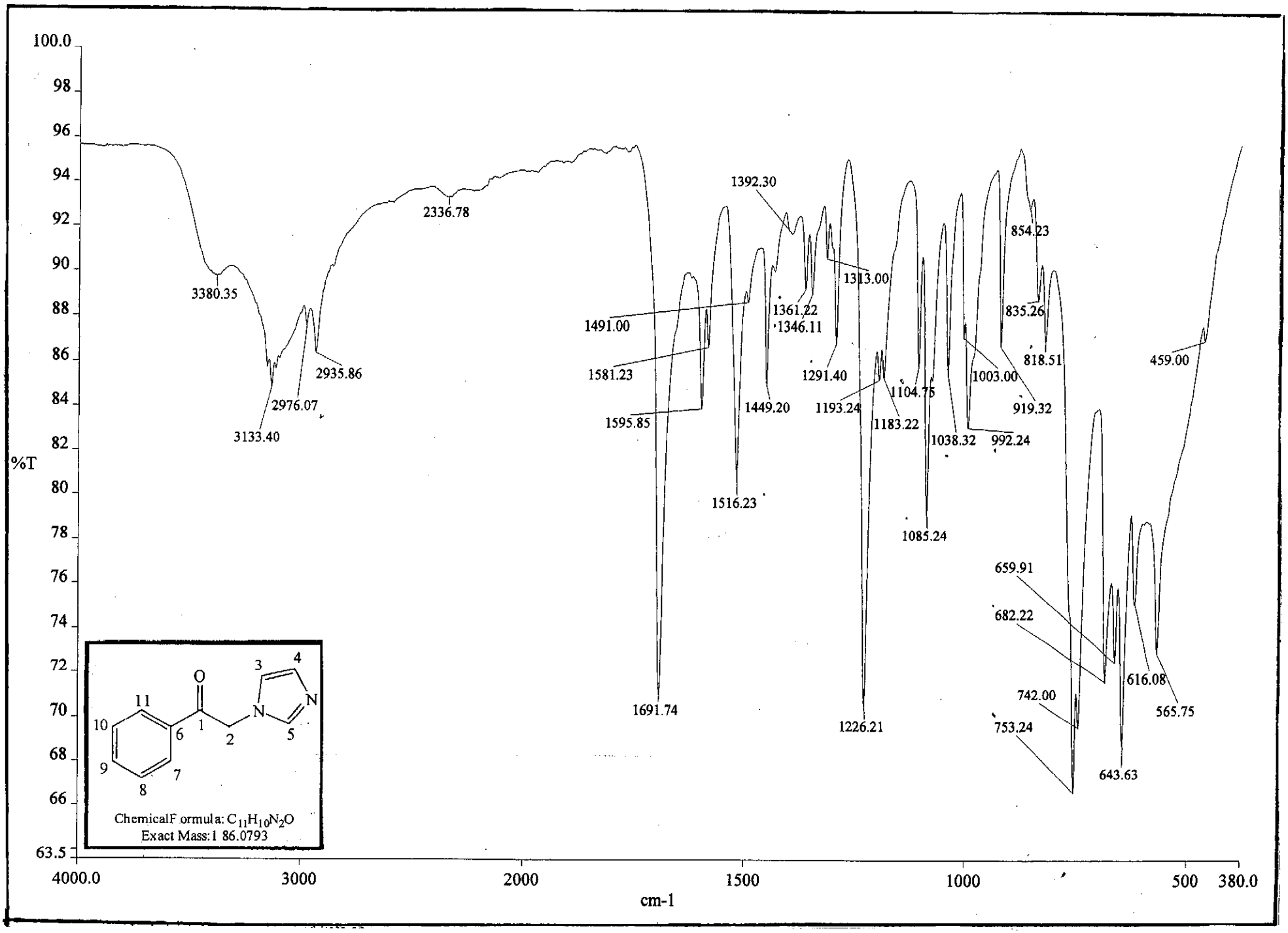

Infrared spectrum of compound 3, 2-Imidazol-1-yl-1-phenyl ethanone

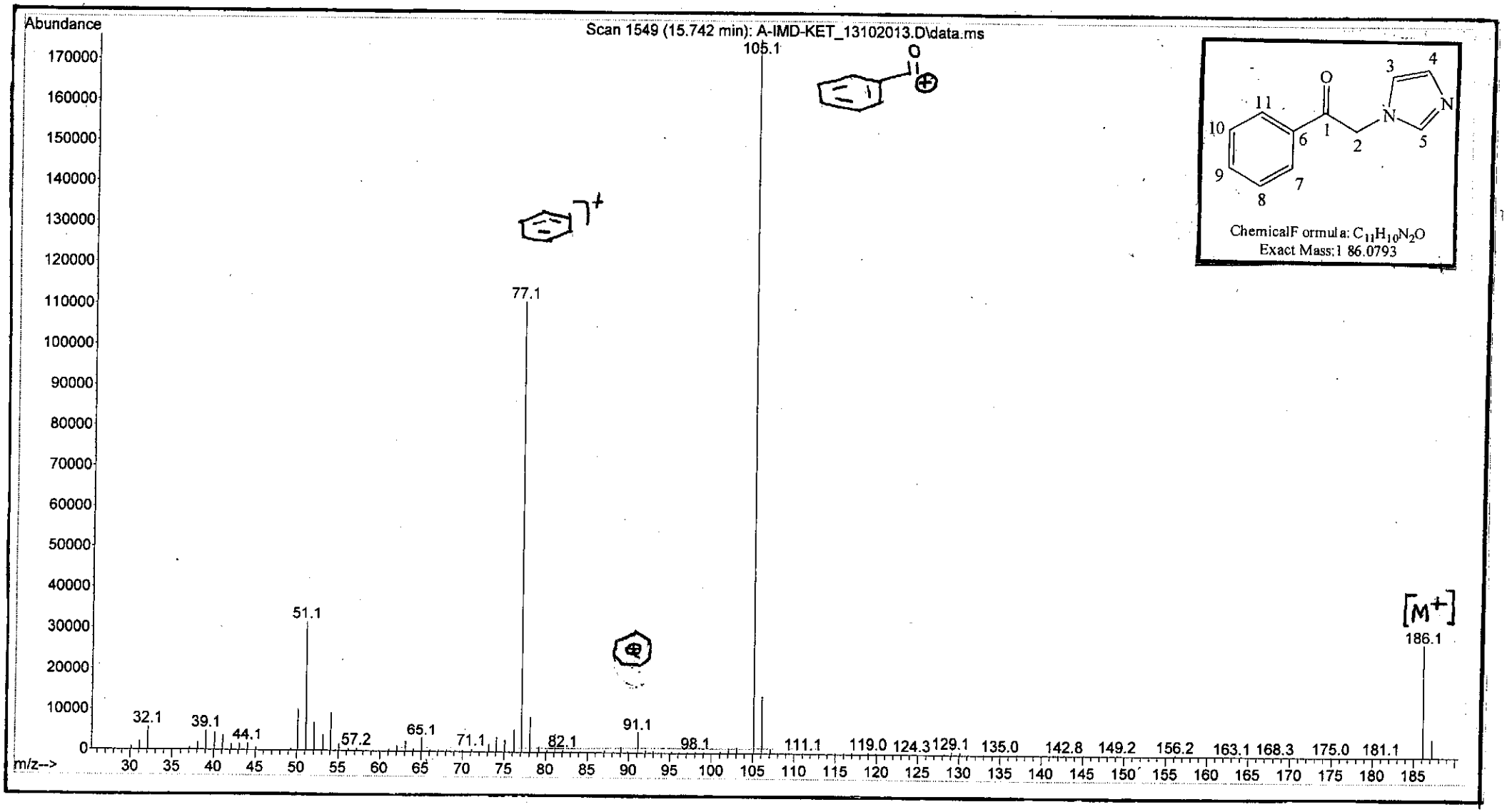

Mass spectrum of compound 3, 2-Imidazol-1-yl-1-phenyl ethanone

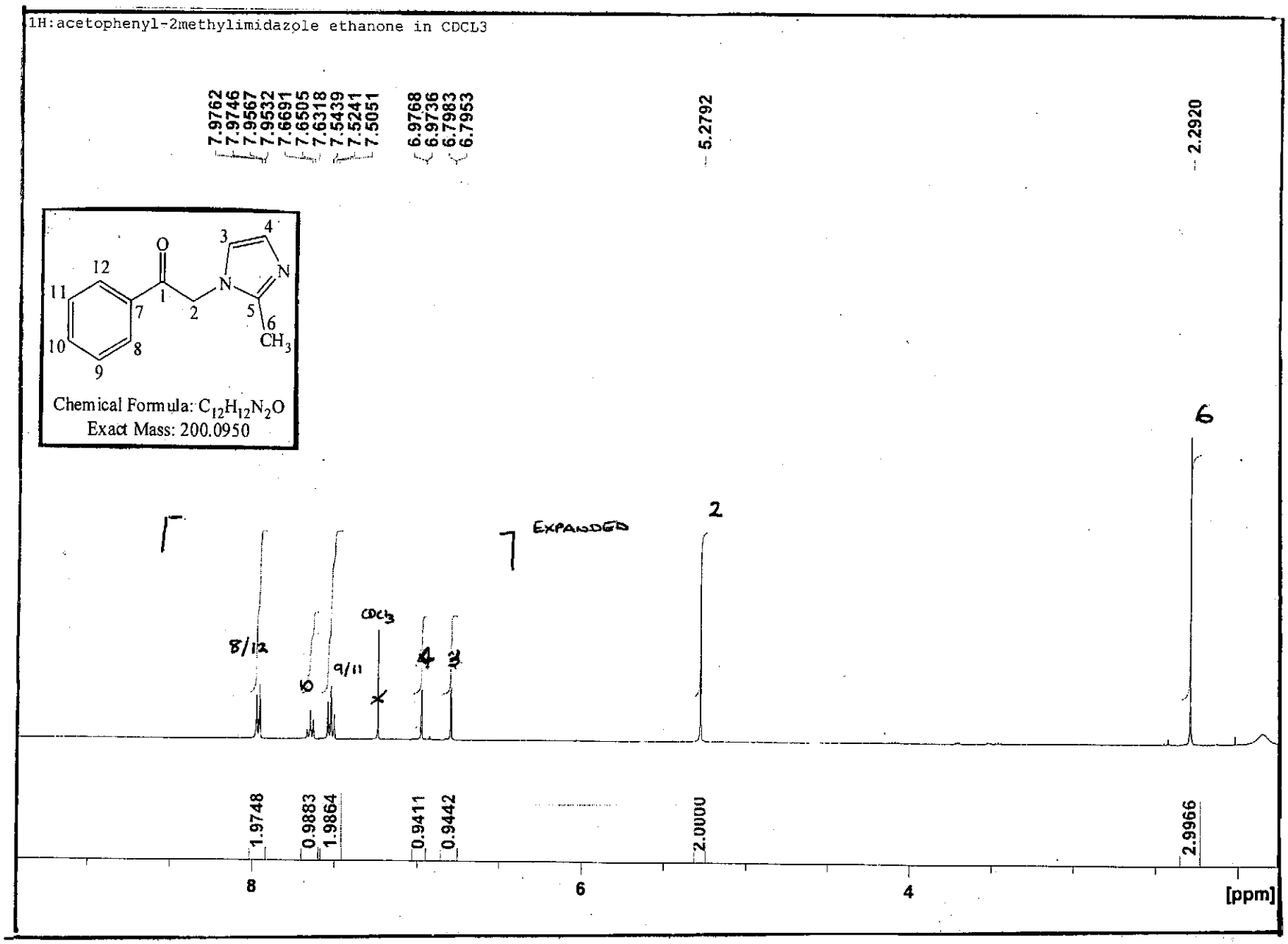

^{1}H NMR spectrum of compound 4, 2-(5-methyl-1H-imidazol-1-yl)-1-phenylethanone

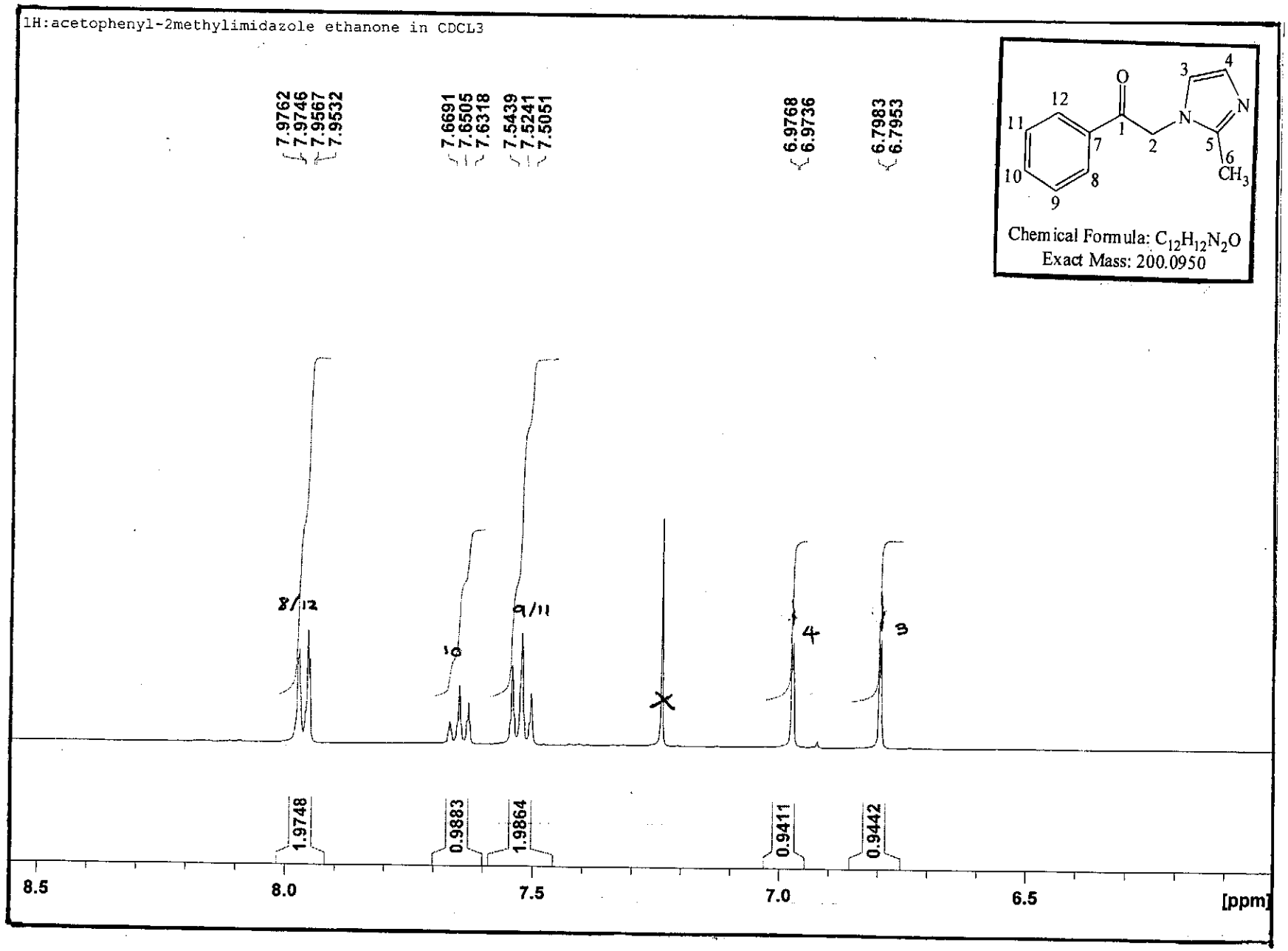

^{1}H NMR spectrum of compound 4, 2-(5-methyl-1H-imidazol-1-yl)-1-phenylethanone

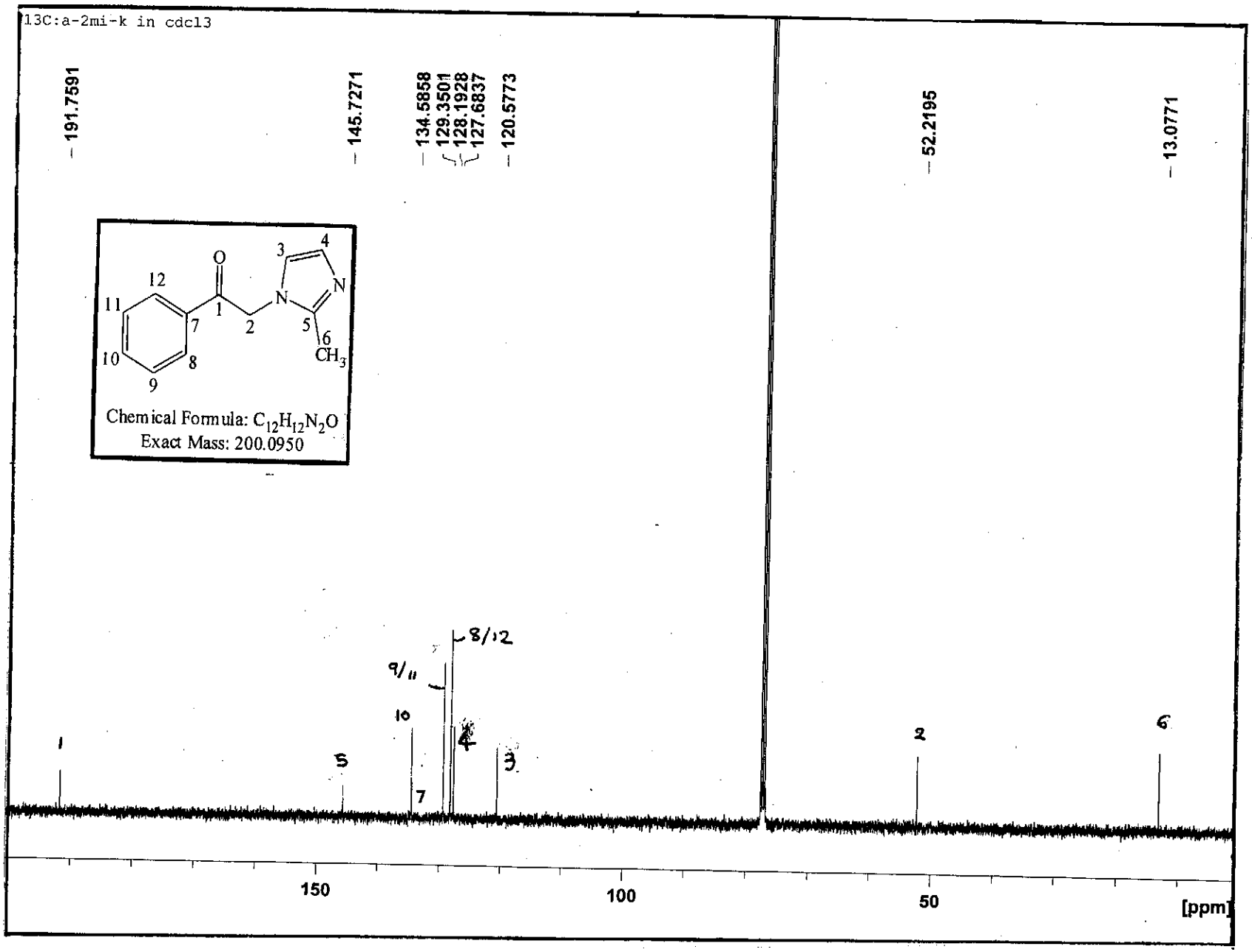

^{13}C NMR of compound 4, 2-(5-methyl-1H-imidazol-1-yl)-1-phenylethanone

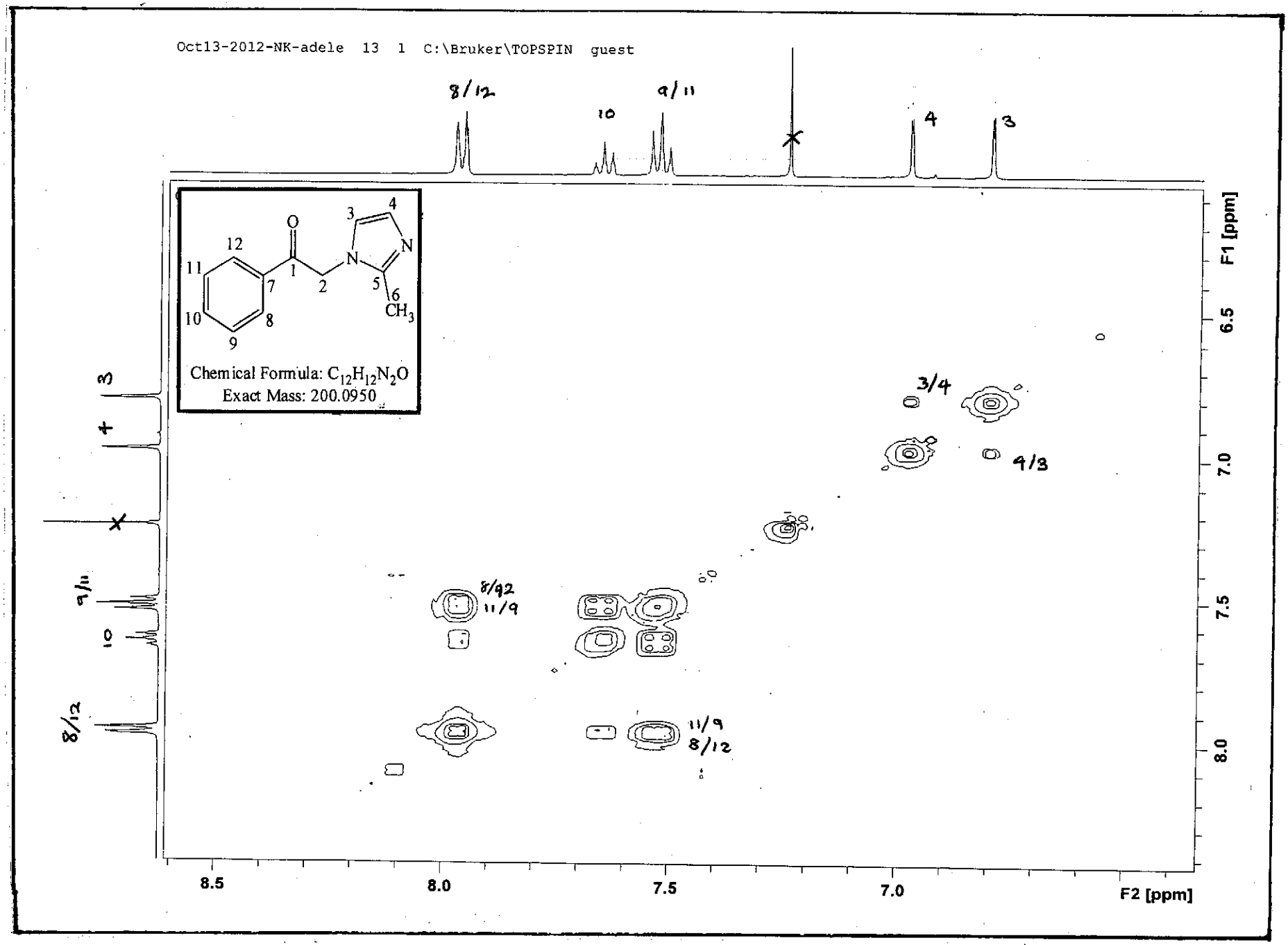

COSY spectrum of compound 4, 2-(5-methyl-1H-imidazol-1-yl)-1-phenylethanone

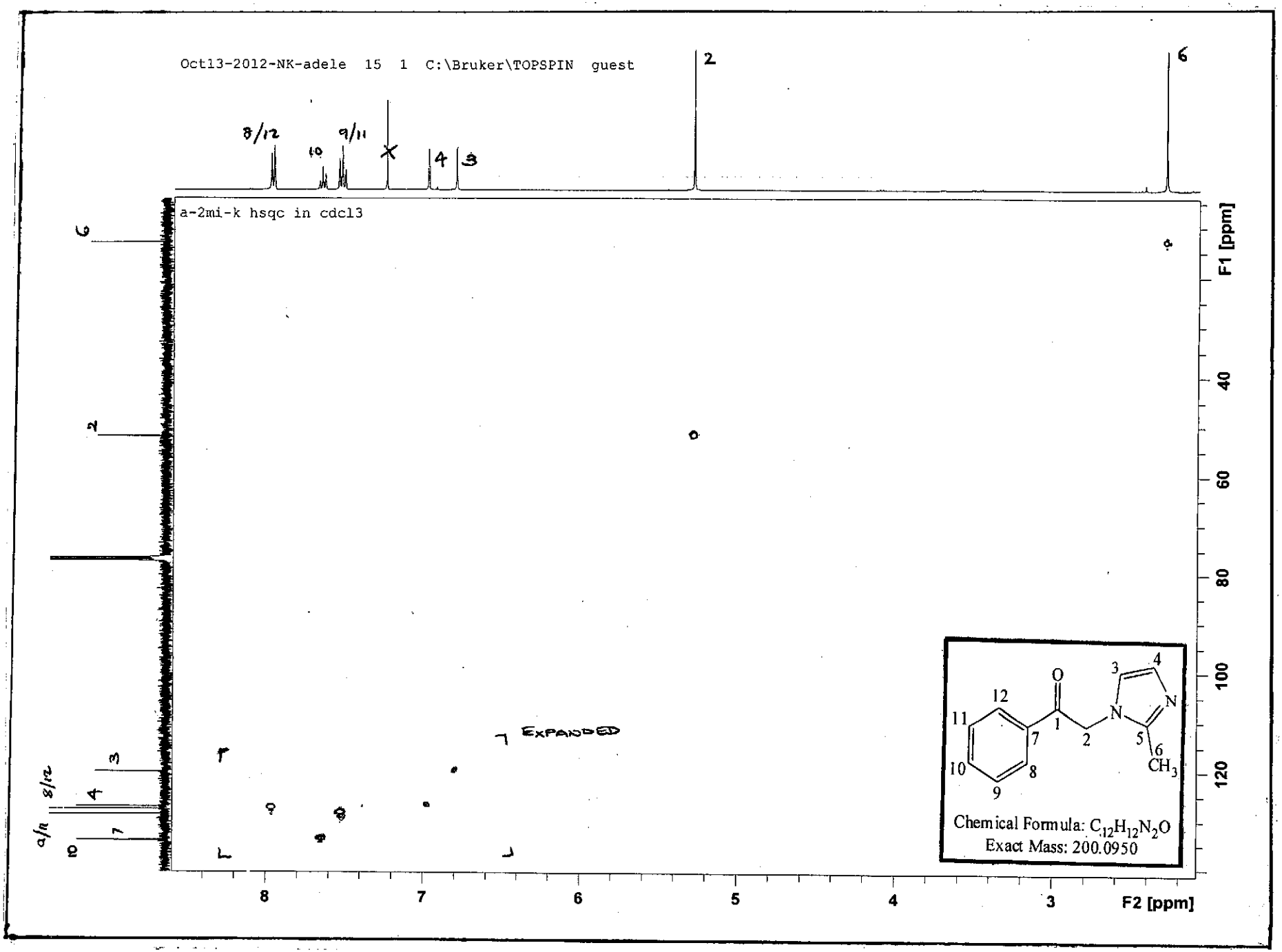

HSQC spectrum of compound 4, 2-(5-methyl-1H-imidazol-1-yl)-1-phenylethanone

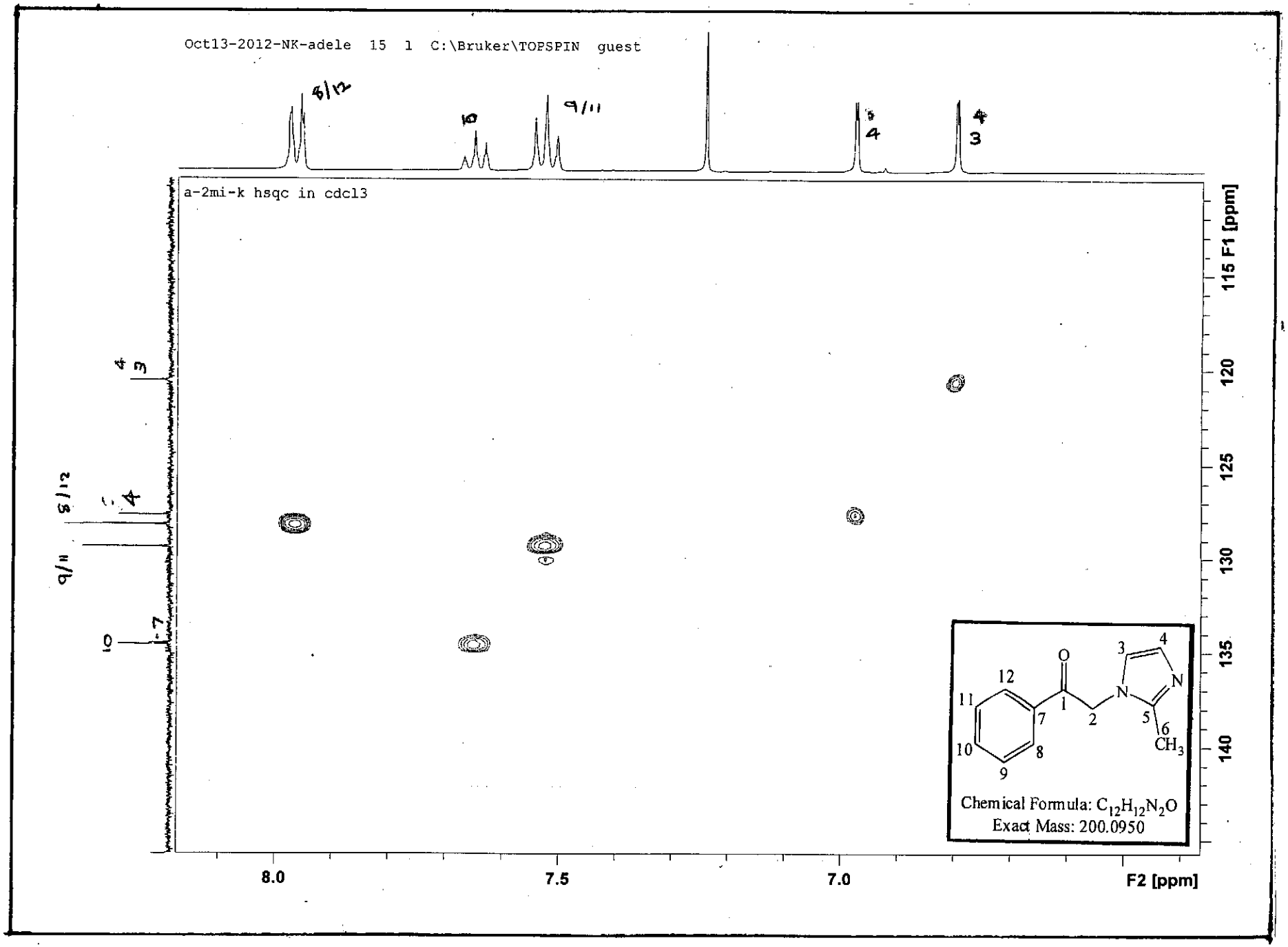

HSQC spectrum of compound 4', 2-(5-methyl-1H-imidazol-1-yl)-1-phenylethanone

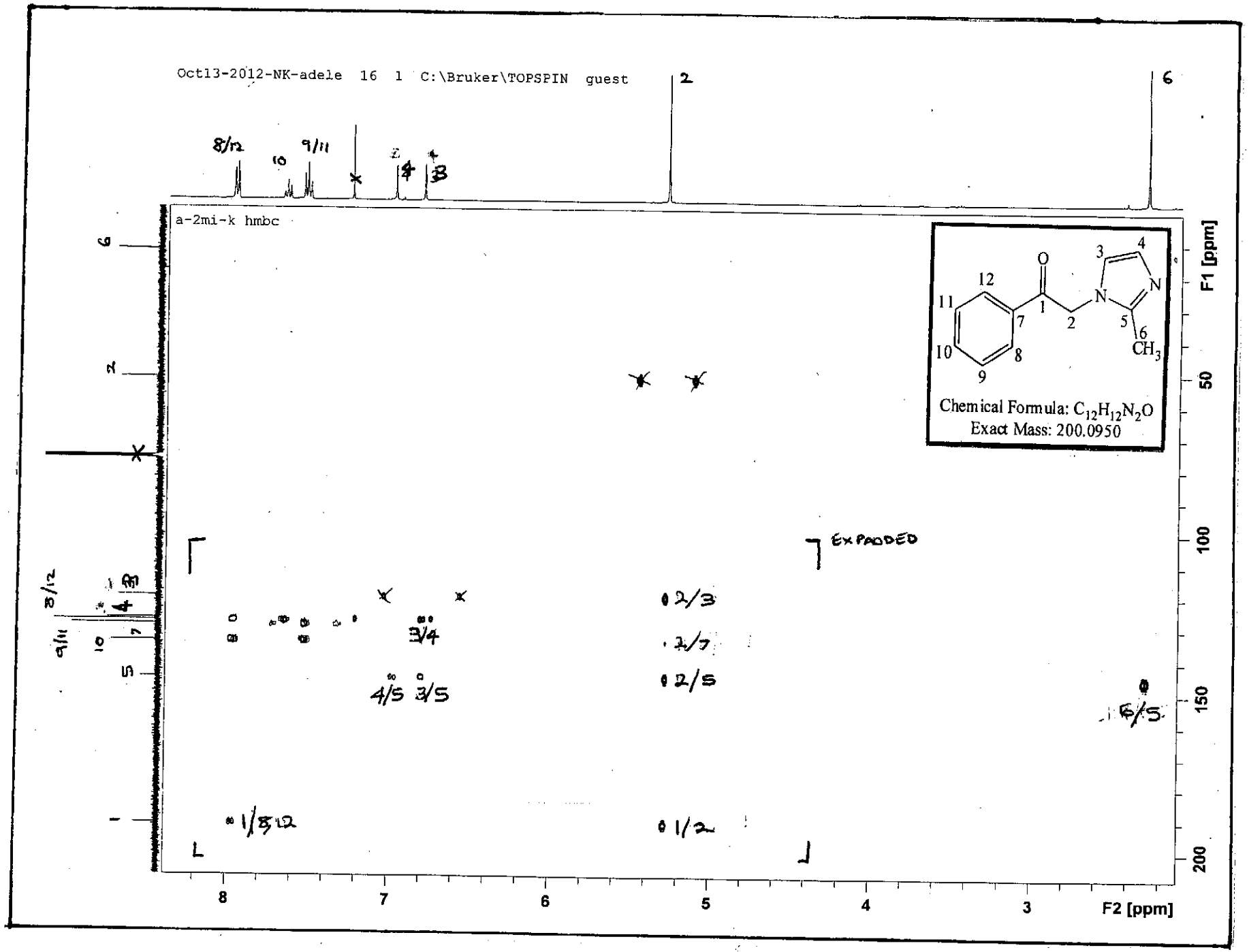

HMBC spectrum of compound 4, 2-(5-methyl-1H-imidazol-1-yl)-1-phenylethanone

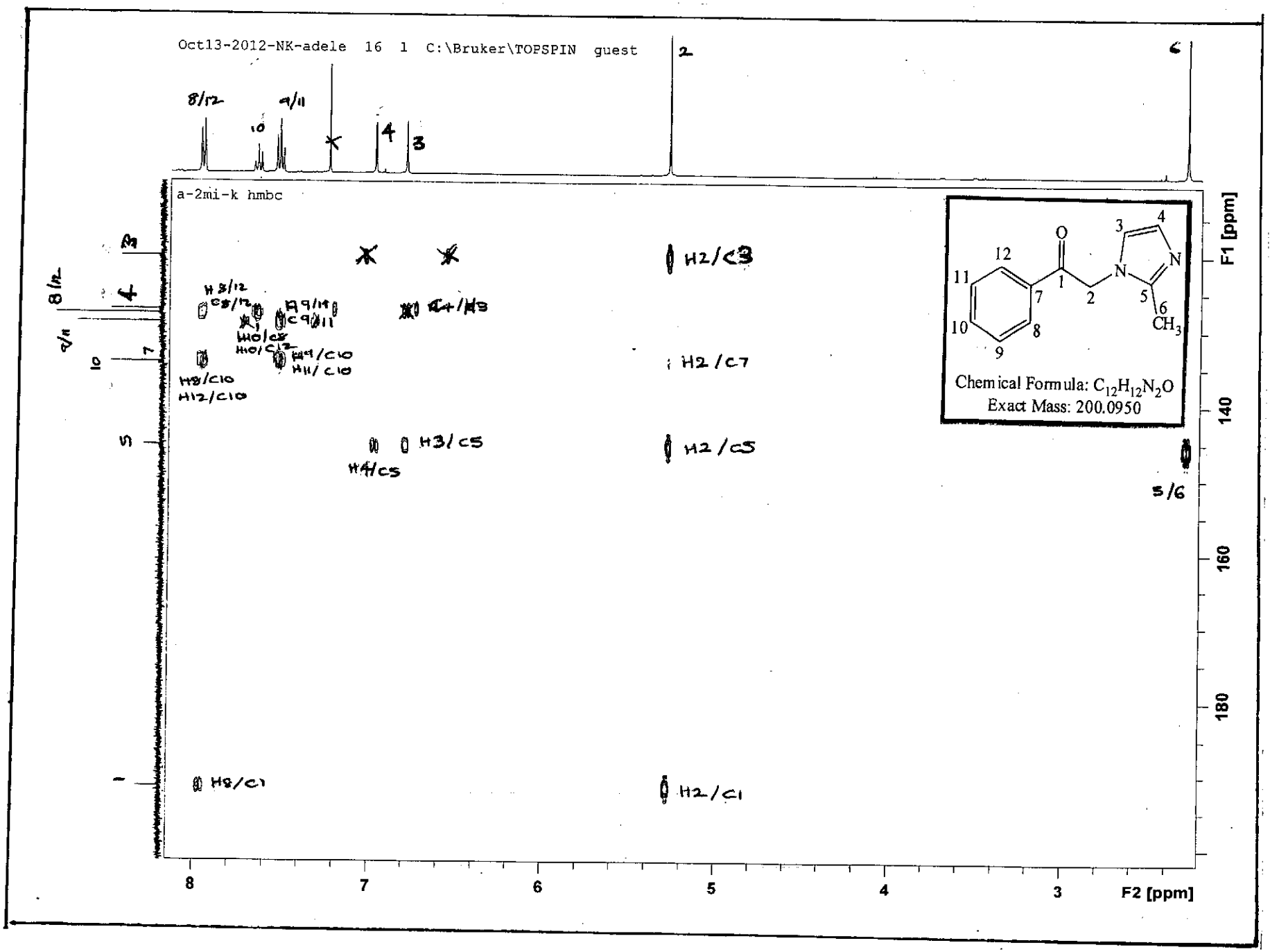

HMBC spectrum of compound 4, 2-(5-methyl-1H-imidazol-1-yl)-1-phenylethanone

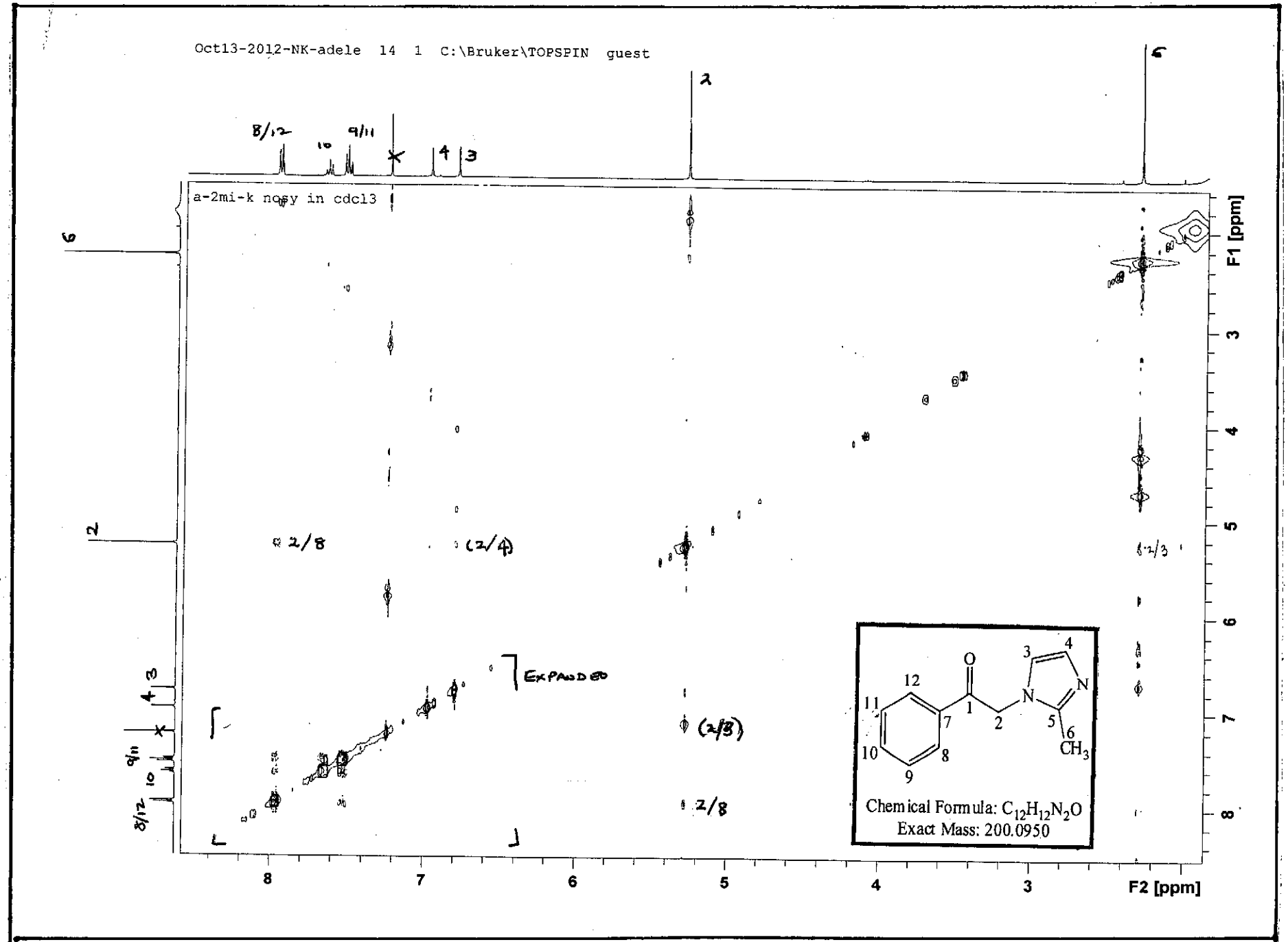

NOESY spectrum of compound 4, 2-(5-methyl-1H-imidazol-1-yl)-1-phenylethanone

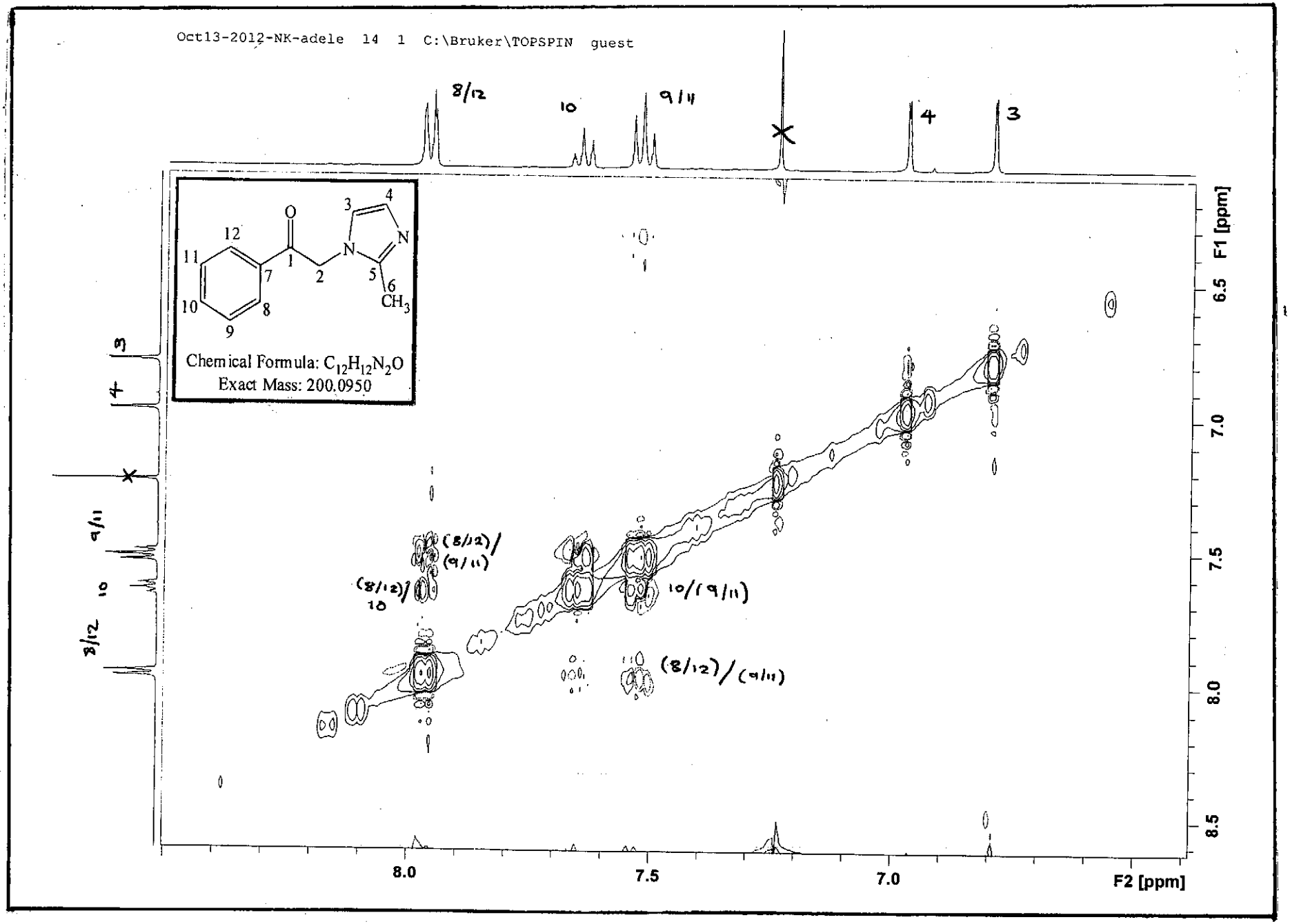

NOESY spectrum of compound 4, 2-(5-methyl-1H-imidazol-1-yl)-1-phenylethanone

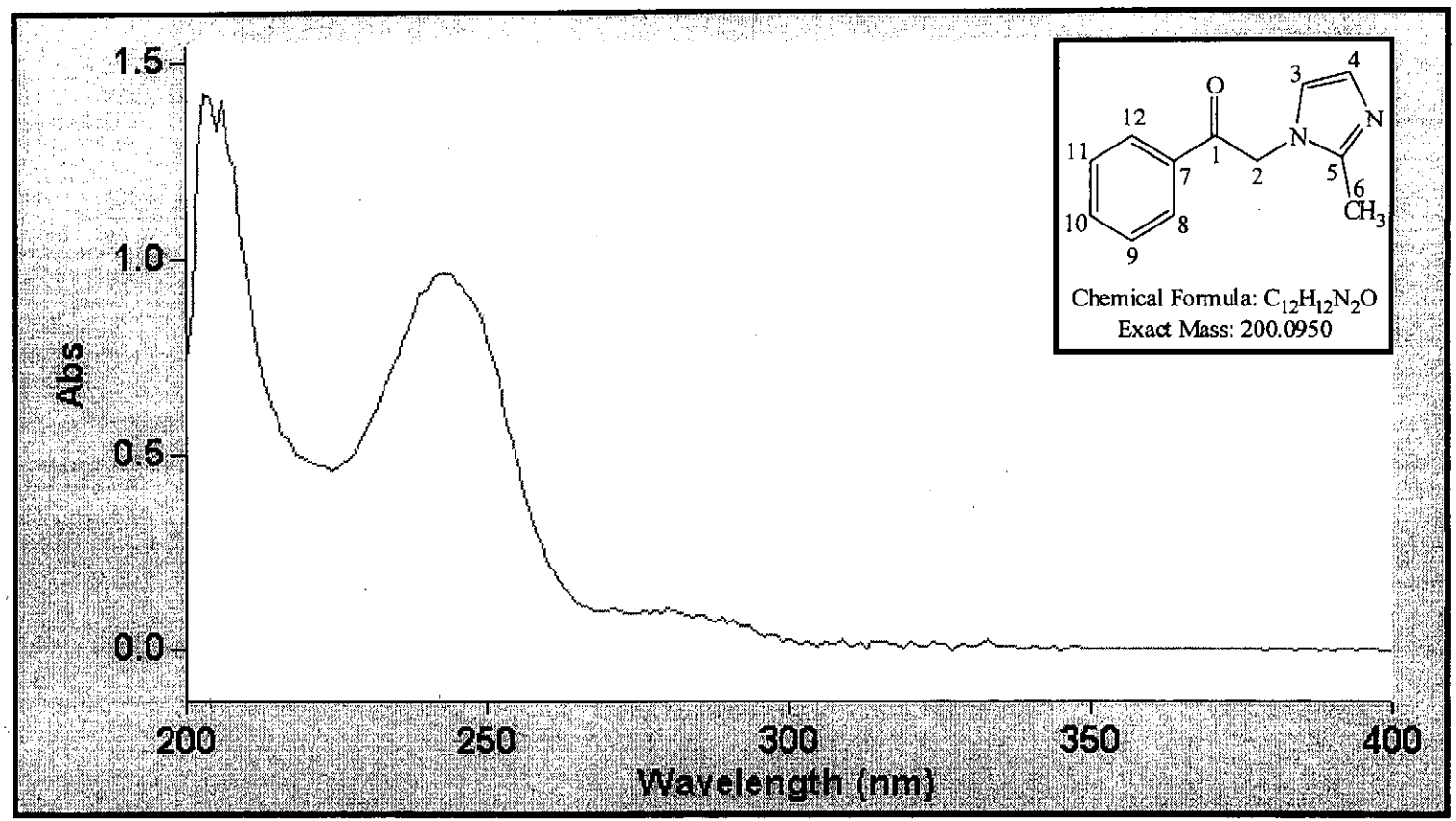

Ultra Violet spectrum of compound 4, 2-(2-methyl-1H-imidazol-1-yl)-1-phenylethanone

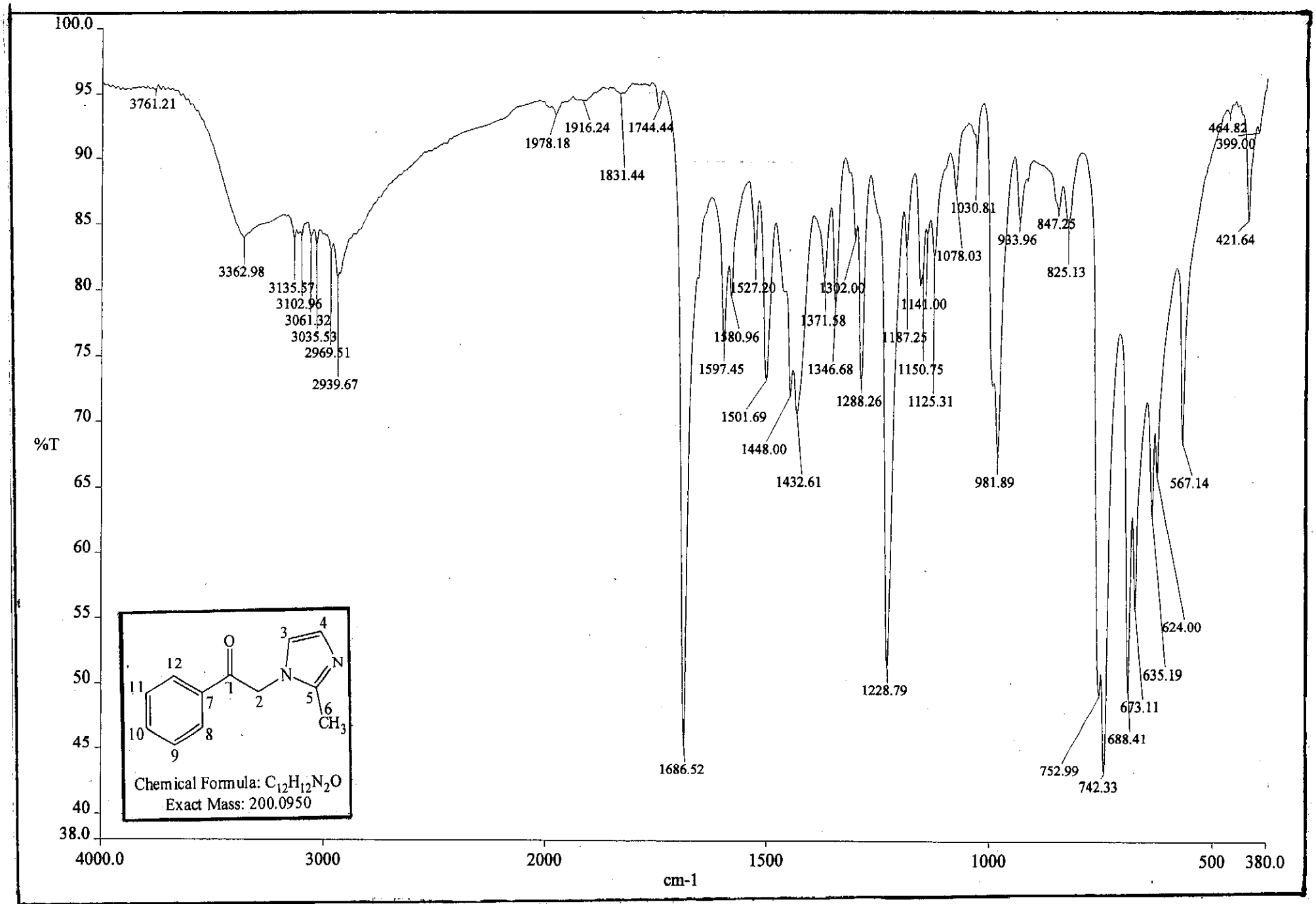

Infrared spectrum of compound 4, 2-(5-methyl-1H-imidazol-1-yl)-1-phenylethanone

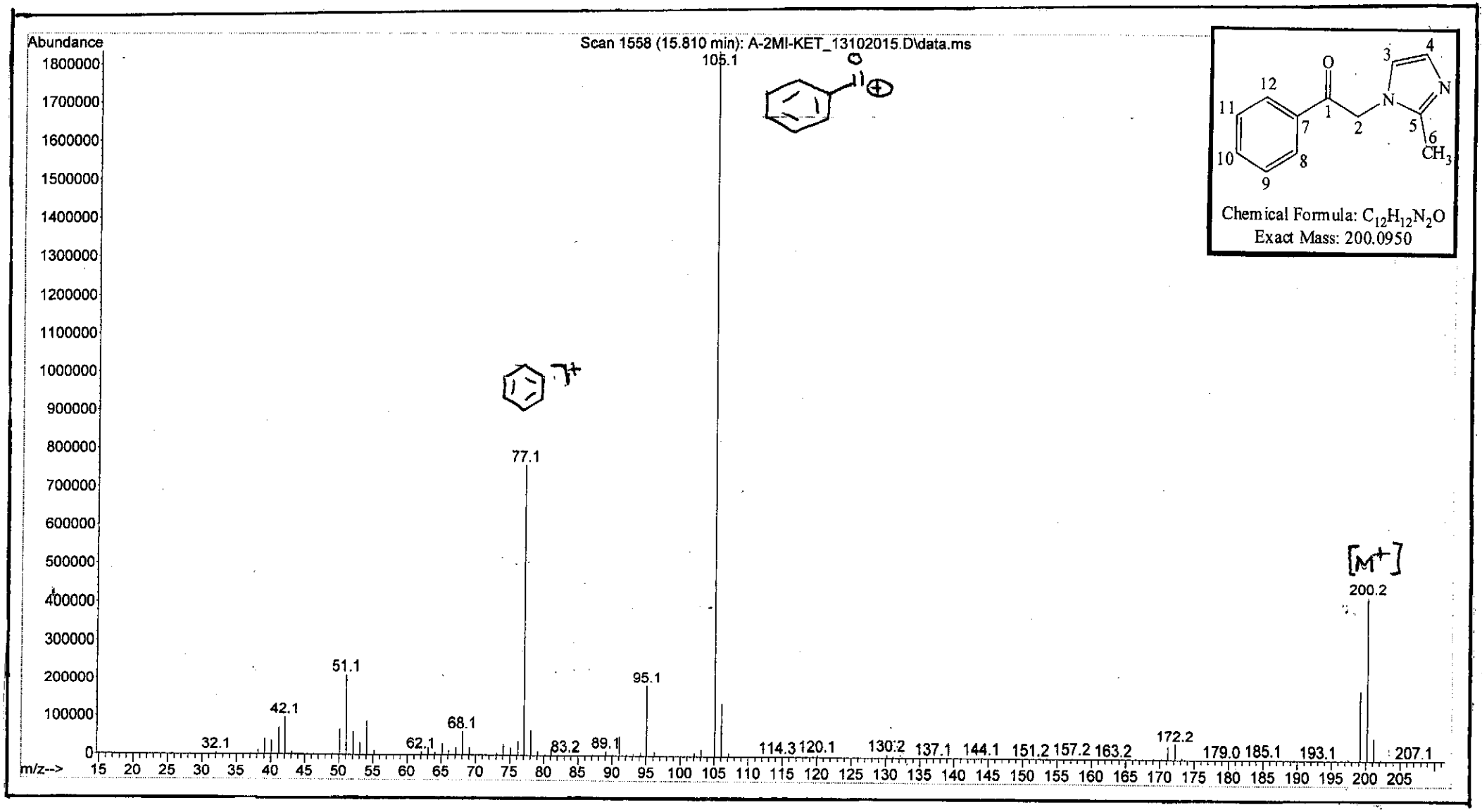

Mass spectrum of compound 4, 2-(5-methyl-1H-imidazol-1-yl)-1-phenylethanone

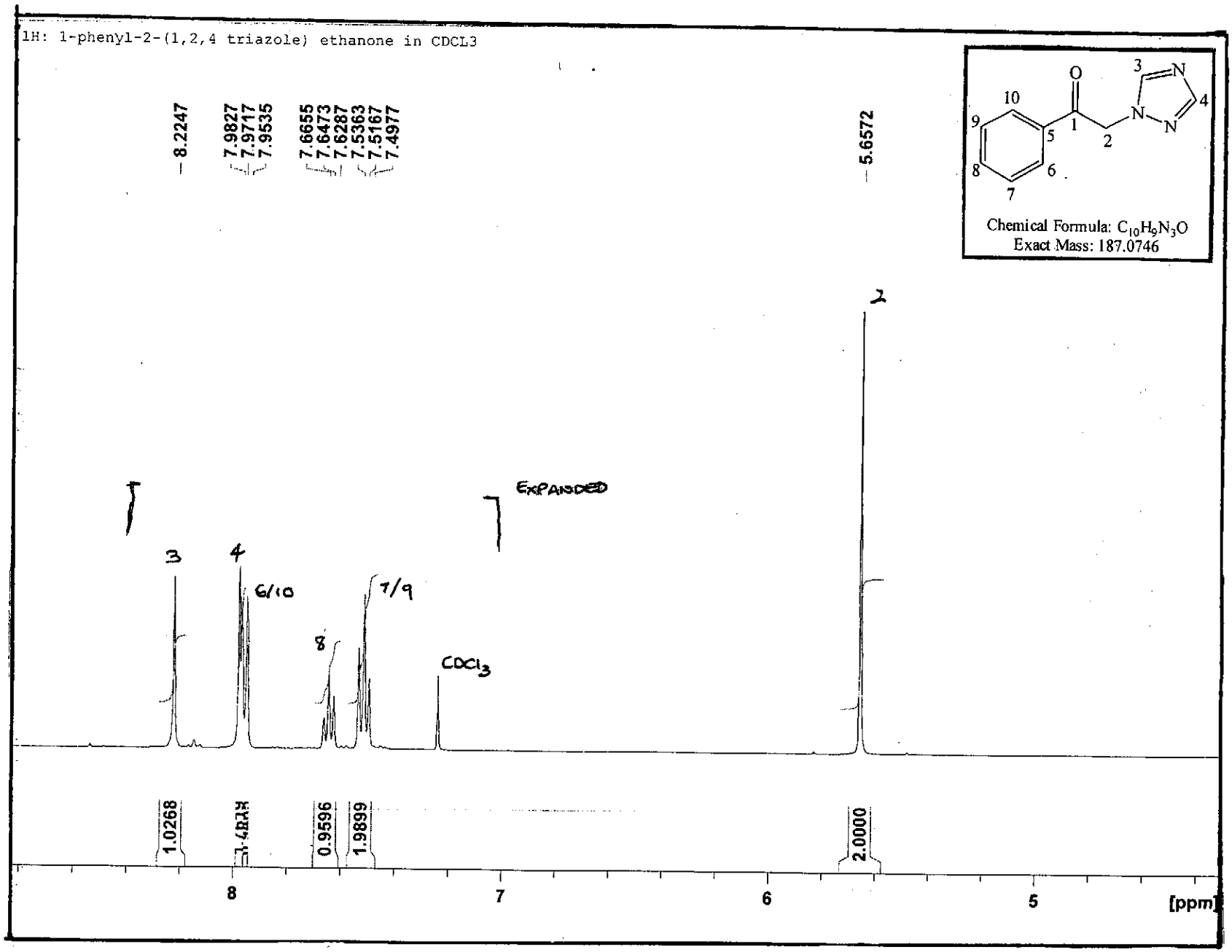

^{1}H NMR spectrum of compound 5, 1-Phenyl-2-[1,2,4]triazol-1-yl ethanone

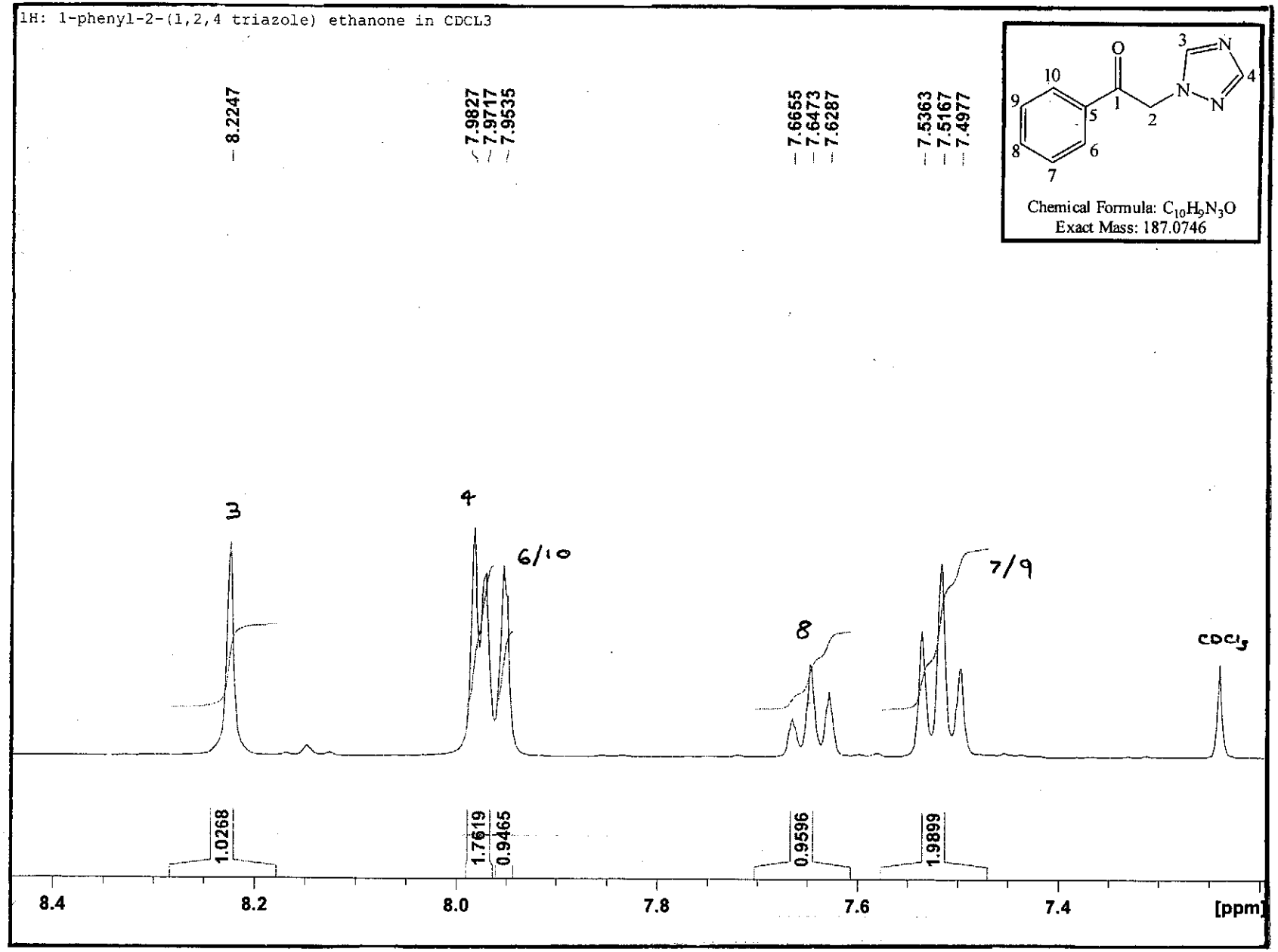

^{1}H NMR spectrum of compound 5, 1-Phenyl-2-[1,2,4]triazol-1-yl ethanone

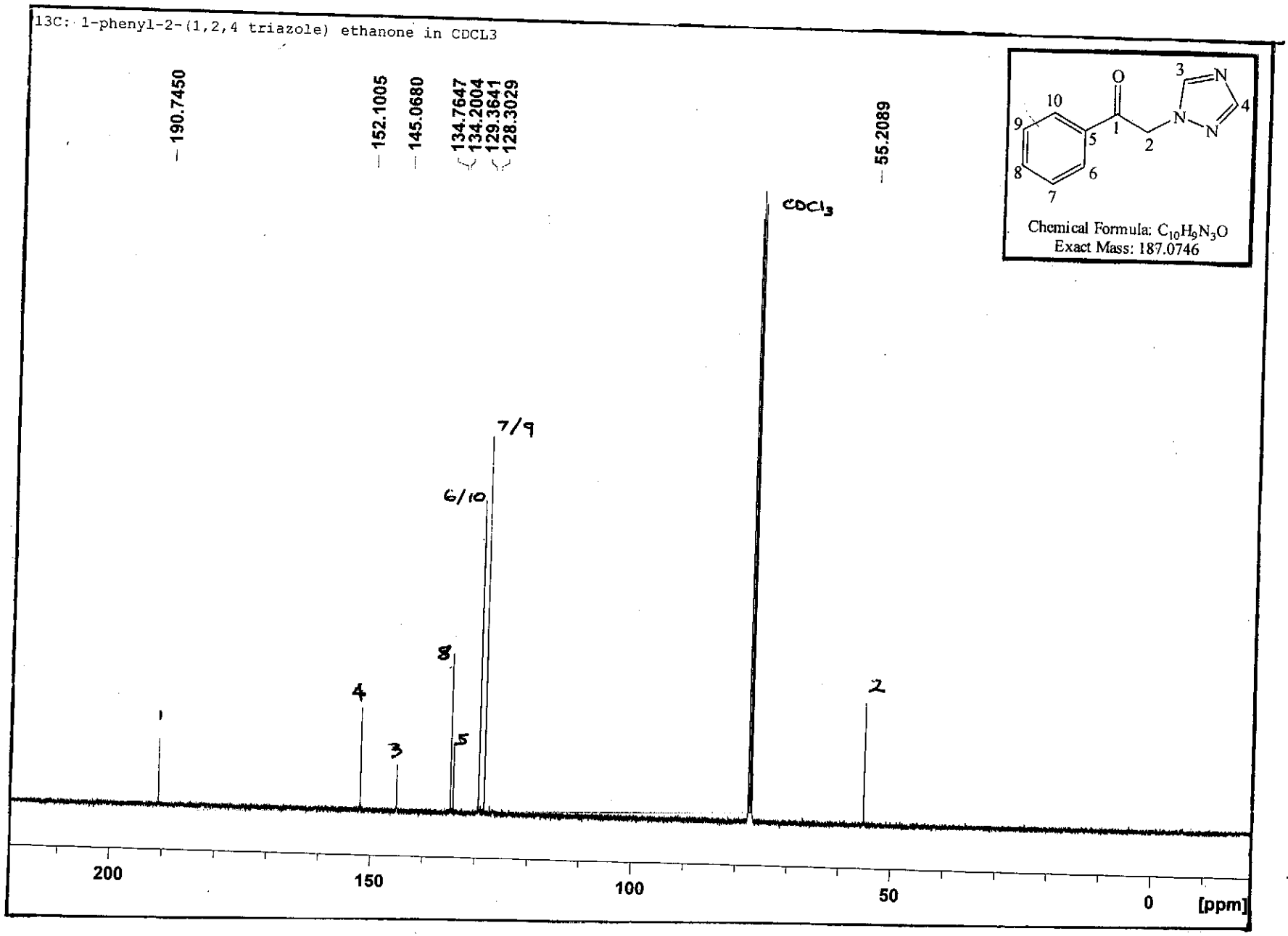

^{13}C NMR of compound 5, 1-Phenyl-2-[1,2,4]triazol-1-yl ethanone

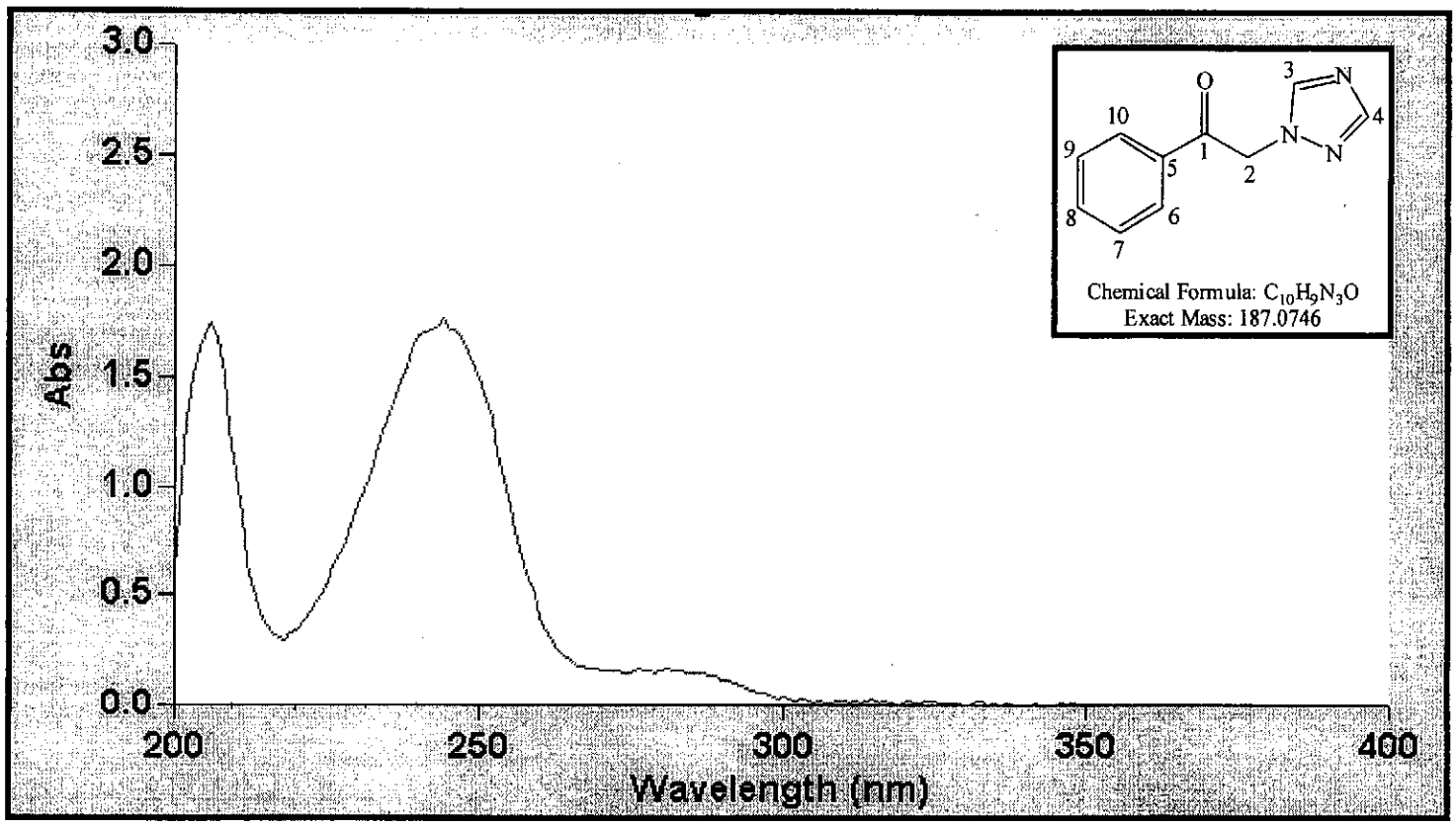

Ultra Violet spectrum of compound 5, 1-phenyl-2-(1H-1,2,4-triazol-1-yl)ethanone

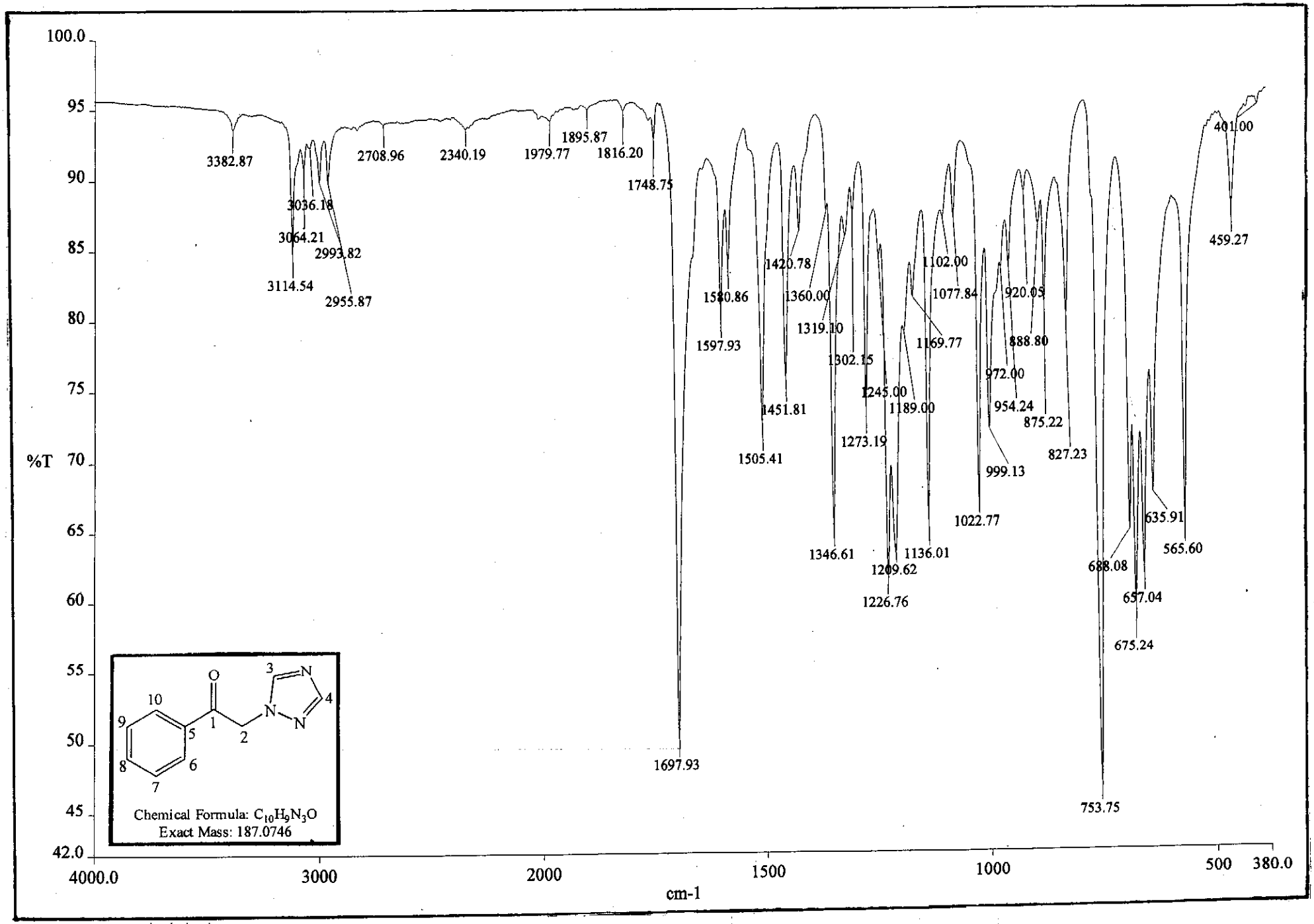

Infrared spectrum of compound 5, 1-Phenyl-2- [1,2,4]triazol-1-yl ethanone

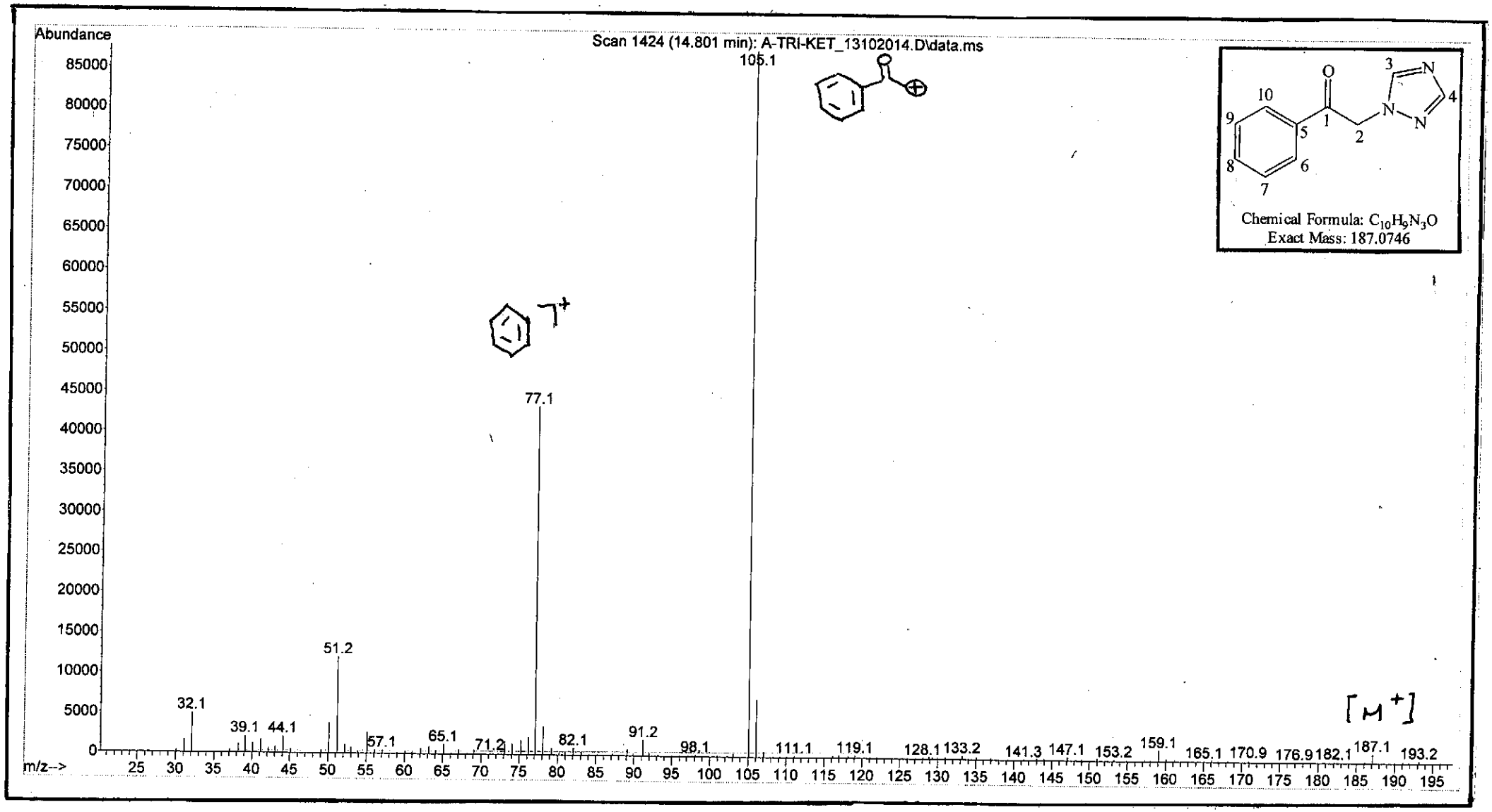

Mass spectrum of compound 5, 1-Phenyl-2-[1,2,4]triazol-1-yl ethanone

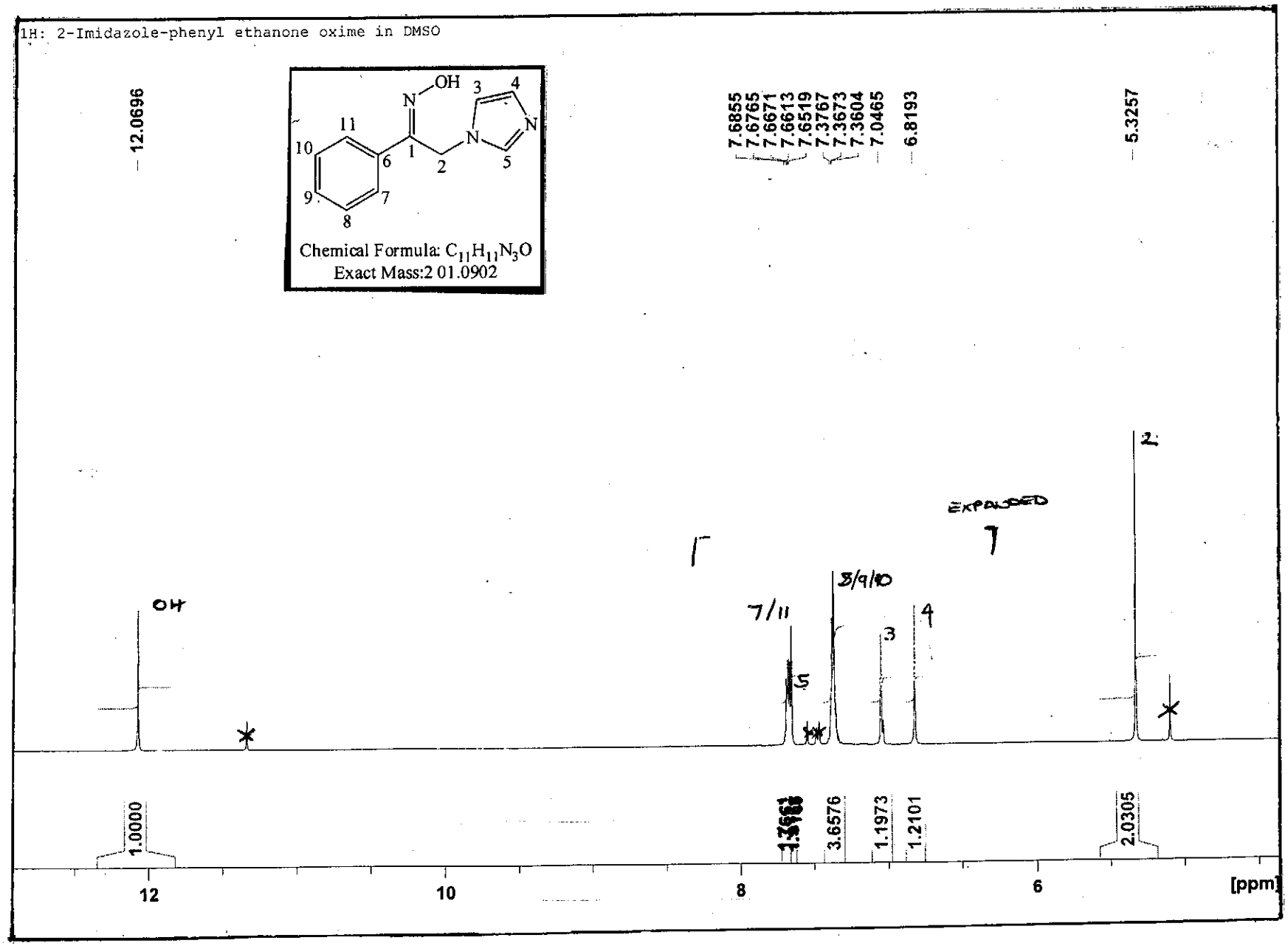

^{1}H NMR spectrum of compound 6, 2-(1H-imidazol-1-yl)-1-phenylethaone oxime

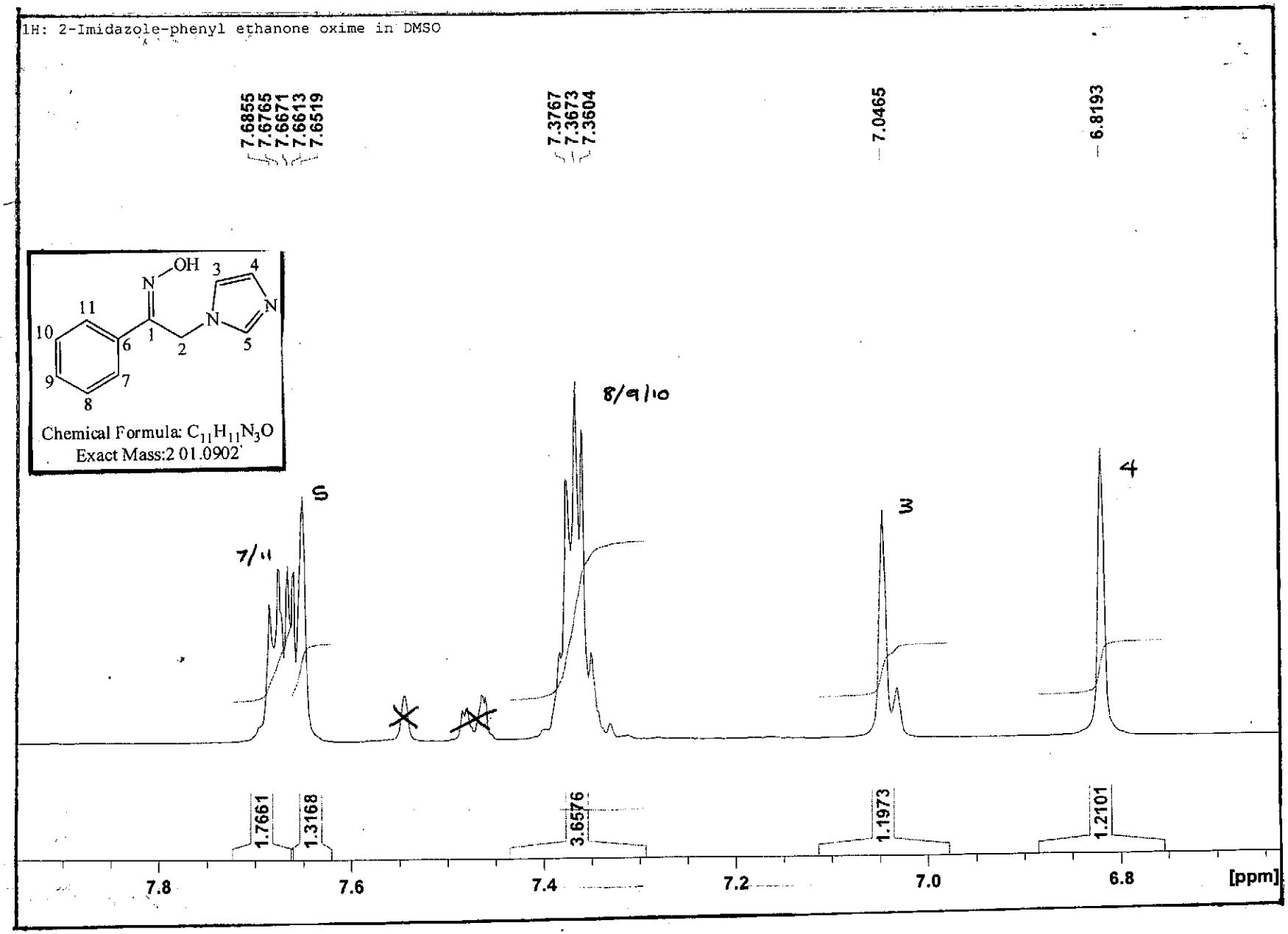

^{1}H NMR spectrum of compound 6, 2-(1H-imidazol-1-yl)-1-phenylethaone oxime

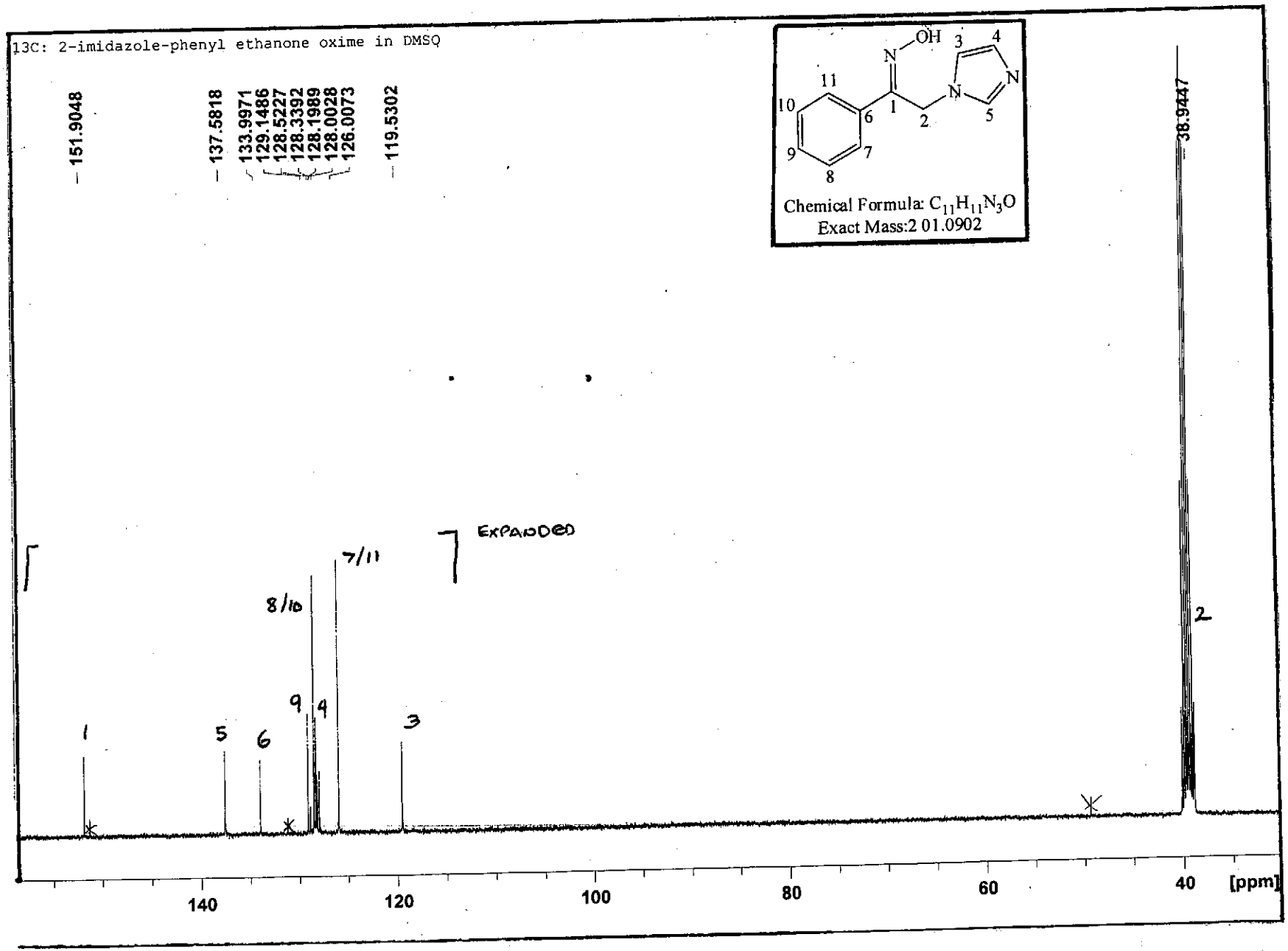

^{13}C NMR of compound 6, 2-(1H-imidazol-1-yl)-1-phenylethaone oxime

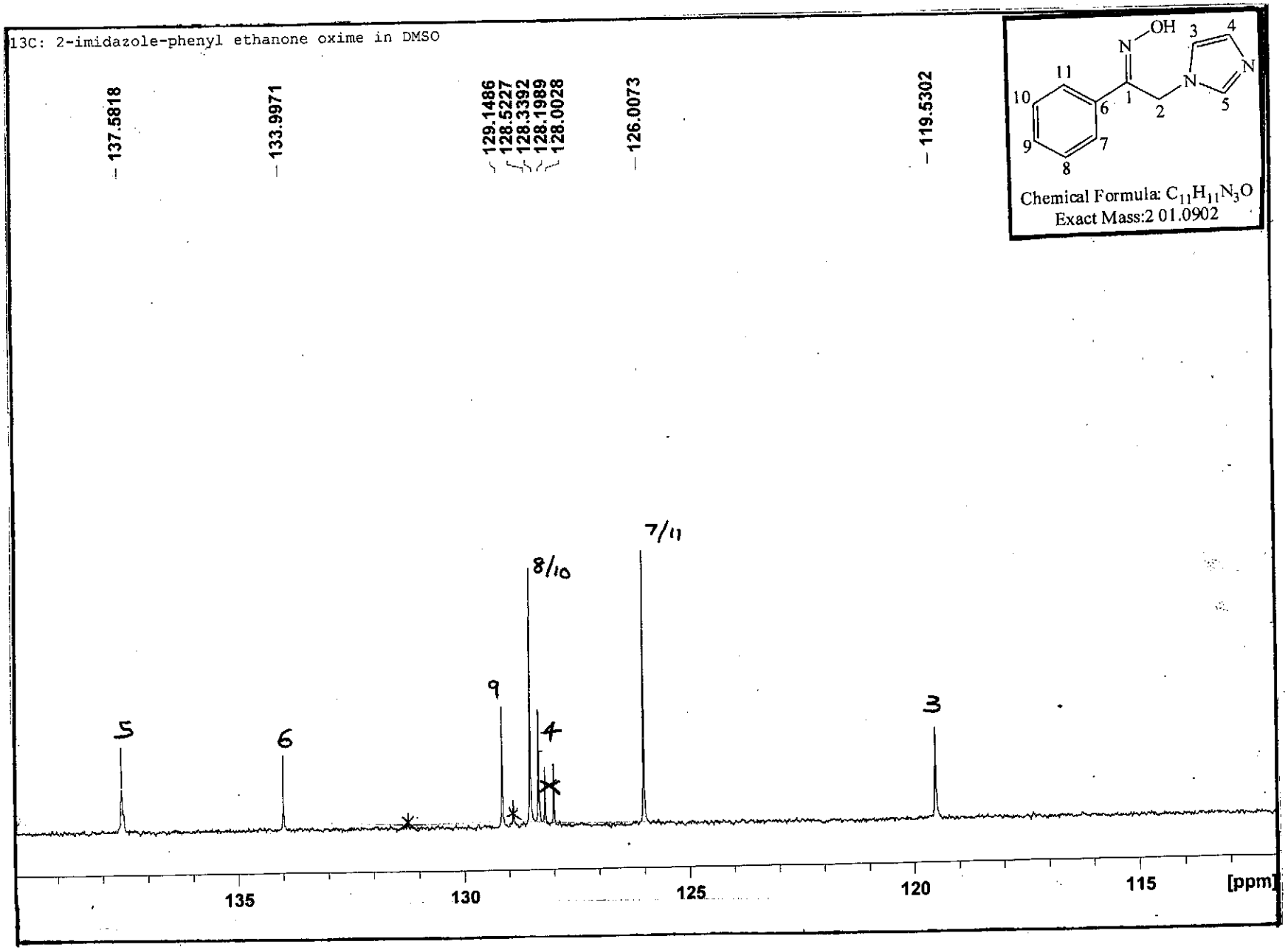

^{13}C NMR of compound 6, 2-(1H-imidazol-1-yl)-1-phenylethaone oxime

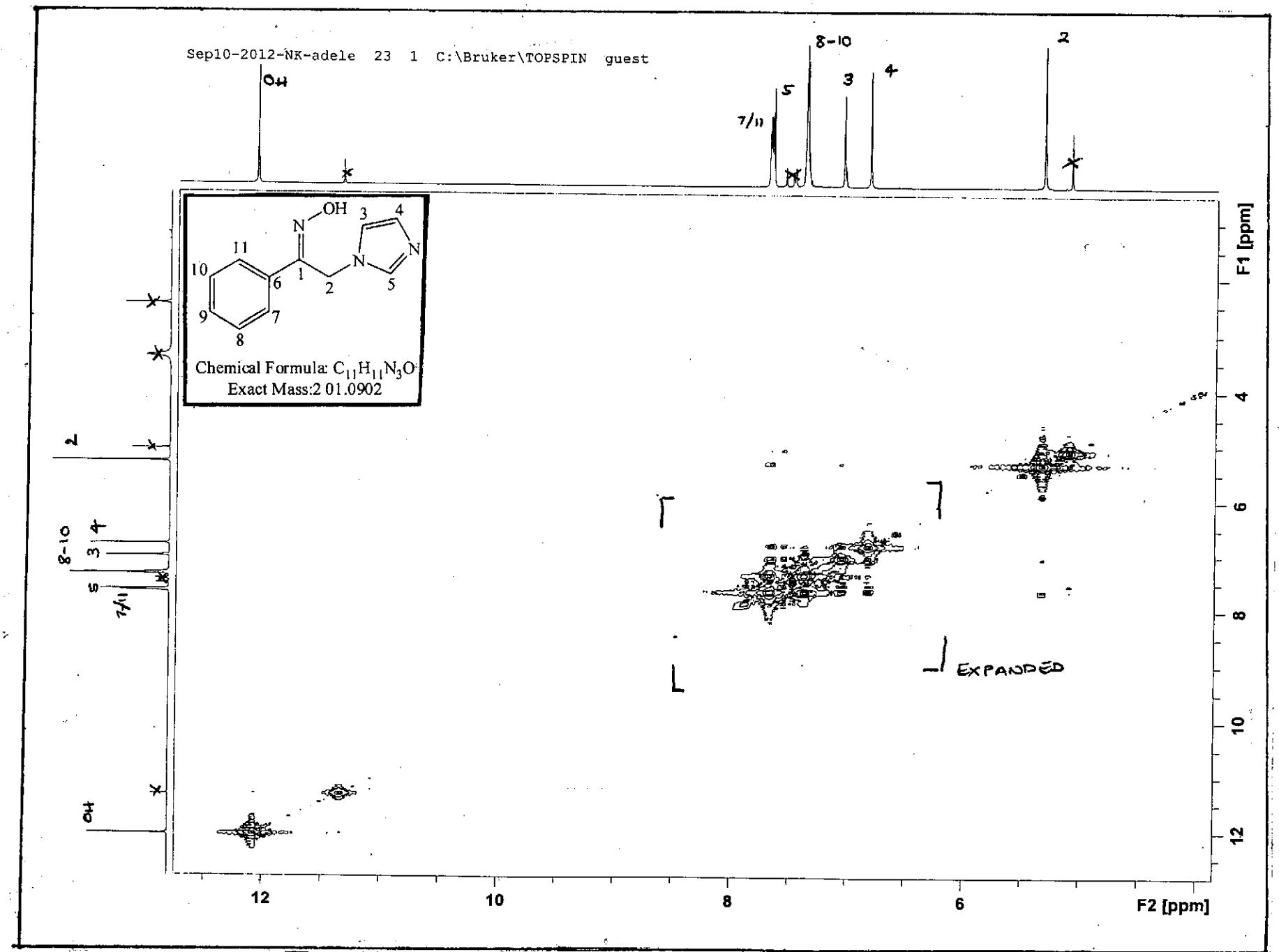

COSY spectrum of compound 6, 2-(1H-imidazol-1-yl)-1-phenylethaone oxime

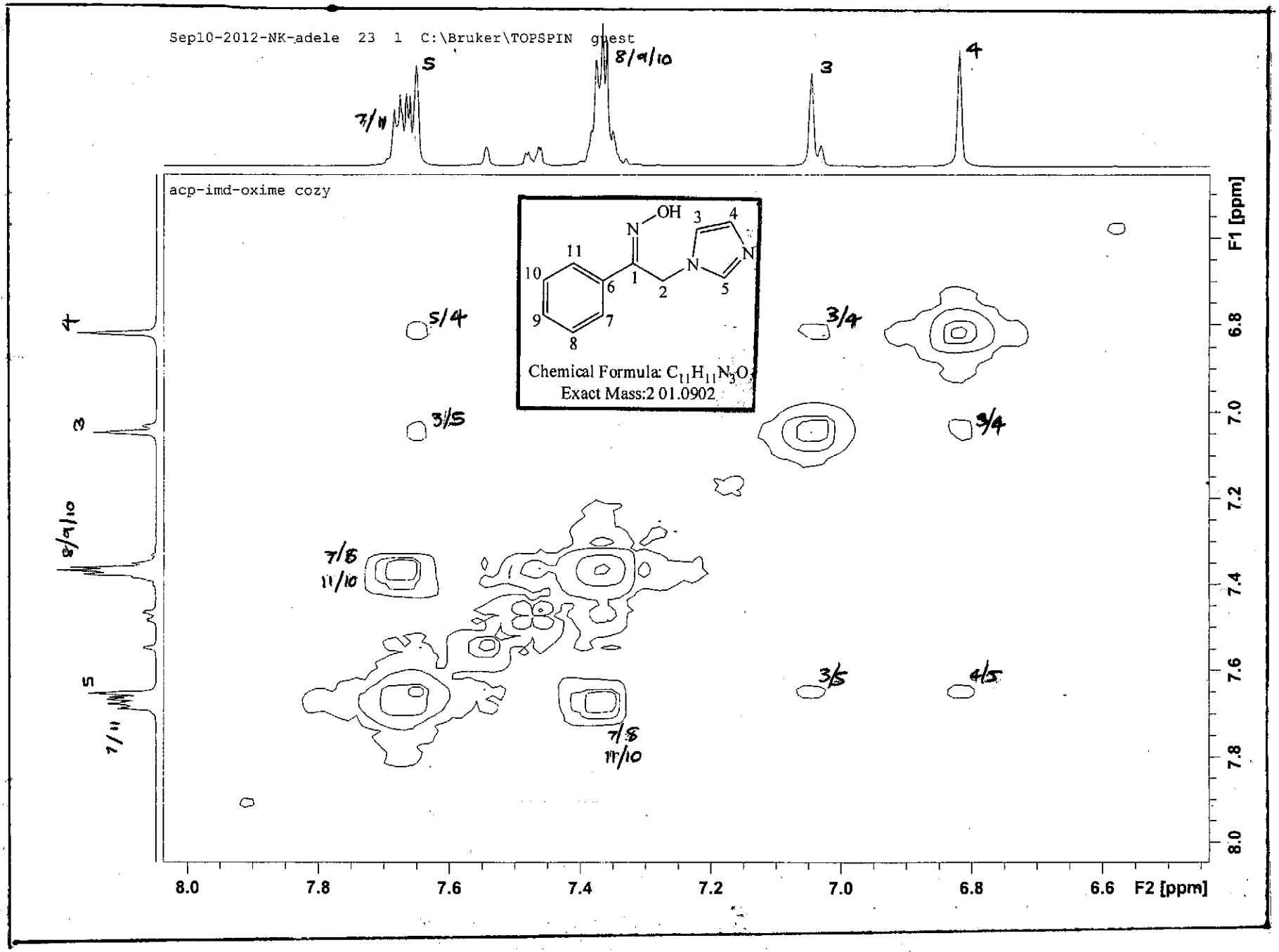

COSY spectrum of compound 6, 2-(1H-imidazol-1-yl)-1-phenylethaone oxime

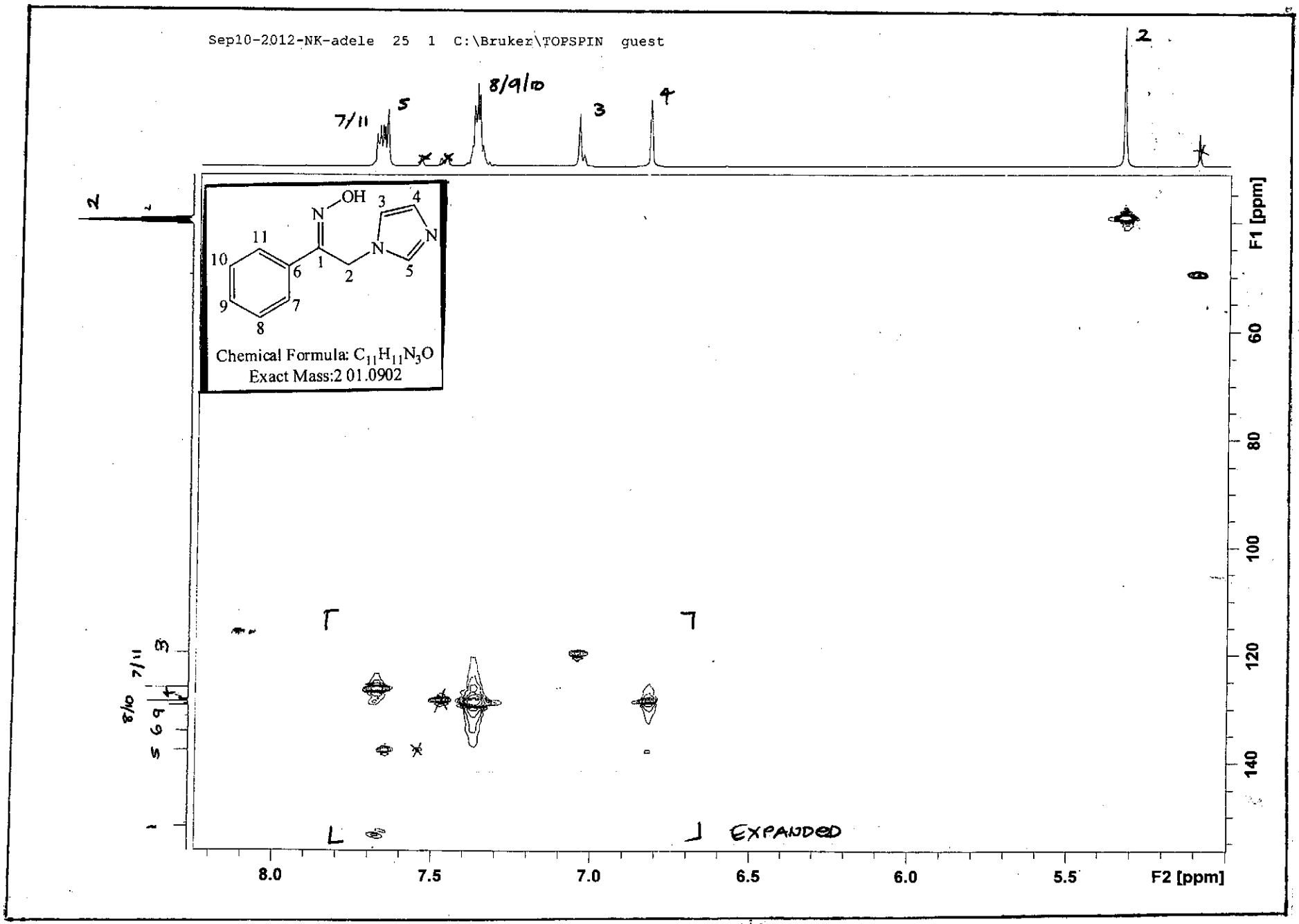

HSQC spectrum of compound 6, 2-(1H-imidazol-1-yl)-1-phenylethaone oxime

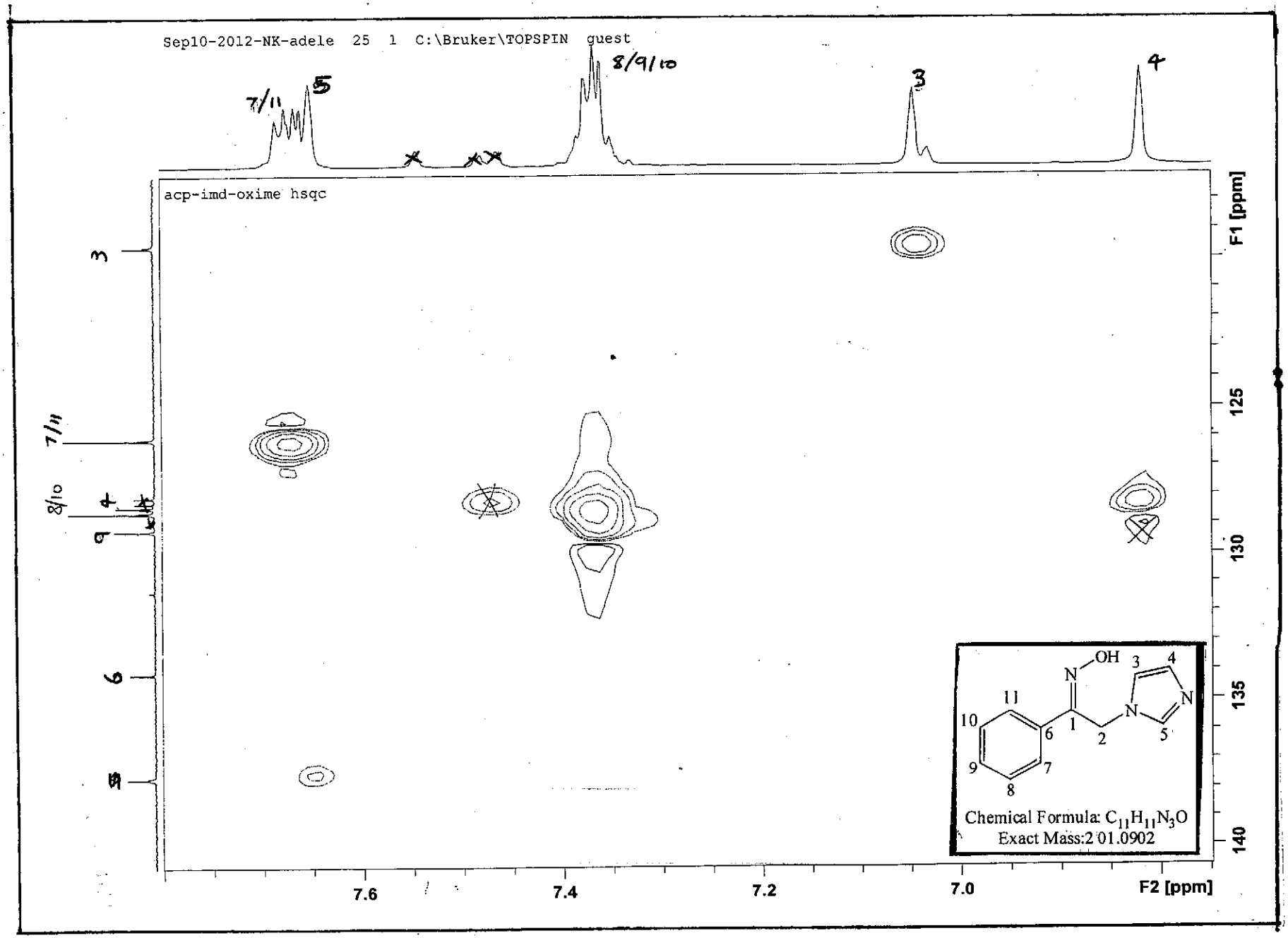

HSQC spectrum of compound 6, 2-(1H-imidazol-1-yl)-1-phenylethaone oxime

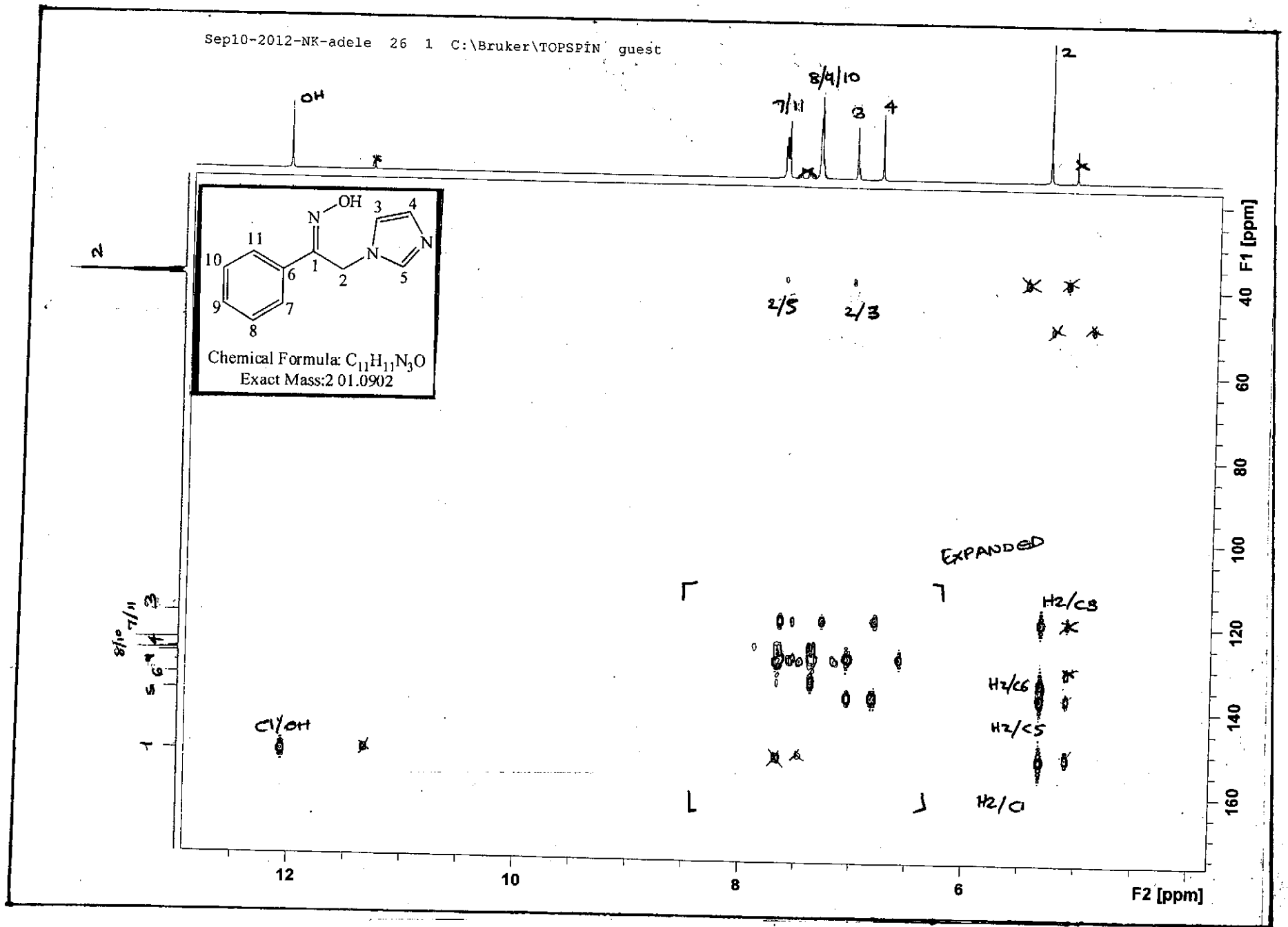

HMBC spectrum of compound 6, 2-(1H-imidazol-1-yl)-1-phenylethaone oxime

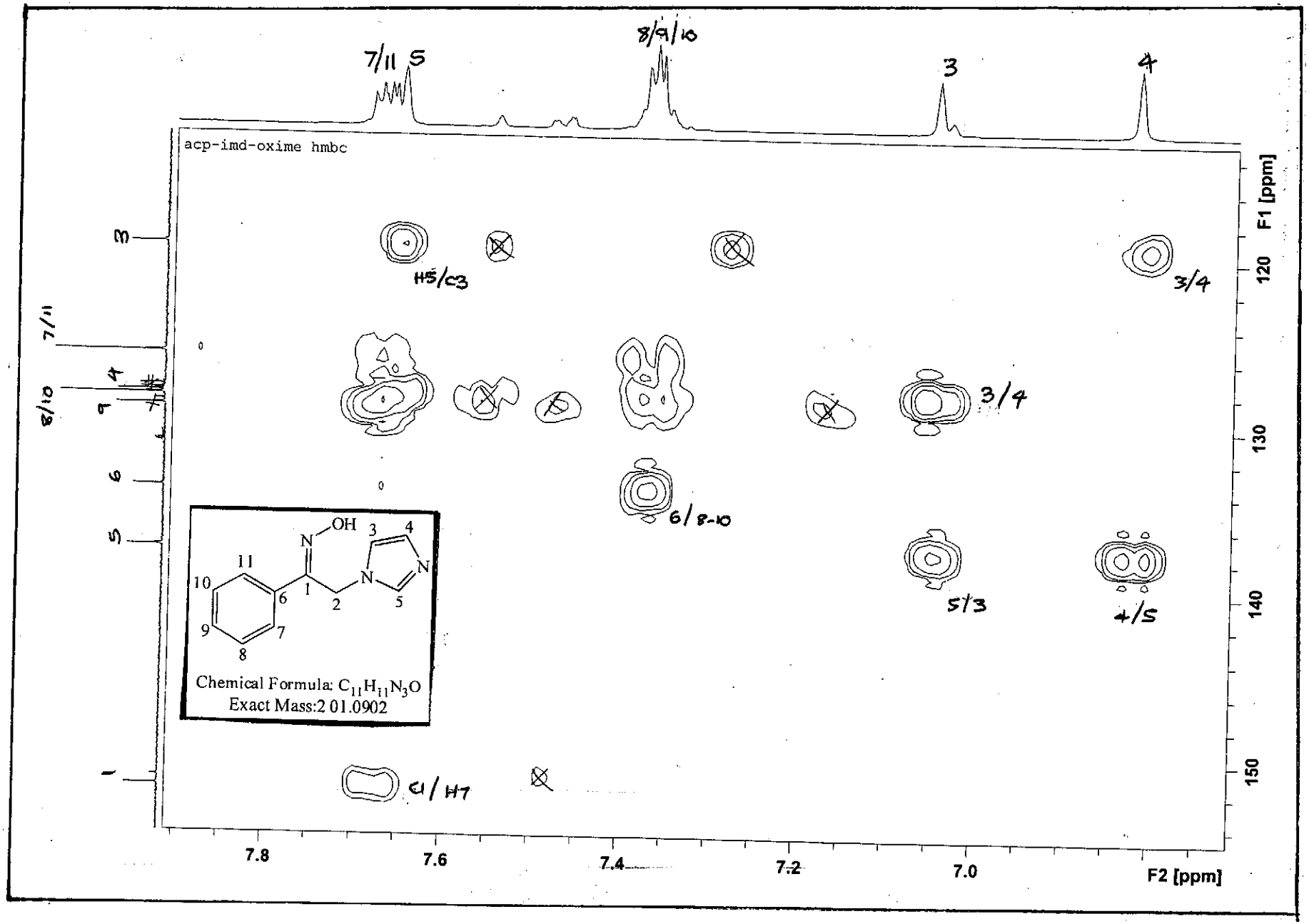

HMBC spectrum of compound 6, 2-(1H-imidazol-1-yl)-1-phenylethaone oxime

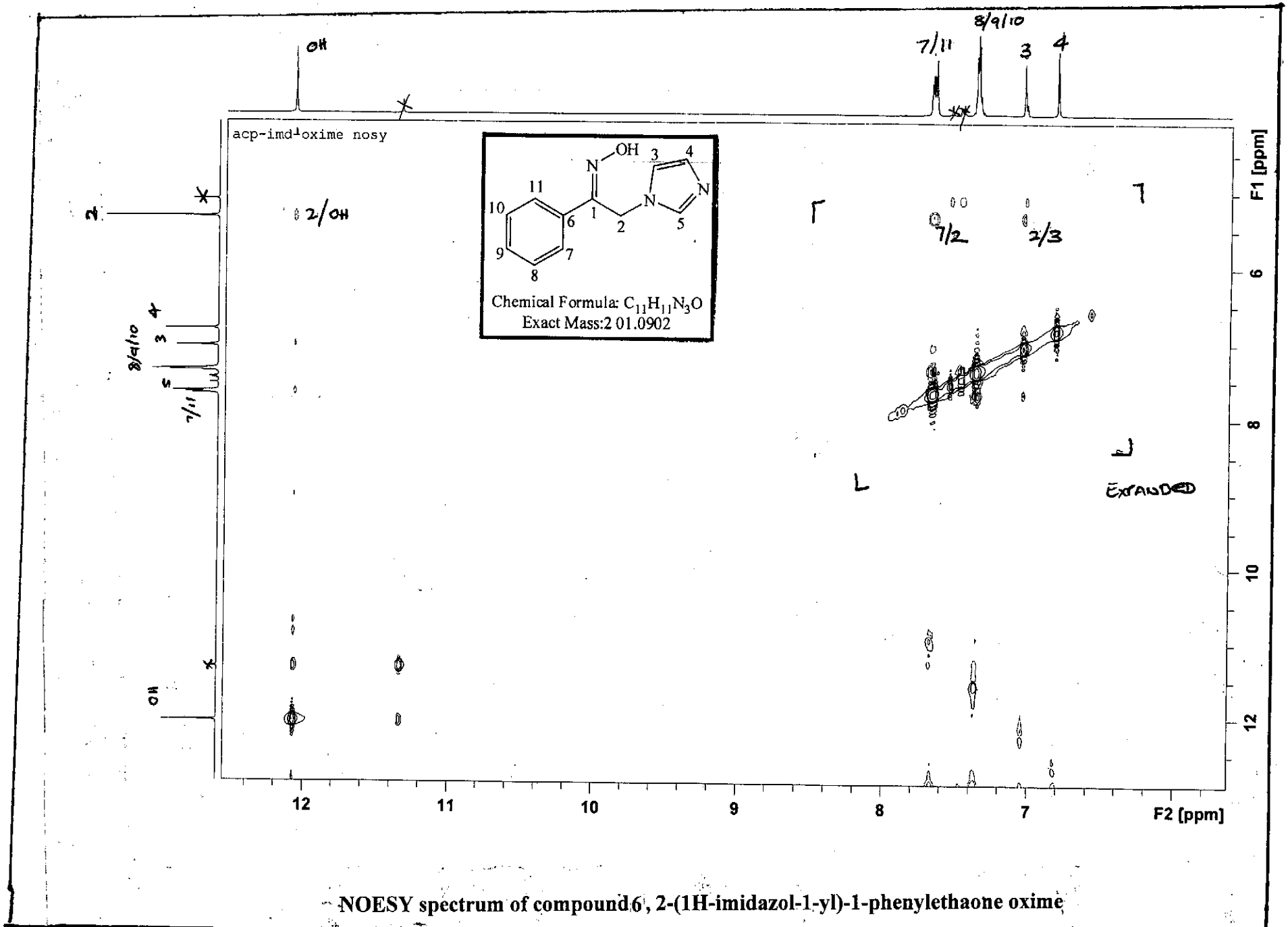

NOESY spectrum of compound 6, 2-(1H-imidazol-1-yl)-1-phenylethaone oxime

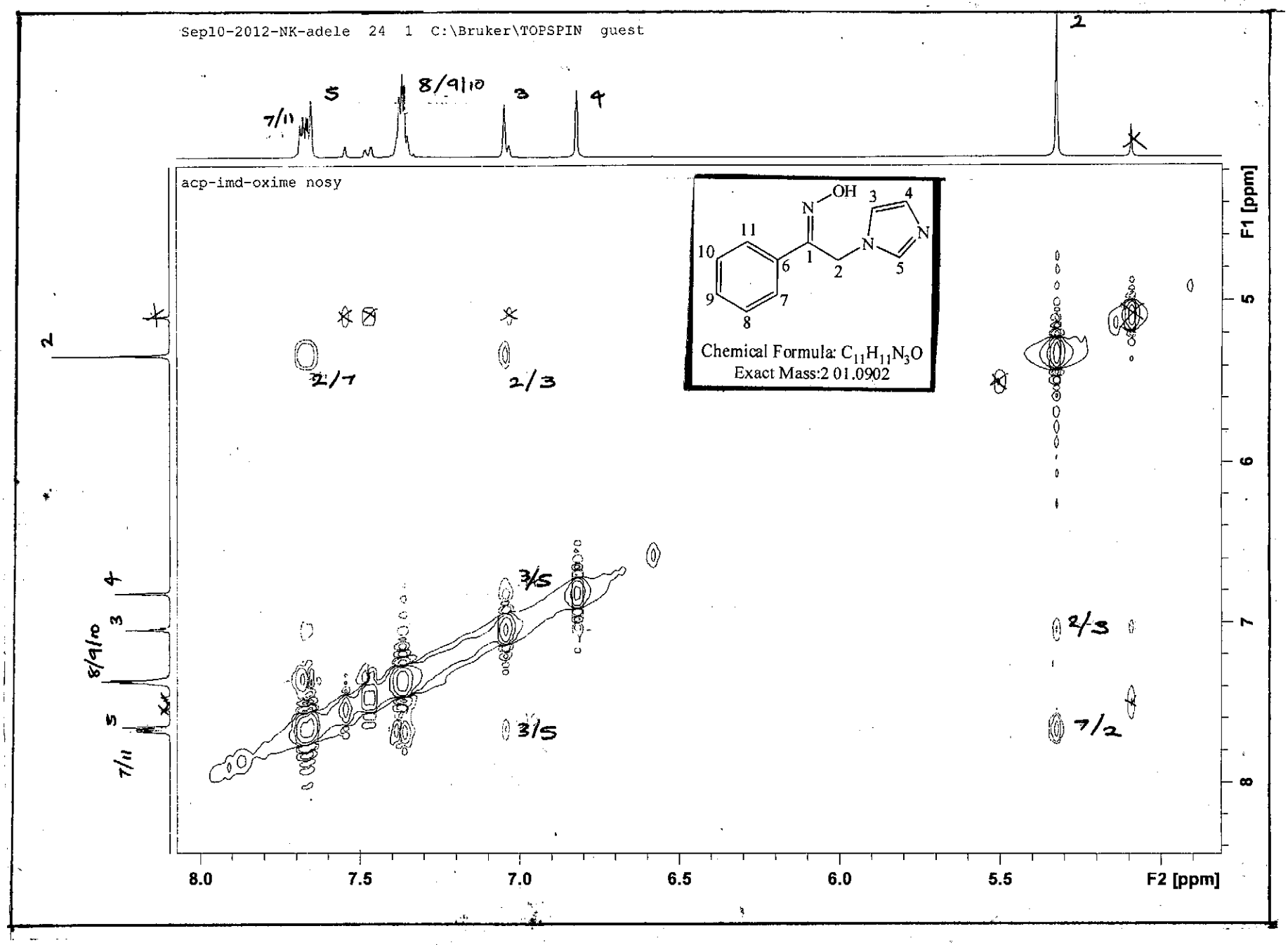

NOESY spectrum of compound 6, 2-(1H-imidazol-1-yl)-1-phenylethaone oxime

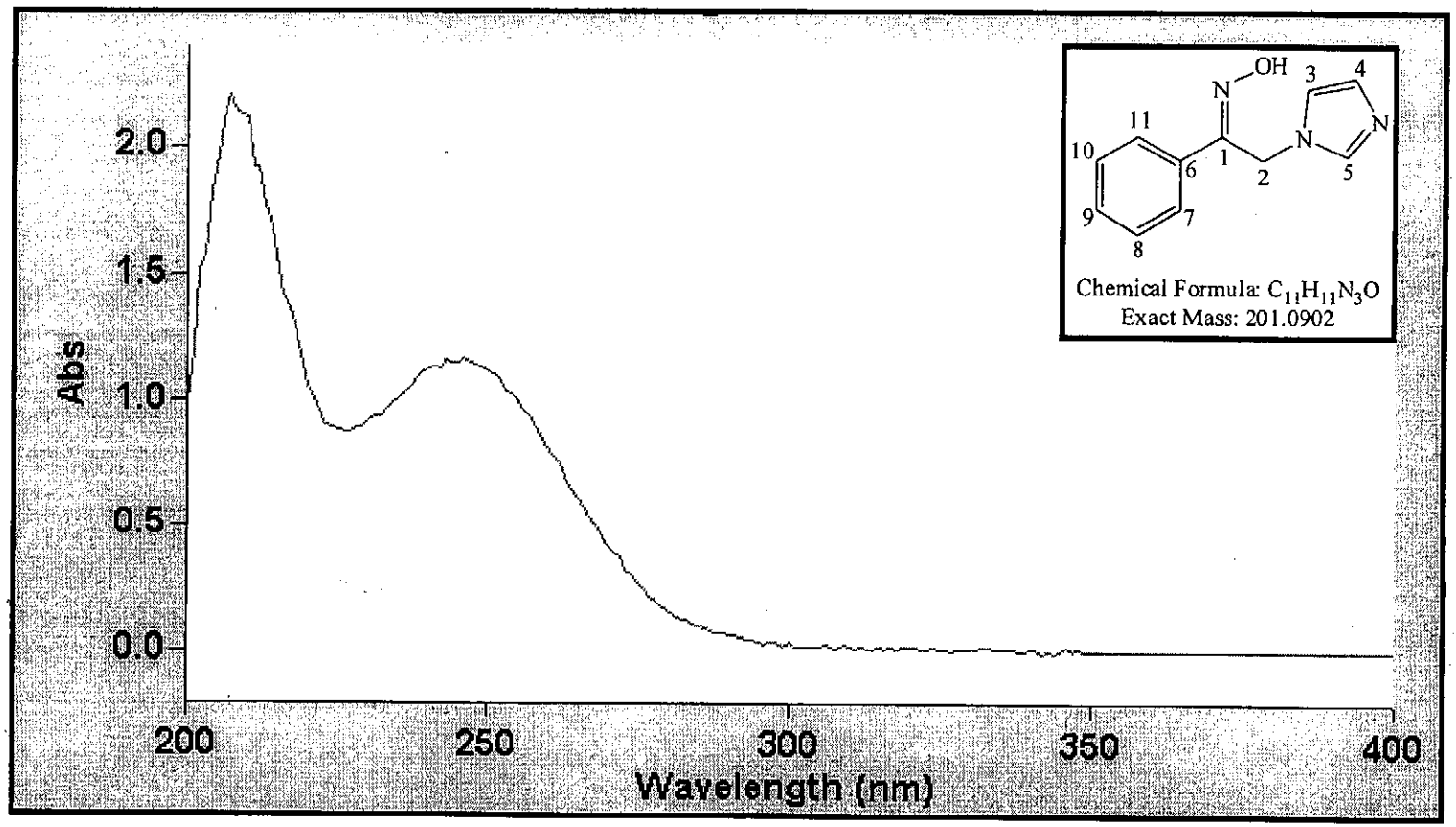

Ultra Violet spectrum of compound 6, 2-(1H-imidazol-1-yl)-1-phenylethanone oxime

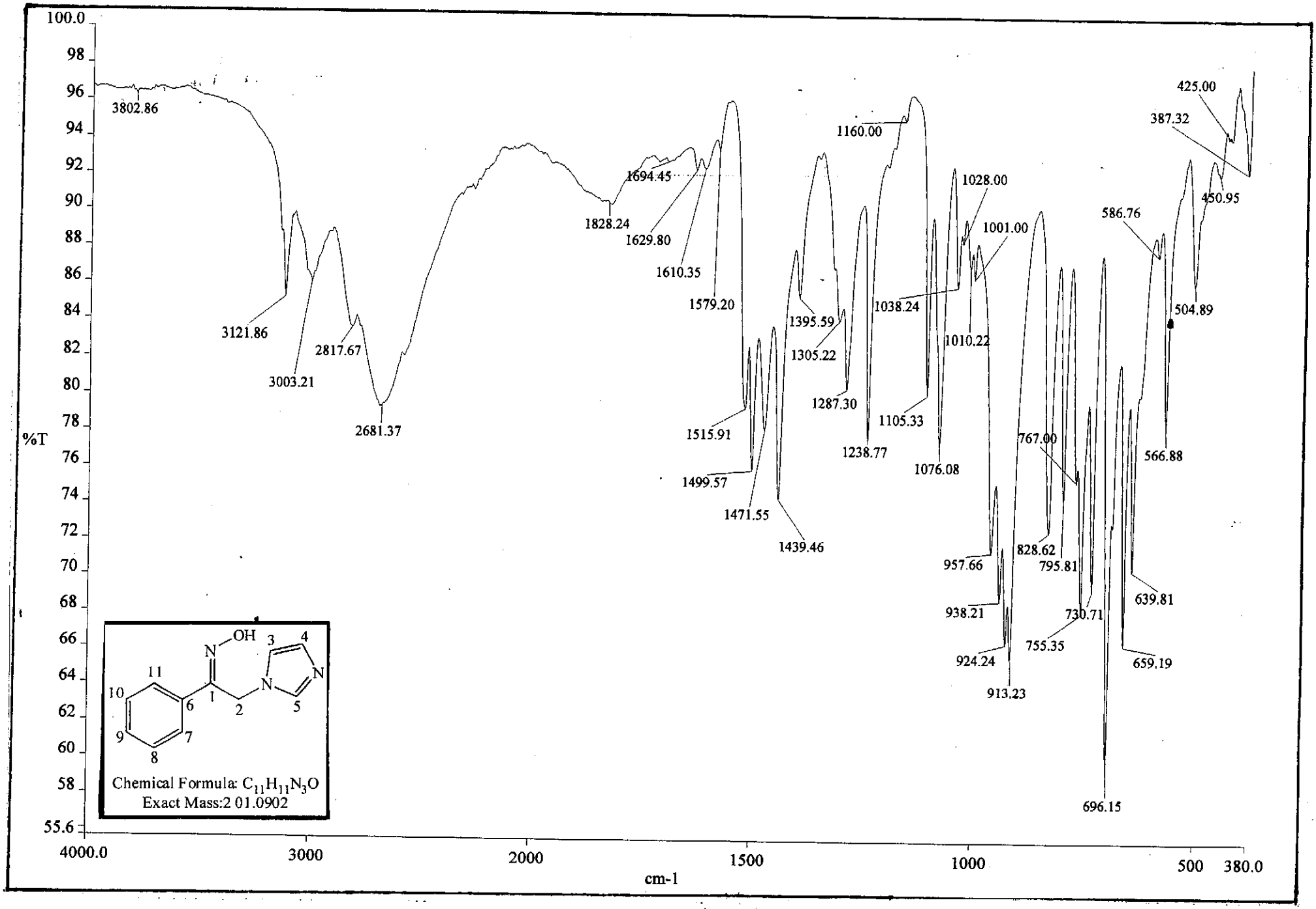

Infrared spectrum of compound 6, 2-(1H-imidazol-1-yl)-1-phenylethaone oxime

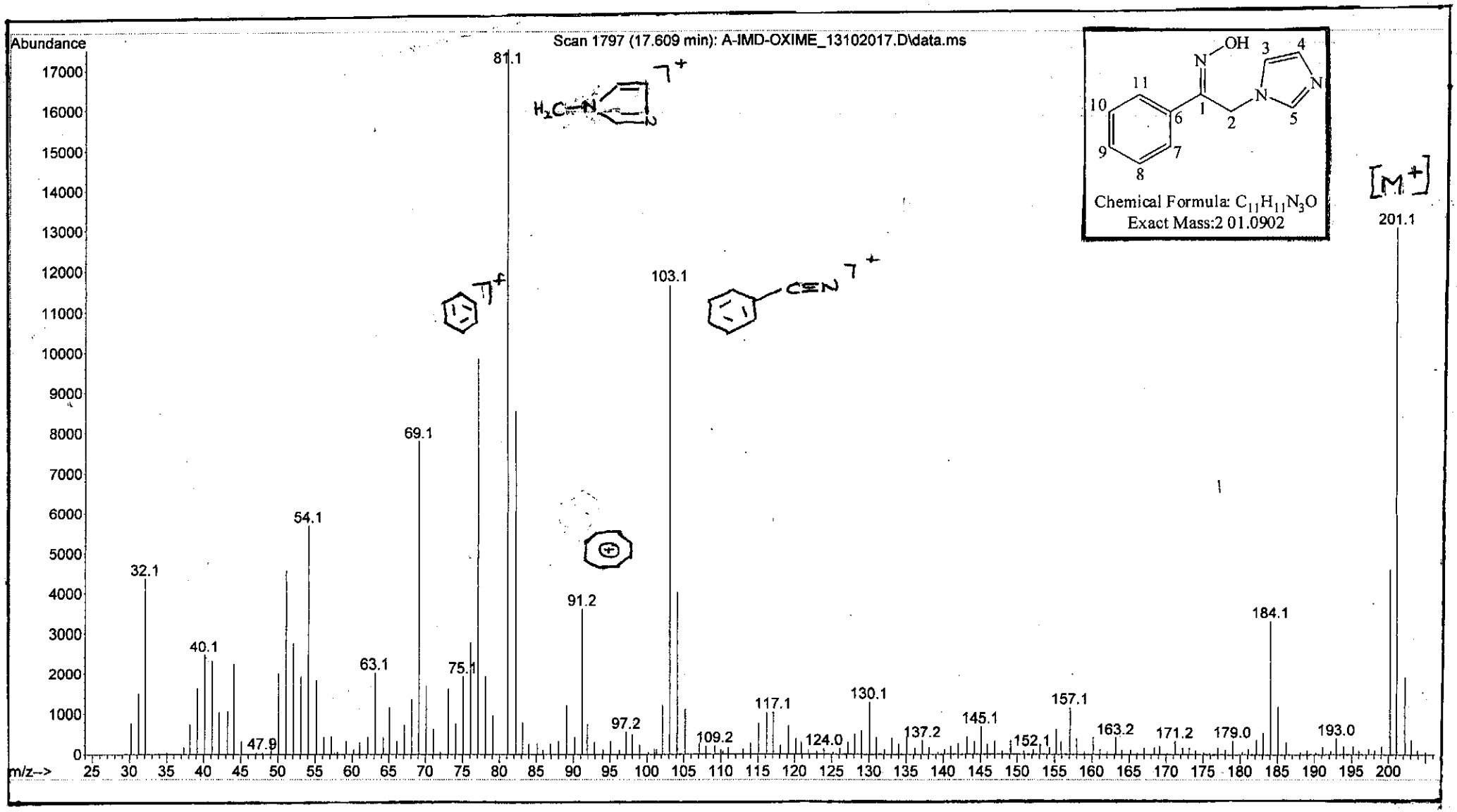

Mass spectrum of compound 6, 2-(1H-imidazol-1-yl)-1-phenylethaone oxime

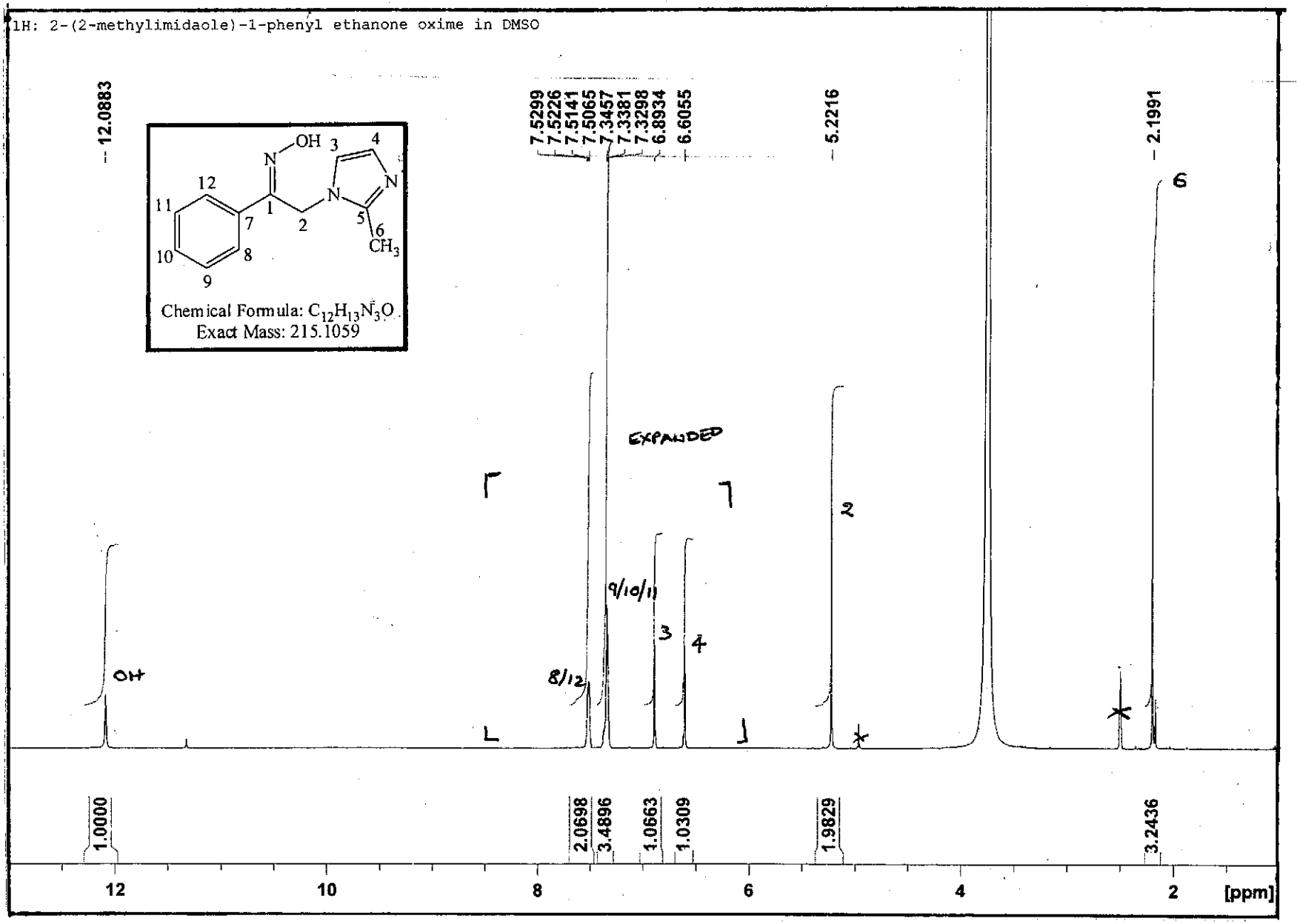

^{1}H NMR spectrum of compound 7 , 2-(2-methyl-1H-imidazol-1-yl)-1-phenyl ethanone oxime

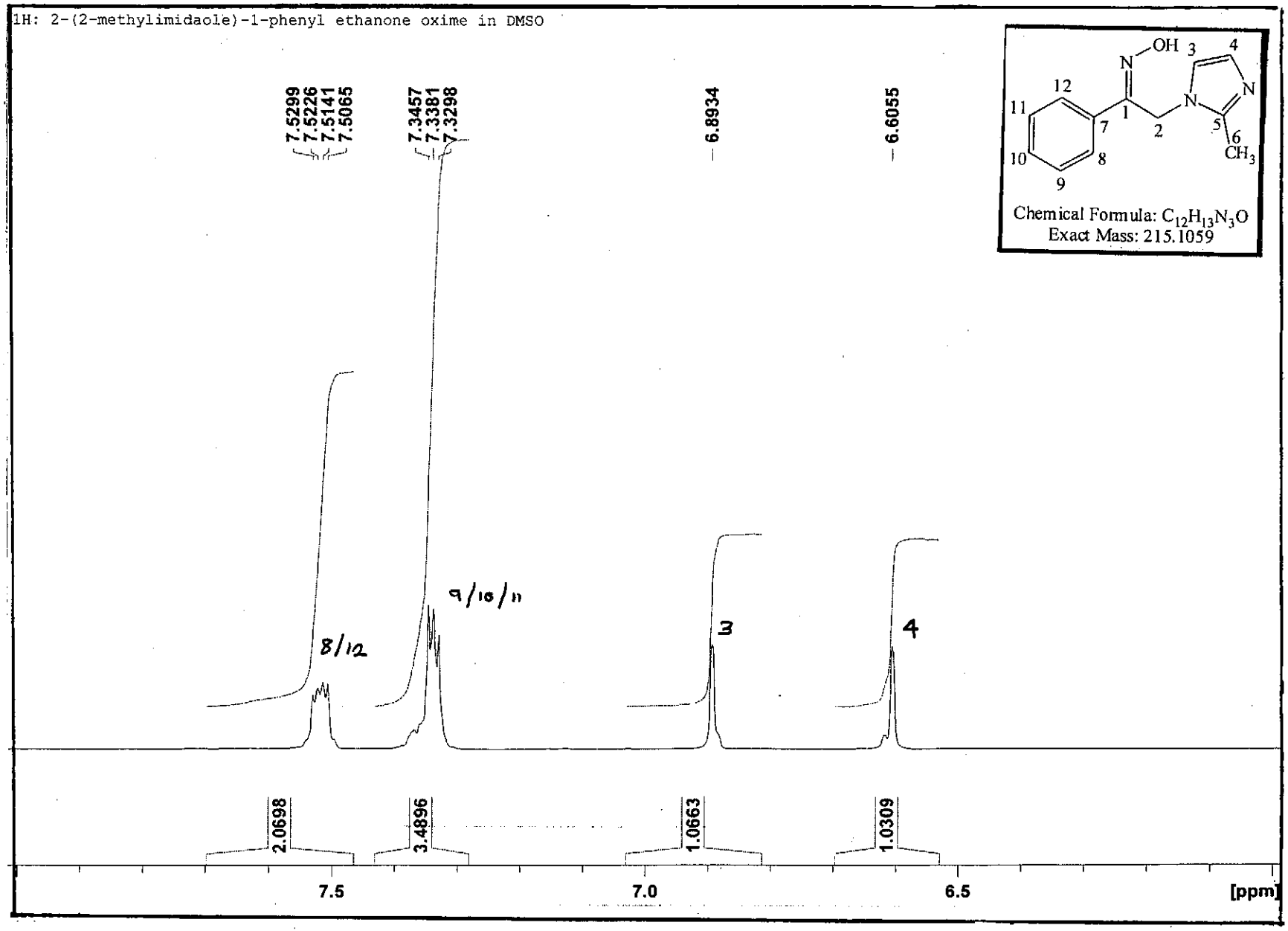

^{1}H NMR spectrum of compound 7 , 2-(2-methyl-1H-imidazol-1-yl)-1-phenyl ethanone oxime

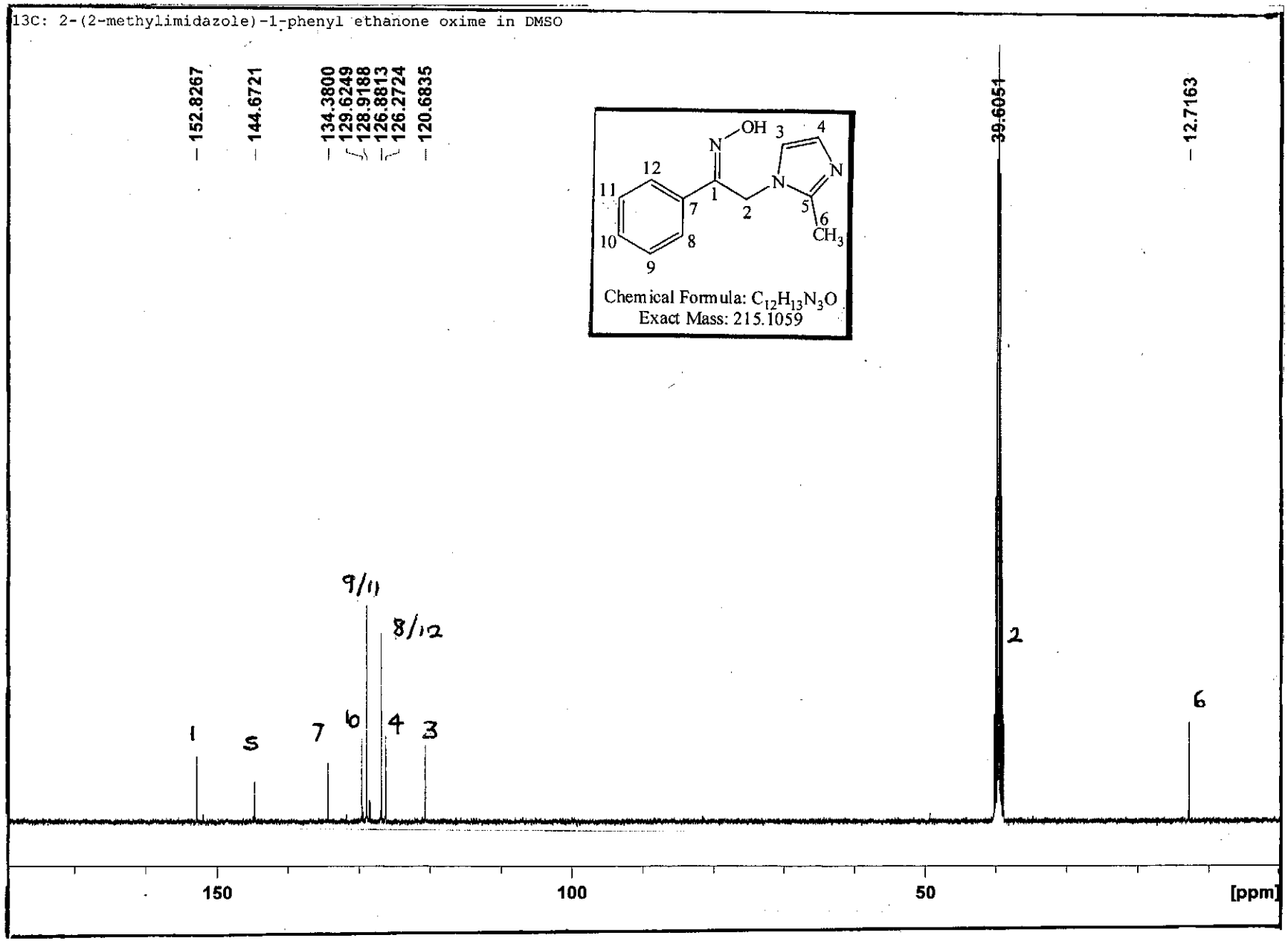

^{13}C NMR of compound 7 , 2-(2-methyl-1H-imidazol-1-yl)-1-phenyl ethanone oxime

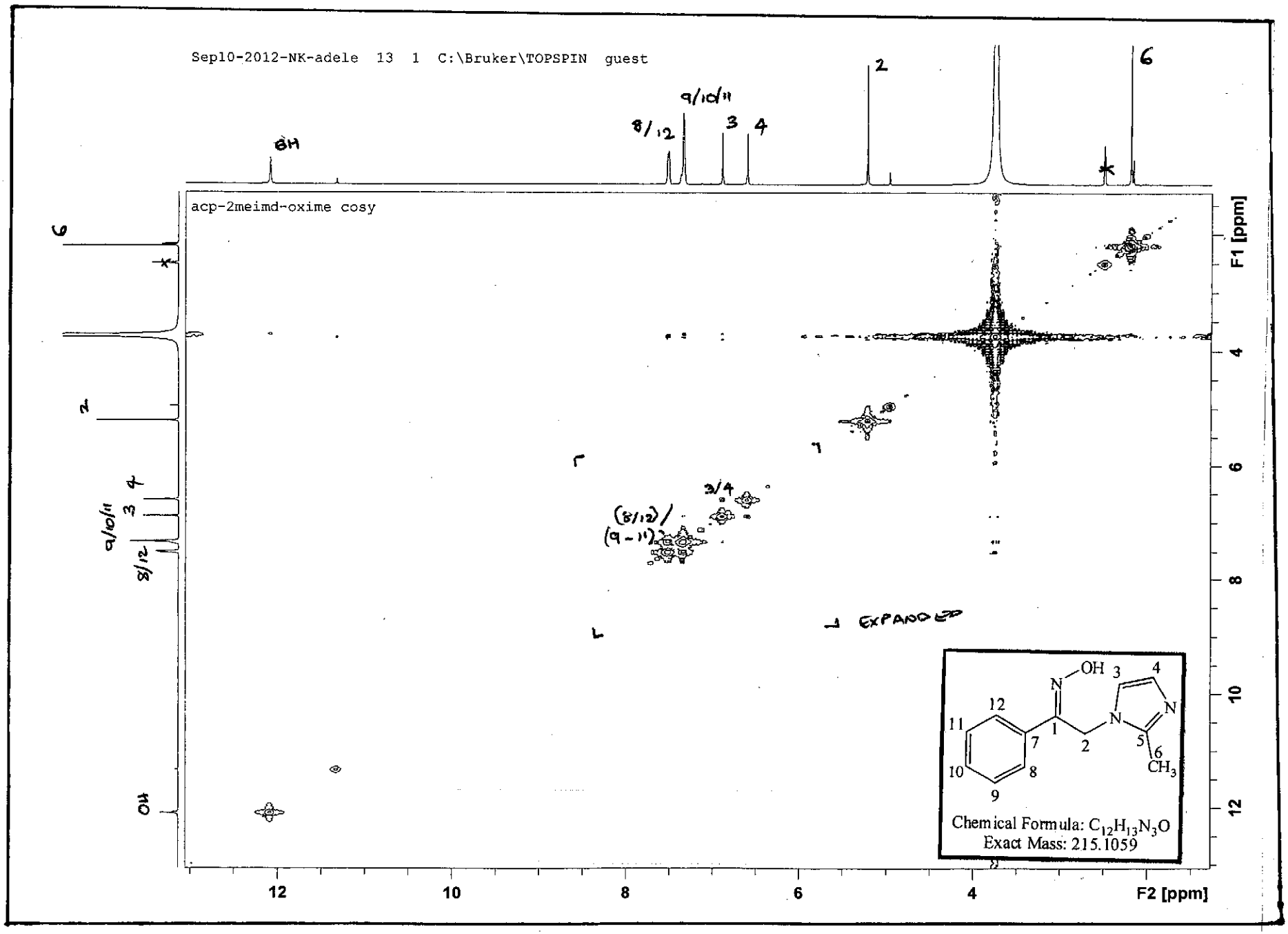

COSY spectrum of compound 7 , 2- (2-methyl-1H-imidazol-1-yl)-1-phenyl ethanone oxime

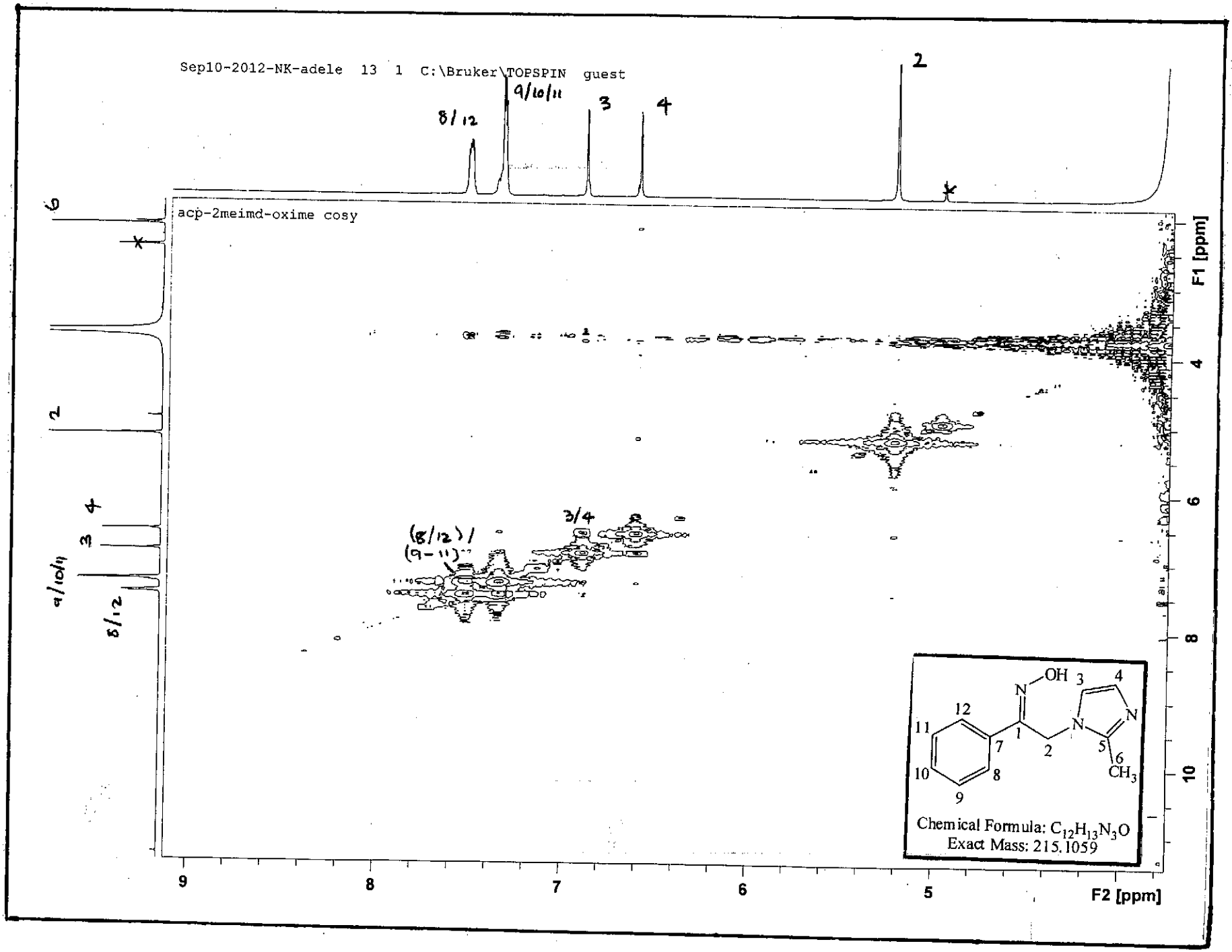

COSY spectrum of compound 7 \, 2-(2-methyl-1H-imidazol-1-yl)-1- phenyl ethanone oxime

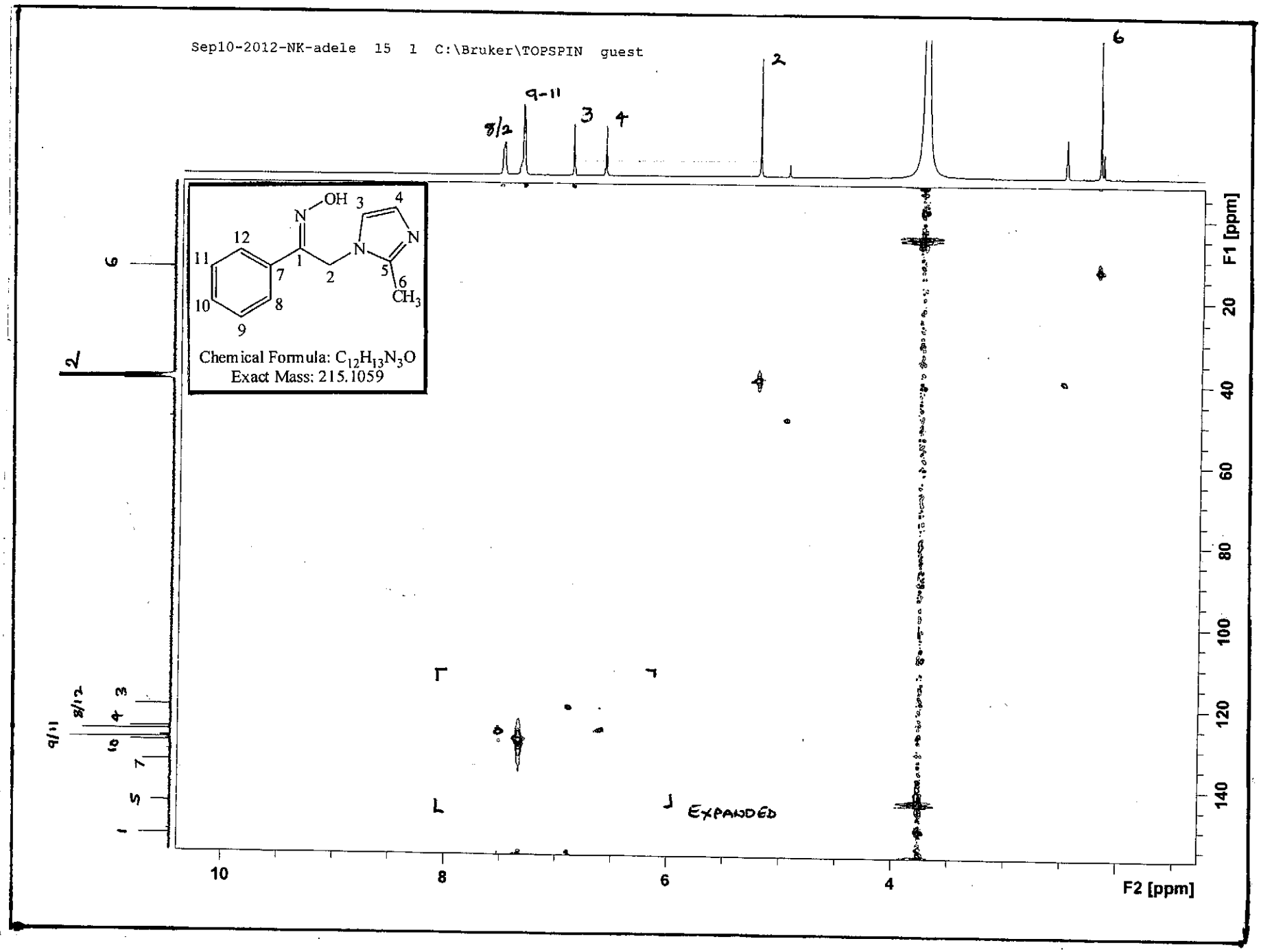

HSQC spectrum of compound 7 , 2-(2-methyl-1H-imidazol-1-yl)-1-phenyl ethanone oxime

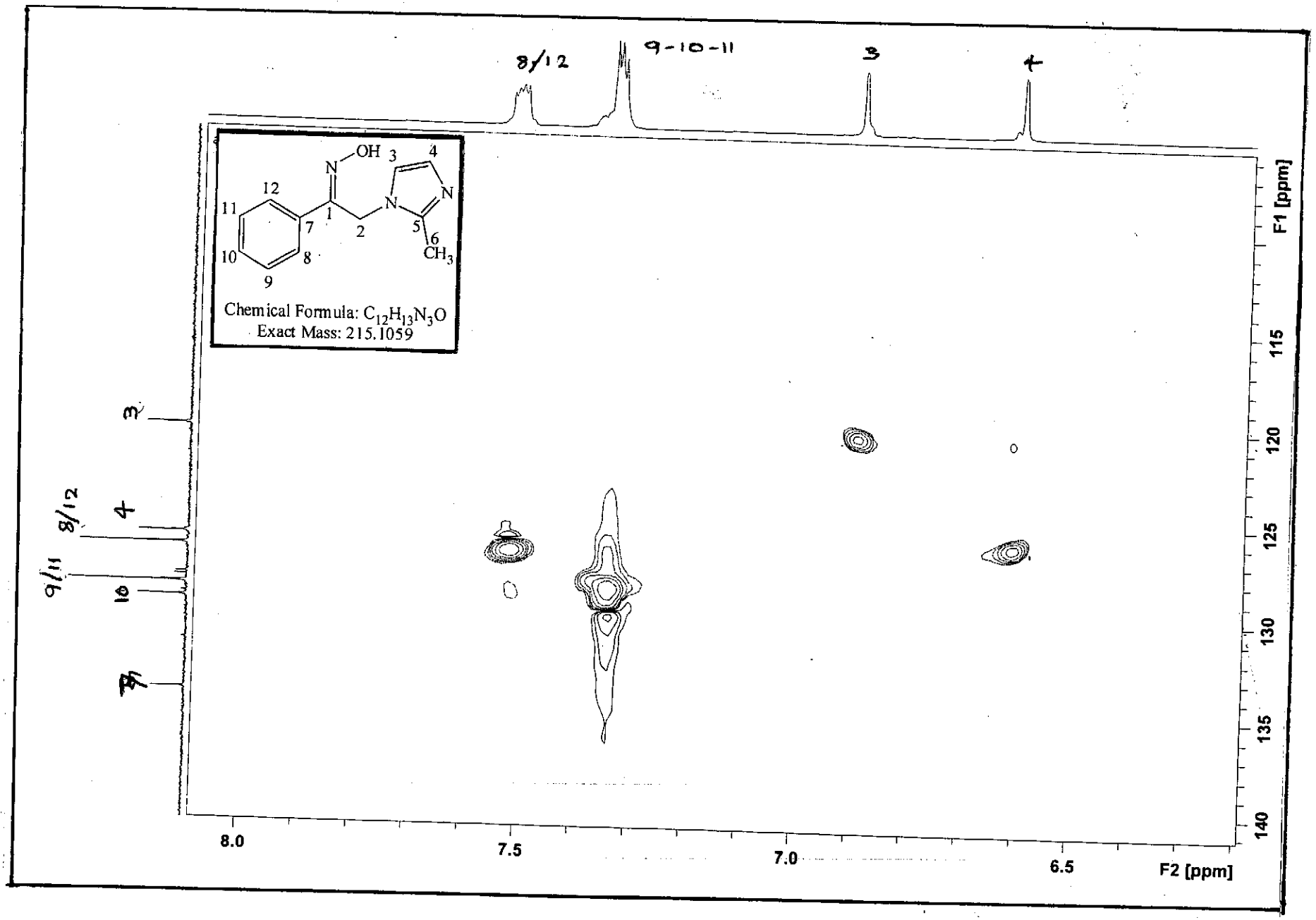

HSQC spectrum of compound 7, 2-(2-methyl-1H-imidazol-1-yl)-1-phenyl ethanone oxime

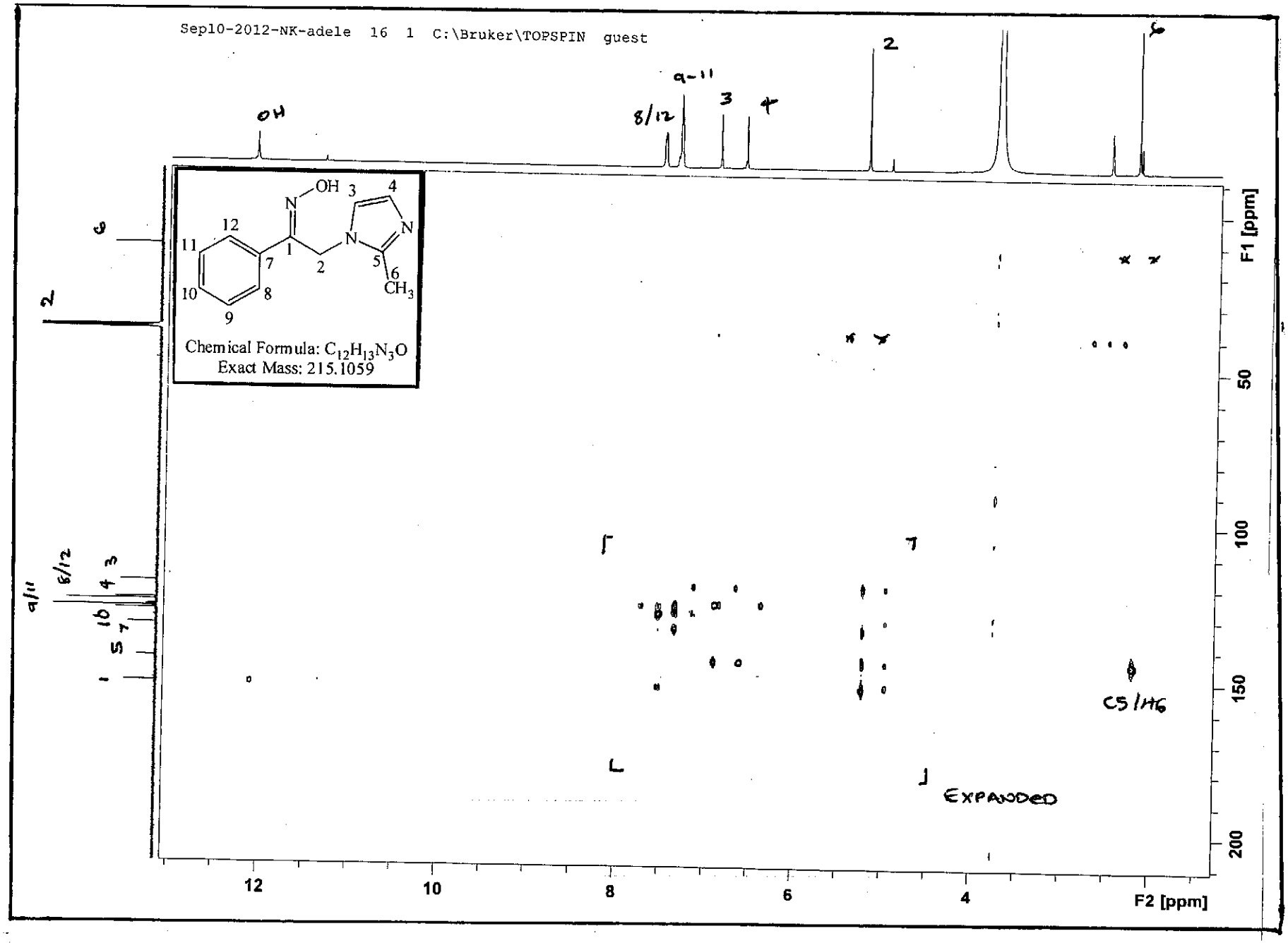

HMBC spectrum of compound 7 , 2-(2-methyl-1H-imidazol-1-yl)-1-phenyl ethanone oxime

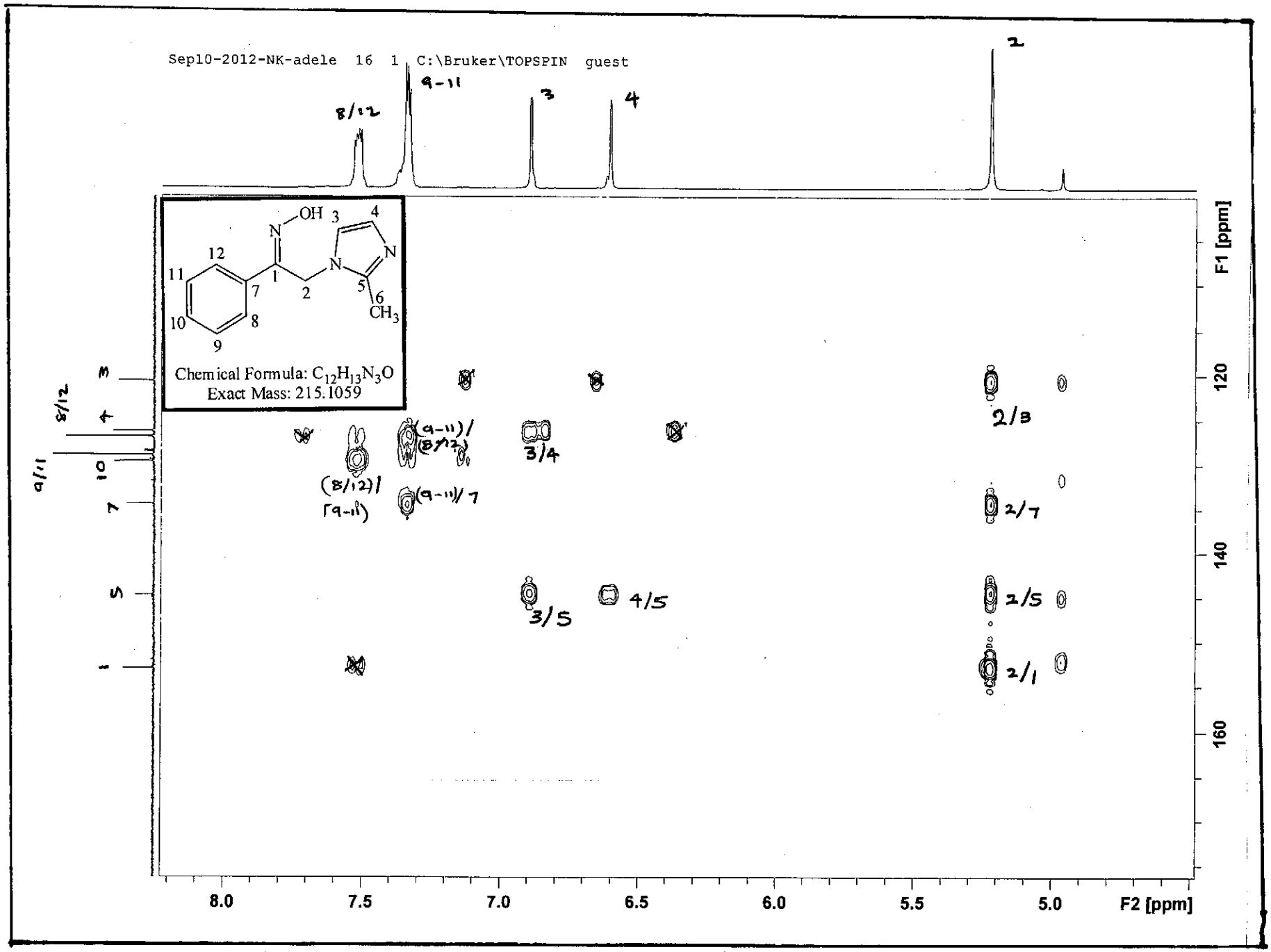

HMBC spectrum of compound 7, 2-(2-methyl-1H-imidazol-1-yl)-1-phenyl ethanone oxime

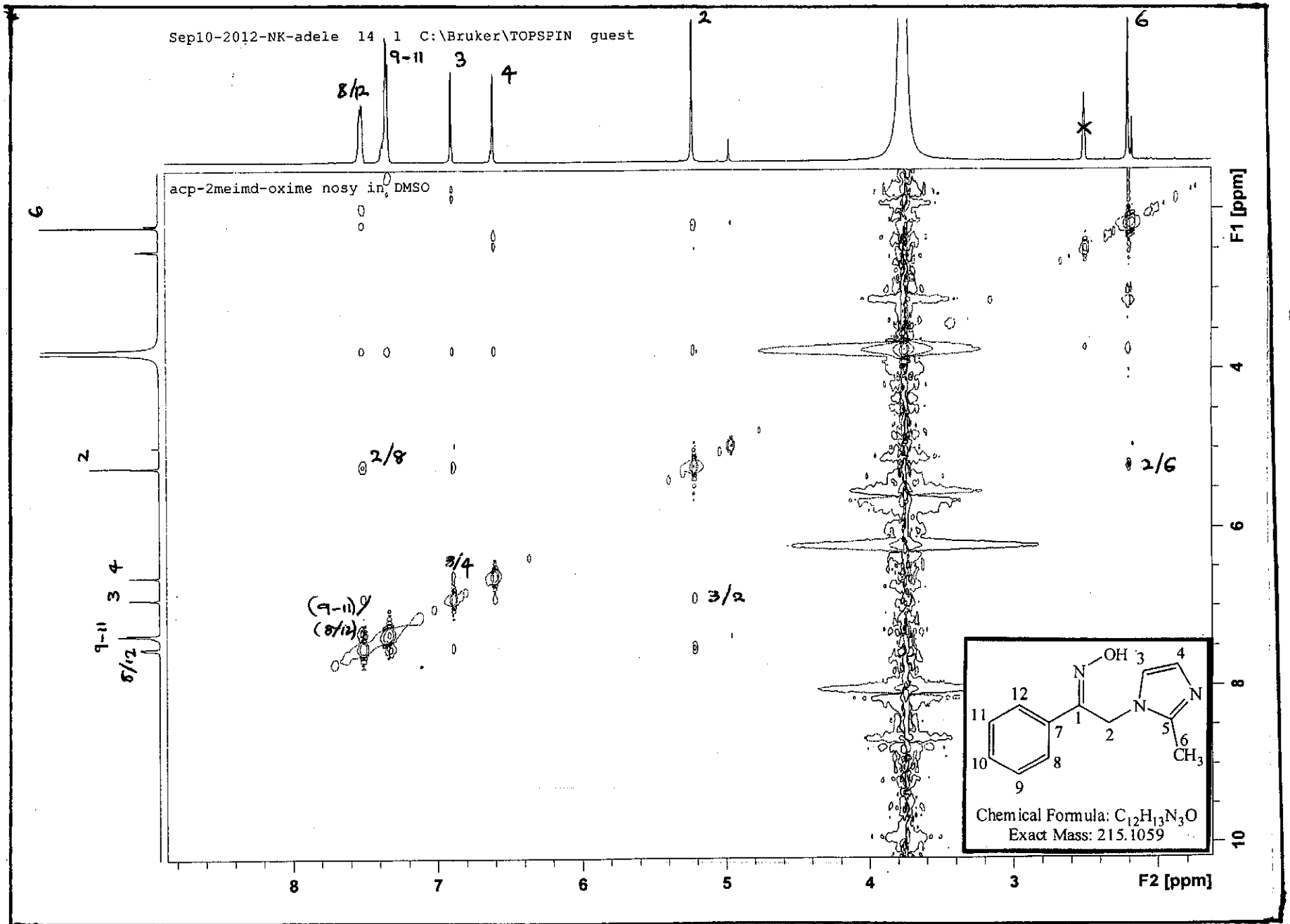

NOESY spectrum of compound 7 , 2-(2-methyl-1H-imidazol-1-yl)-1-phenyl ethanone oxime

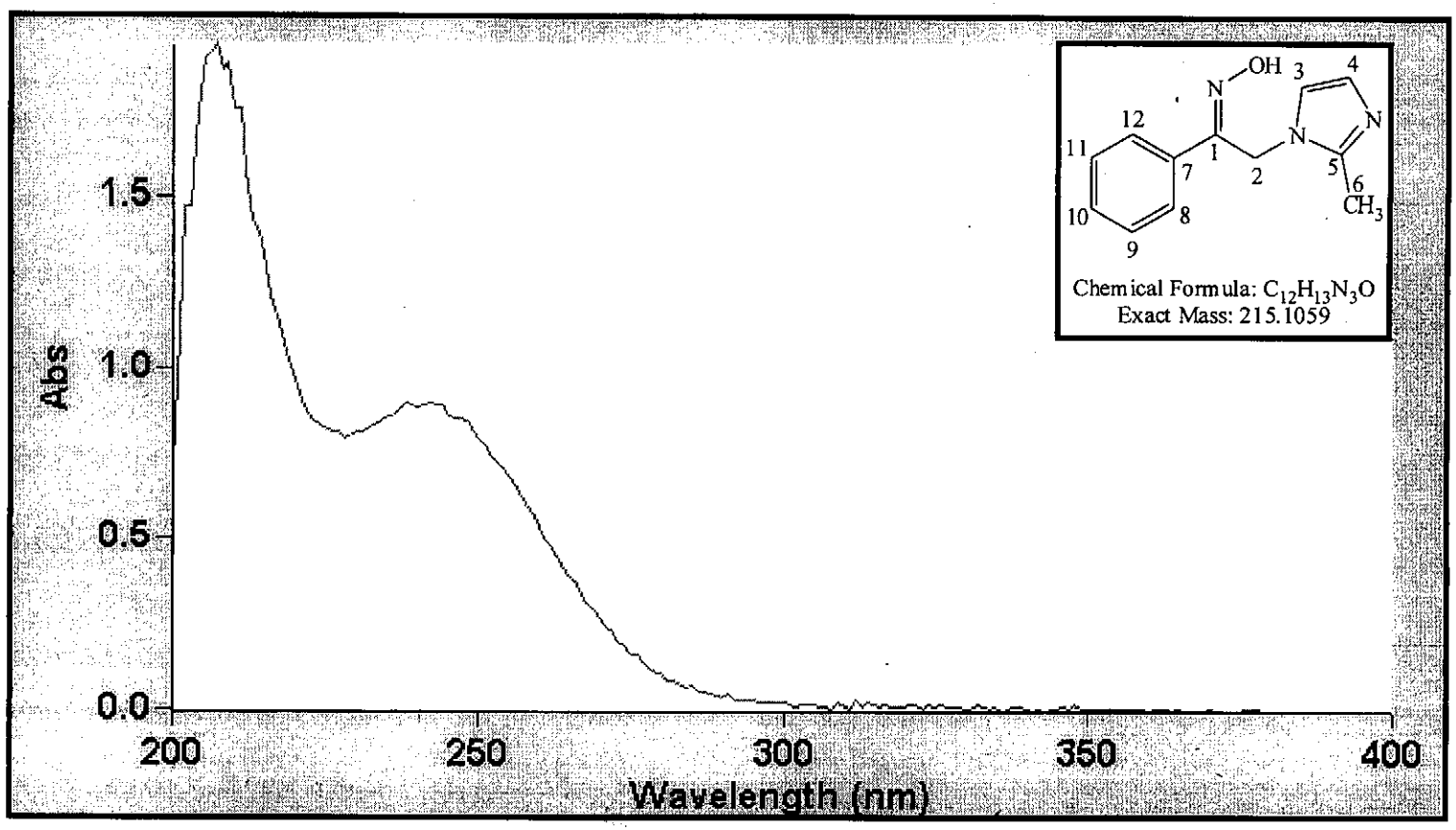

Ultra Violet spectrum of compound 7 , 2-(2-methyl-1H-imidazol-1-yl)-1-phenylethanone oxime

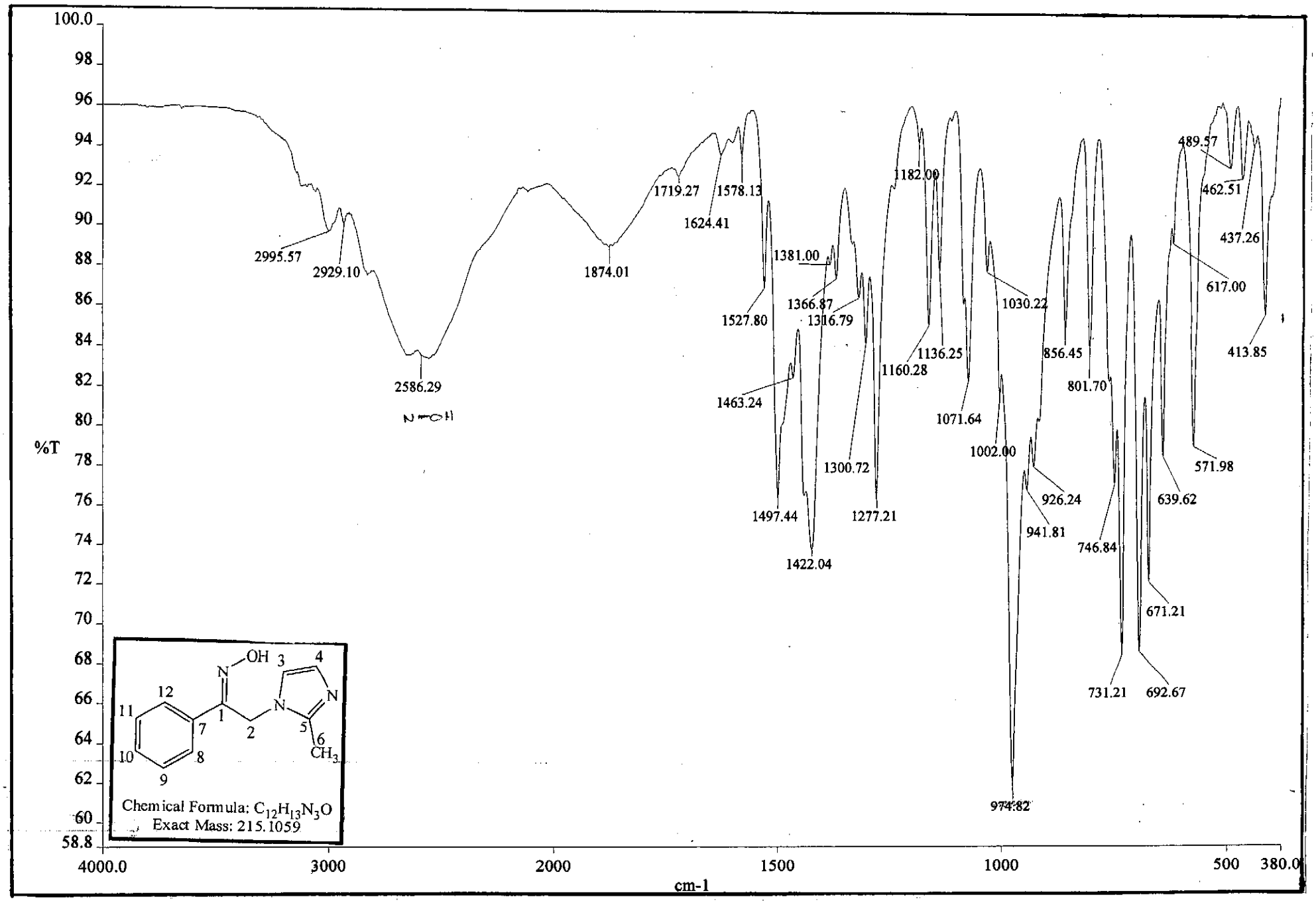

Infrared spectrum of compound 7 , 2-(2-methyl-1H-imidazol-1-yl)-1-phenyl ethanone oxime

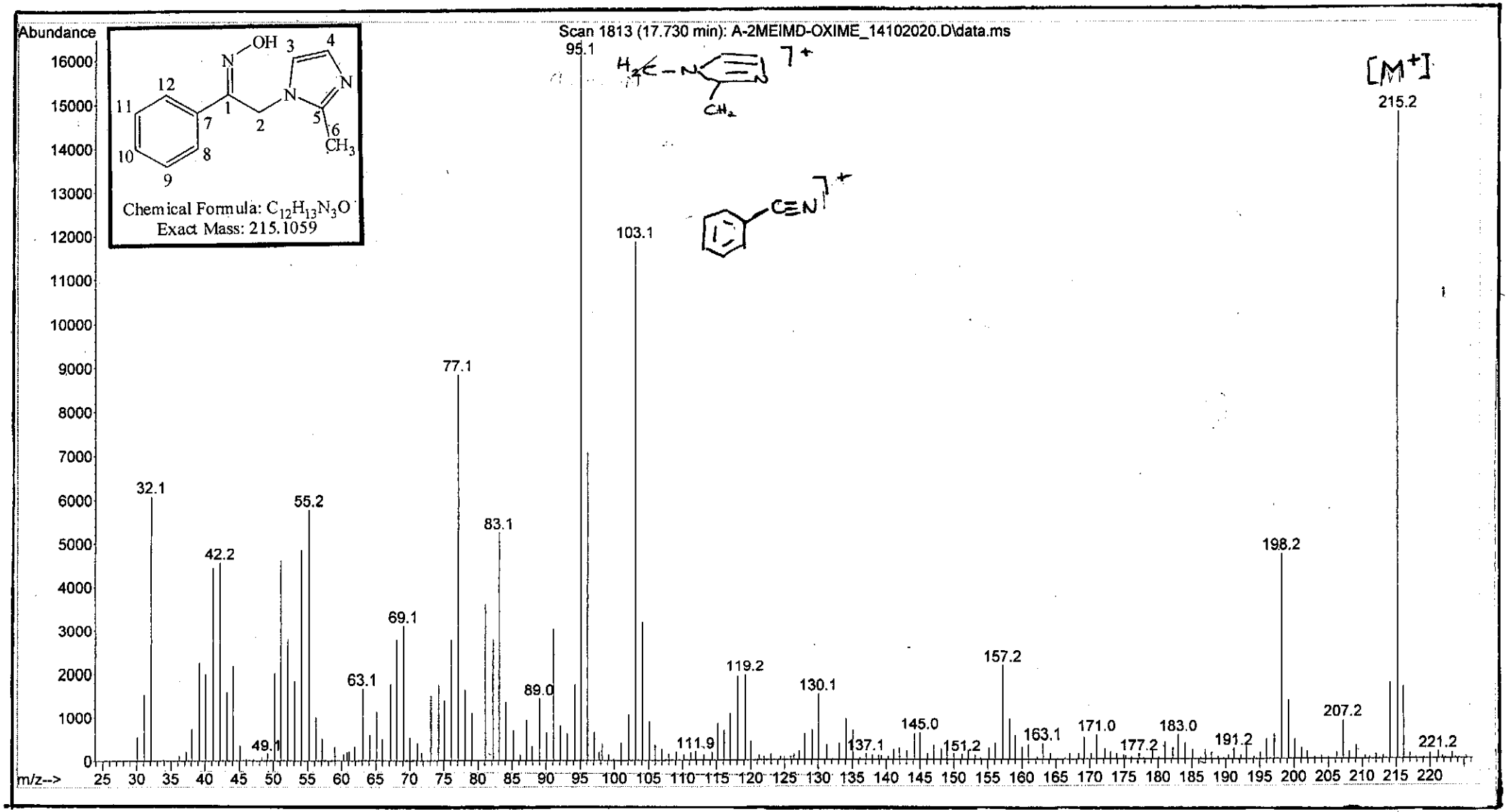

Mass spectrum of compound 7 , 2-(2-methyl-1H-imidazol-1-yl)-1-phenyl ethanone oxime

Elemental Composition Report

Single Mass Analysis
Tolerance = 5.0 PPM / DBE: min = -1.5, max = 50.0
Element prediction: Off
Number of isotope peaks used for i-FIT = 3

Monoisotopic Mass, Even Electron Ions
18 formula(e) evaluated with 1 results within limits (up to 50 best isotopic matches for each mass)
Elements Used:
C: 10-15 H: 10-15 N: 0-5 O: 0-5
Adele 3 2 (0.017) Cm (1:31)
TOF MS ES+

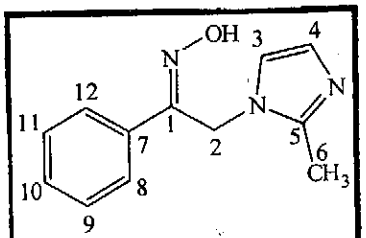

Chemical Formula: $C_{12}H_{13}N_3O$
Exact Mass: 215.1059

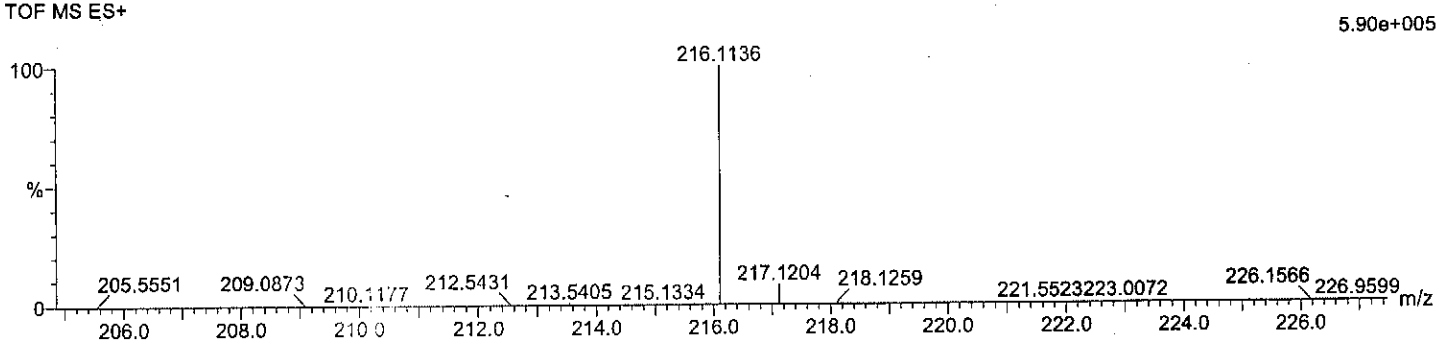

Minimum:				-1.5			
Maximum:		5.0	5.0	50.0			
Mass	Calc. Mass	mDa	PPM	DBE	i-FIT	i-FIT (Norm)	Formula
216.1136	216.1137	-0.1	-0.5	7.5	327.6	0.0	C12 H14 N3 O

HRMS spectrum of compound 7, 2-(2-methyl-1H-imidazol-1-yl)-1-phenyl ethanone oxime

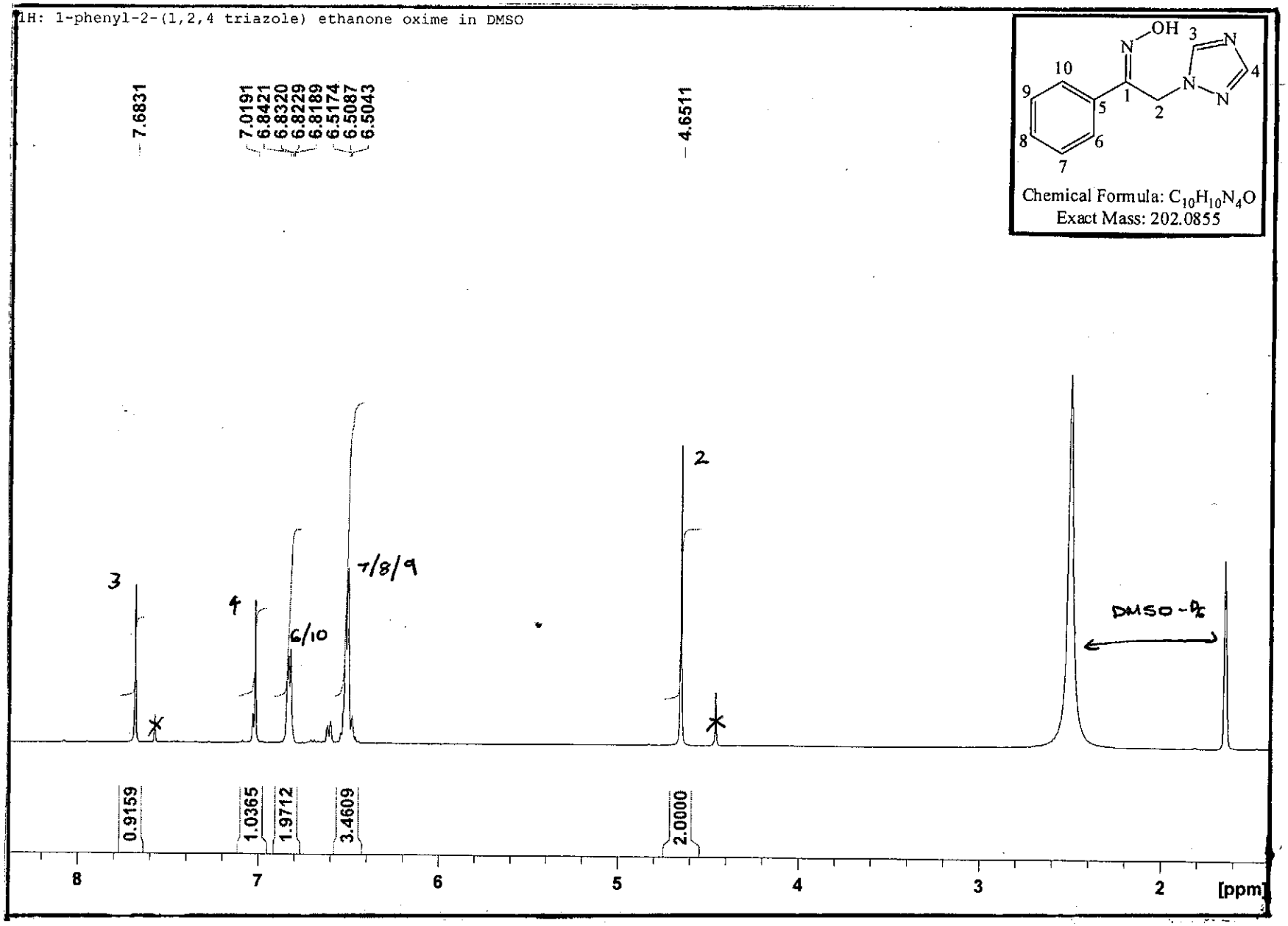

^{1}H NMR spectrum of compound 8., 1-phenyl-2-[1,2,4]triazol-1-yl-ethanone oxime

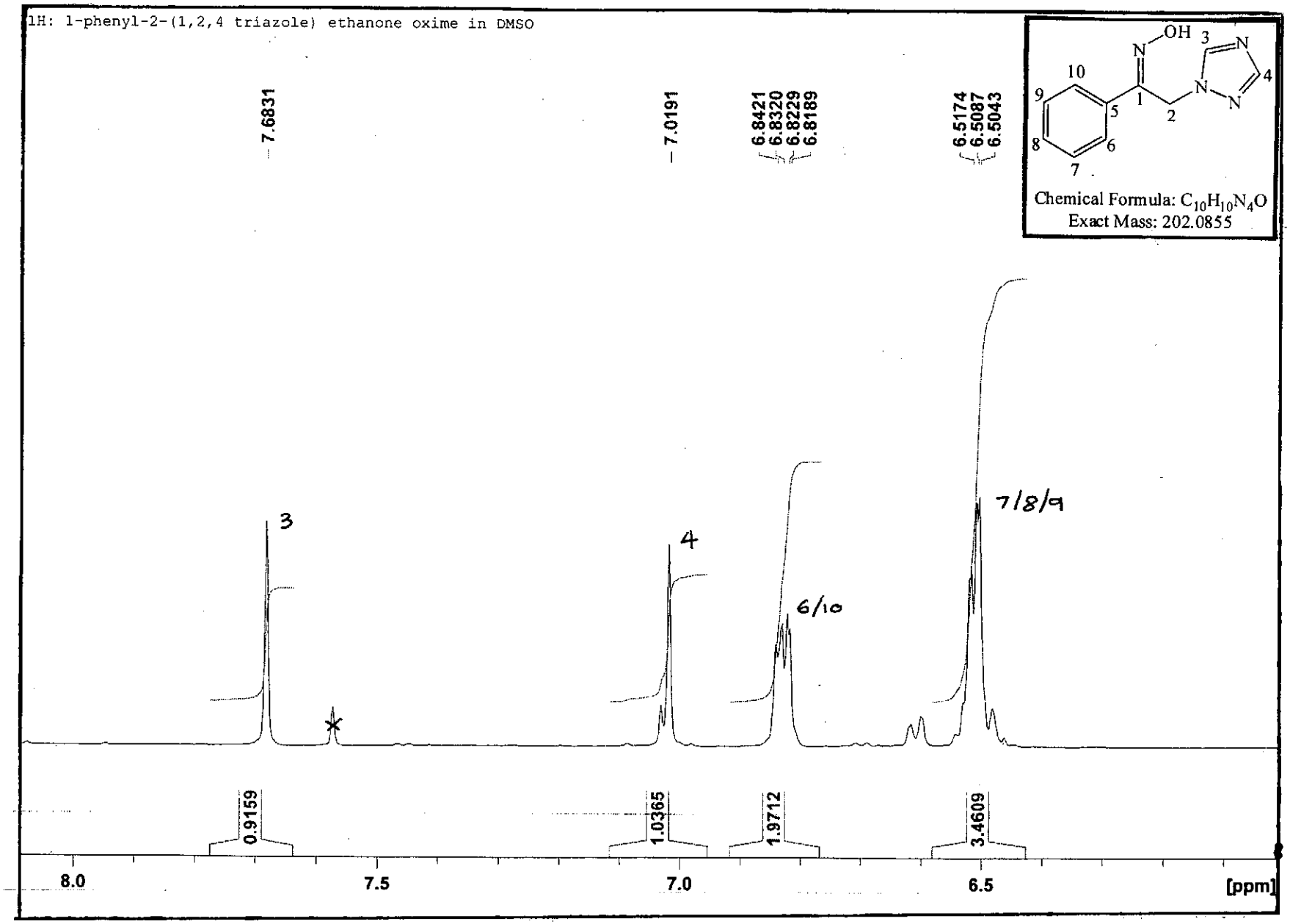

^{1}H NMR spectrum of compound 8., 1-phenyl-2-[1,2,4]triazol-1-yl-ethanone oxime

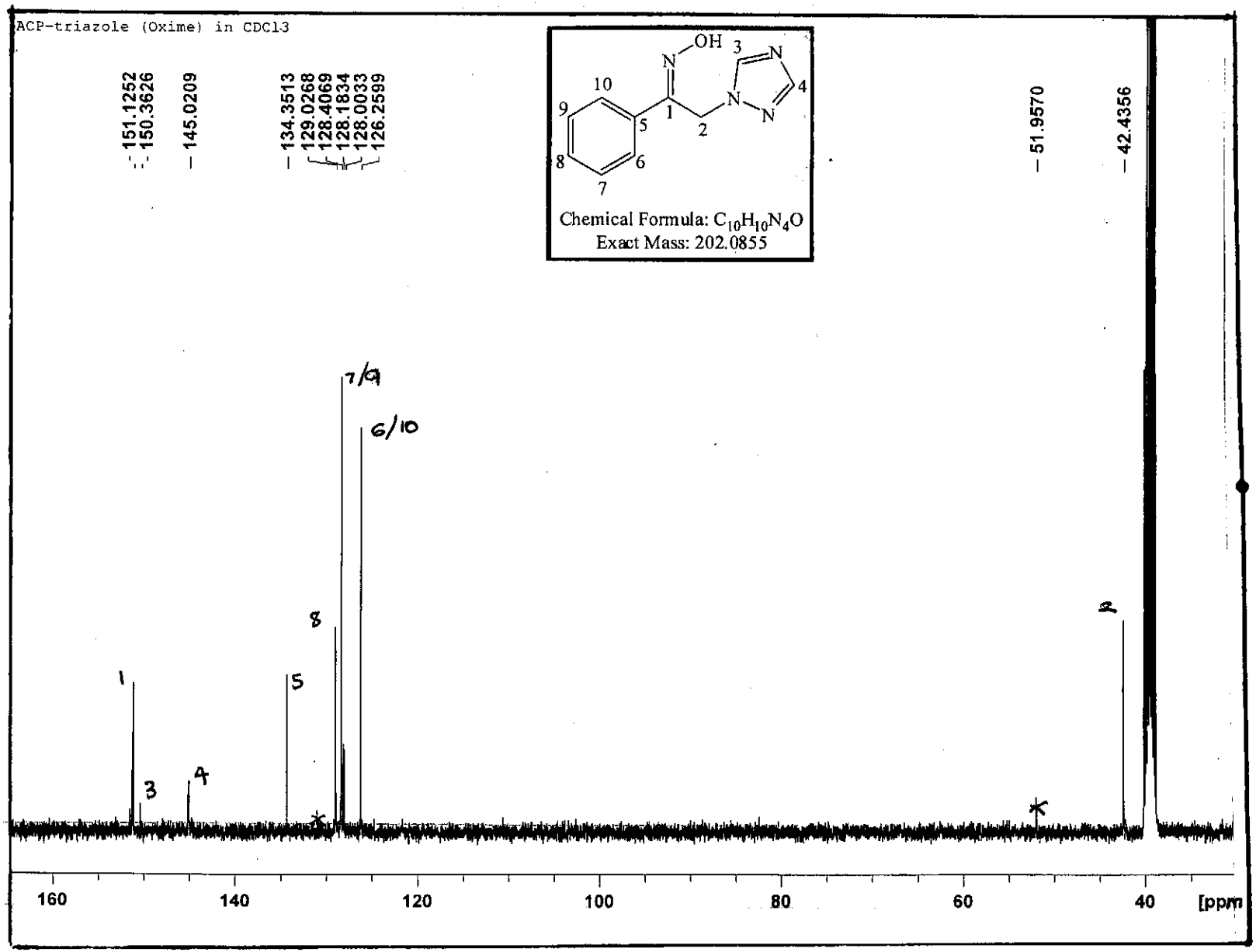

^{13}C NMR of compound 8 |, 1-phenyl-2-[1,2,4]triazol-1-yl-ethanone oxime

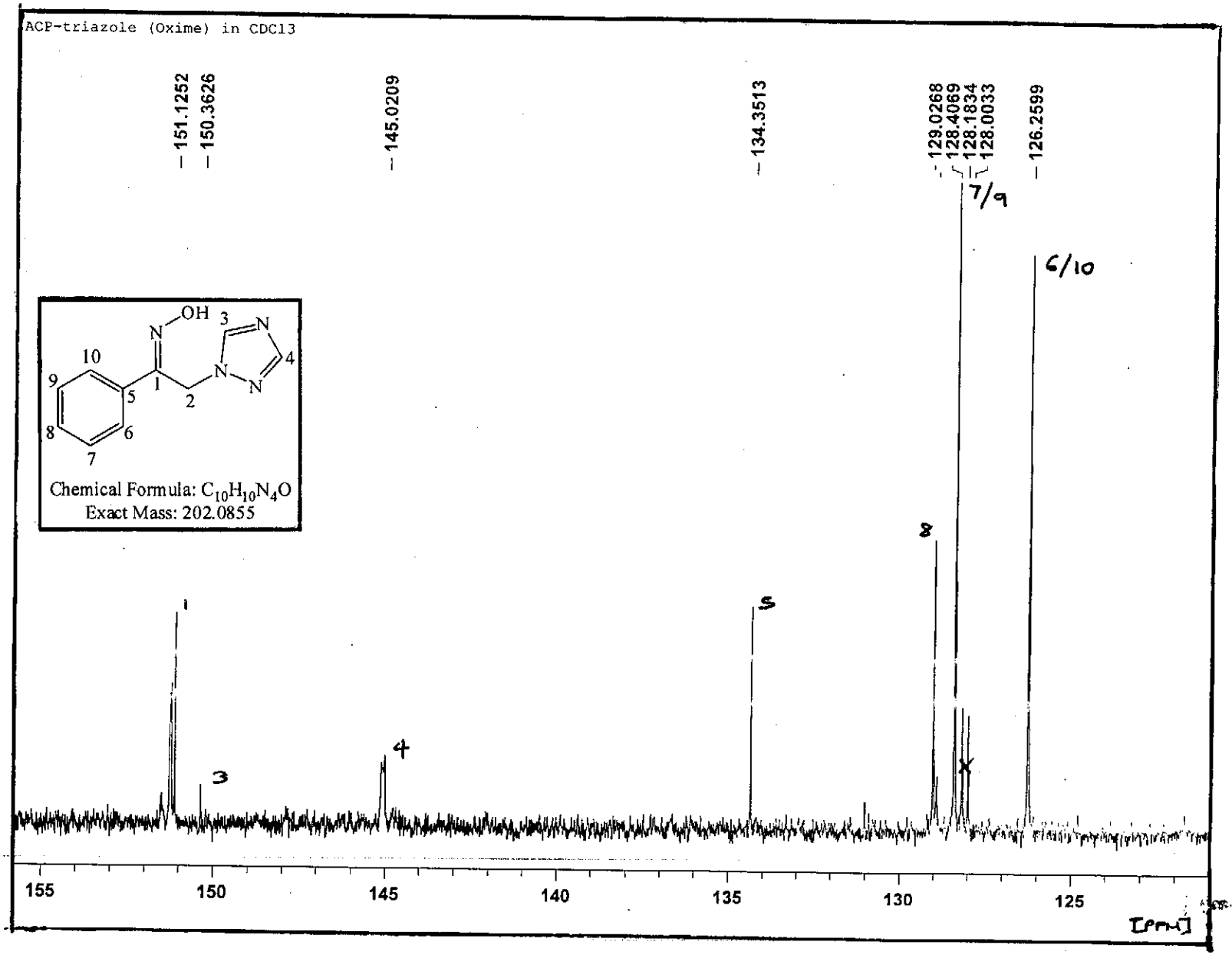

^{13}C NMR of compound 8, 1-phenyl-2-[1,2,4]triazol-1-yl-ethanone oxime

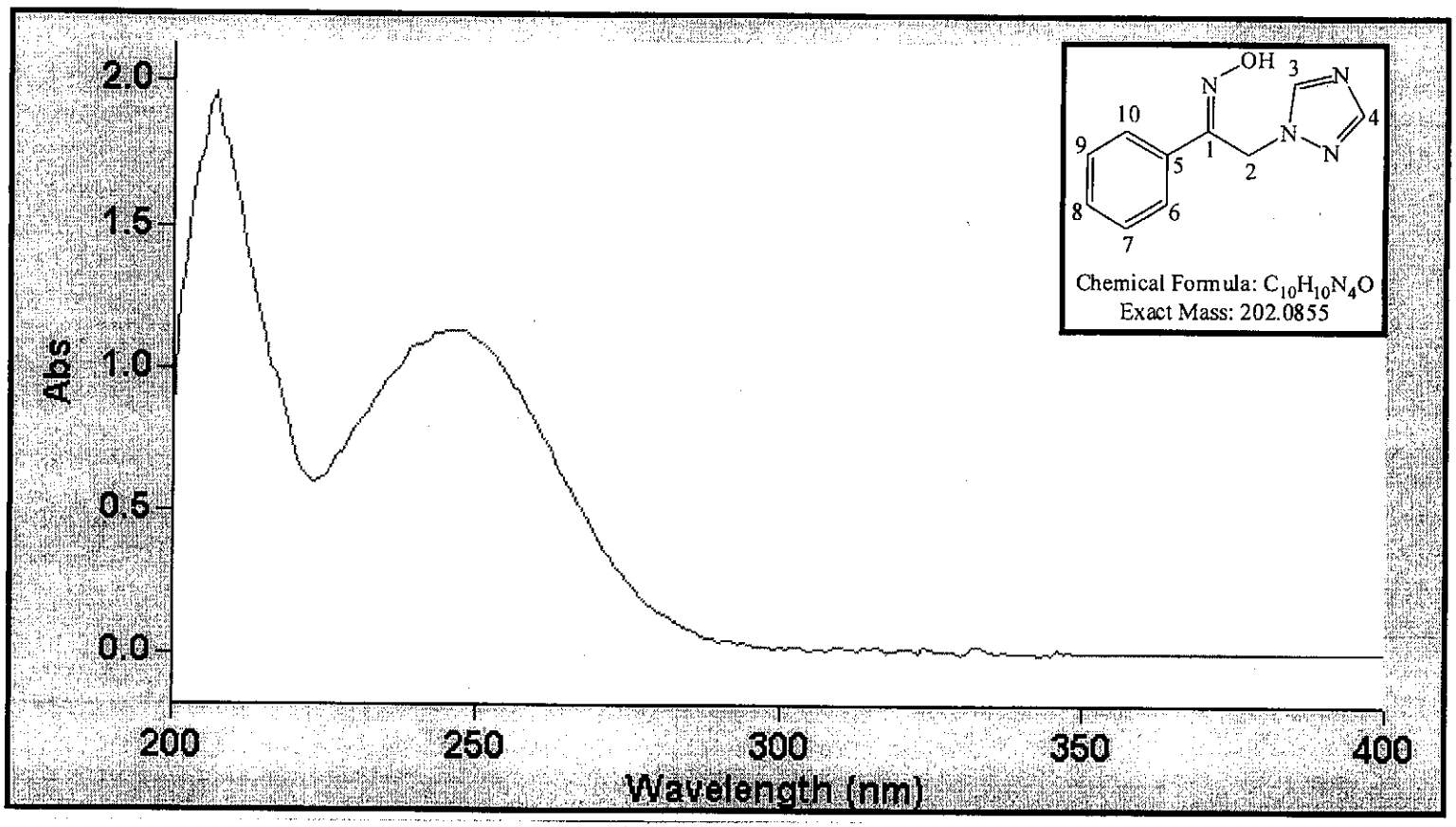

Ultra Violet spectrum of compound 8l, 1-phenyl-2-(1H-1,2,4-triazol-1-yl)ethanone oxime

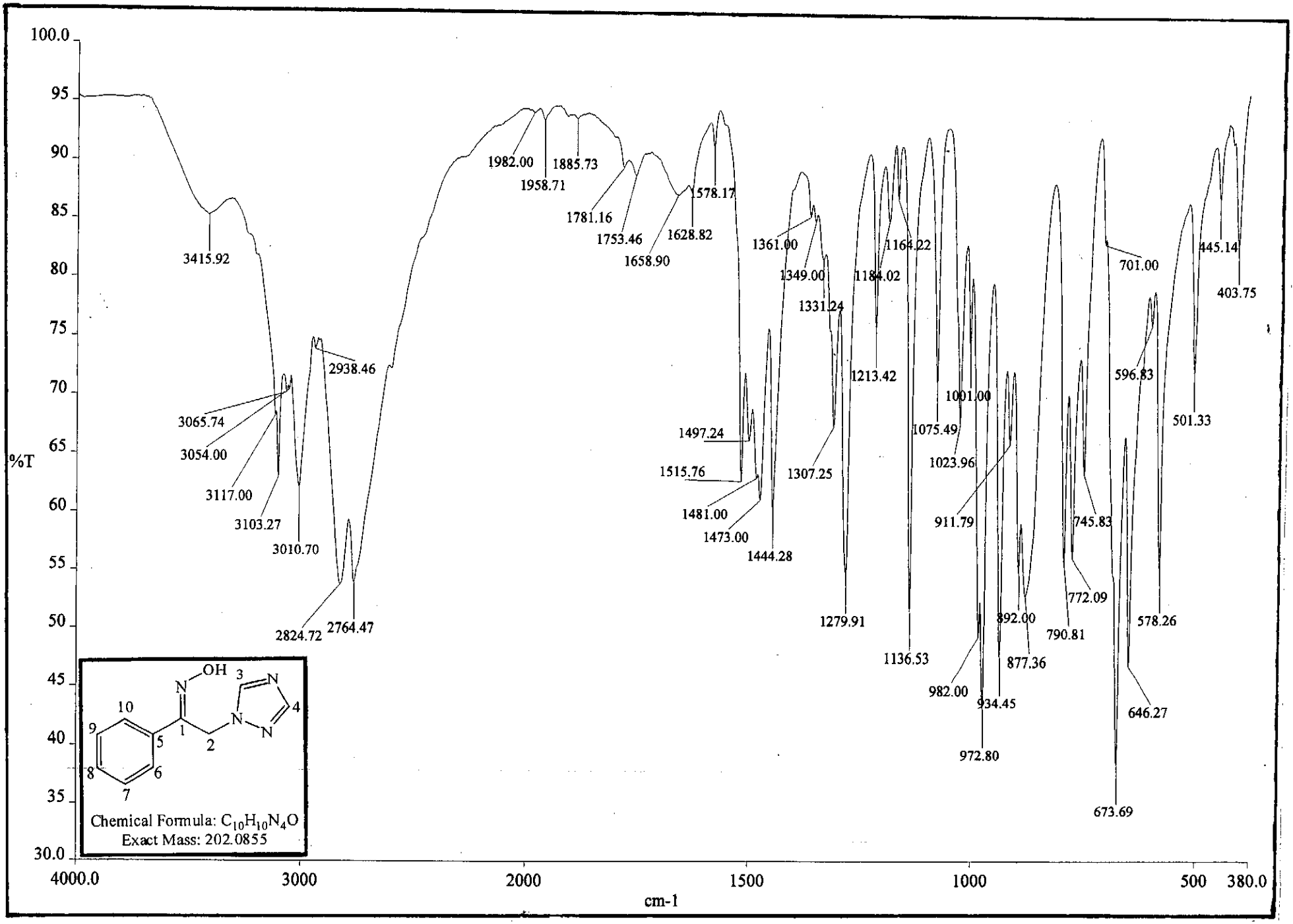

Infrared spectrum of compound 8, 1-phenyl-2-[1,2,4]triazol-1-yl-ethanone oxime

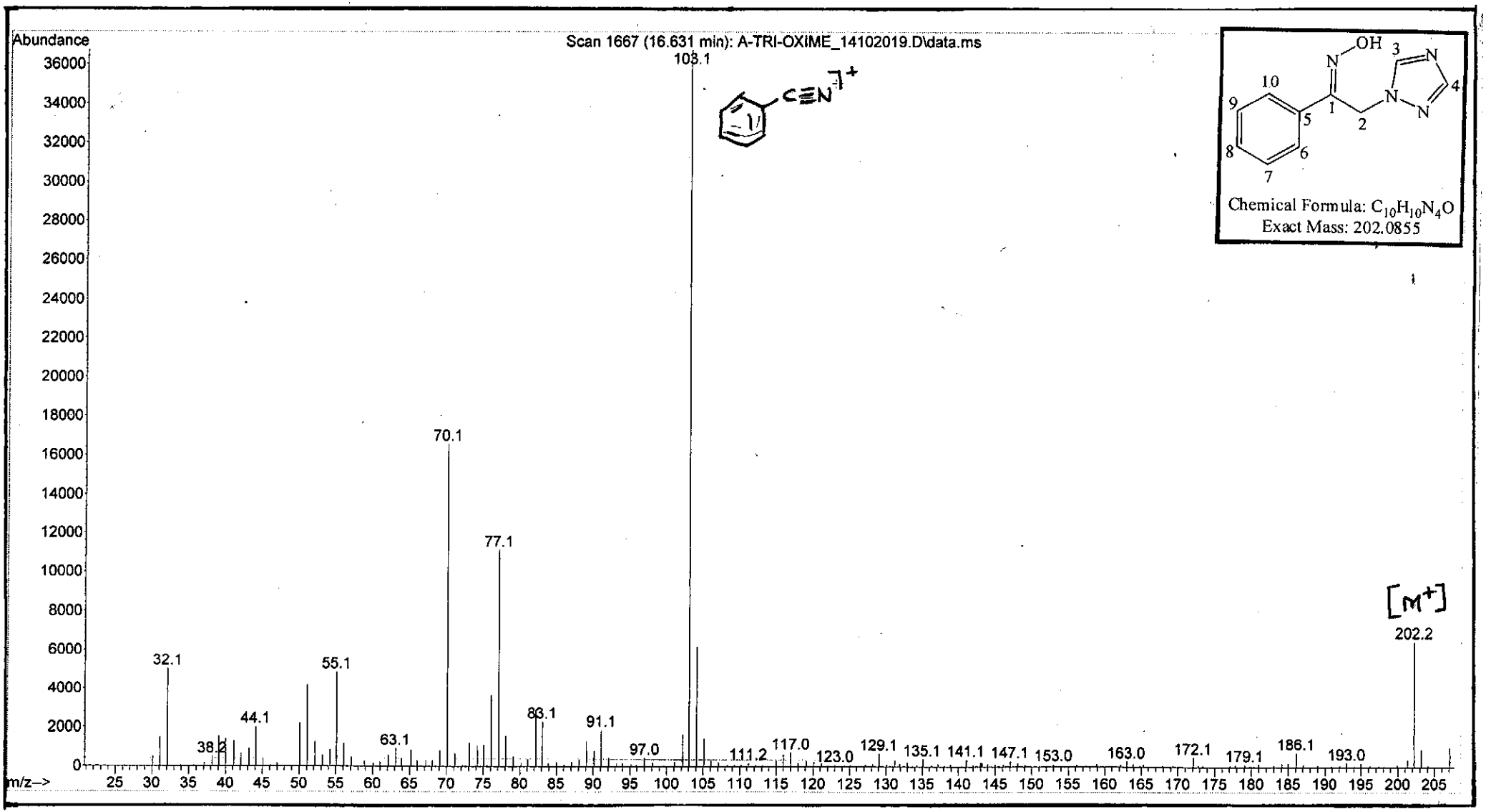

Mass spectrum of compound 8l, 1-phenyl-2-[1,2,4]triazol-1-yl-ethanone oxime

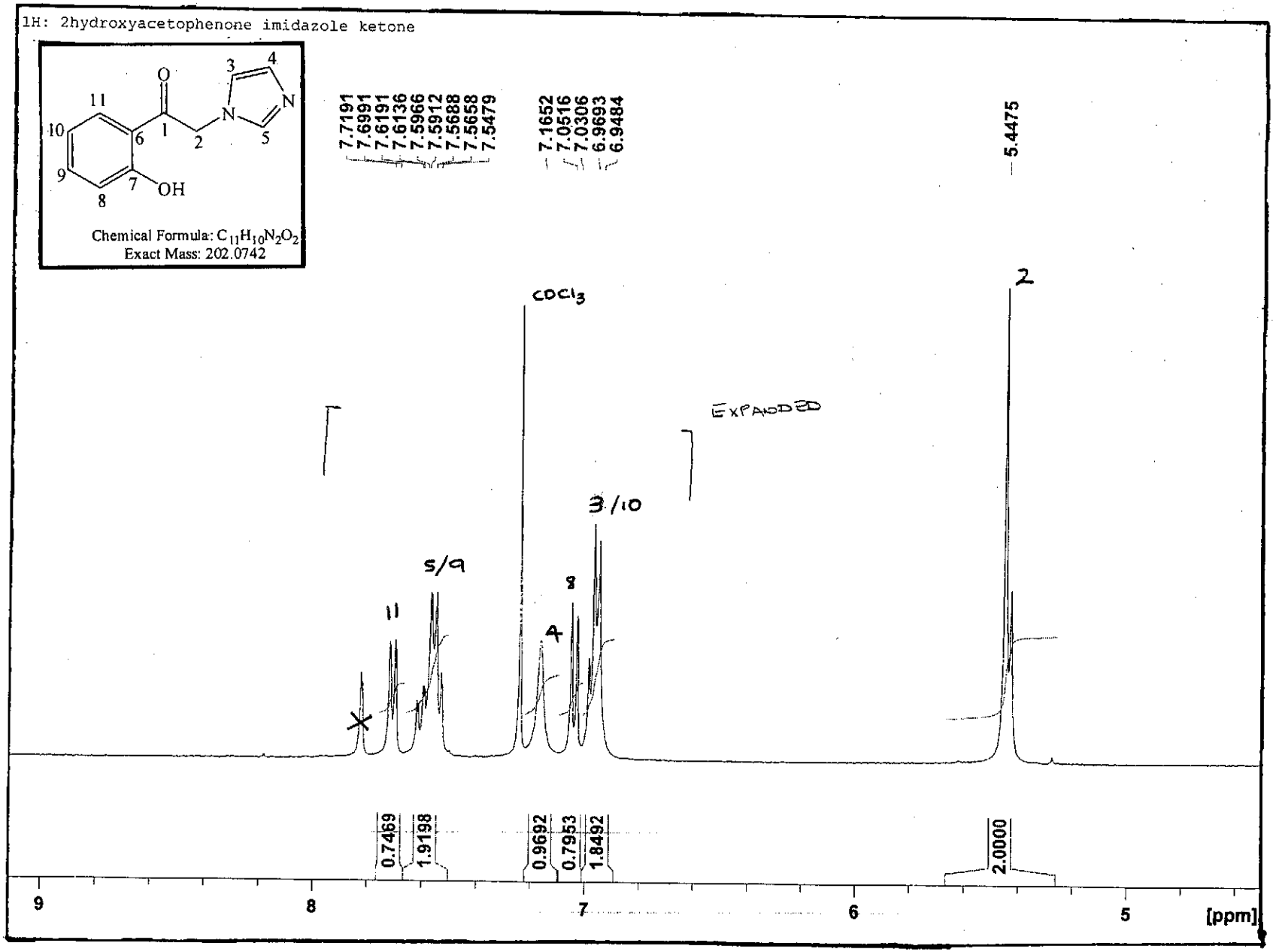

^{1}H NMR spectrum of compound 9 ,1-(2-hydroxy-phenyl)-2-imidazol-1-yl ethanone

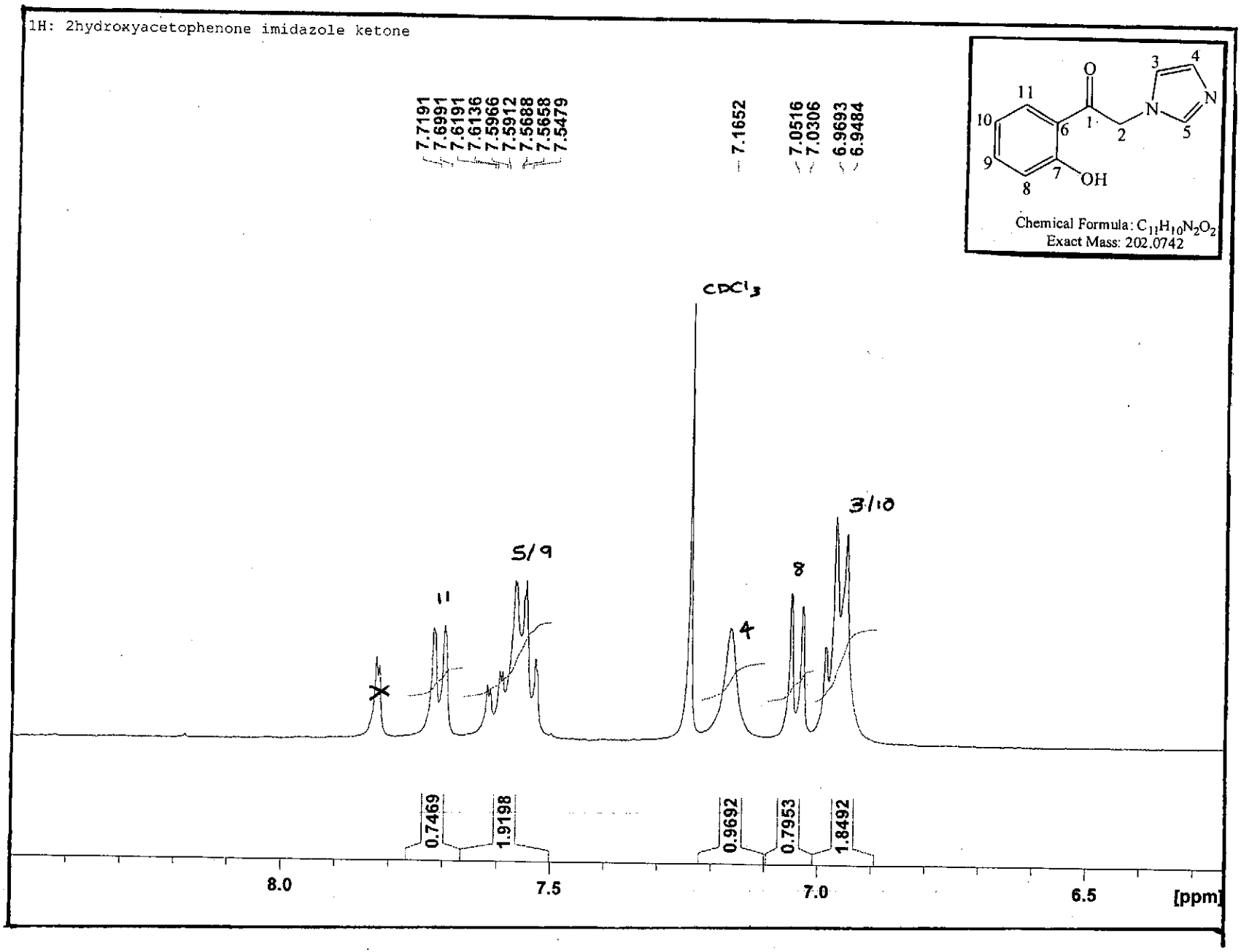

^{1}H NMR spectrum of compound 9, 1-(2-hydroxy-phenyl)-2-imidazol-1-yl ethanone

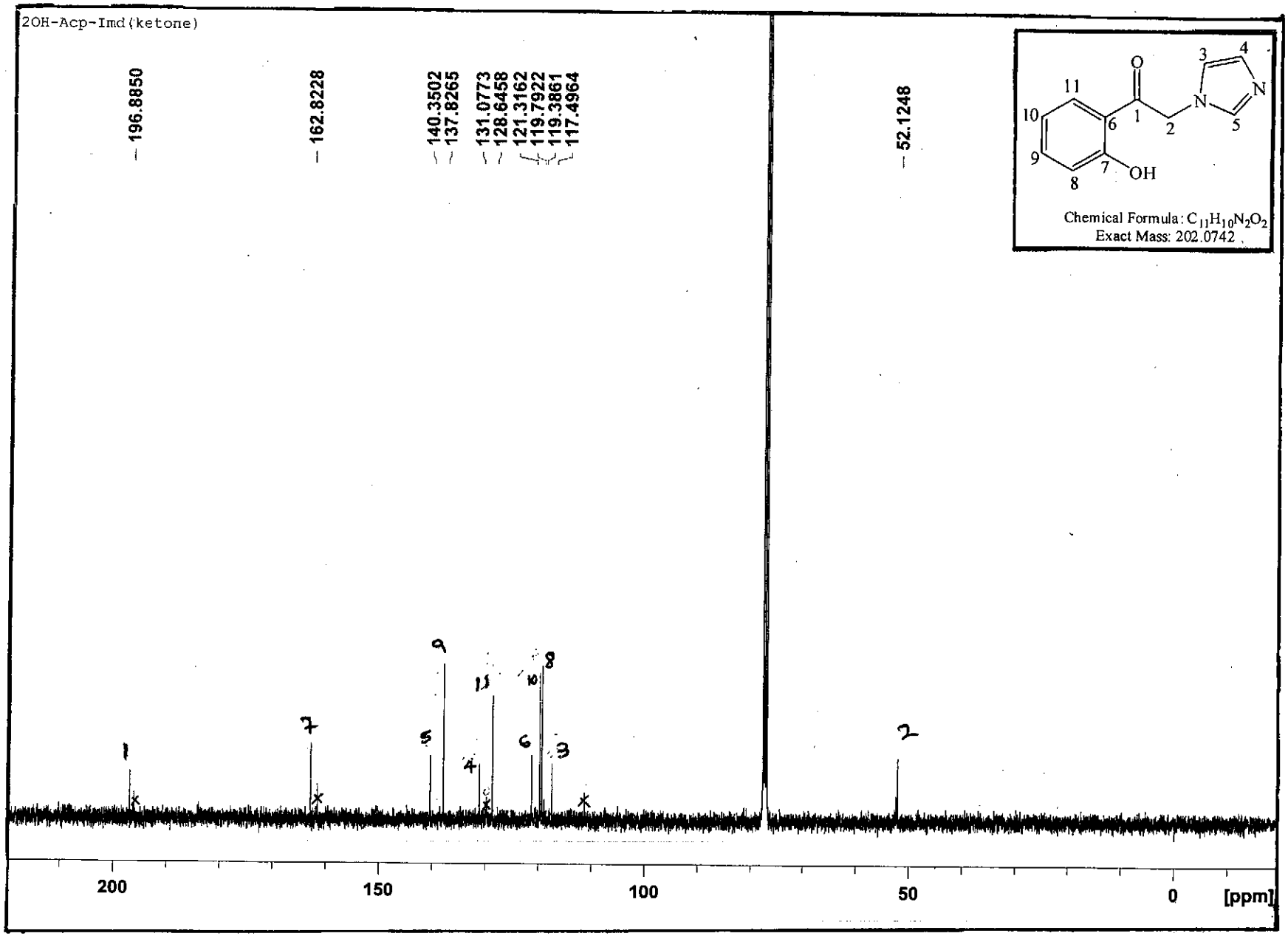

^{13}C NMR of compound 9, 1-(2-hydroxy-phenyl)-2-imidazol-1-yl ethanone

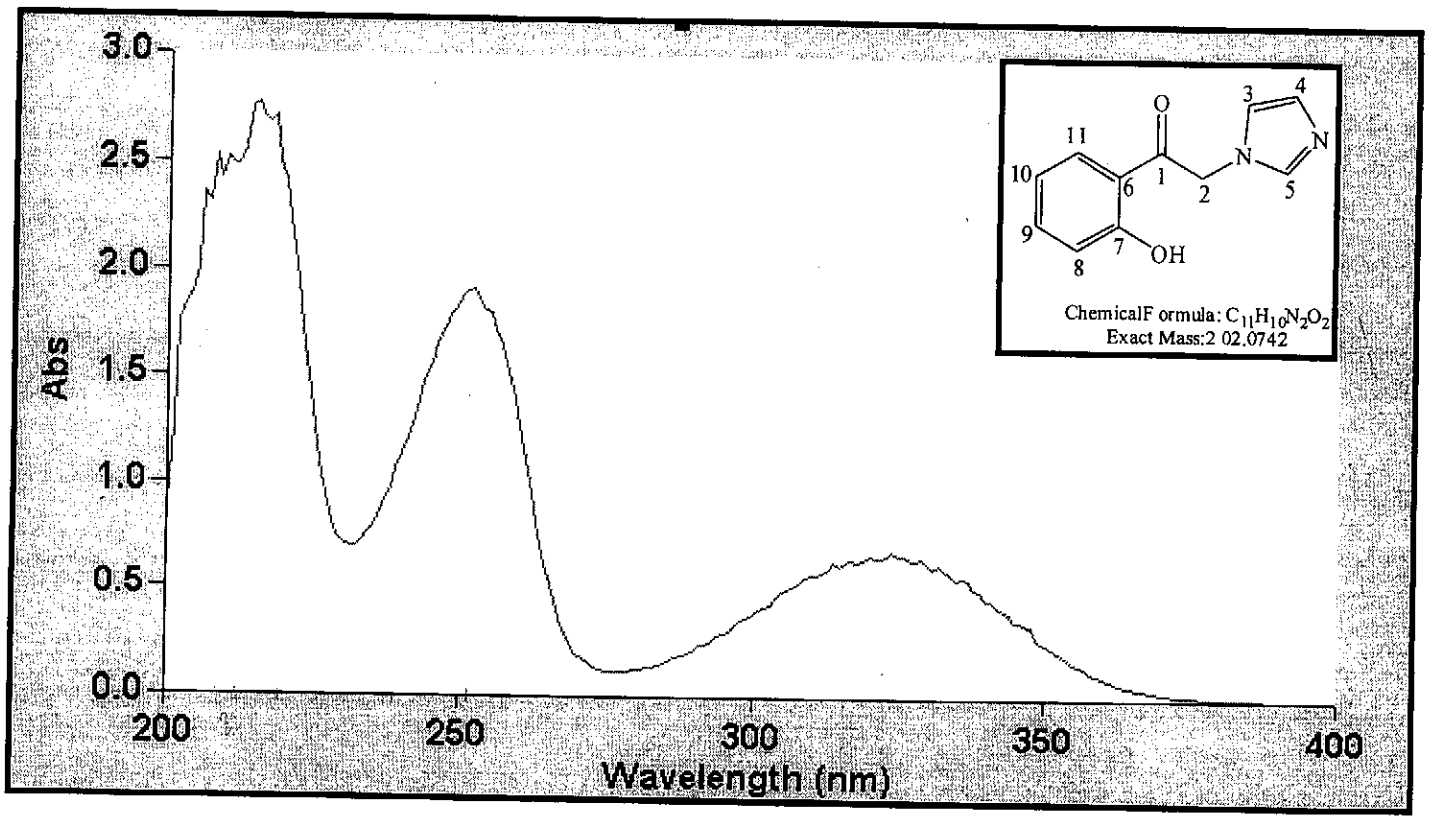

Ultra Violet spectrum of compound 9, 1-(2-hydroxyphenyl)-2-(1H-imidazol-1-yl)ethanone

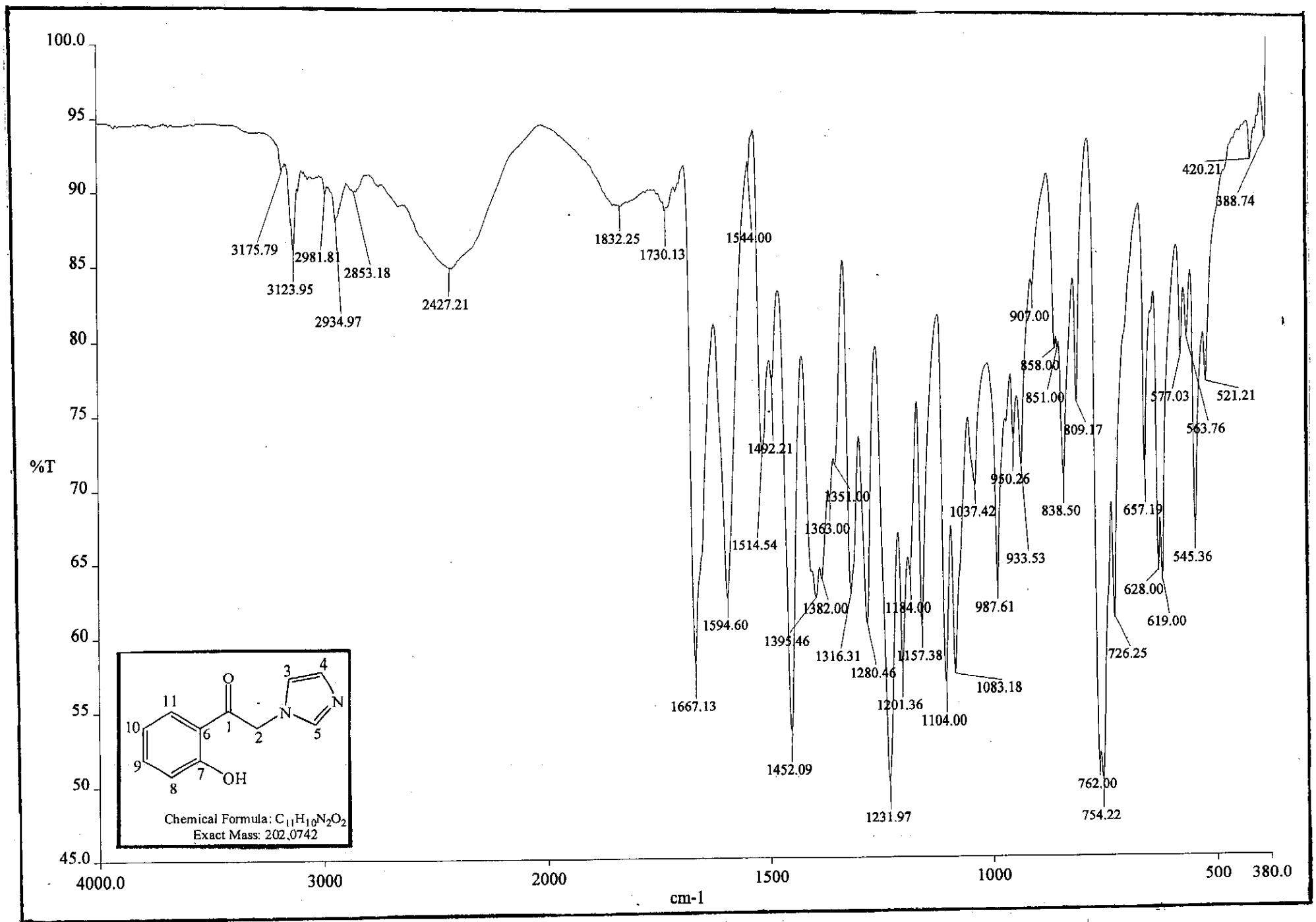

Infrared spectrum of compound 9, 1-(2-hydroxy-phenyl)-2-imidazol-1-yl ethanone

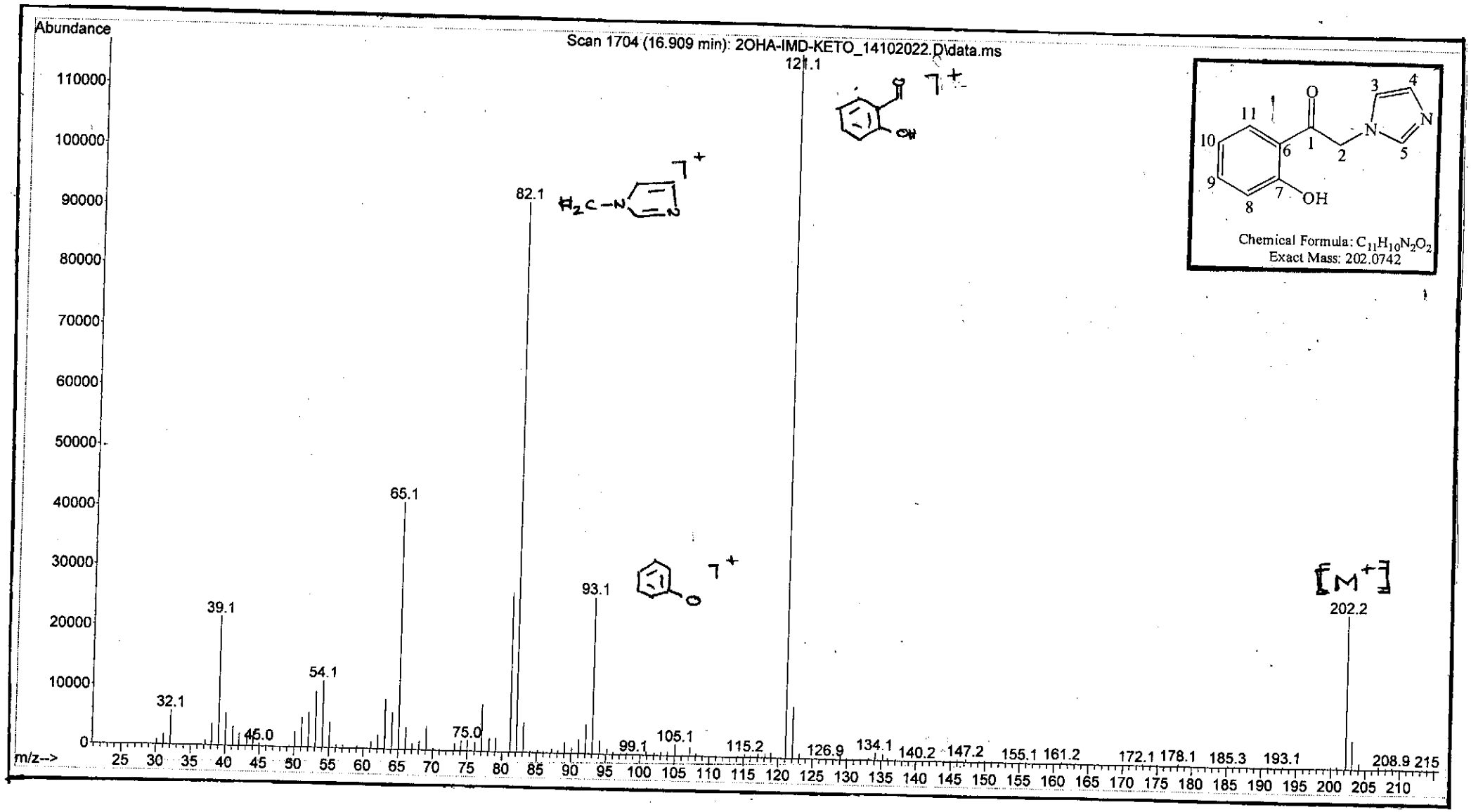

Mass spectrum of compound 9, 1-(2-hydroxy-phenyl)-2-imidazol-1-yl ethanone

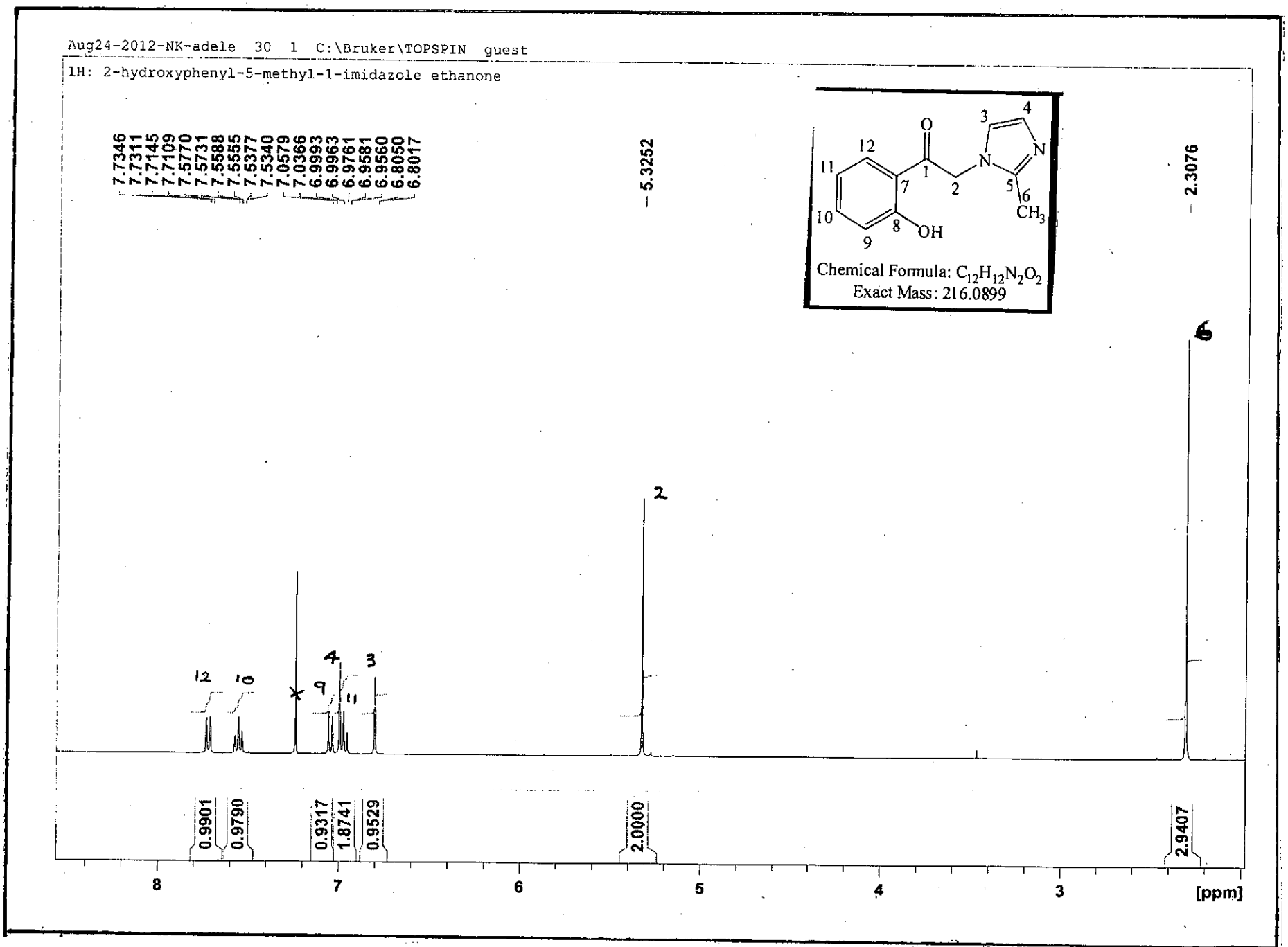

^{1}H NMR spectrum of compound 10, 1-(2-hydroxyphenyl)-2-(5-methyl-1H-imidazol-1-yl)ethanone

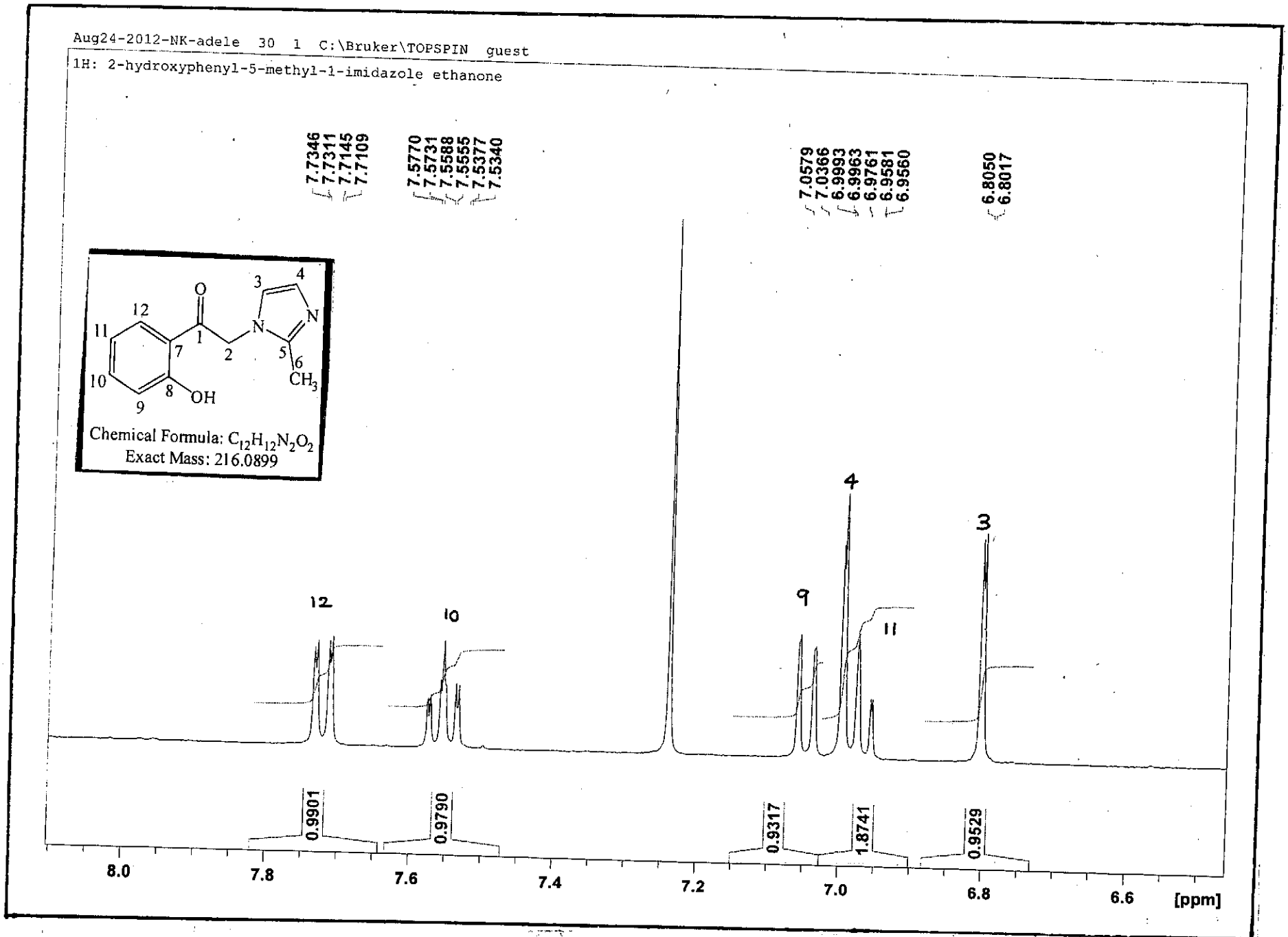

^{1}H NMR spectrum of compound10, 1-(2-hydroxyphenyl)-2-(5-methyl-1H-imidazol-1-yl)ethanone

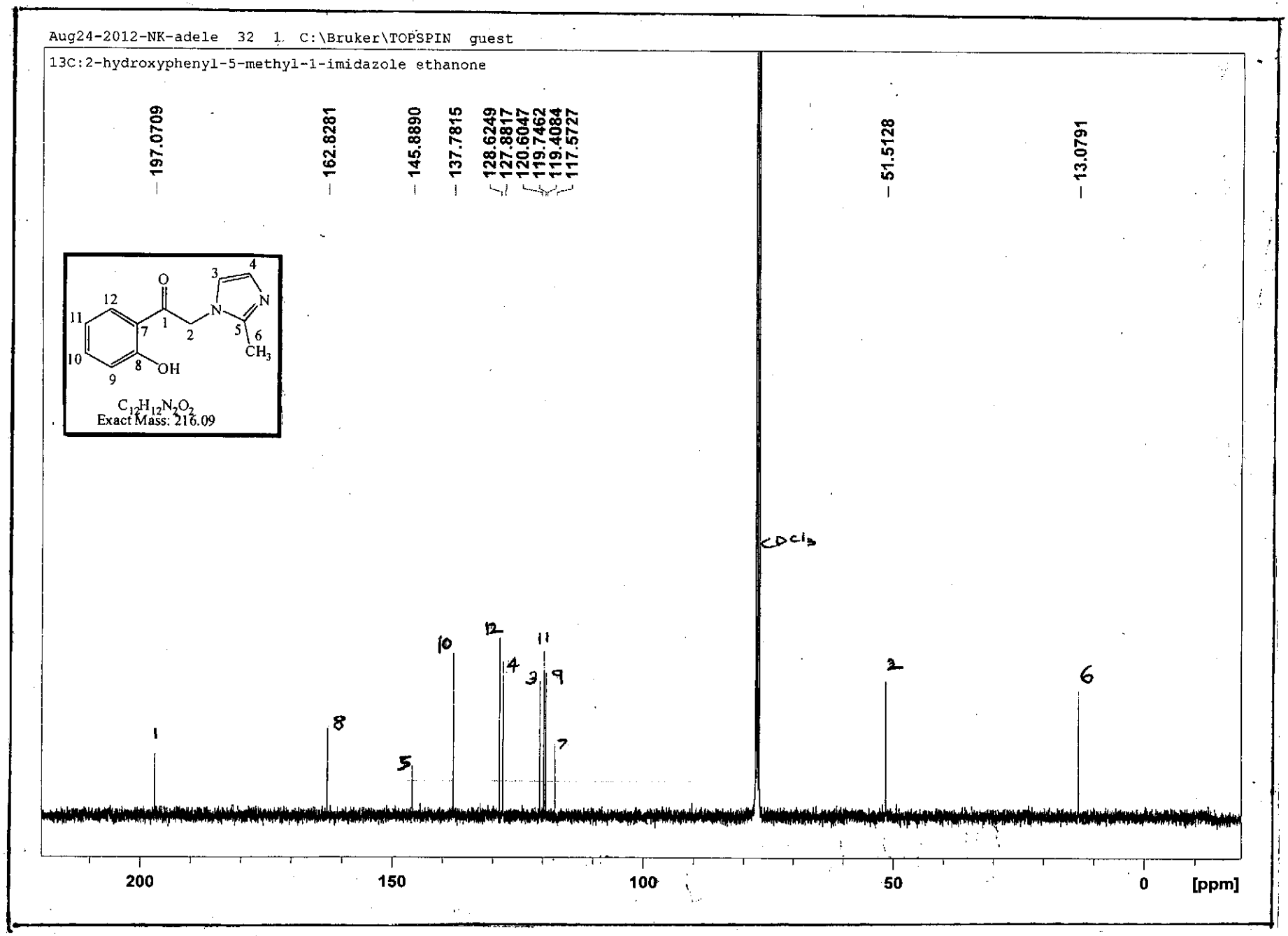

^{13}C NMR of compound10,1-(2-hydroxyphenyl)-2-(5-methyl-1H-imidazol-1-yl)ethanone

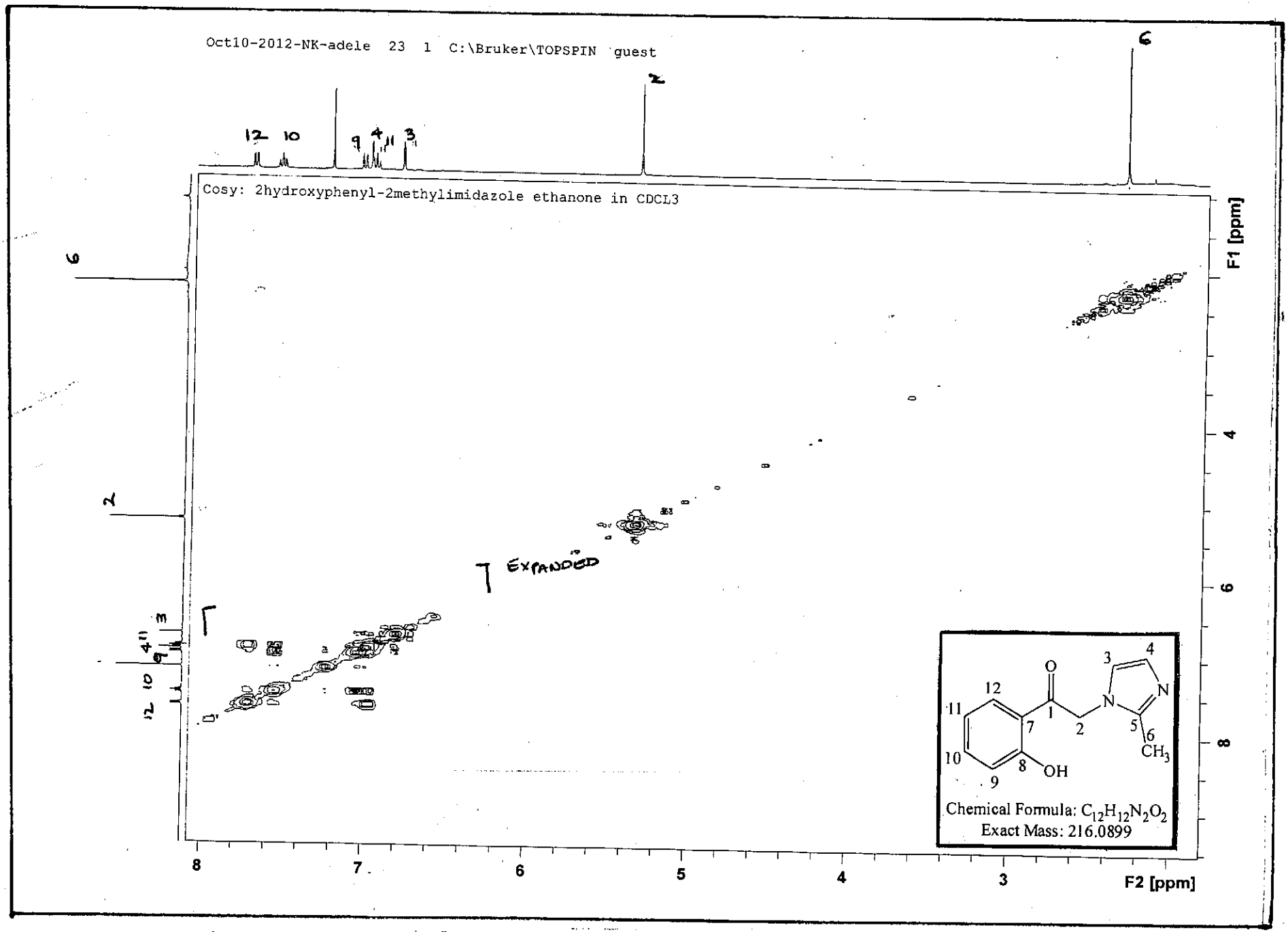

COSY spectrum of compound10,1-(2-hydroxyphenyl)-2-(5-methyl-1H-imidazol-1-yl)ethanone

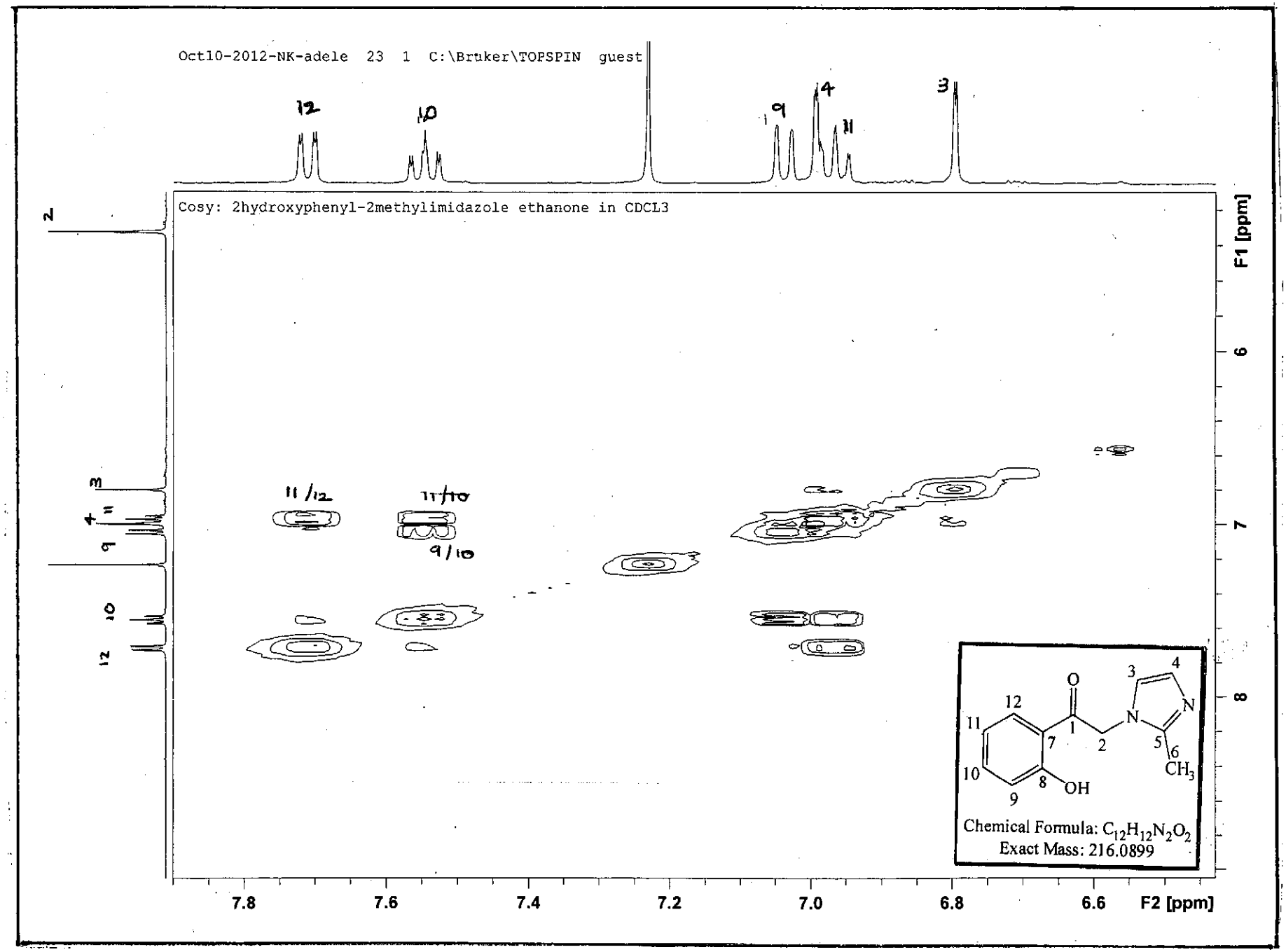

COSY spectrum of compound 10, 1-(2-hydroxyphenyl)-2-(5-methyl-1H-imidazol-1-yl)ethanone

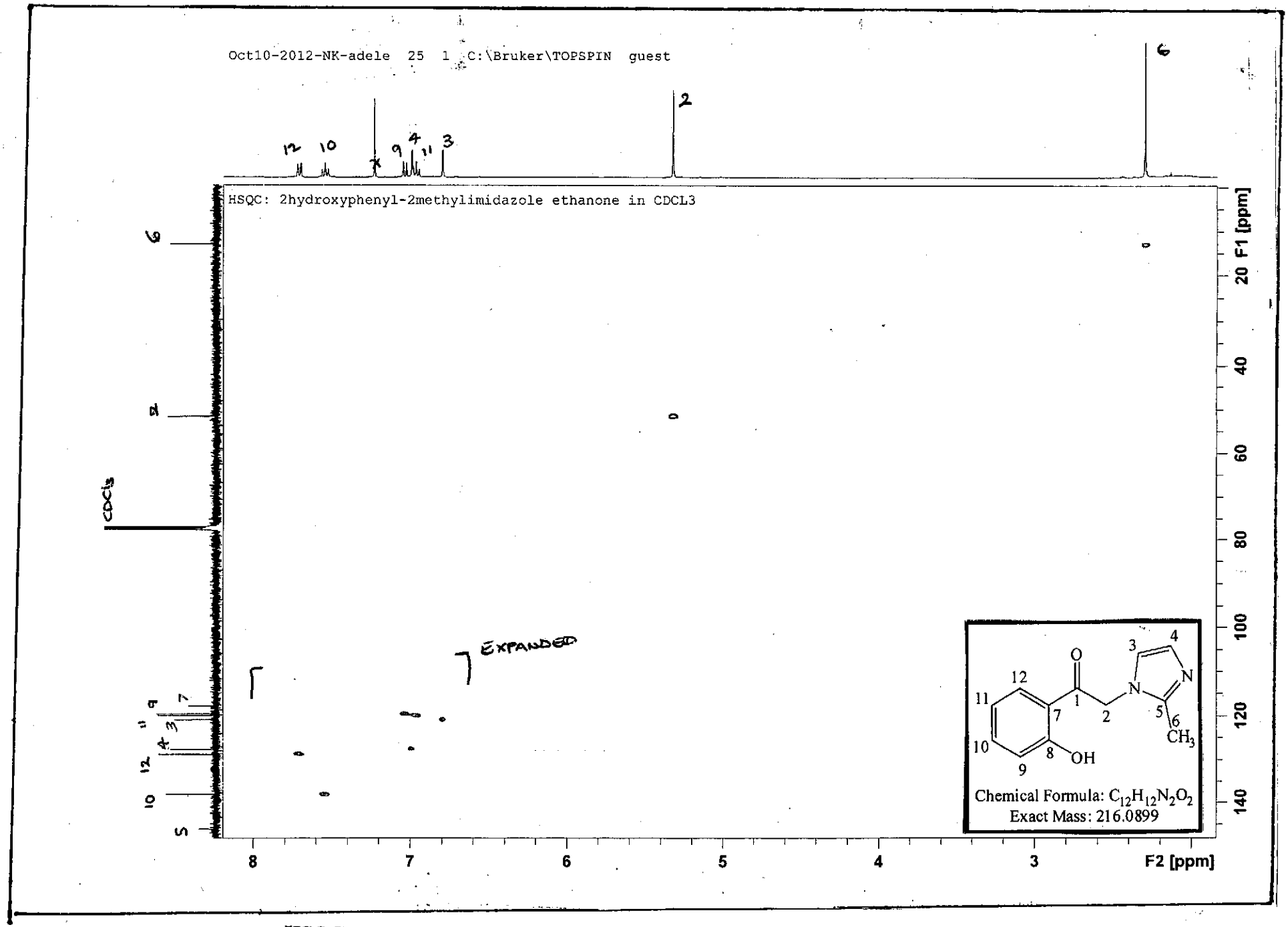

HSQC spectrum of compound10,1-(2-hydroxyphenyl)-2-(5-methyl-1H-imidazol-1-yl)ethanone

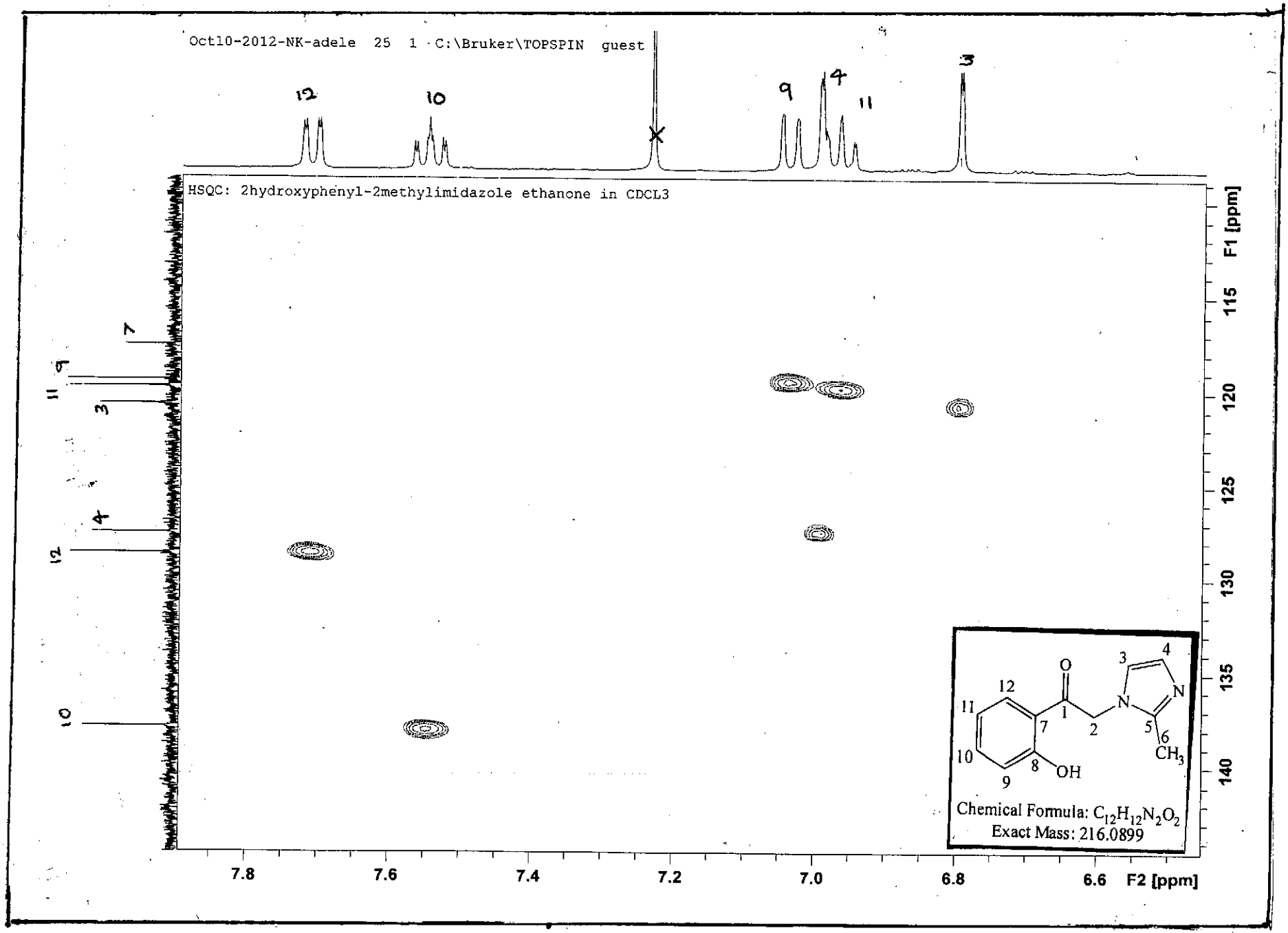

HSQC spectrum of compound10,1-(2-hydroxyphenyl)-2-(5-methyl-1H-imidazol-1-yl)ethanone

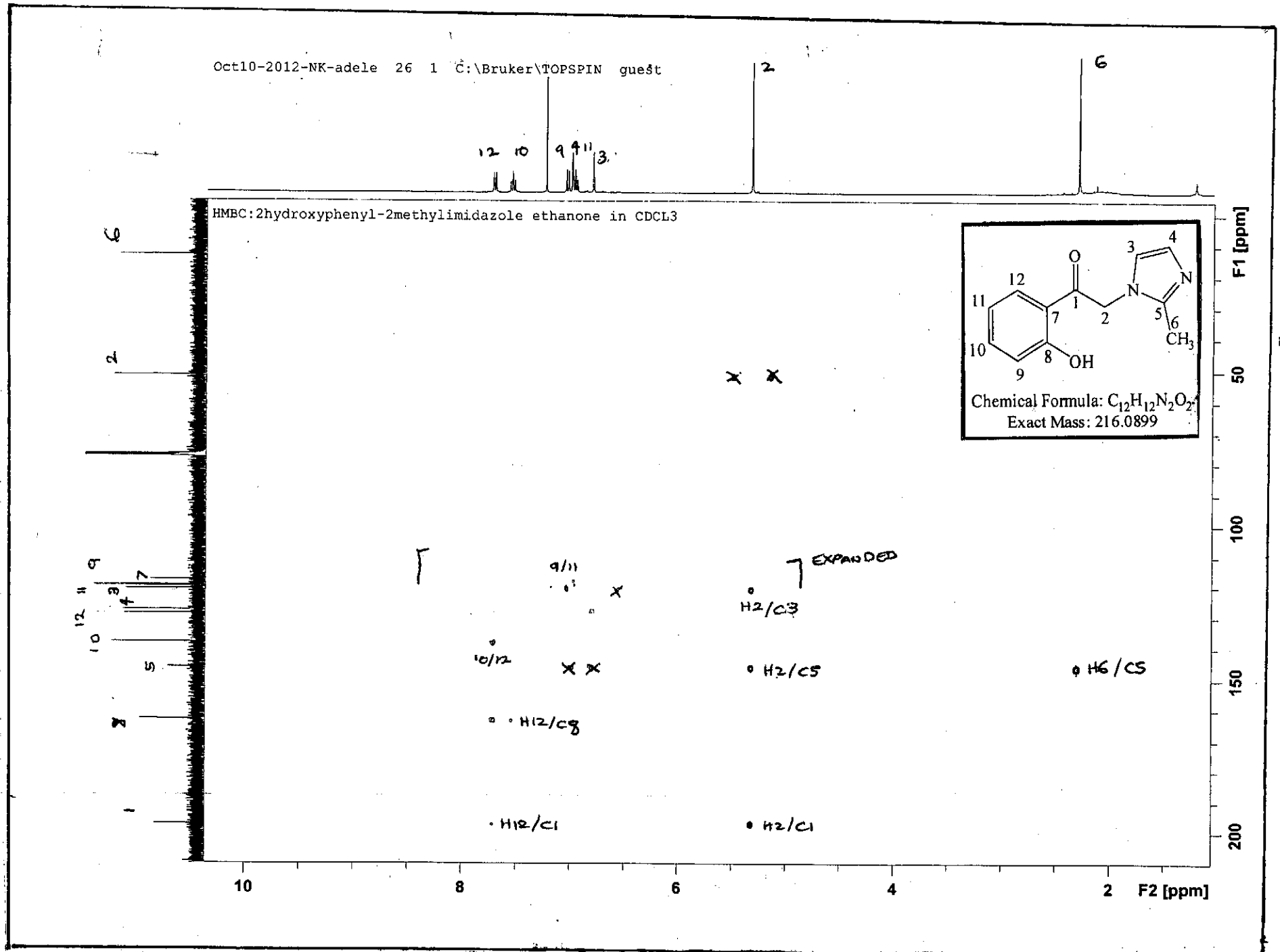

HMBC spectrum of compound10,1-(2-hydroxyphenyl)-2-(5-methyl-1H-imidazol-1-yl)ethanone

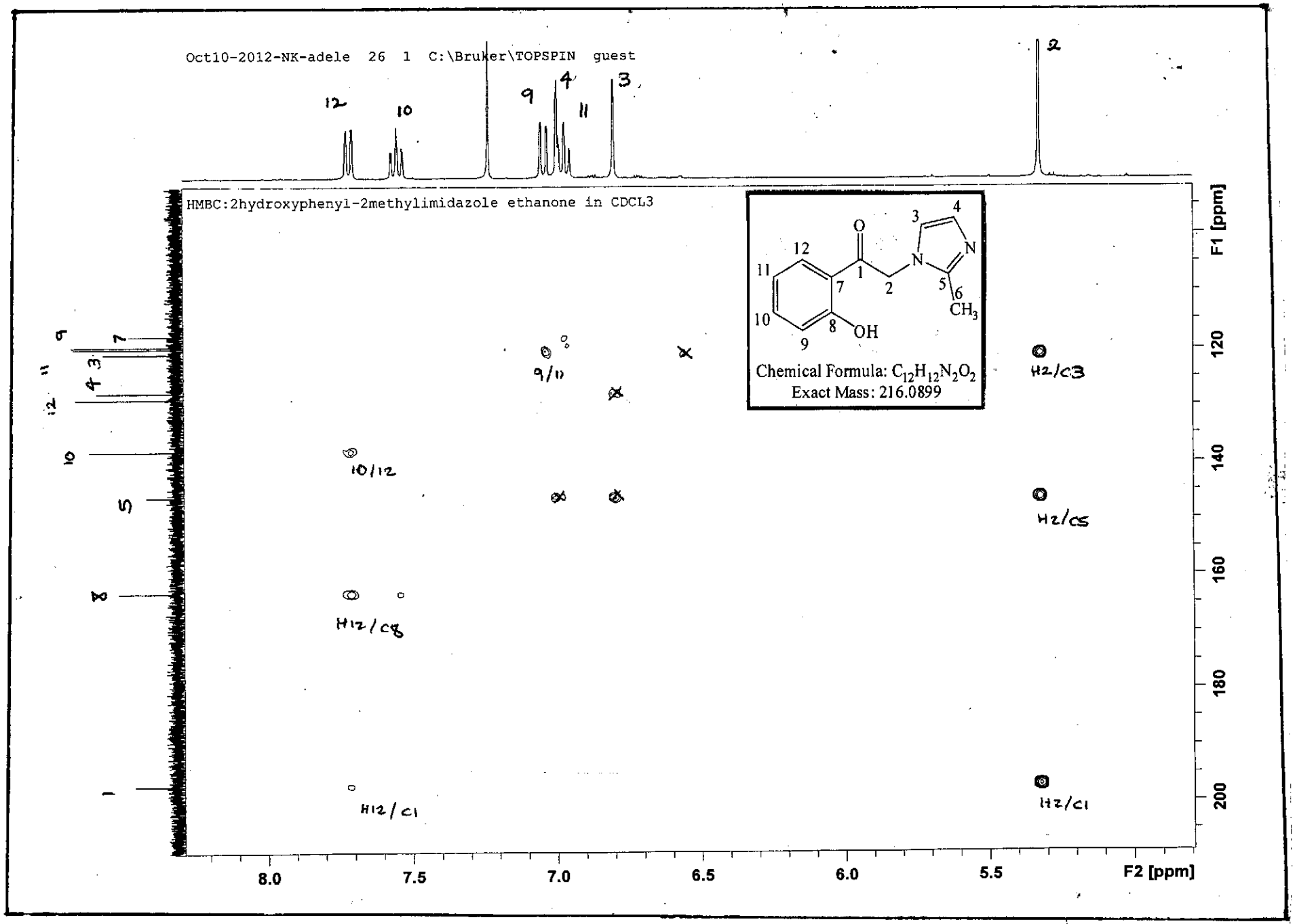

HMBC spectrum of compound10,1-(2-hydroxyphenyl)-2-(5-methyl-1H-imidazol-1-yl)ethanone

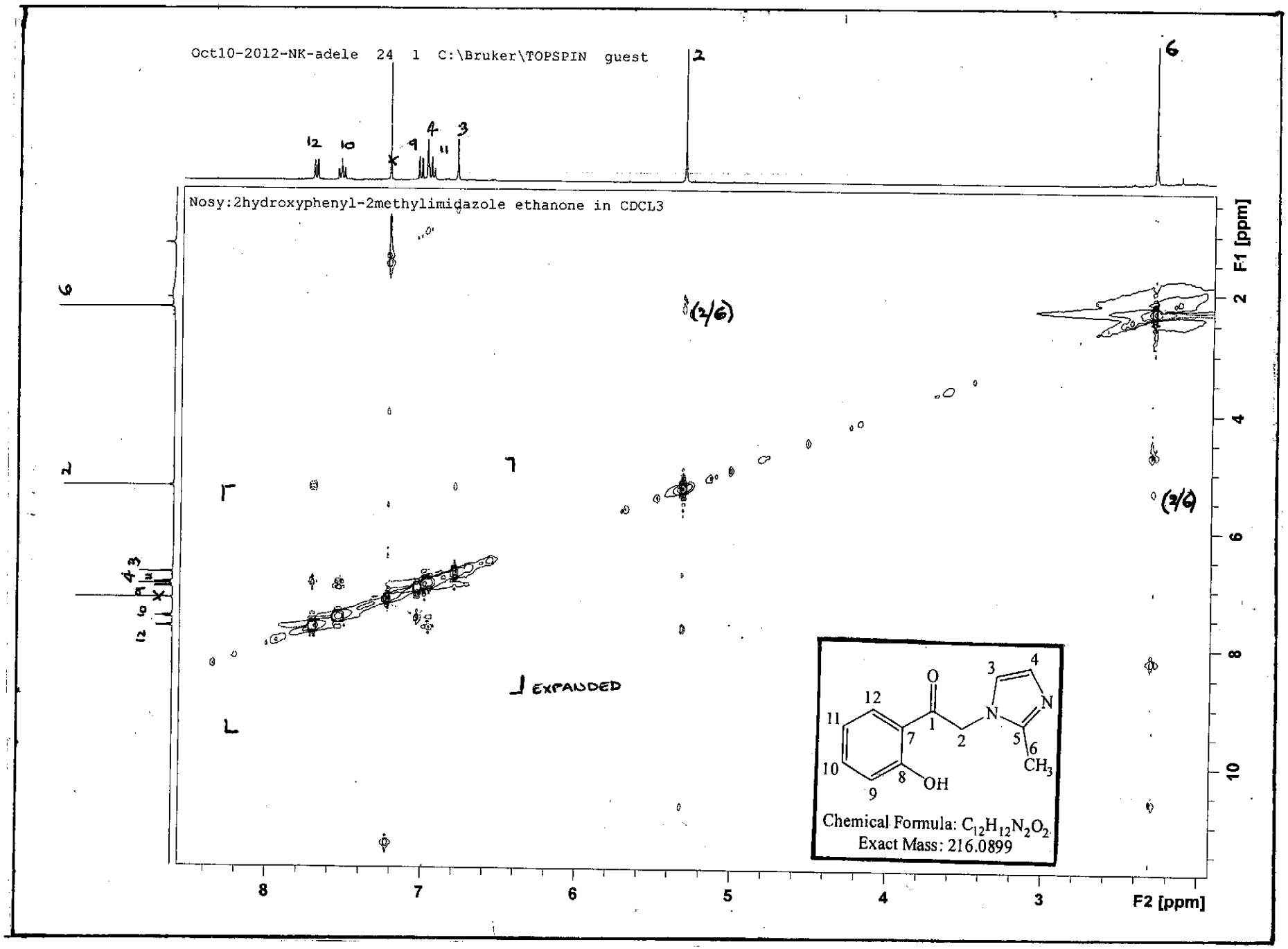

NOESY spectrum of compound10,1-(2-hydroxyphenyl)-2-(5-methyl-1H-imidazol-1-yl)ethanone

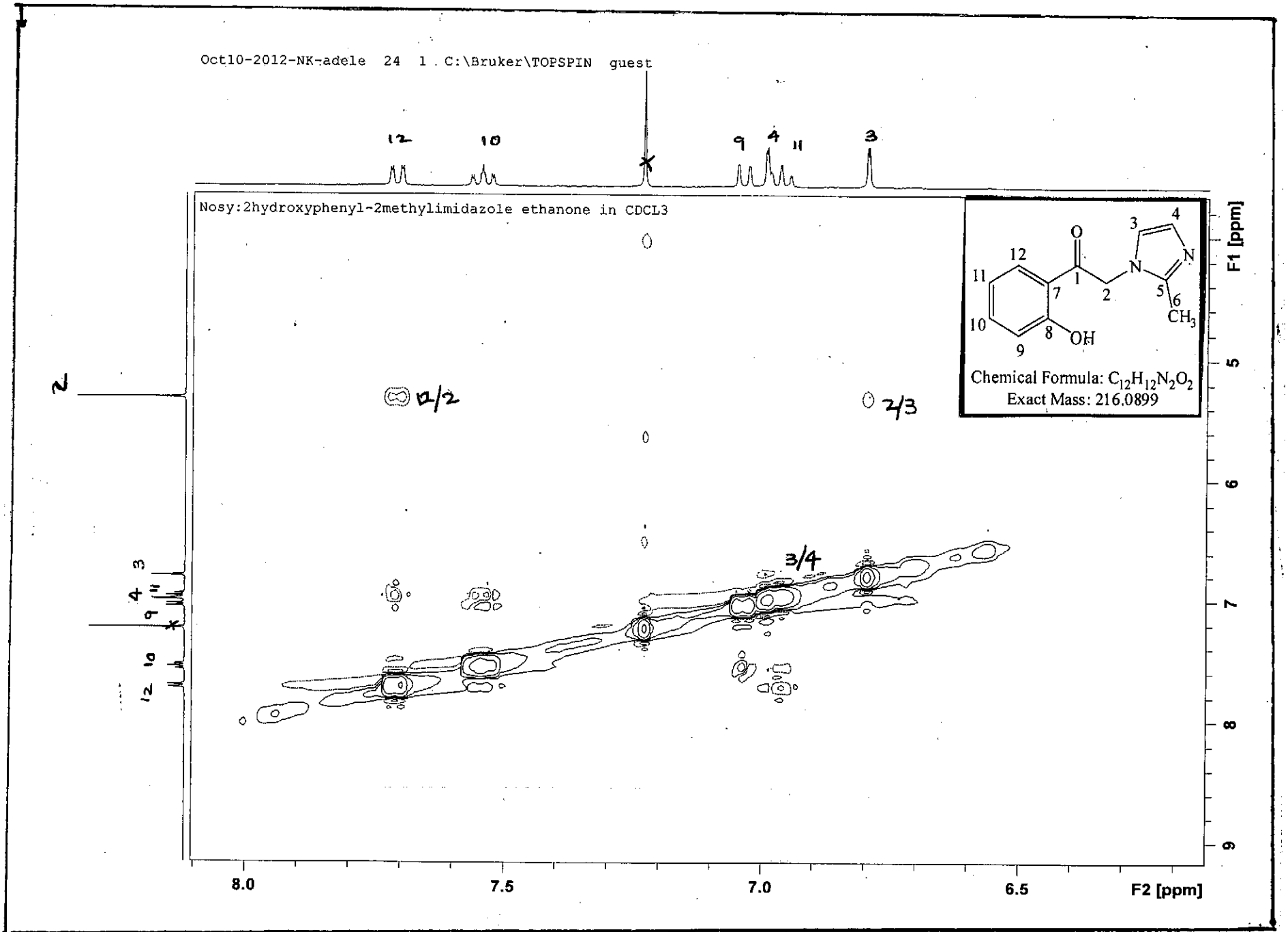

NOESY spectrum of compound 10,1-(2-hydroxyphenyl)-2-(5-methyl-1H-imidazol-1-yl)ethanone

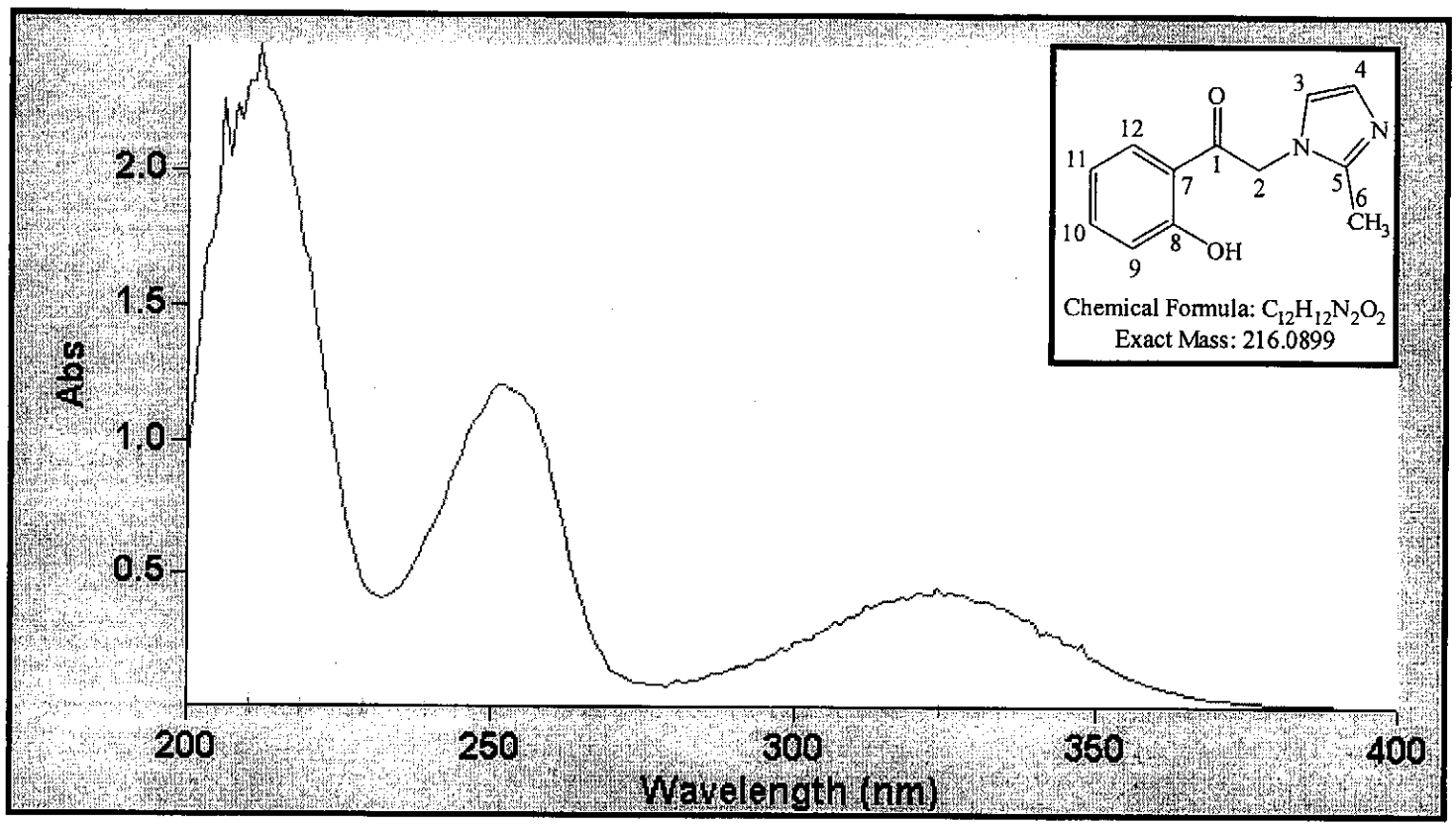

Ultra Violet spectrum of compound10,1-(2-hydroxyphenyl)-2-(2-methyl-1H-imidazol-1-yl)ethanone

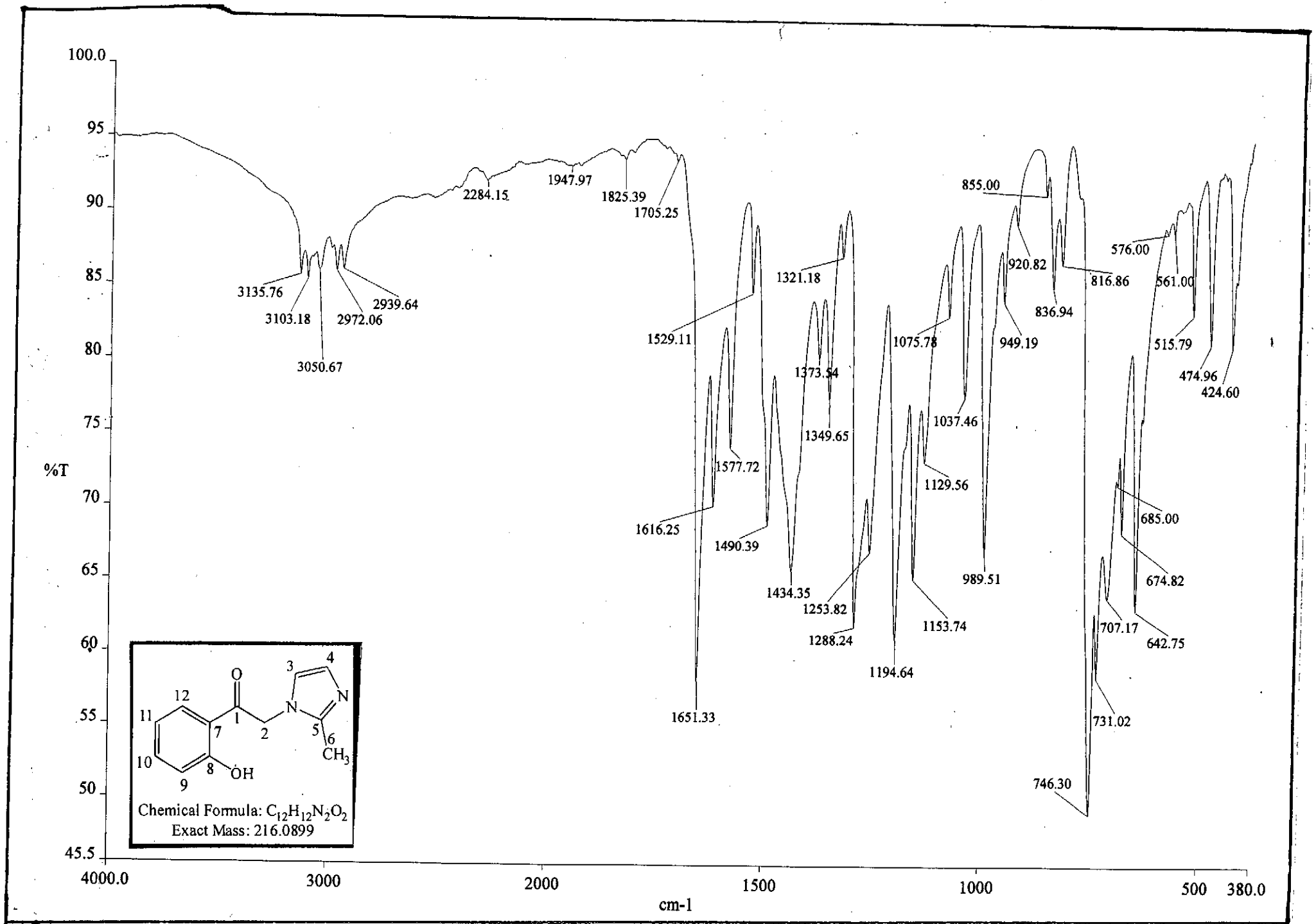

Infrared spectrum of compound 10, 1-(2-hydroxyphenyl)-2-(5-methyl-1H-imidazol-1-yl)ethanone

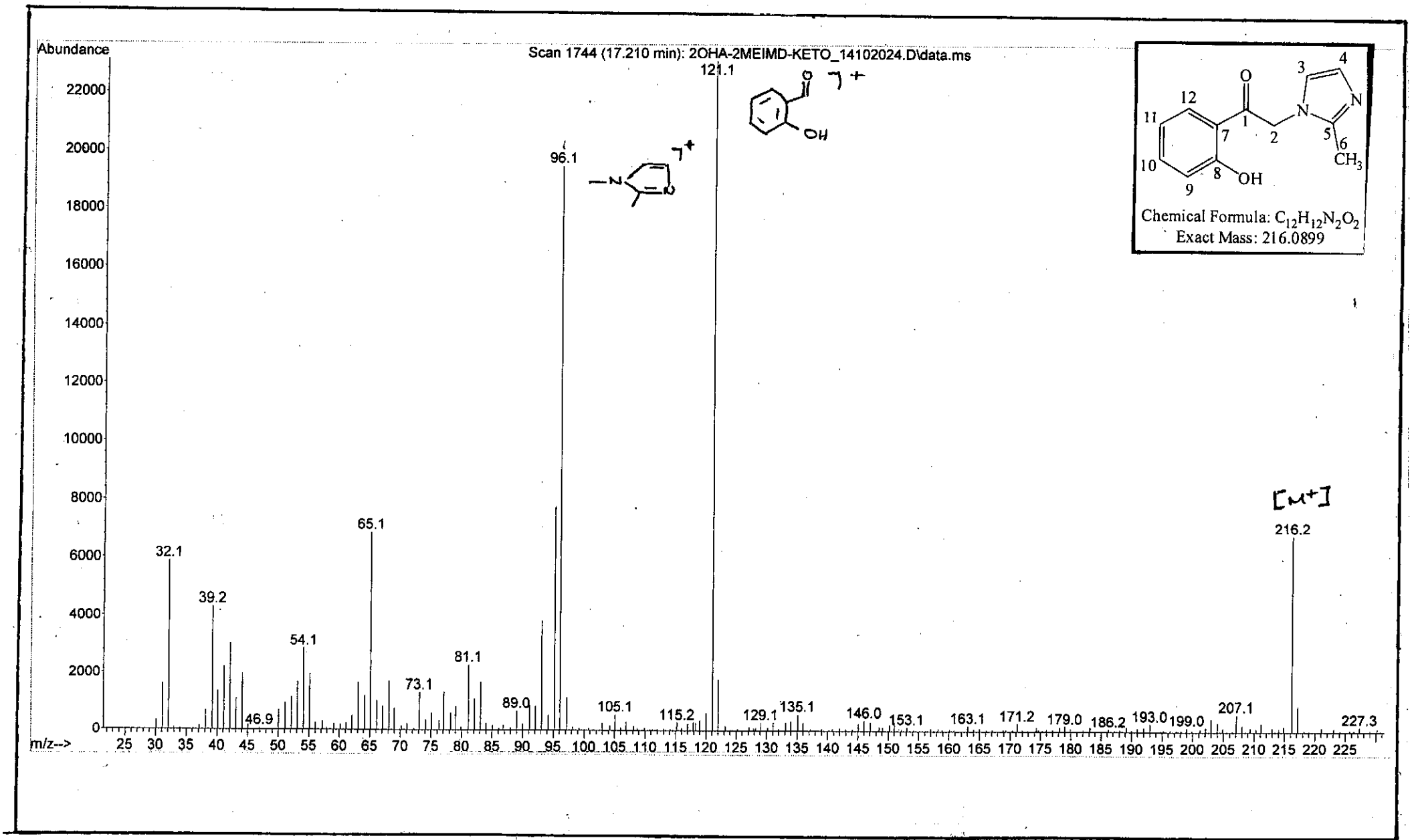

Mass spectrum of compound 10, 1-(2-hydroxyphenyl)-2-(5-methyl-1H-imidazol-1-yl)ethanone

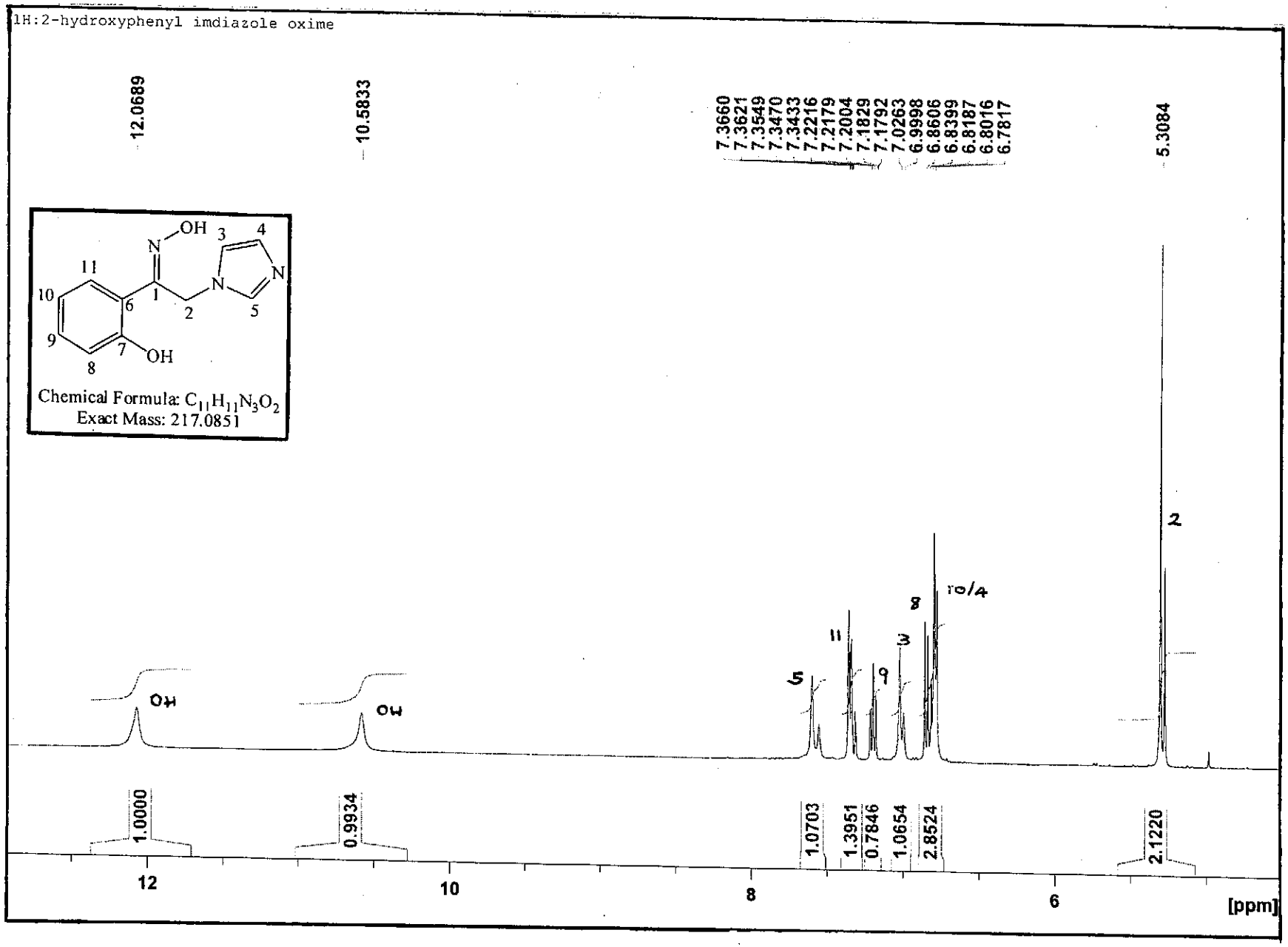

^{1}H NMR spectrum of compound 12, 1-(2-hydroxyphenyl)-2-(1H-imidazol-1-yl) ethanone oxime

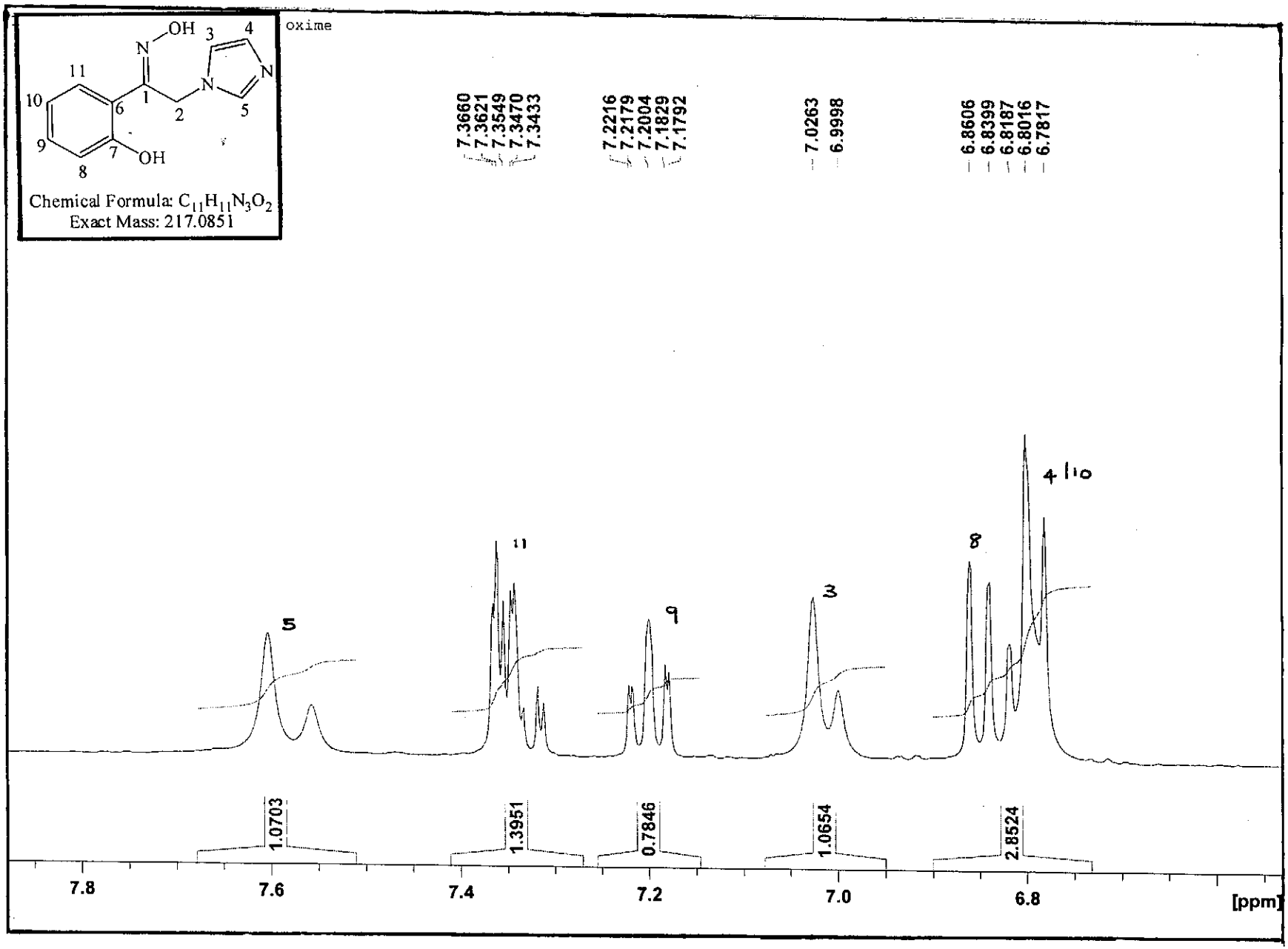

^{1}H NMR spectrum of compound 12, 1-(2-hydroxyphenyl)-2-(1H-imidazol-1-yl) ethanone oxime

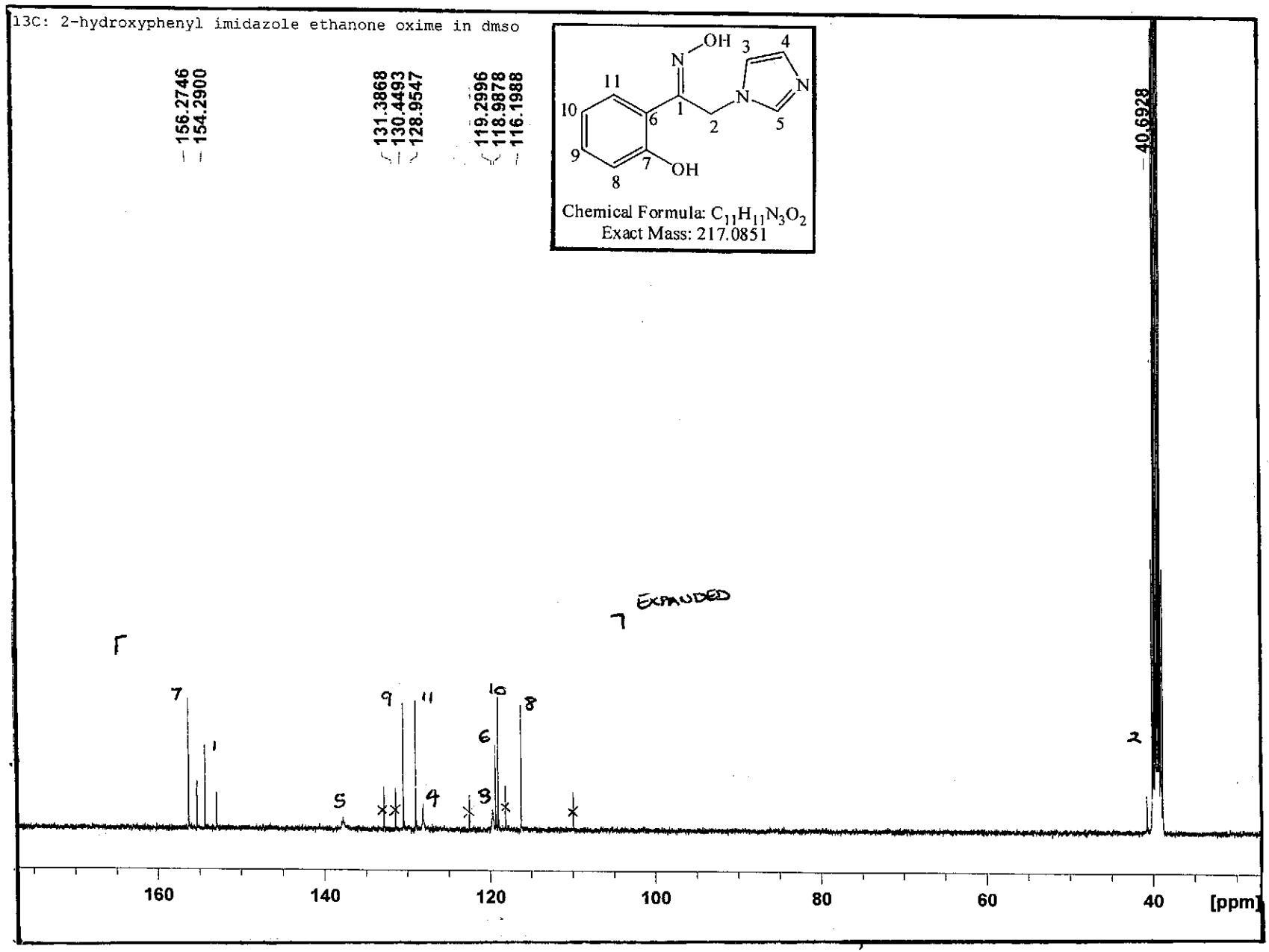

^{13}C NMR of compound 12, 1-(2-hydroxyphenyl)-2-(1H-imidazol-1-yl) ethanone oxime

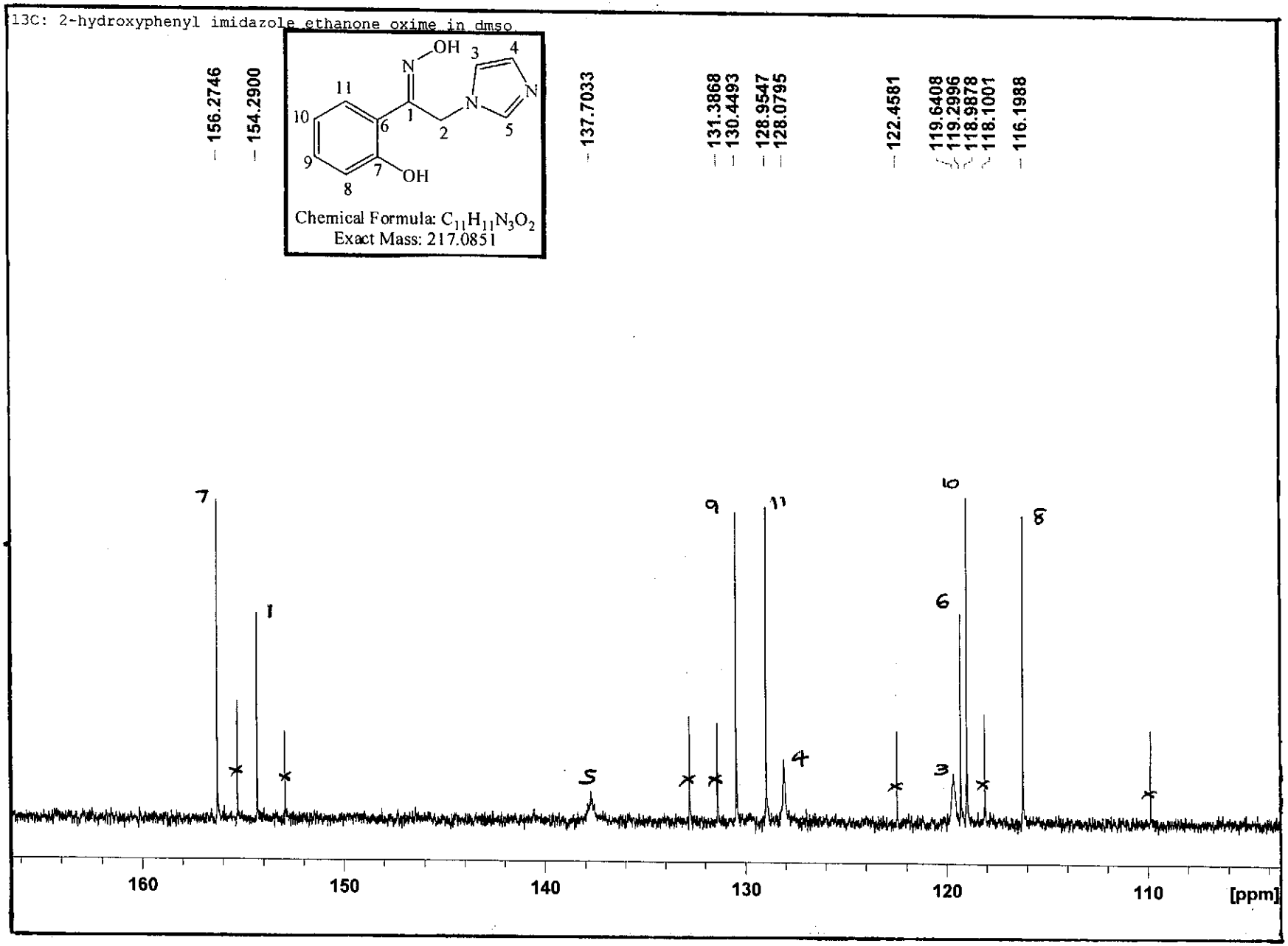

^{13}C NMR of compound 12, 1-(2-hydroxyphenyl)-2-(1H-imidazol-1-yl) ethanone oxime

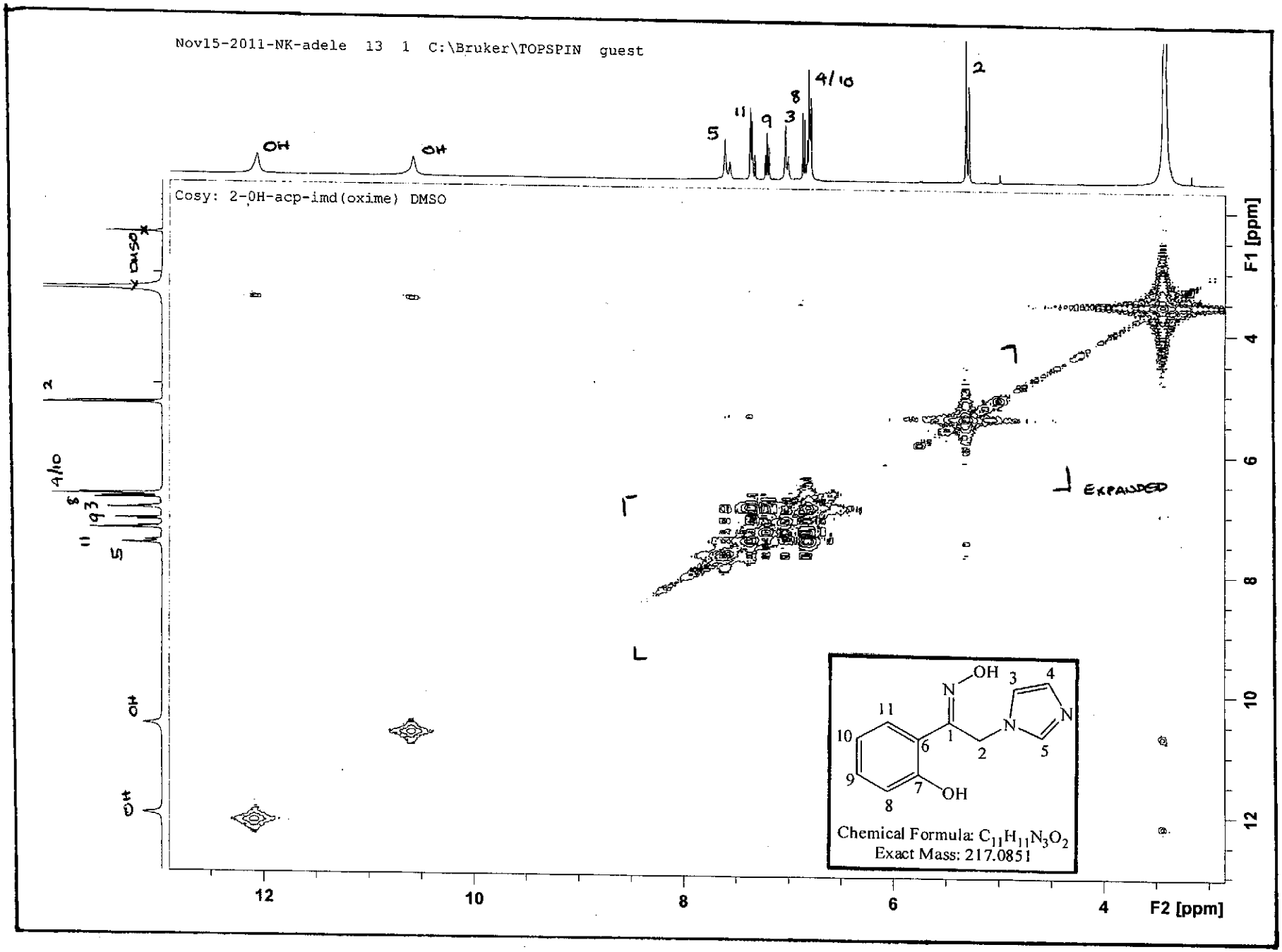

COSY spectrum of compound 12, 1-(2-hydroxyphenyl)-2-(1H-imidazol-1-yl) ethanone oxime

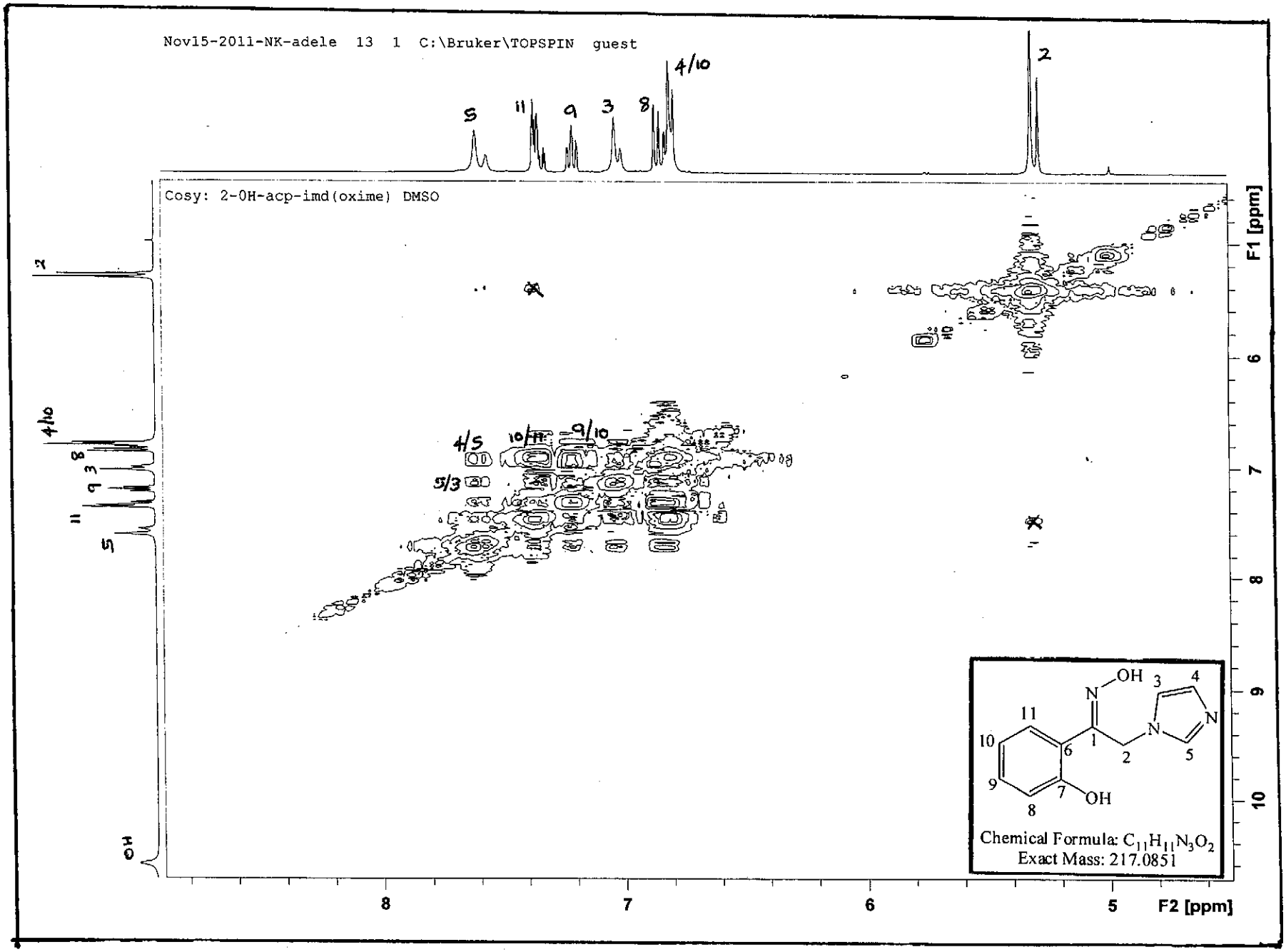

COSY spectrum of compound 12, 1-(2-hydroxyphenyl)-2-(1H-imidazol-1-yl) ethanone oxime

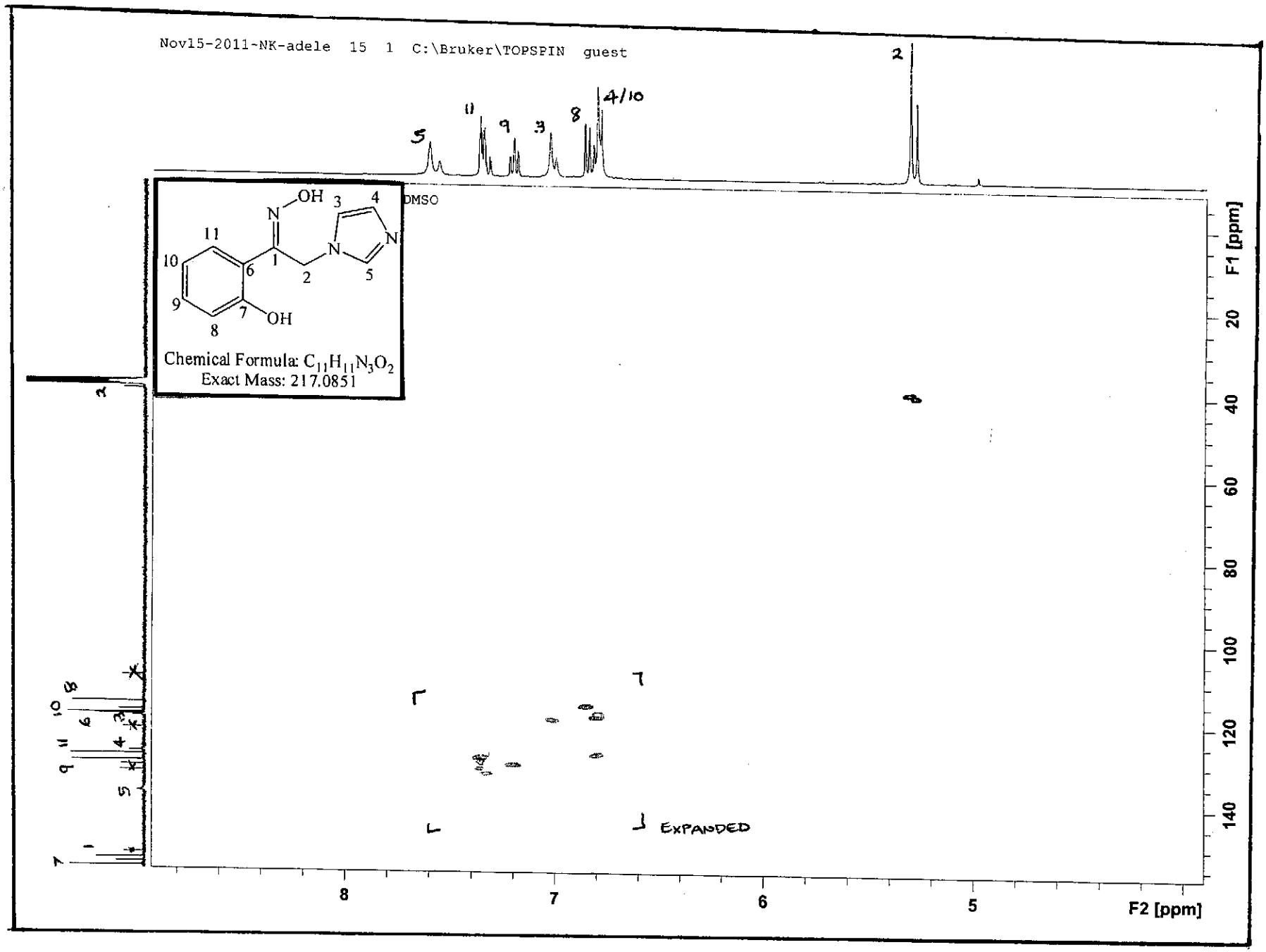

HSQC spectrum of compound 12, 1-(2-hydroxyphenyl)-2-(1H-imidazol-1-yl) ethanone oxime

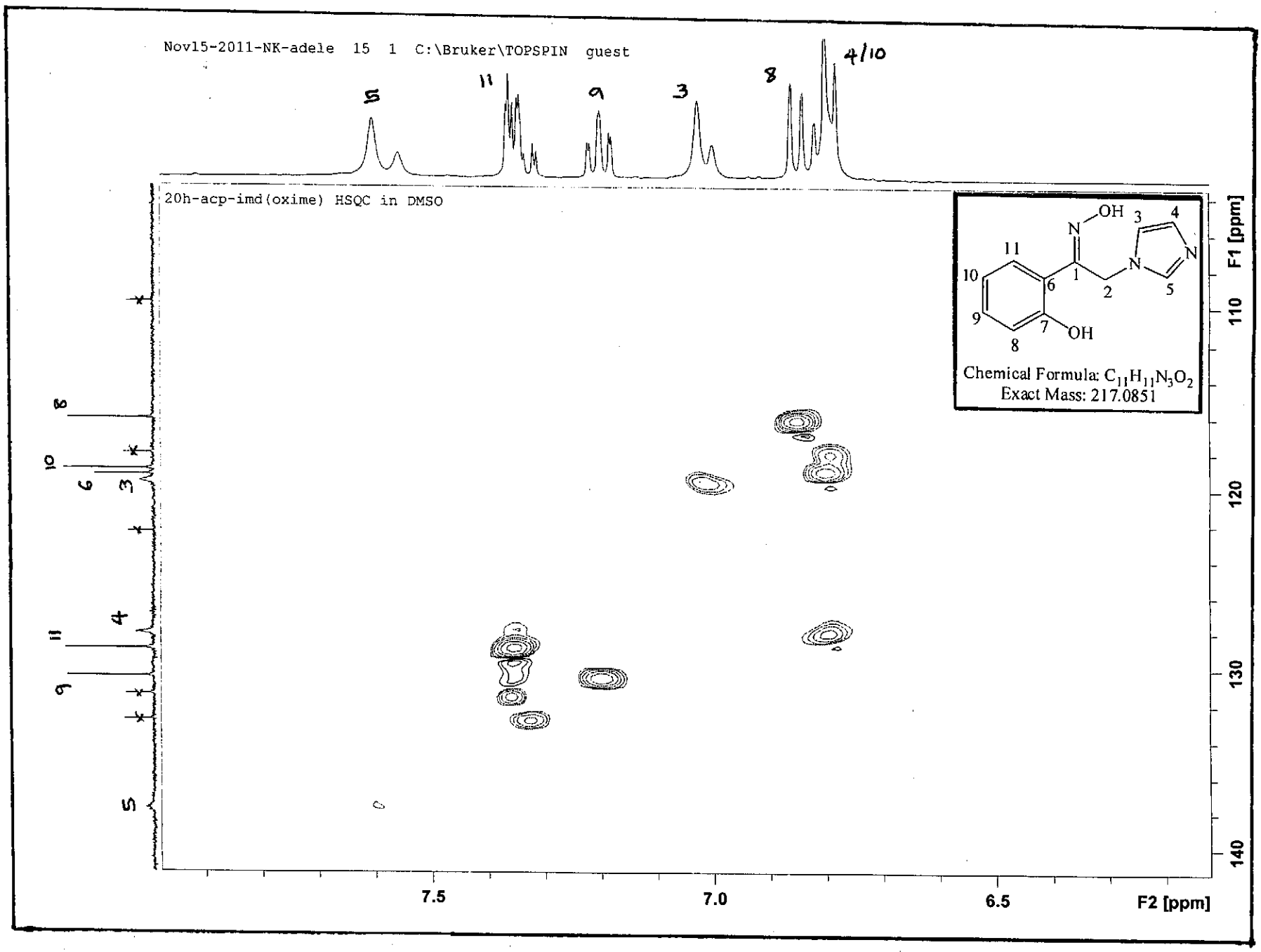

HSQC spectrum of compound 12, 1-(2-hydroxyphenyl)-2-(1H-imidazol-1-yl) ethanone oxime

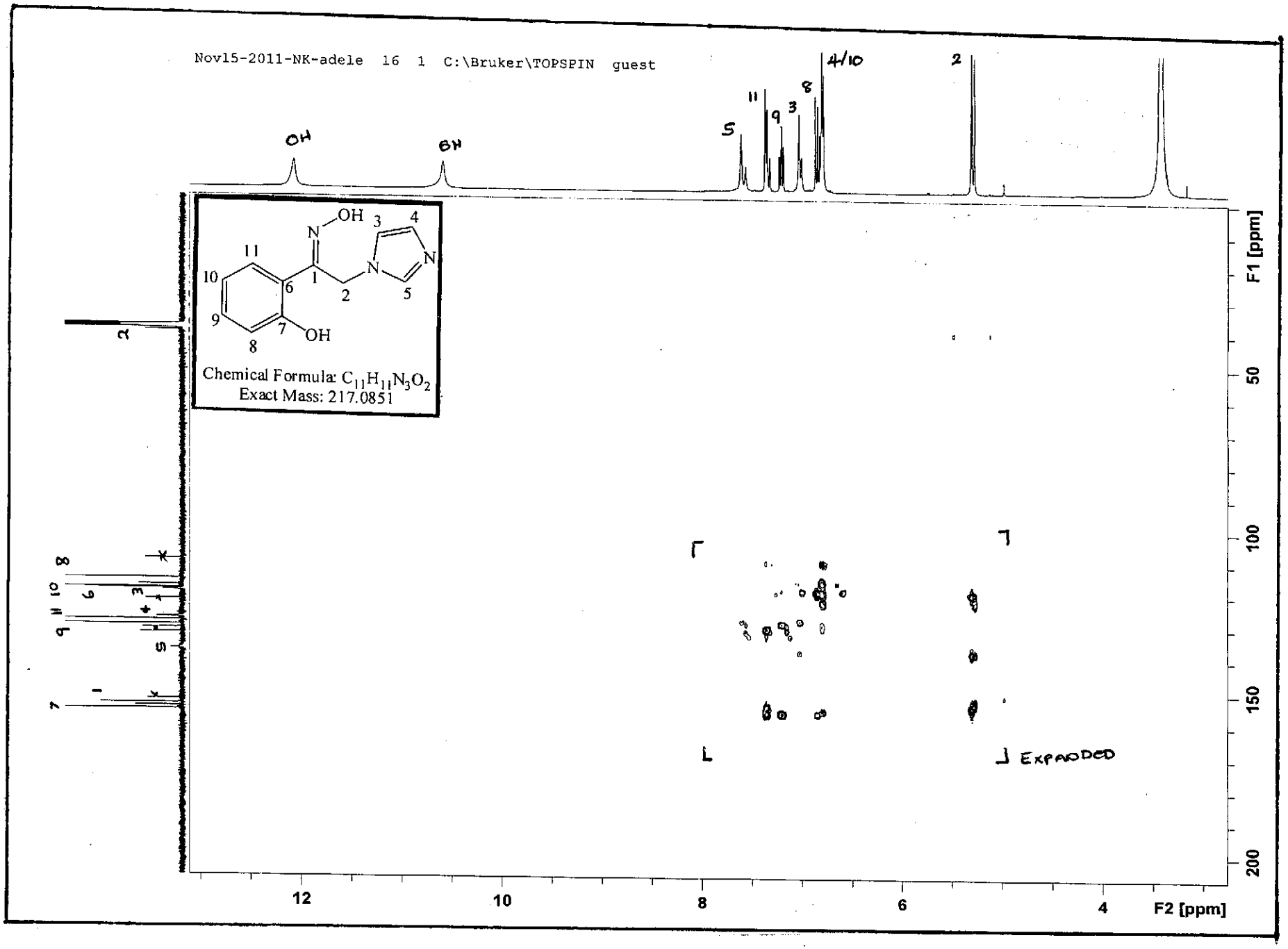

HMBC spectrum of compound 12, 1-(2-hydroxyphenyl)-2-(1H-imidazol-1-yl) ethanone oxime

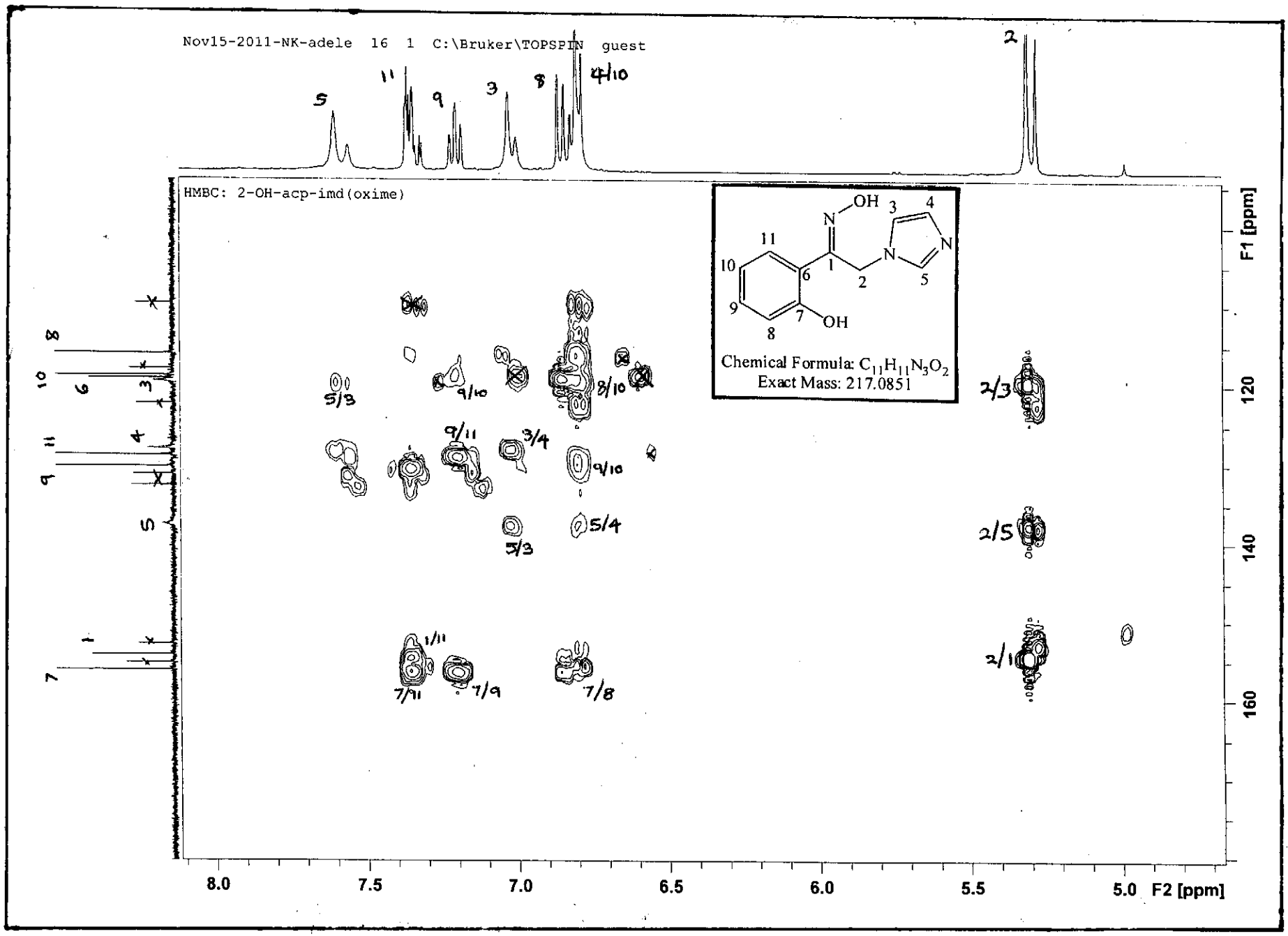

HMBC spectrum of compound 12, 1-(2-hydroxyphenyl)-2-(1H-imidazol-1-yl) ethanone oxime

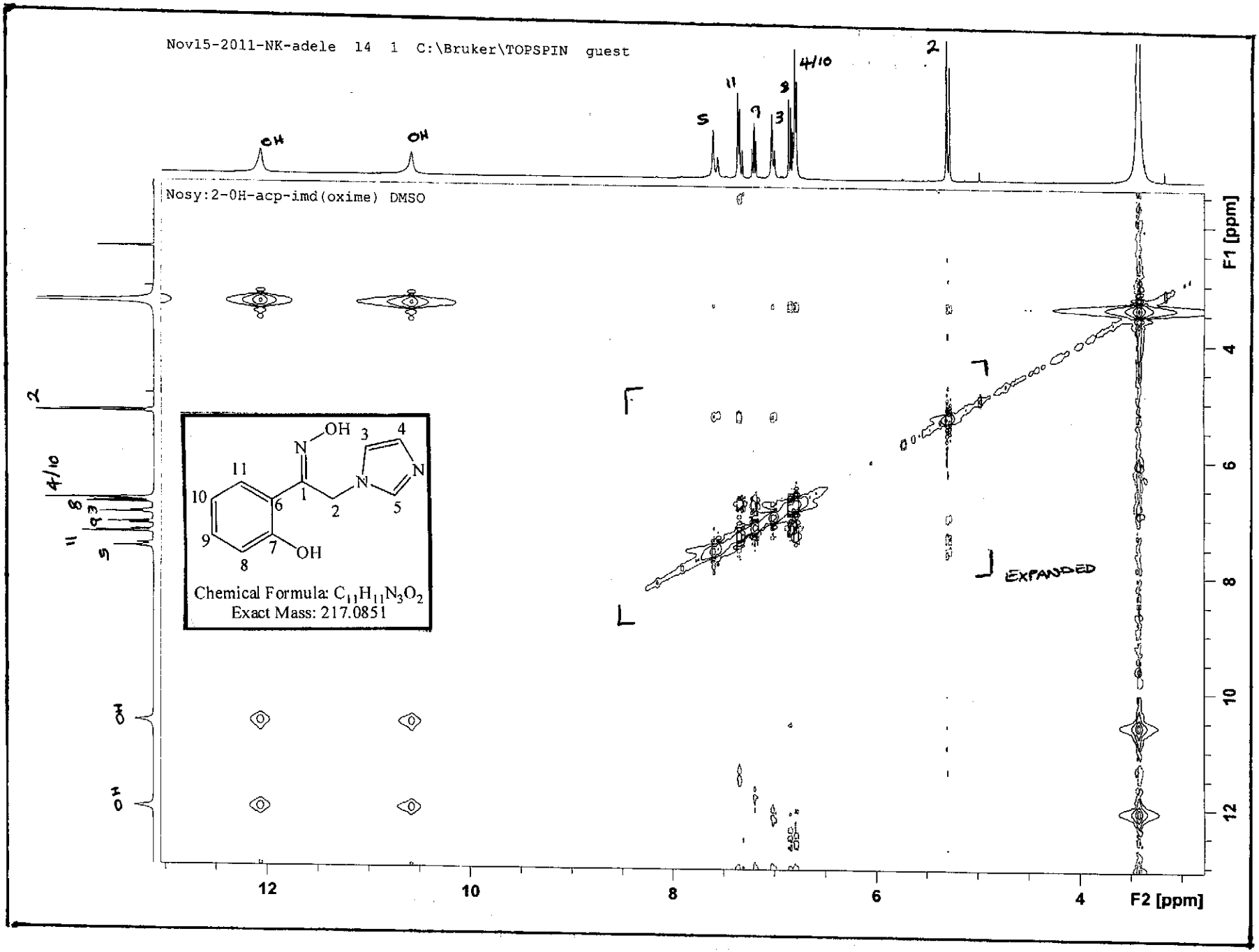

NOESY spectrum of compound 12, 1-(2-hydroxyphenyl)-2-(1H-imidazol-1-yl) ethanone oxime

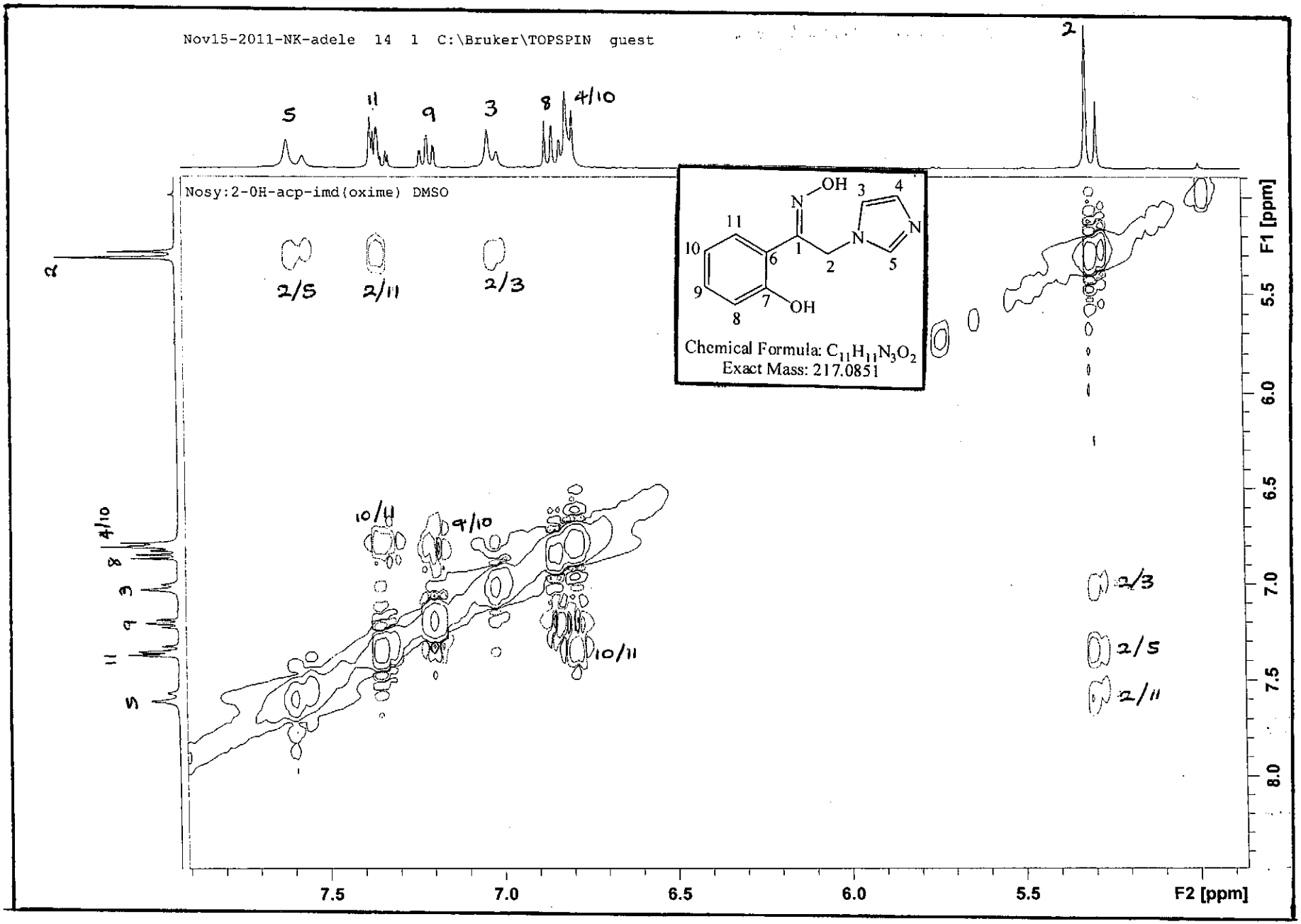

NOESY spectrum of compound12 , 1-(2-hydroxyphenyl)-2-(1H-imidazol-1-yl) ethanone oxime

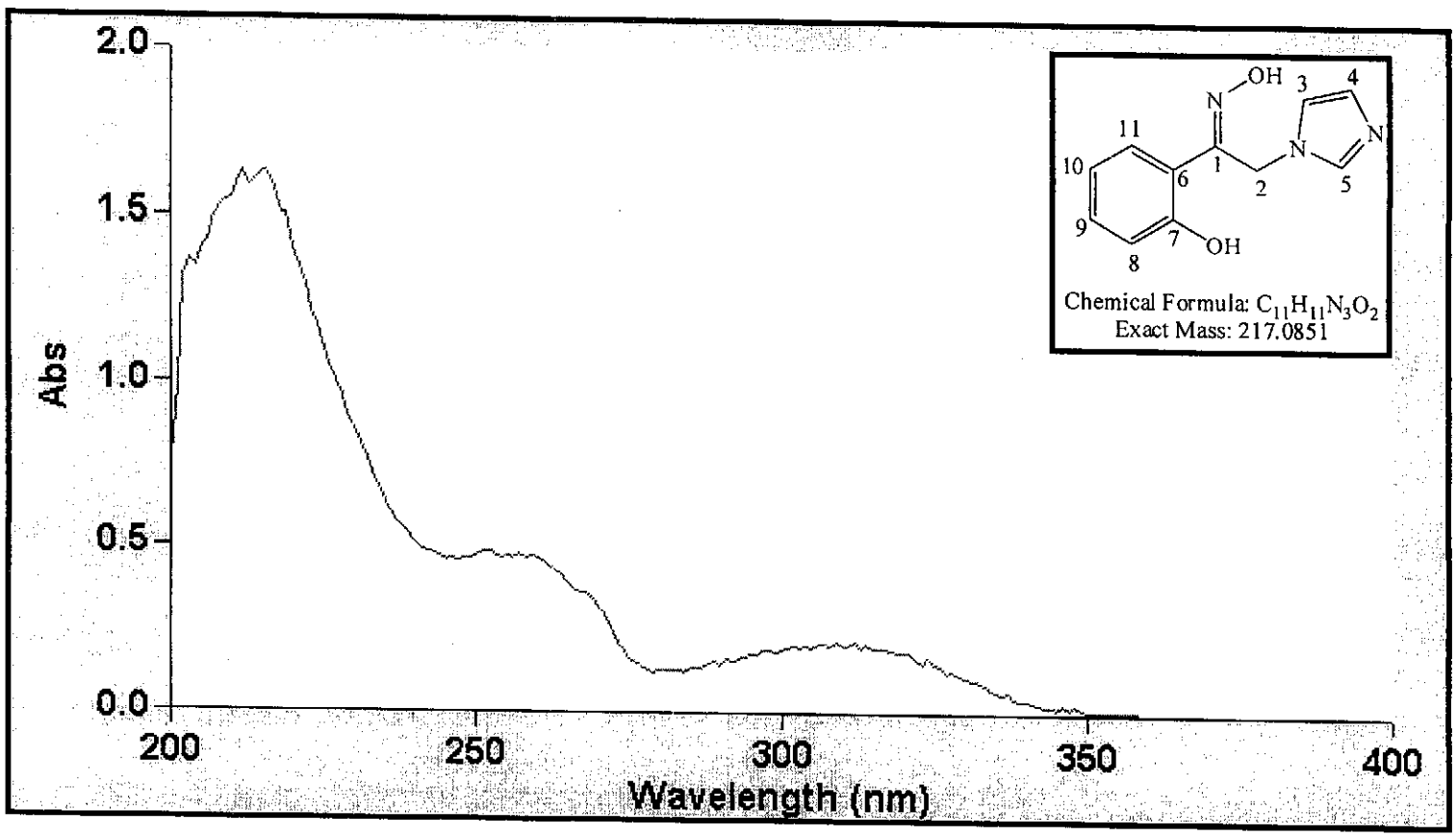

Ultra Violet spectrum of compound 12, 1-(2-hydroxyphenyl)-2-(1H-imidazol-1-yl)ethanone oxime

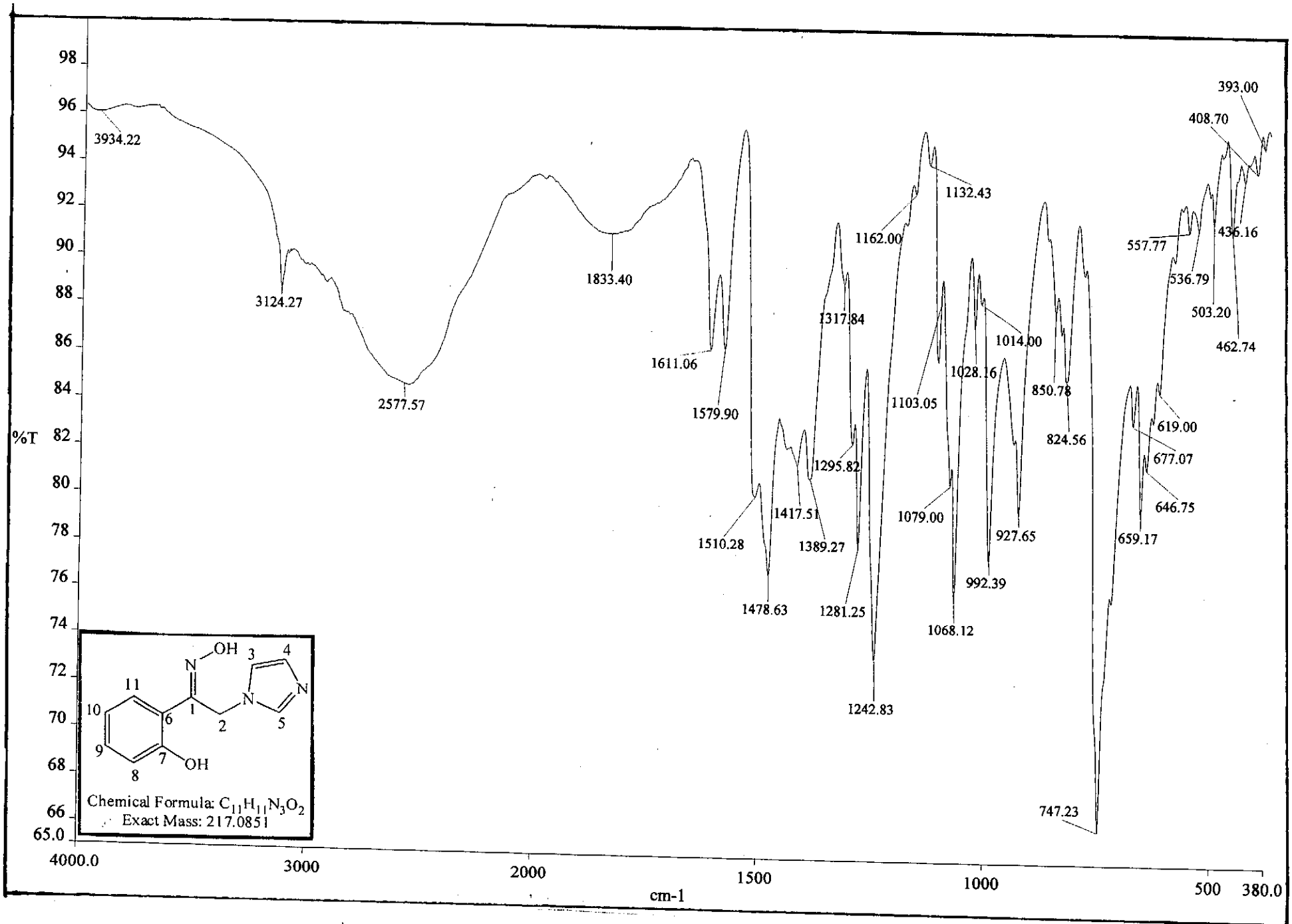

Infrared spectrum of compound 12, 1-(2-hydroxyphenyl)-2-(1H-imidazol-1-yl) ethanone oxime

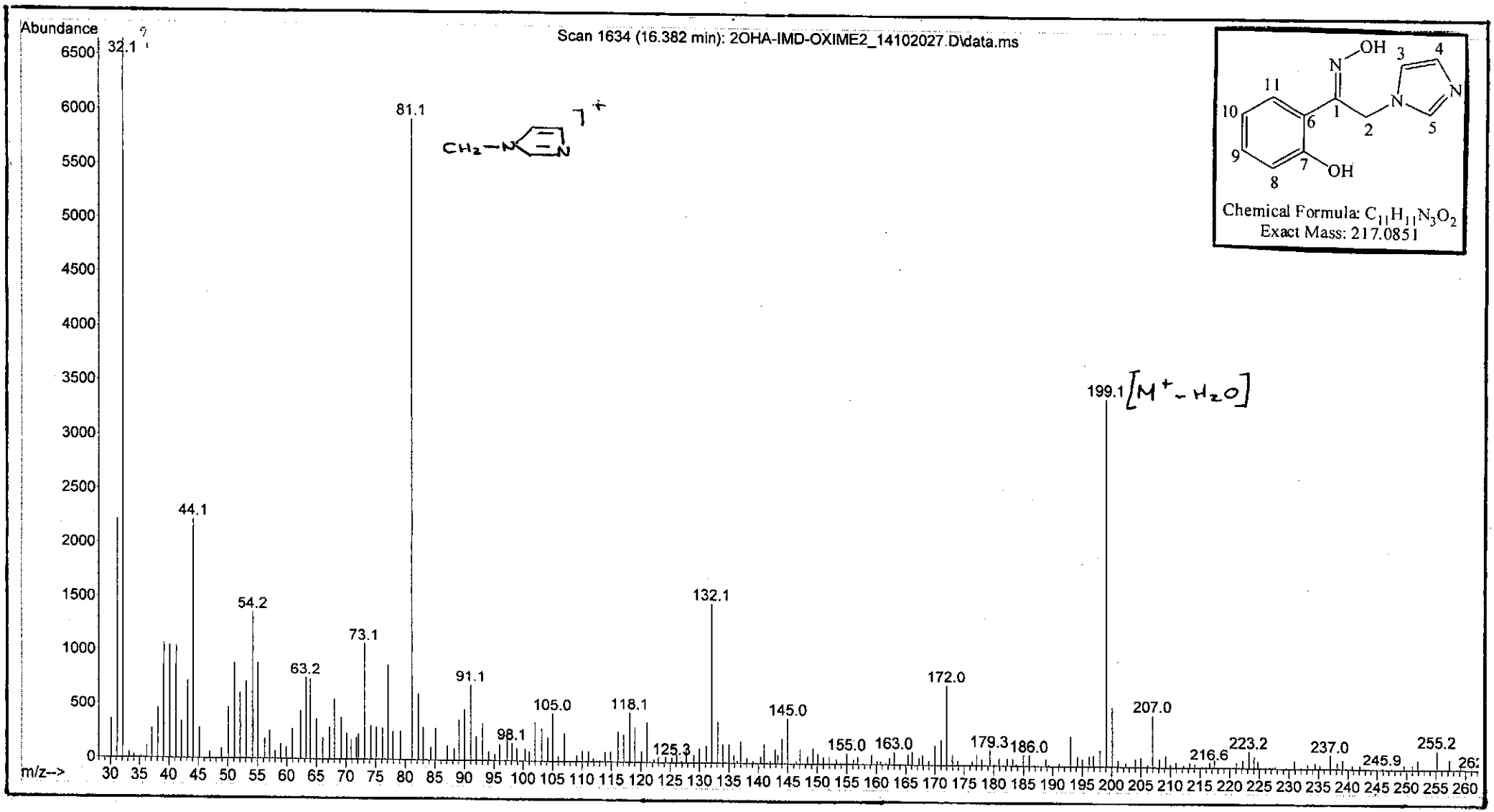

Mass spectrum of compound 12, 1-(2-hydroxyphenyl)-2-(1H-imidazol-1-yl) ethanone oxime

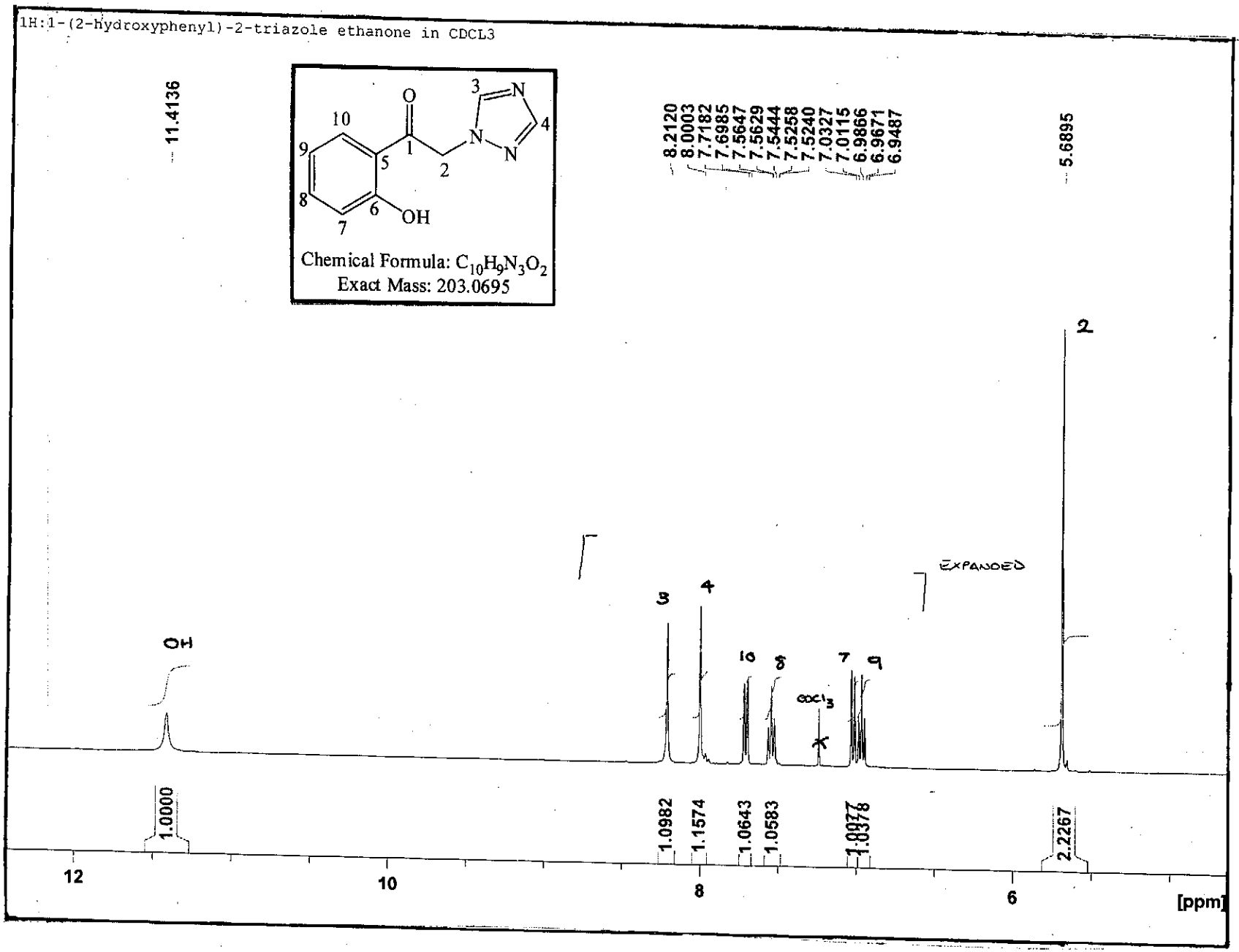

^{1}H NMR spectrum of compound11,1-(2-hydroxyphenyl)-2-(1H-1,2,4-triazol-1-yl)ethanone

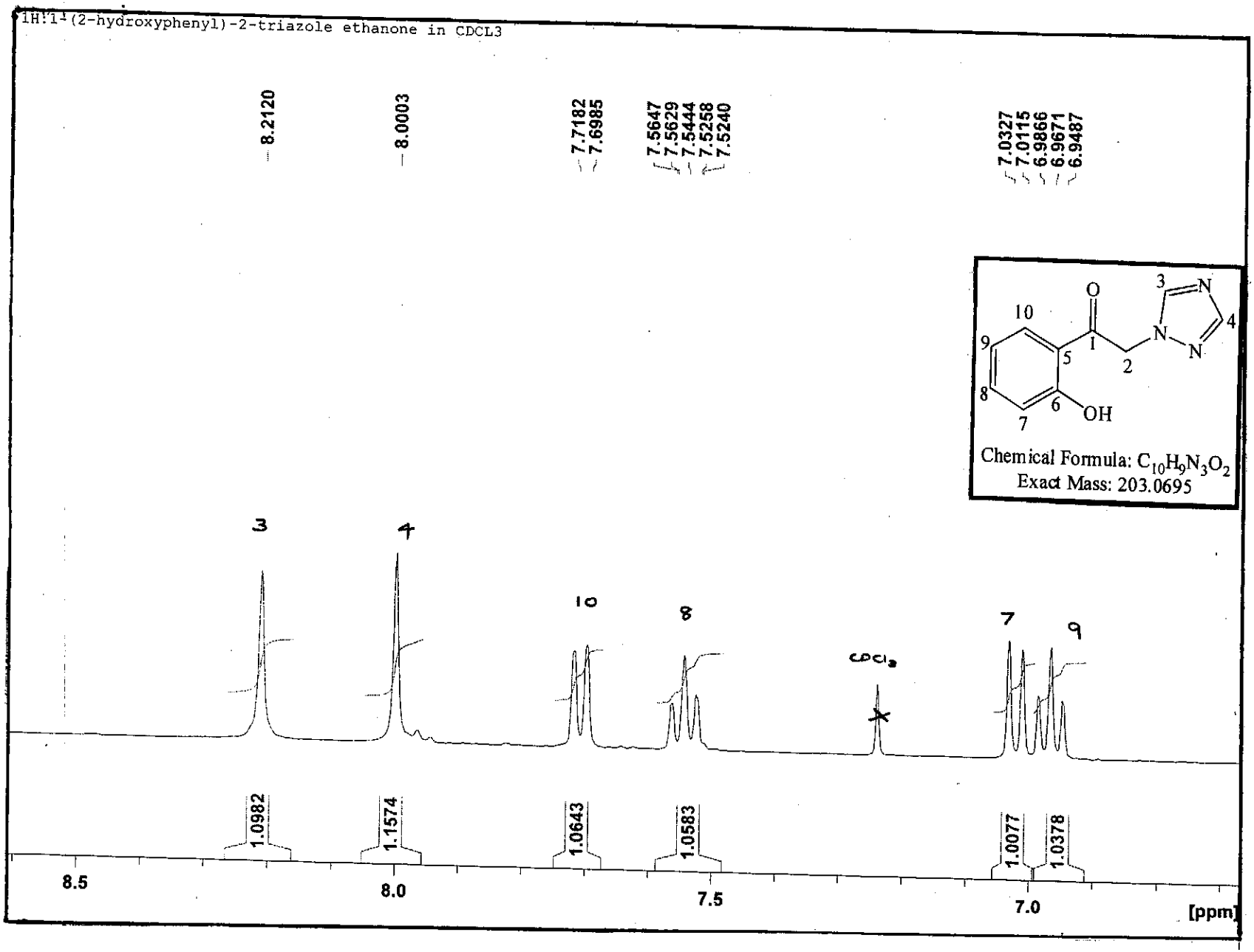

^{1}H NMR spectrum of compound11,1-(2-hydroxyphenyl)-2-(1H-1,2,4-triazol-1-yl)ethanone

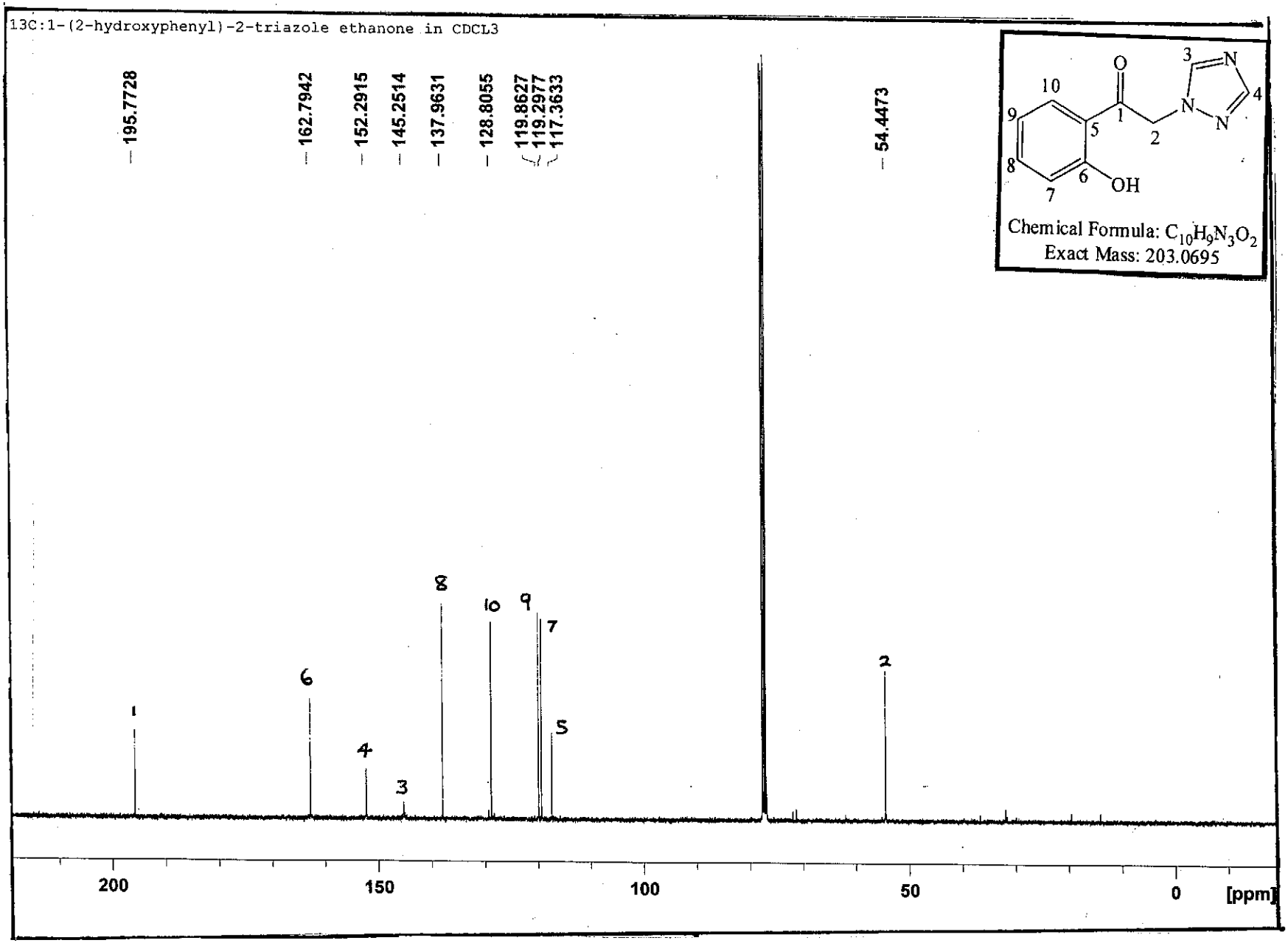

^{13}C NMR of compound 1 1-(2-hydroxyphenyl)-2-(1H-1,2,4-triazol-1-yl)ethanone

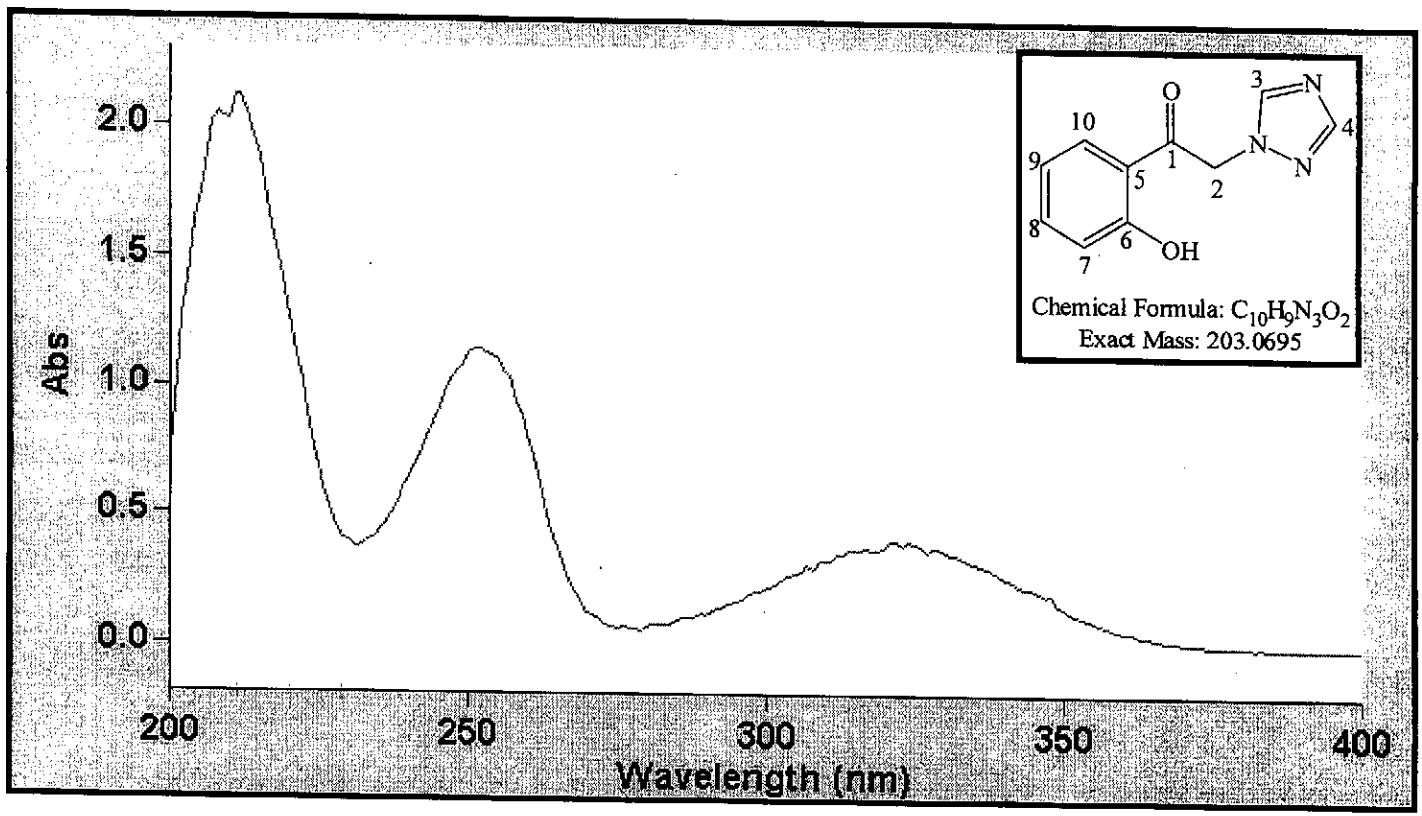

Ultra Violet spectrum of compound11,1-(2-hydroxyphenyl)-2-(1H-1,2,4-triazol-1-yl)ethanone

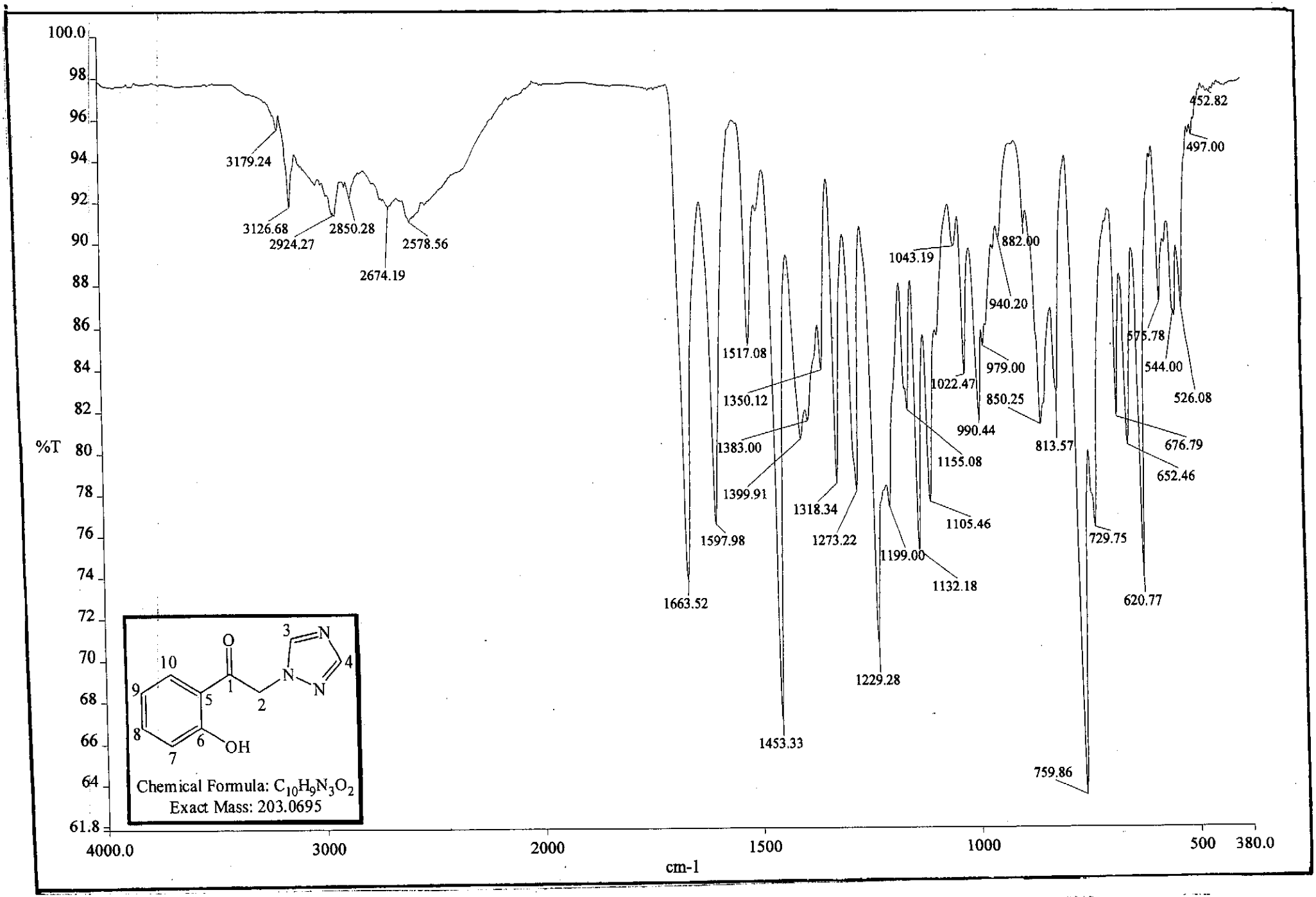

Infrared spectrum of compound11,1-(2-hydroxyphenyl)-2-(1H-1,2,4-triazol-1-yl)ethanone

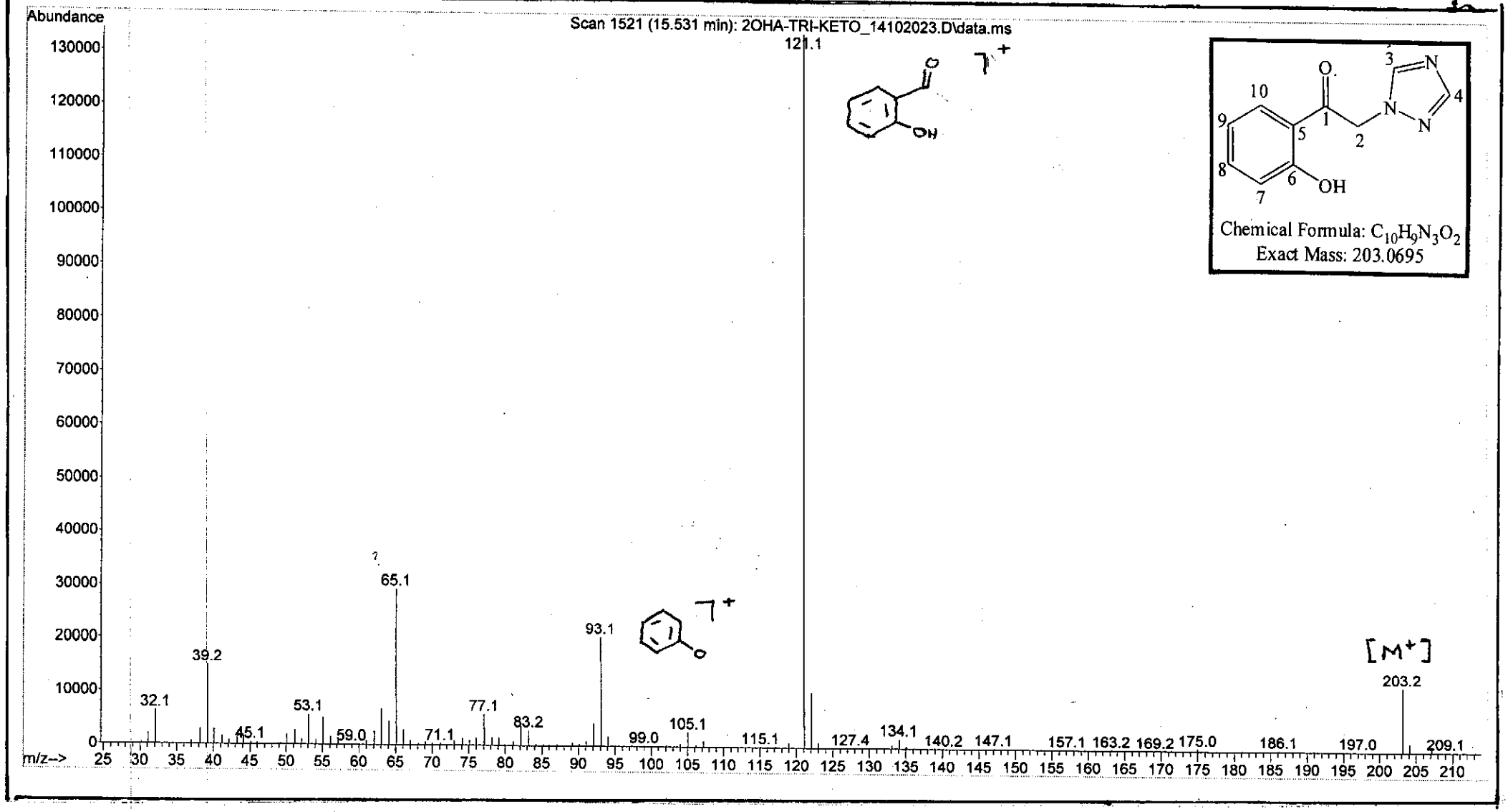

Mass spectrum of compound 11,1-(2-hydroxyphenyl)-2-(1H-1,2,4-triazol-1-yl)ethanone

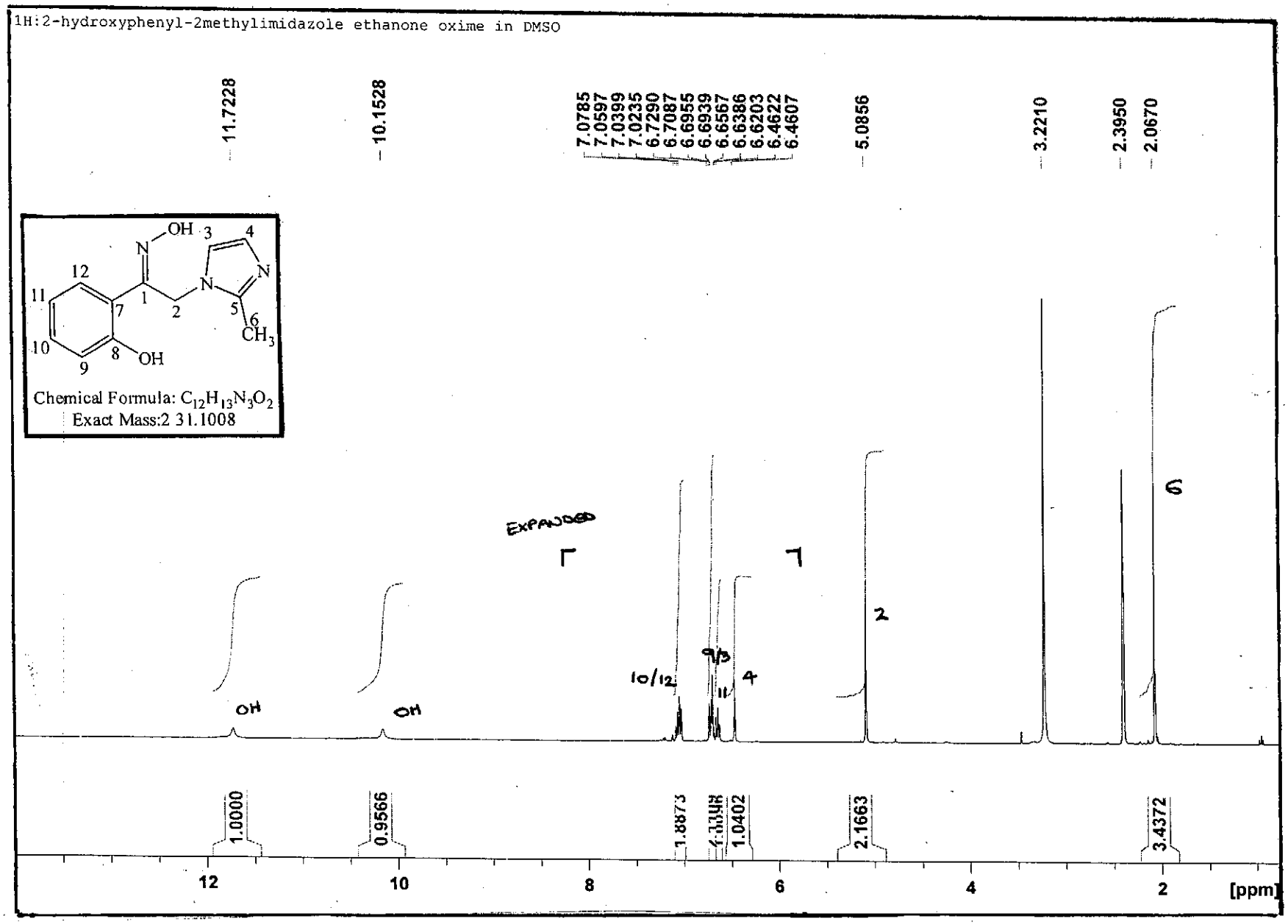

^{1}H NMR spectrum of compound 13, 1-(2-hydroxyphenyl)-2-(2-methyl-1H-imidazol-1-yl) ethanone oxime

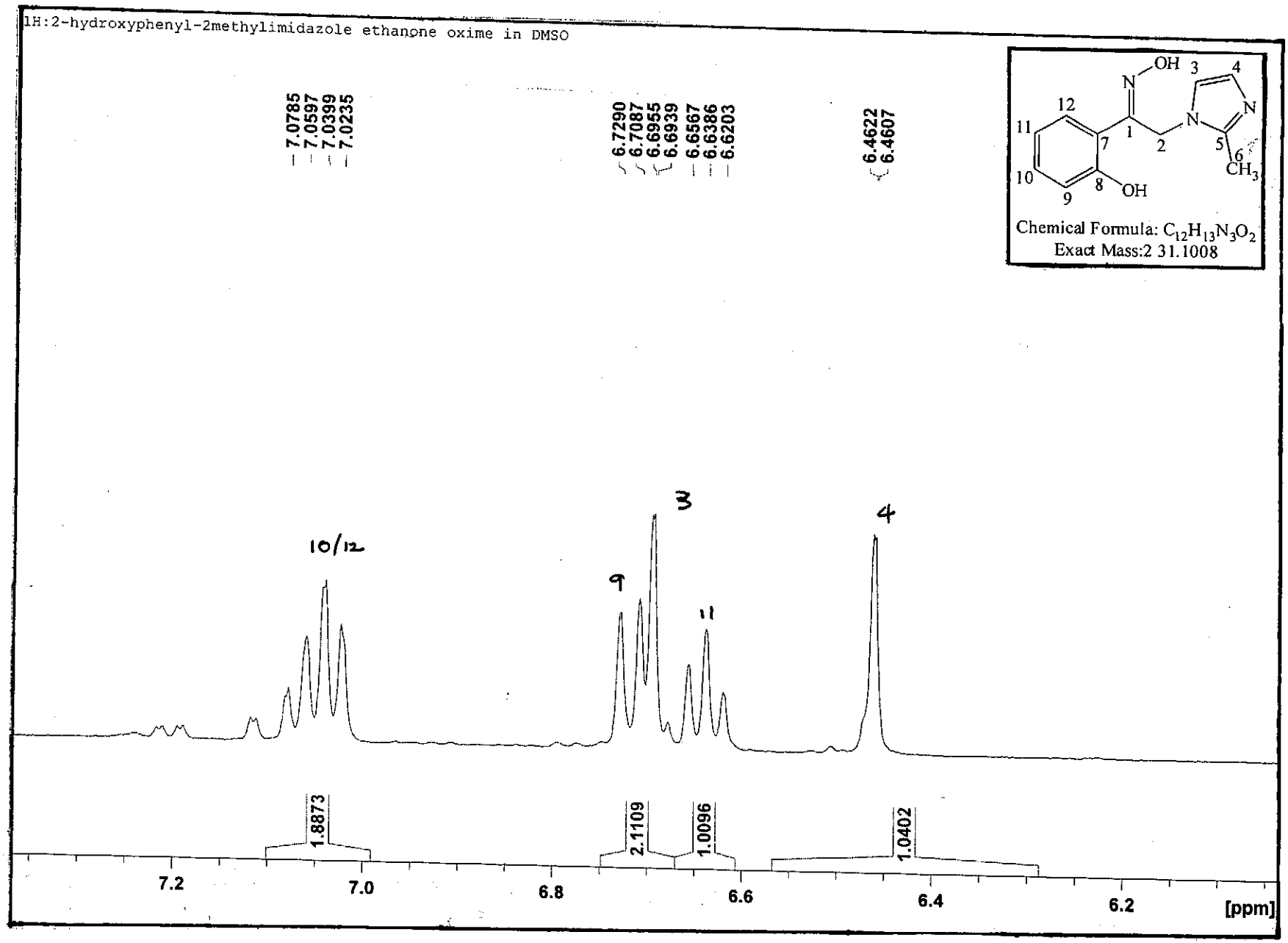

^{1}H NMR spectrum of compound 13, 1-(2-hydroxyphenyl)-2-(2-methyl-1H-imidazol-1-yl) ethanone oxime

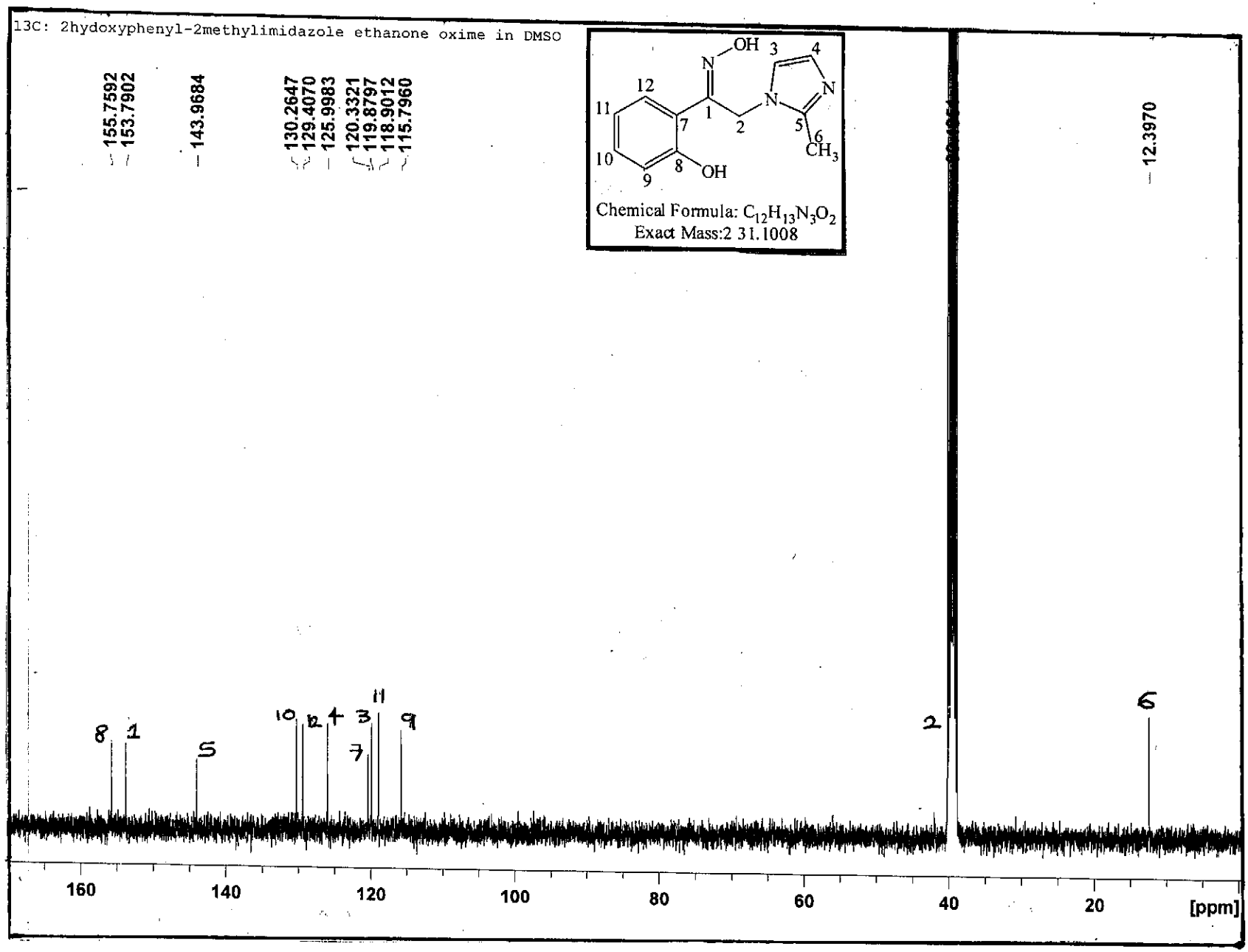

^{13}C NMR of compound 13, 1-(2-hydroxyphenyl)-2-(2-methyl-1H-imidazol-1-yl) ethanone oxime

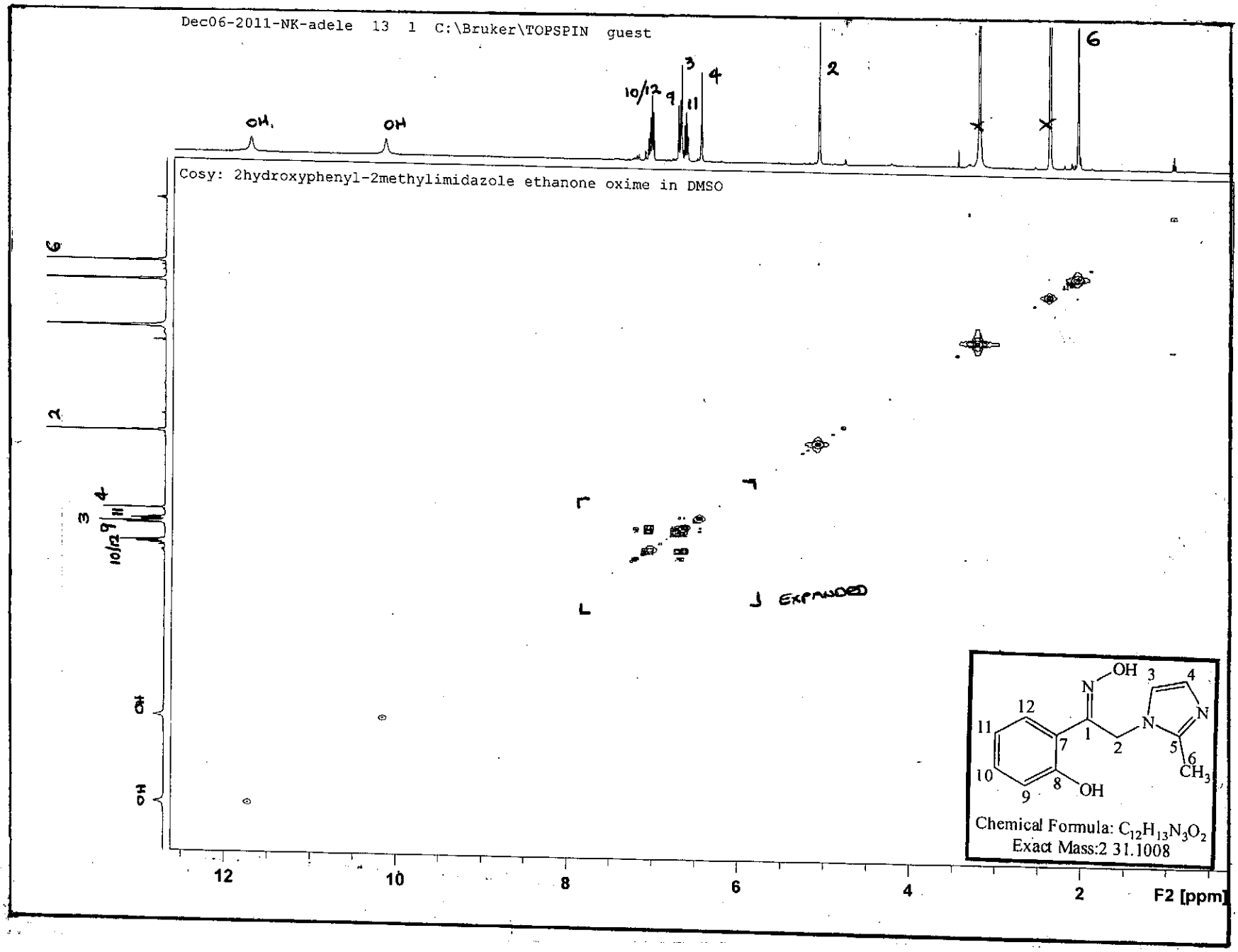

COSY spectrum of compound 13, 1-(2-hydroxyphenyl)-2-(2-methyl-1H-imidazol-1-yl) ethanone oxime

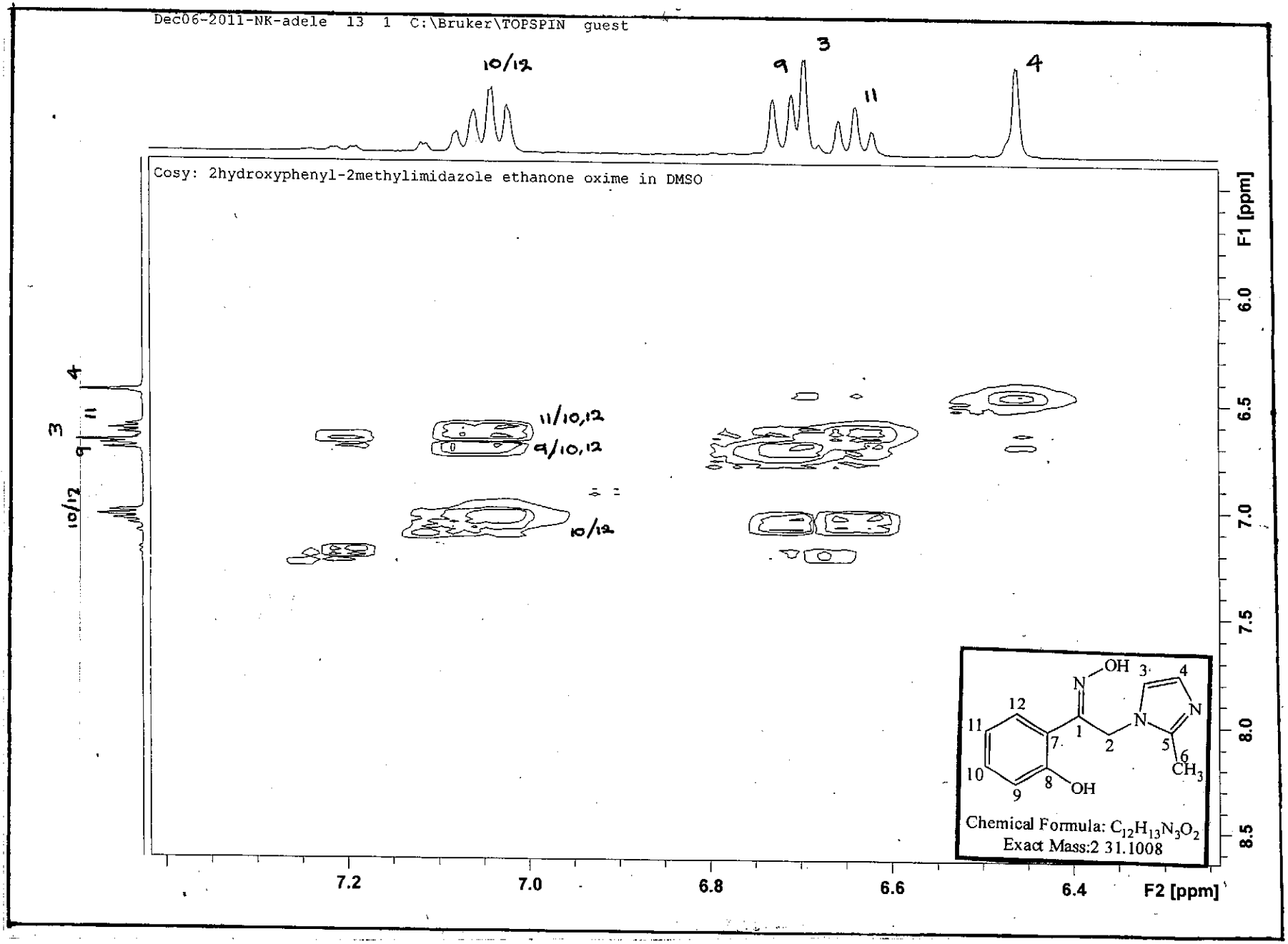

COSY spectrum of compound 13, 1-(2-hydroxyphenyl)-2-(2-methyl-1H-imidazol-1-yl) ethanone oxime

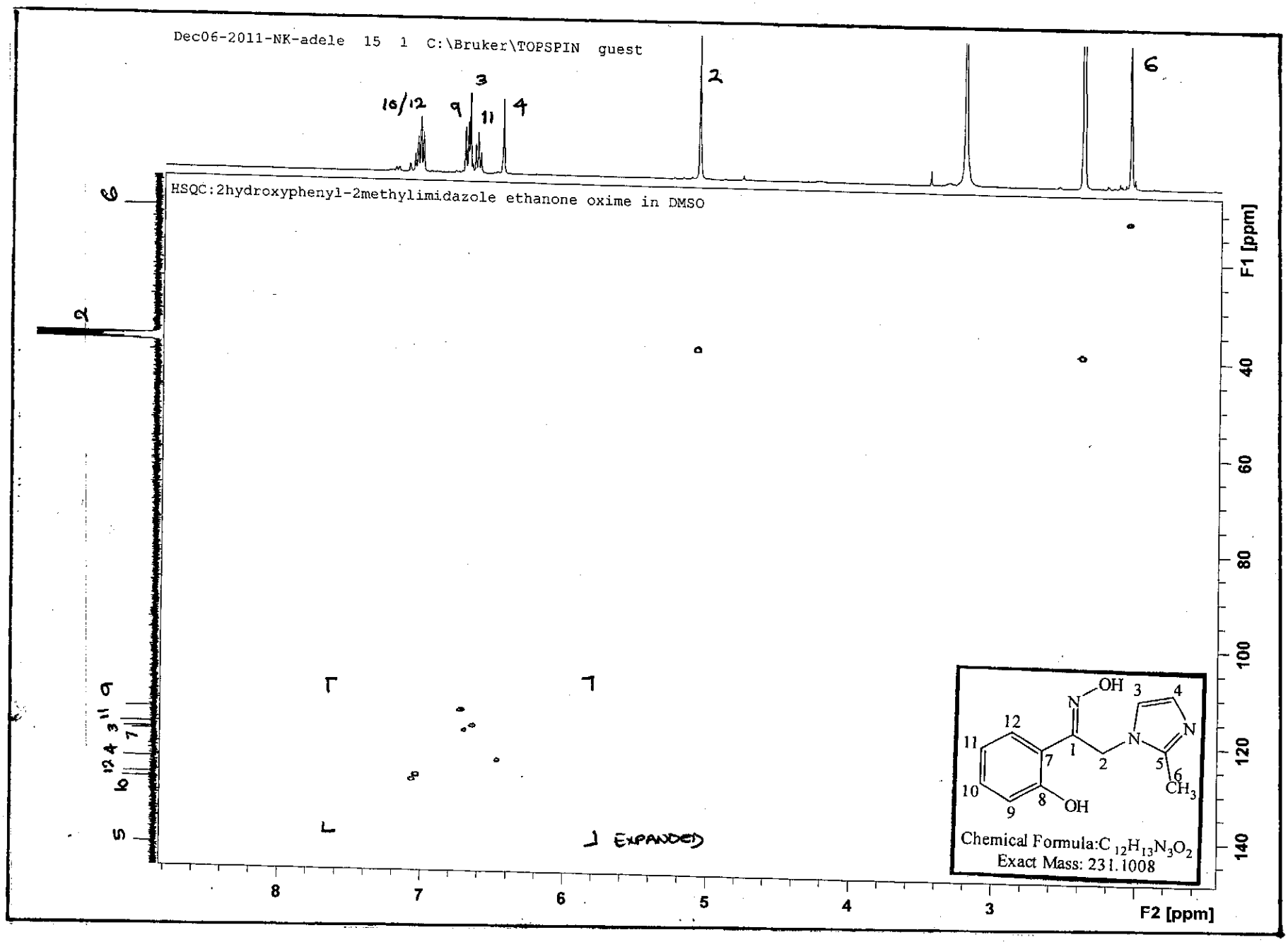

HSQC spectrum of compound 13, 1-(2-hydroxyphenyl)-2-(2-methyl-1H-imidazol-1-yl) ethanone oxime

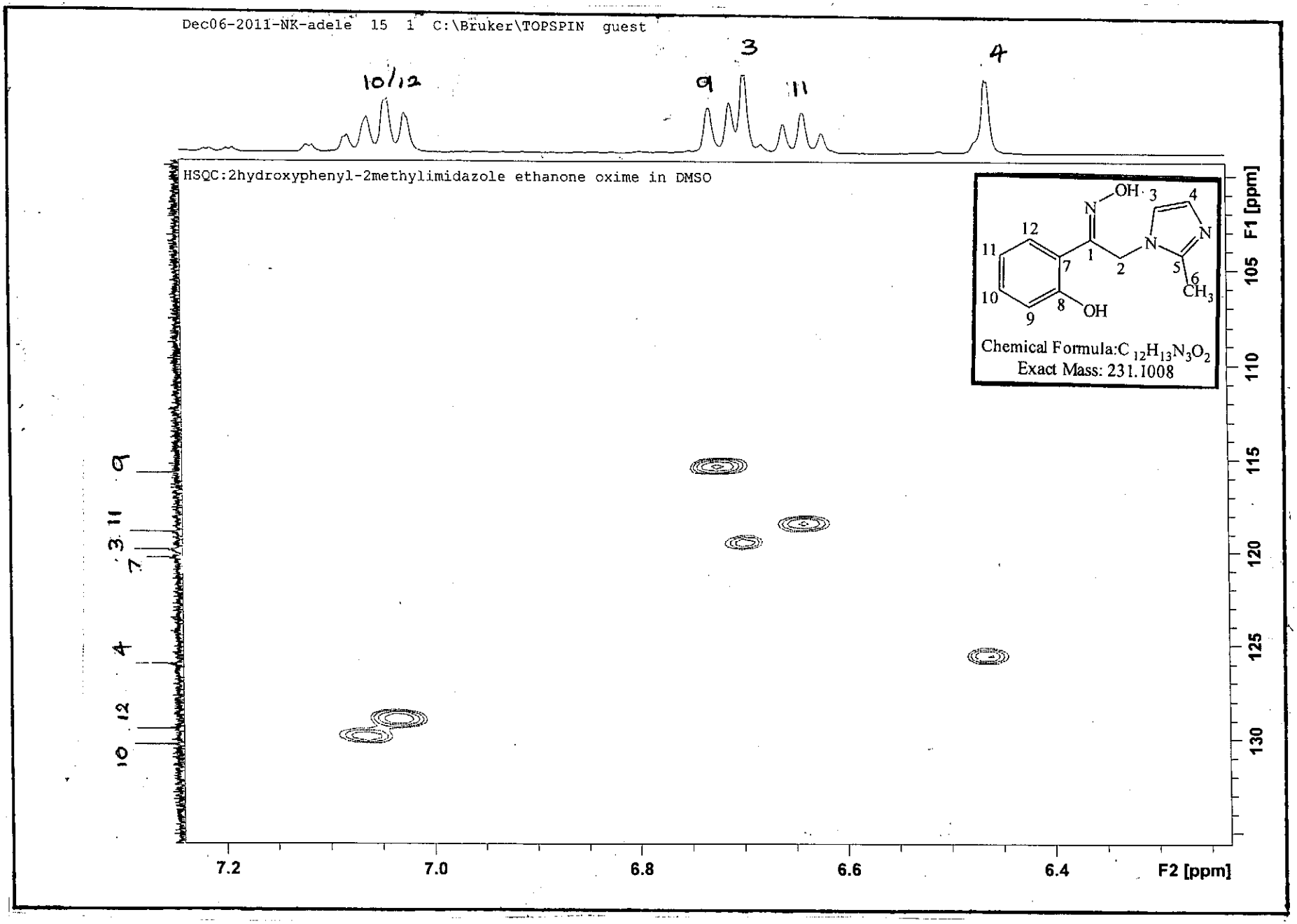

HSQC spectrum of compound 13, 1-(2-hydroxyphenyl)-2-(2-methyl-1H-imidazol-1-yl) ethanone oxime

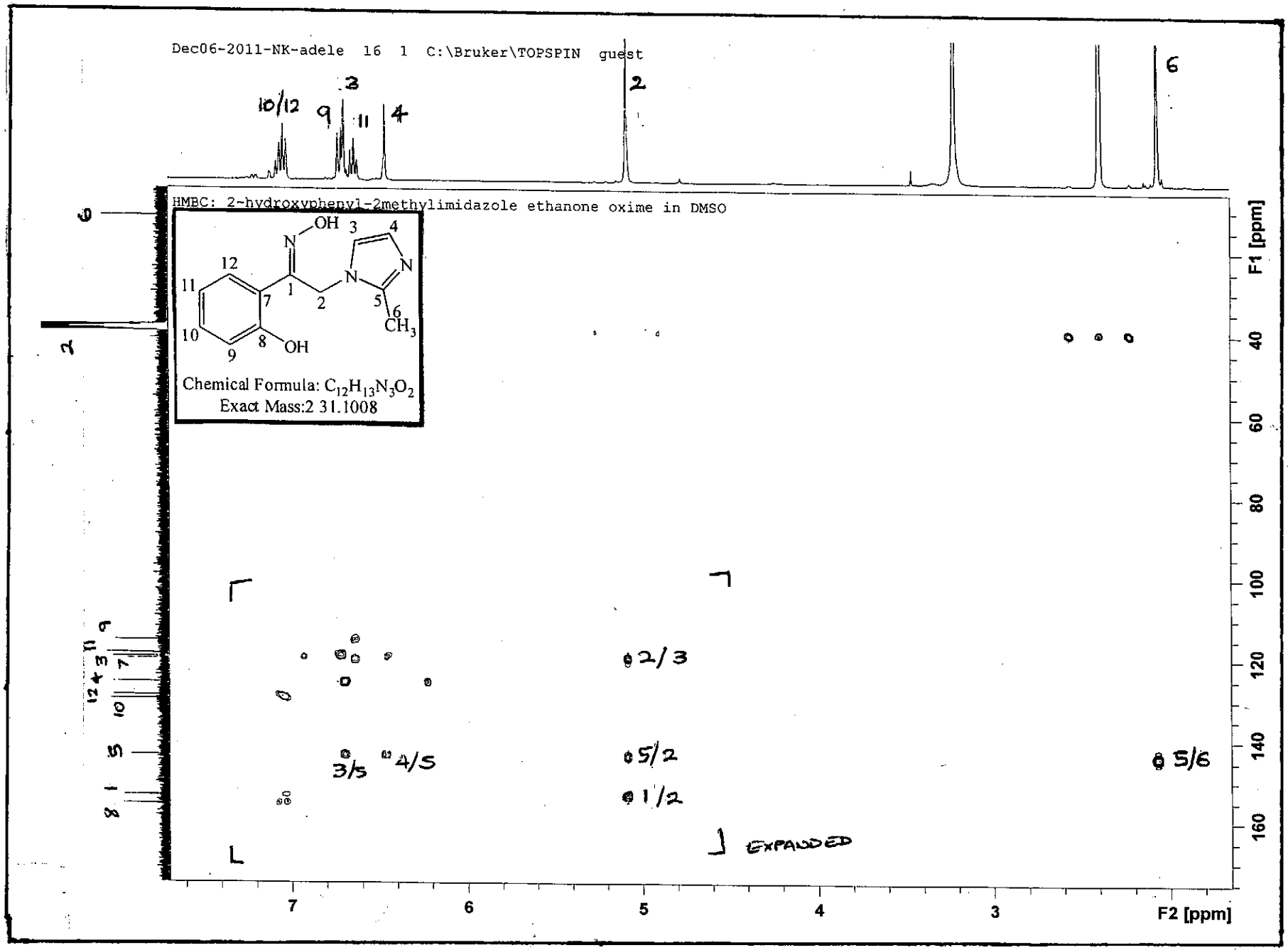

HMBC spectrum of compound 13, 1-(2-hydroxyphenyl)-2-(2-methyl-1H-imidazol-1-yl) ethanone oxime

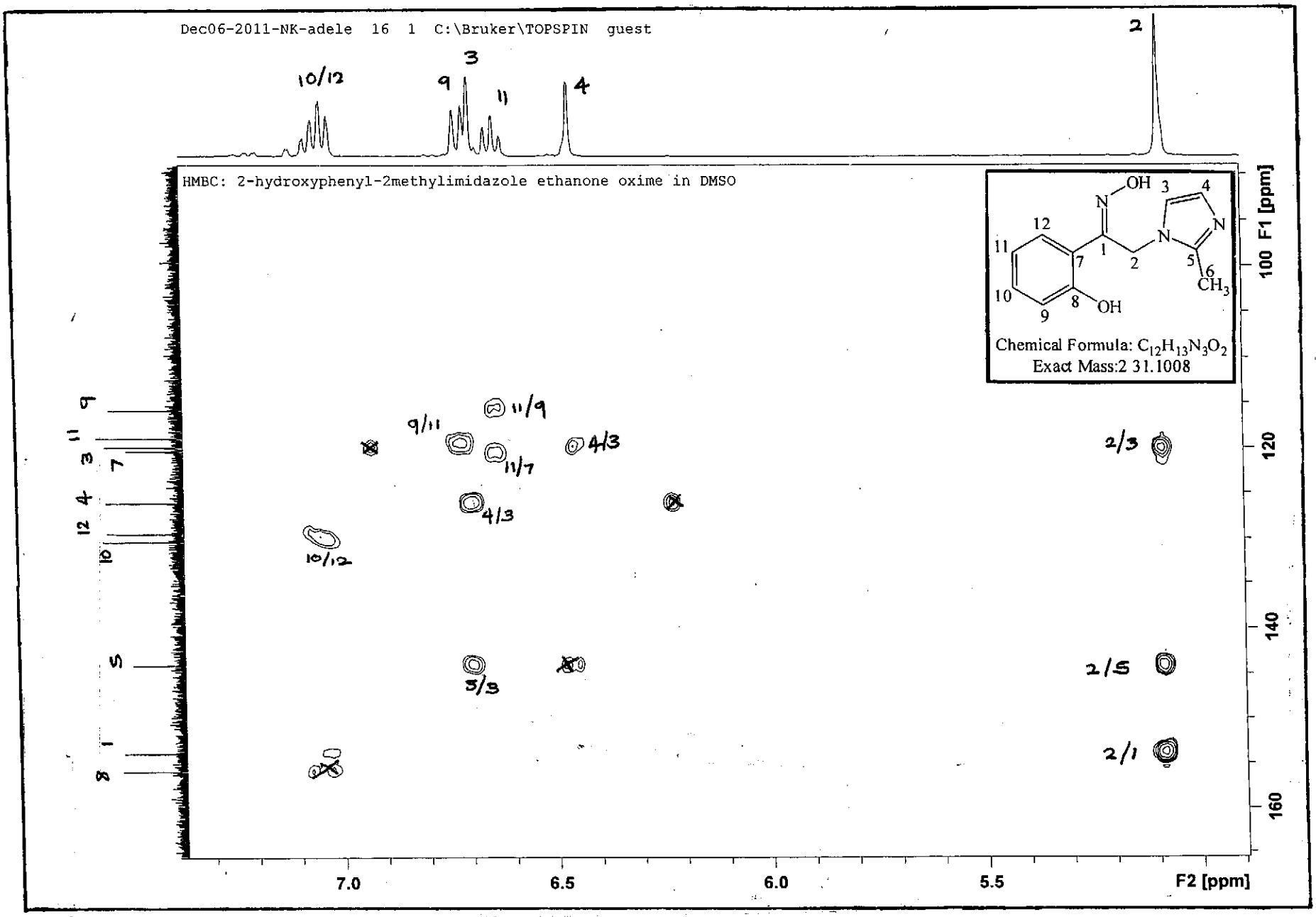

HMBC spectrum of compound 13, 1-(2-hydroxyphenyl)-2-(2-methyl-1H-imidazol-1-yl) ethanone oxime

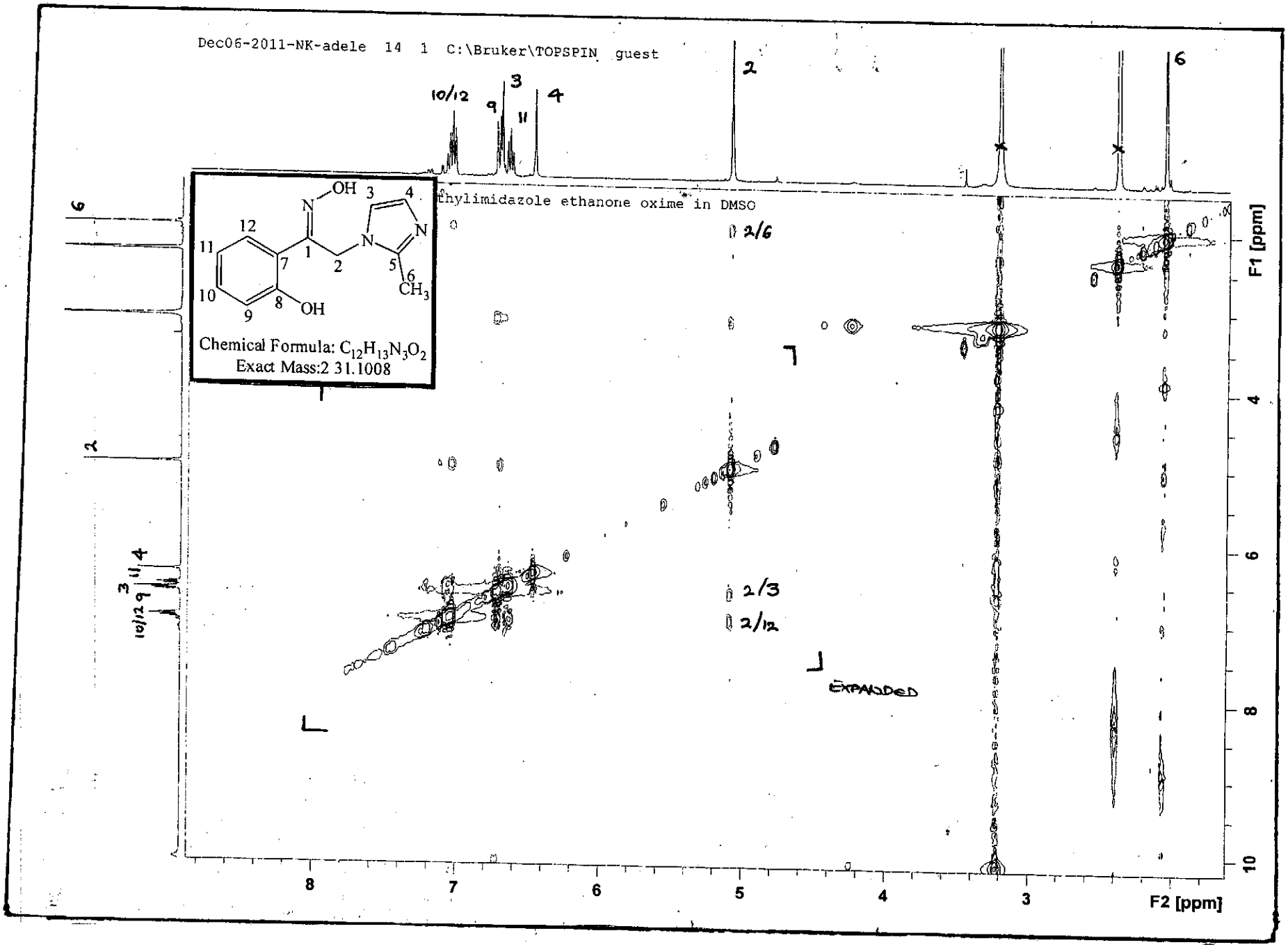

NOESY spectrum of compound 13, 1-(2-hydroxyphenyl)-2-(2-methyl-1H-imidazol-1-yl) ethanone oxime

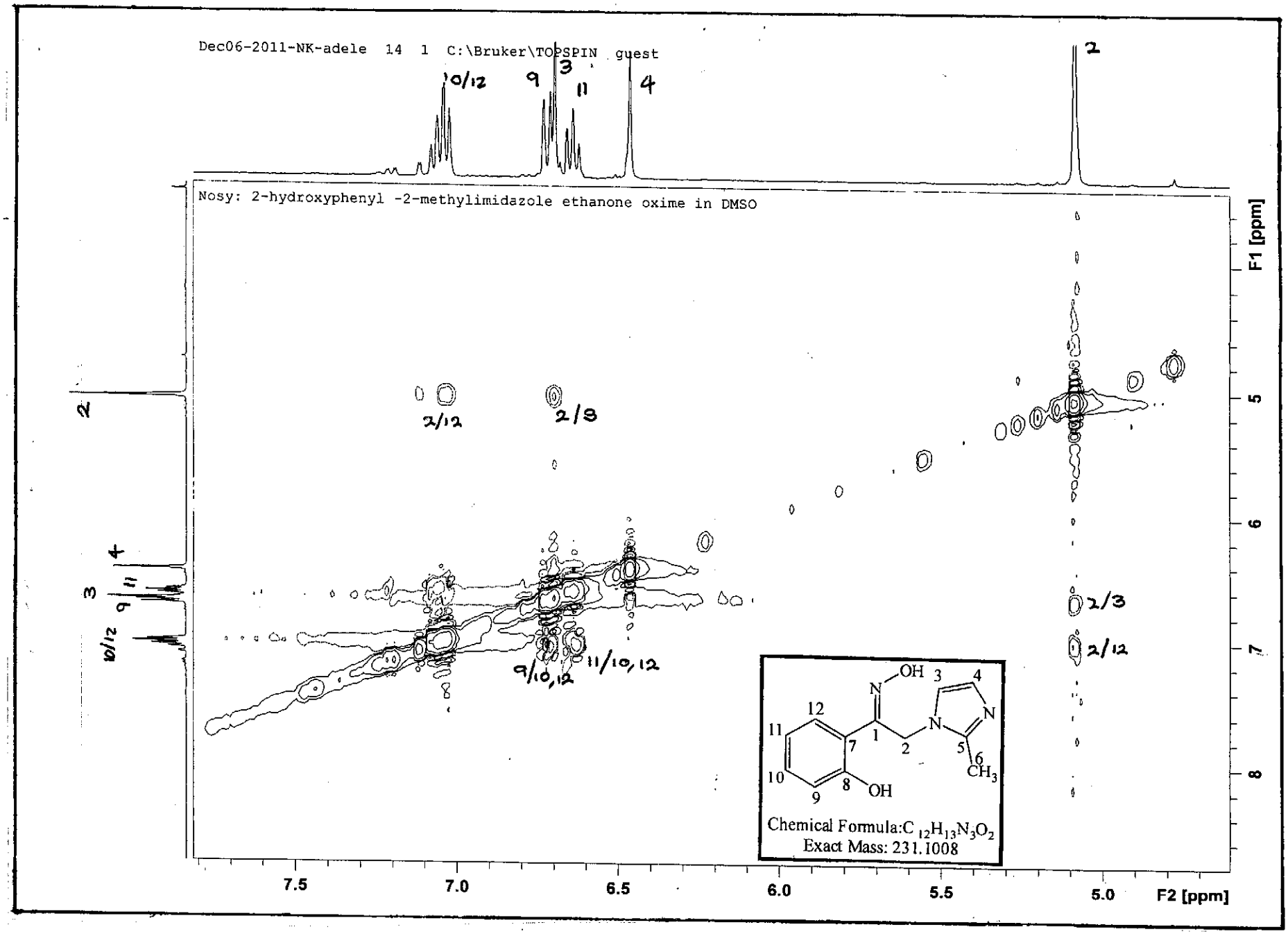

NOESY spectrum of compound 13, 1-(2-hydroxyphenyl)-2-(2-methyl-1H-imidazol-1-yl) ethanone oxime

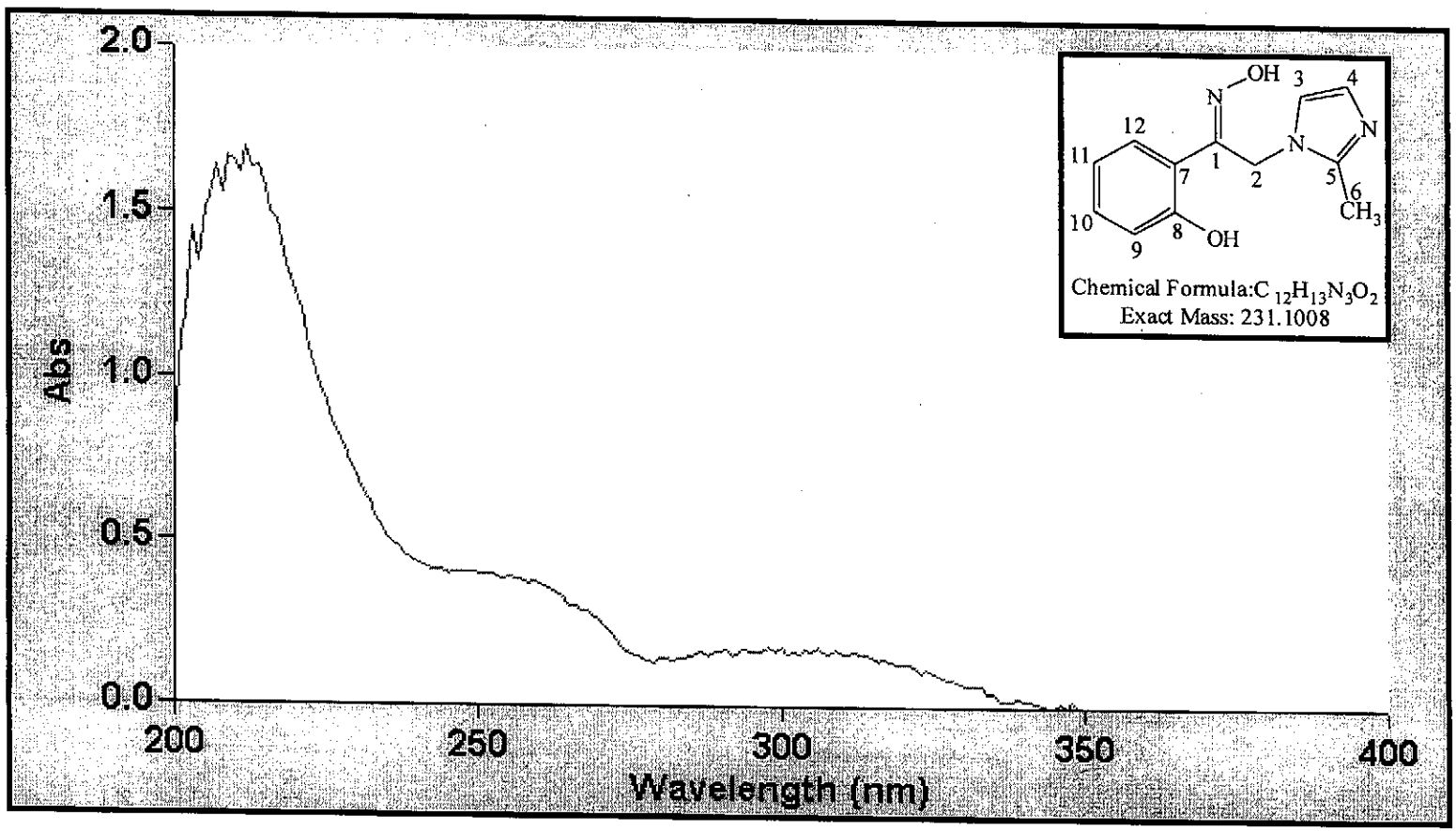

Ultra Violet spectrum of compound 13, 1-(2-hydroxyphenyl)-2-(2-methyl-1H-imidazol-1-yl)ethanone oxime

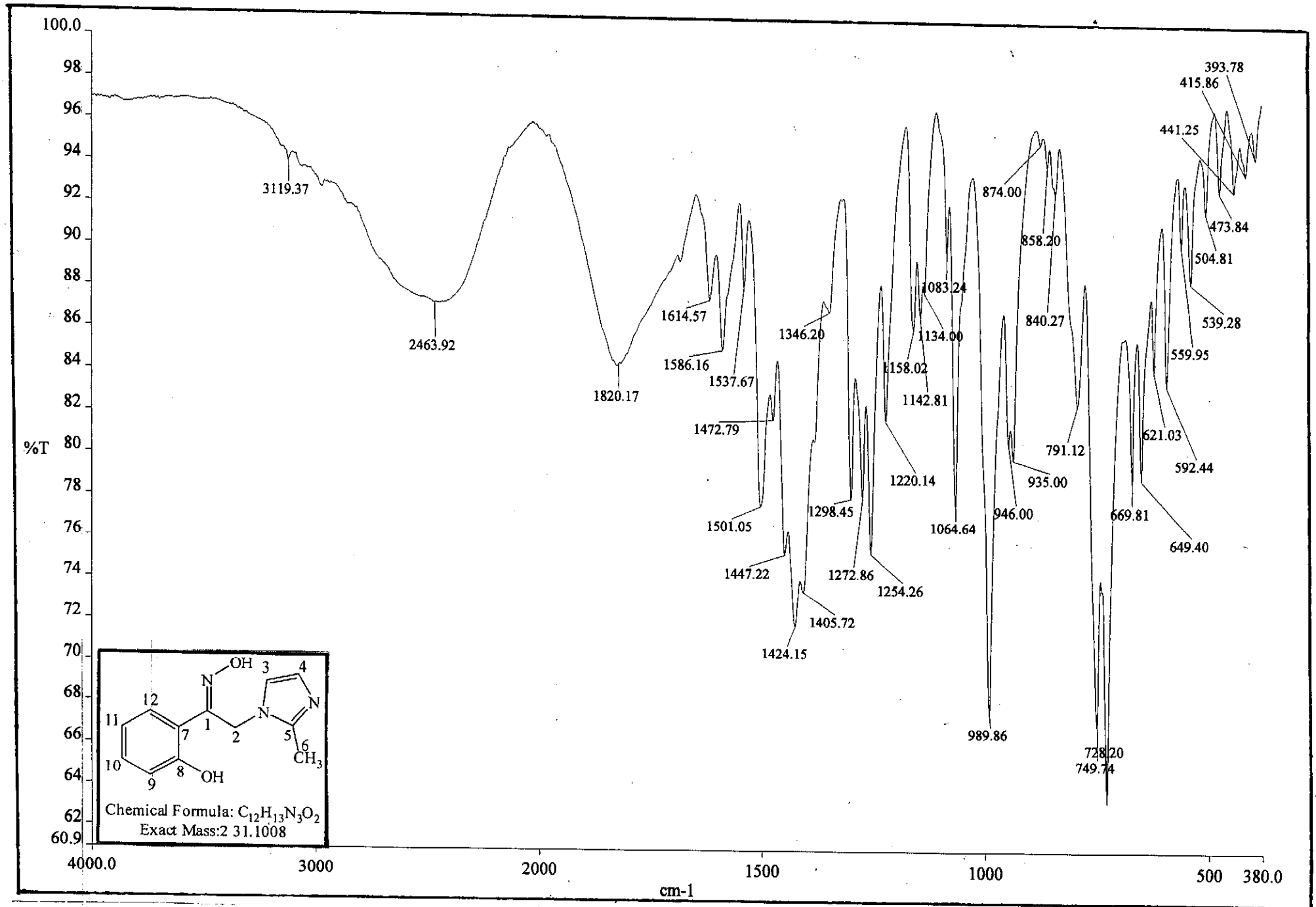

Infrared spectrum of compound 13, 1-(2-hydroxyphenyl)-2-(2-methyl-1H-imidazol-1-yl) ethanone oxime

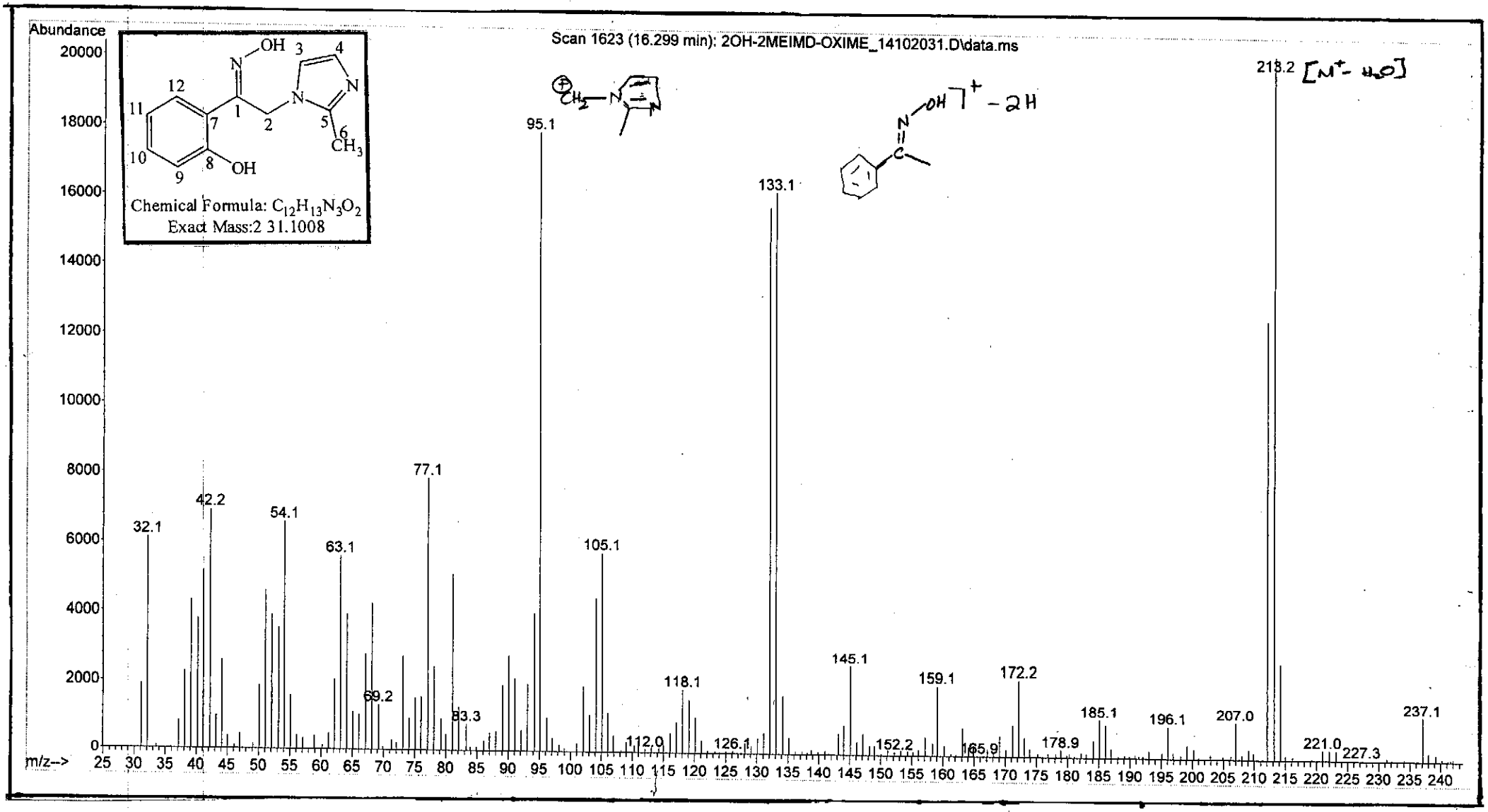

Mass spectrum of compound 13, 1-(2-hydroxyphenyl)-2-(2-methyl-1H-imidazol-1-yl) ethanone oxime

Elemental Composition Report

Single Mass Analysis
Tolerance = 5.0 PPM / DBE: min = -1.5, max = 50.0
Element prediction: Off
Number of isotope peaks used for i-FIT = 3

Monoisotopic Mass, Even Electron Ions
16 formula(e) evaluated with 1 results within limits (up to 50 best isotopic matches for each mass)
Elements Used:
C: 10-15 H: 10-15 N: 0-5 O: 0-5
Adele 2 8 (0.119) Cm (1:31)
TOF MS ES+

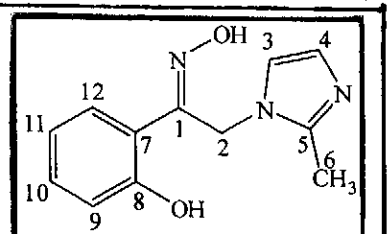

Chemical Formula: $C_{12}H_{13}N_3O_2$
Exact Mass: 231.1008

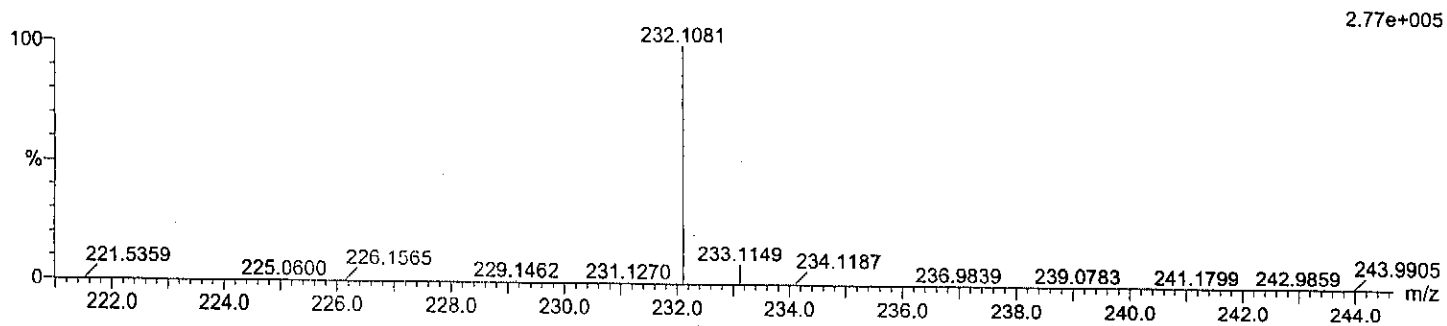

Minimum:				-1.5			
Maximum:		5.0	5.0	50.0			
Mass	Calc. Mass	mDa	PPM	DBE	i-FIT	i-FIT (Norm)	Formula
232.1081	232.1086	-0.5	-2.2	7.5	335.0	0.0	C12 H14 N3 O2

HRMS spectrum of compound 13, 1-(2-hydroxyphenyl)-2-(2-methyl-1H-imidazol-1-yl) ethanone oxime

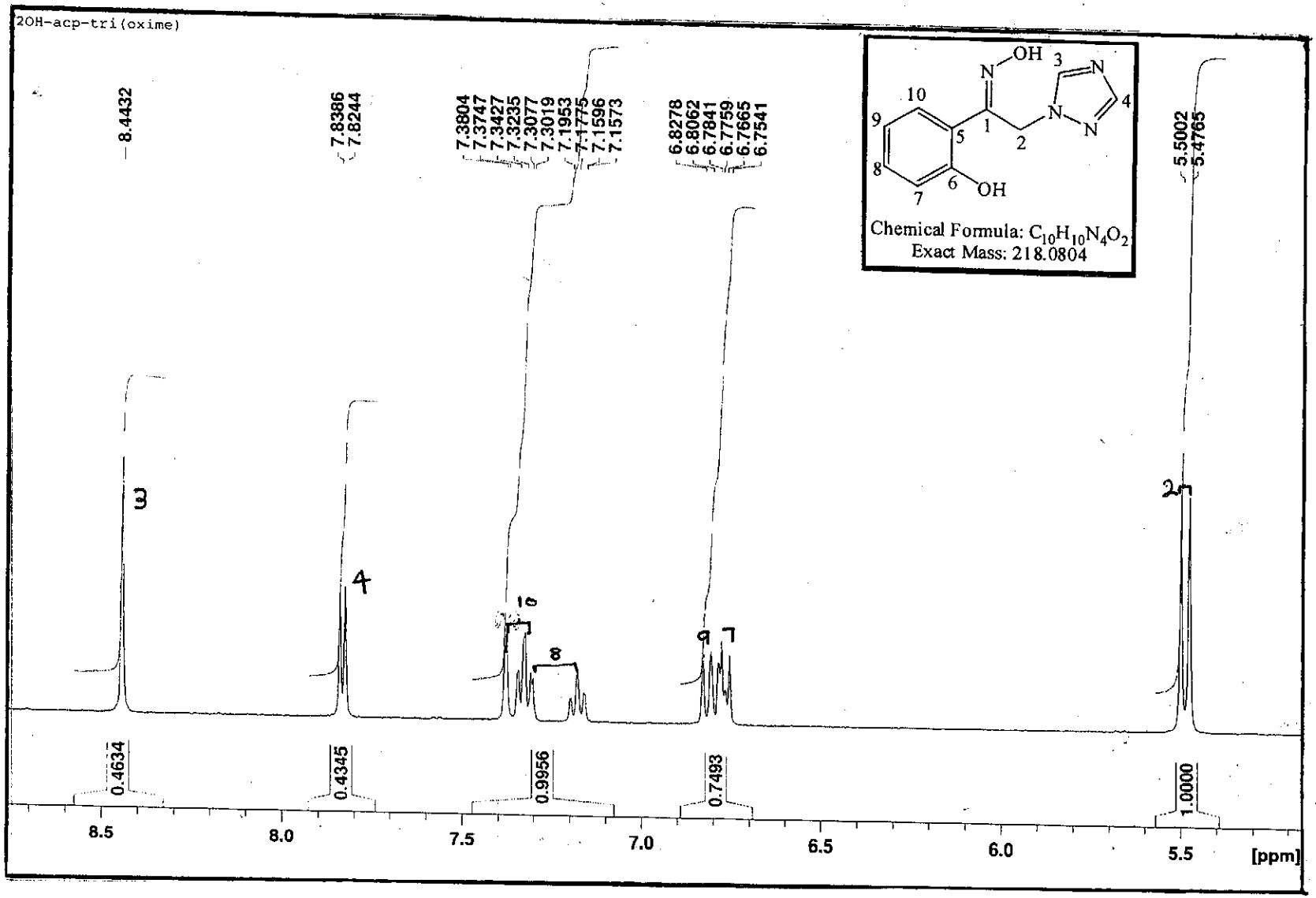

^{1}H NMR spectrum of compound 14, 1-(2-hydroxyphenyl)-2-(1 H- 1,2,4 triazol-1-yl) ethanone oxime

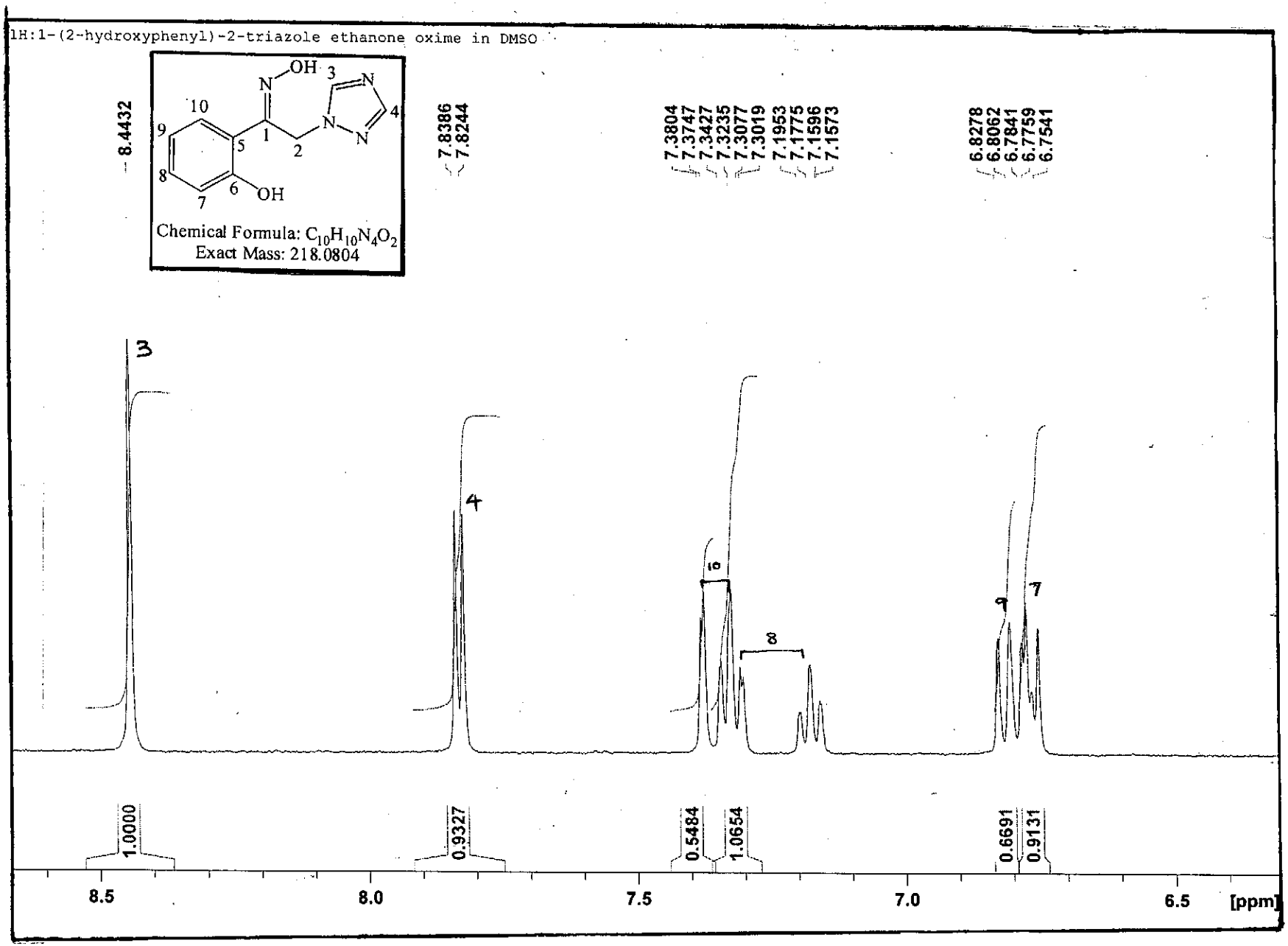

^{1}H NMR spectrum of compound 14., 1-(2-hydroxyphenyl)-2-(1 H- 1,2,4 triazol-1-yl) ethanone oxime

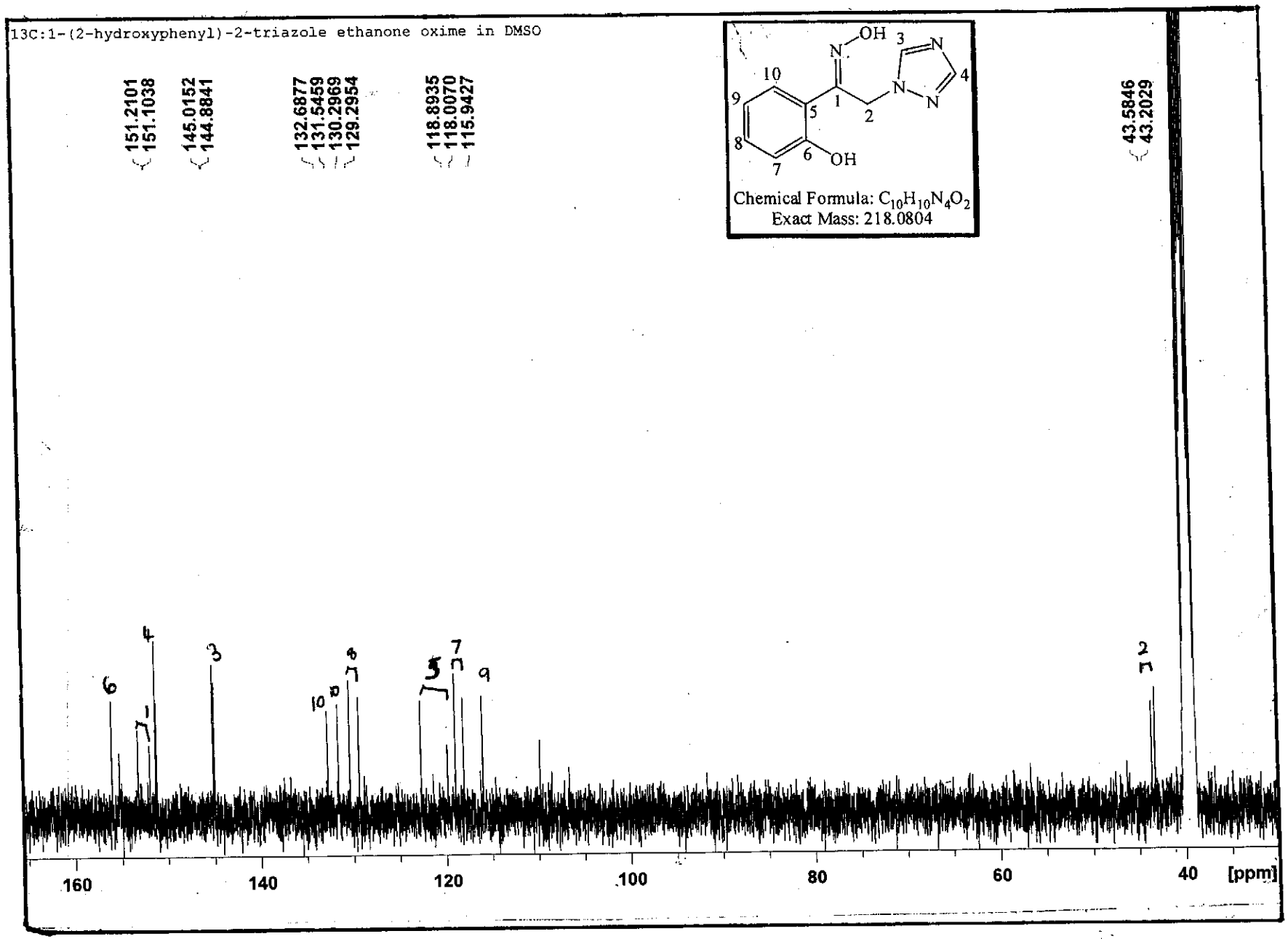

^{13}C NMR of compound 14., 1-(2-hydroxyphenyl)-2-(1 H- 1,2,4 triazol-1-yl) ethanone oxime

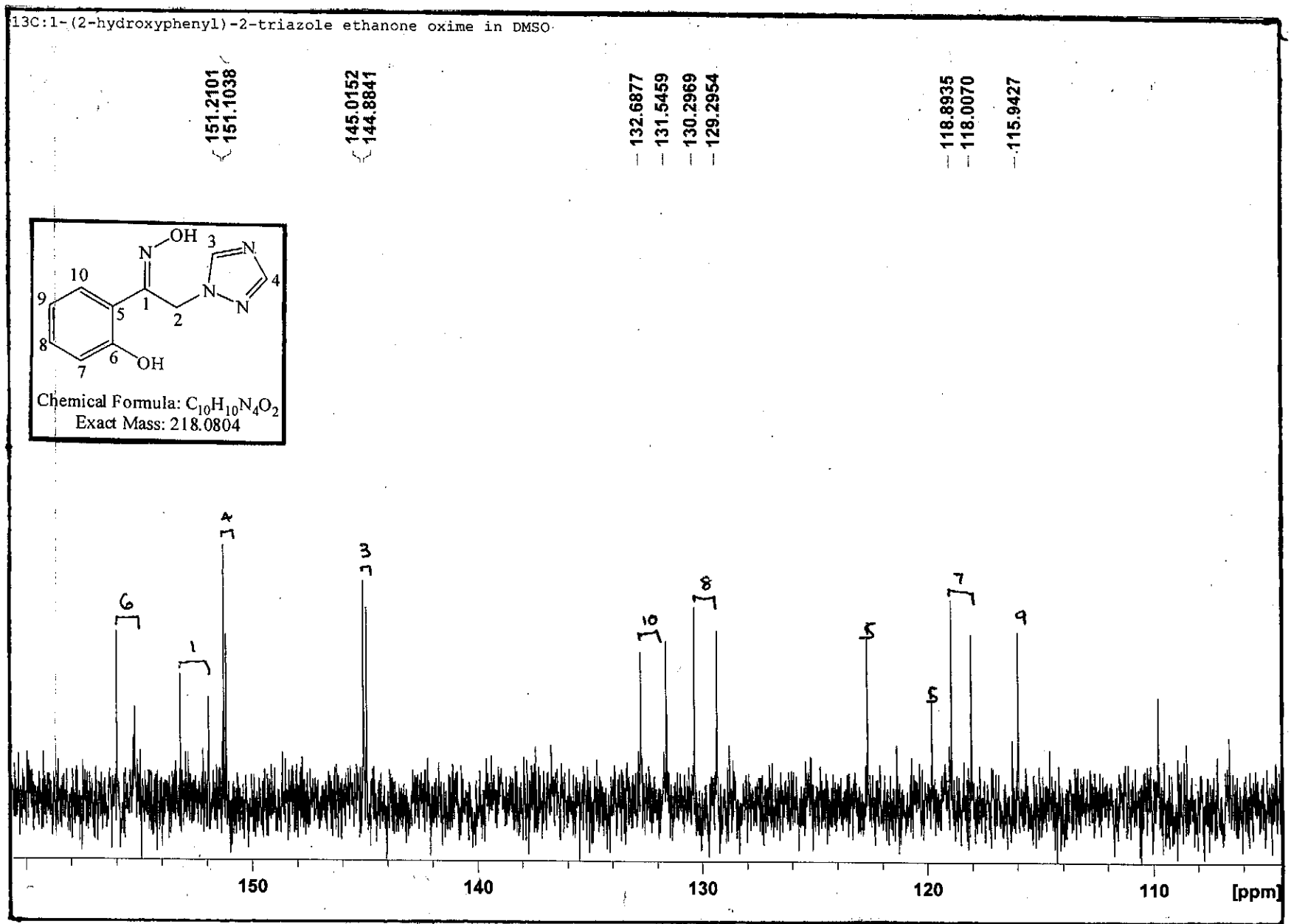

^{13}C NMR of compound 14, 1-(2-hydroxyphenyl)-2-(1 H- 1,2,4 triazol-1-yl) ethanone oxime

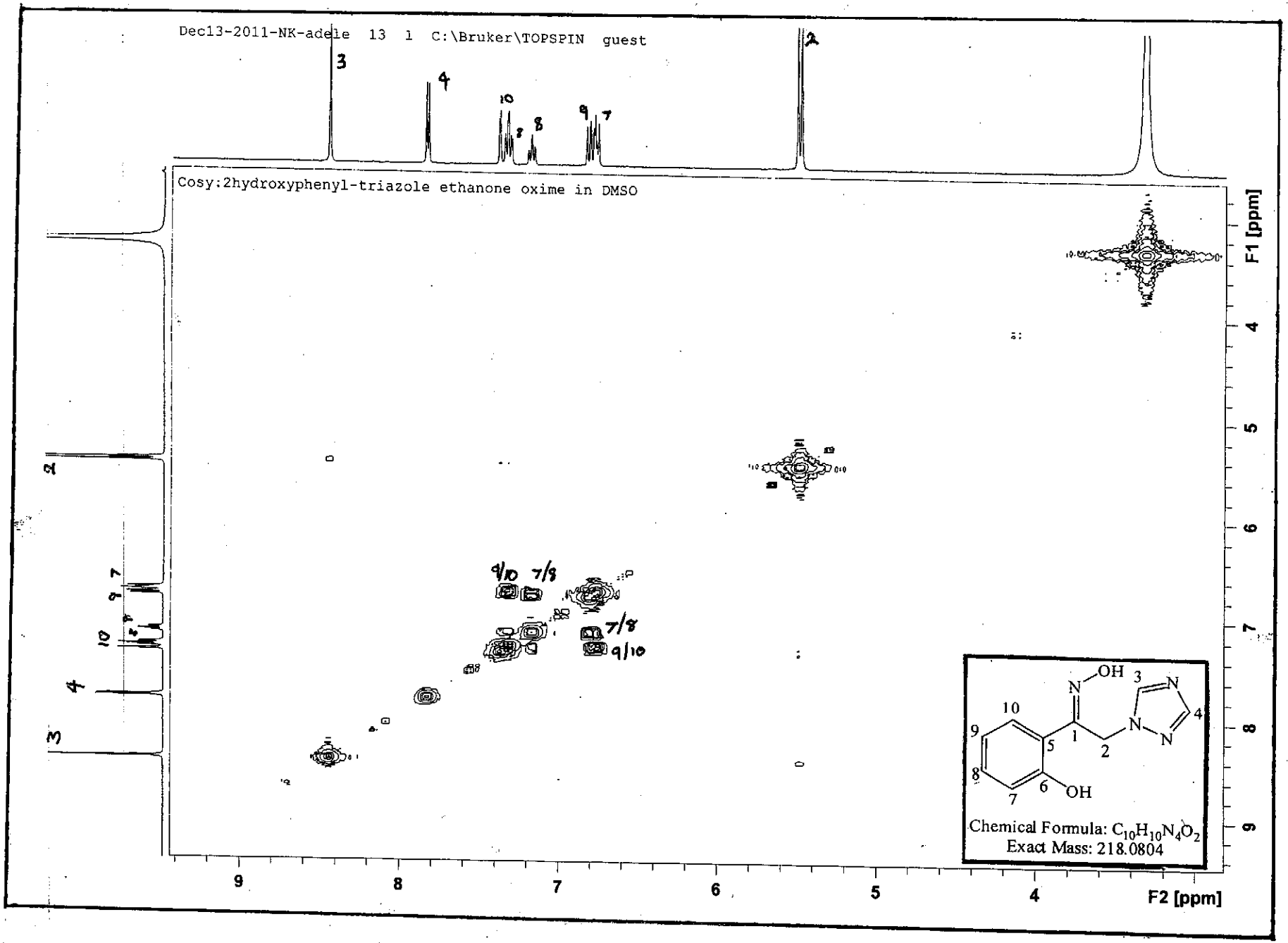

COSY spectrum of compound 14, 1-(2-hydroxyphenyl)-2-(1 H- 1,2,4 triazol-1-yl) ethanone oxime

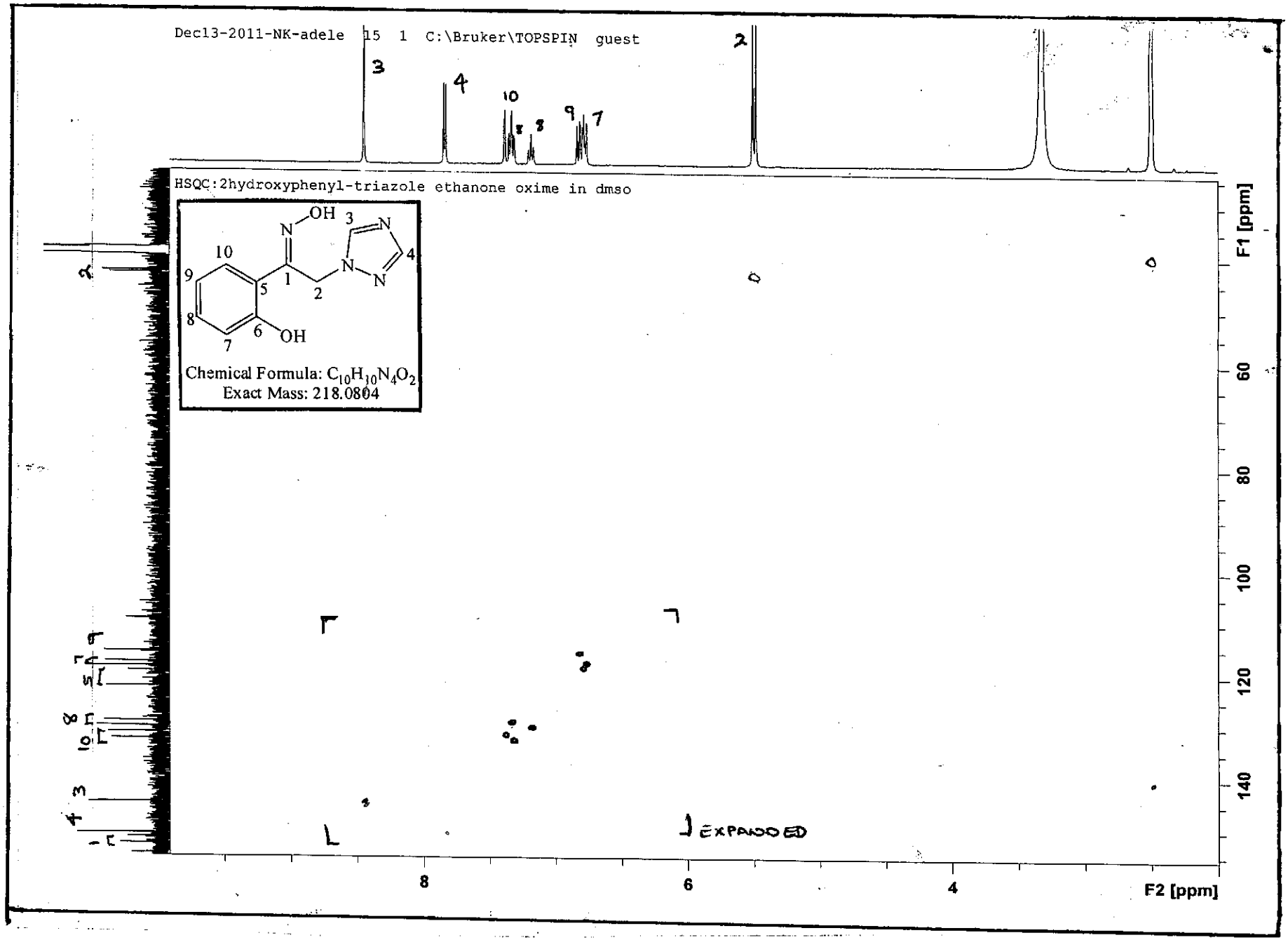

HSQC spectrum of compound 14, 1-(2-hydroxyphenyl)-2-(1 H- 1,2,4 triazol-1-yl) ethanone oxime

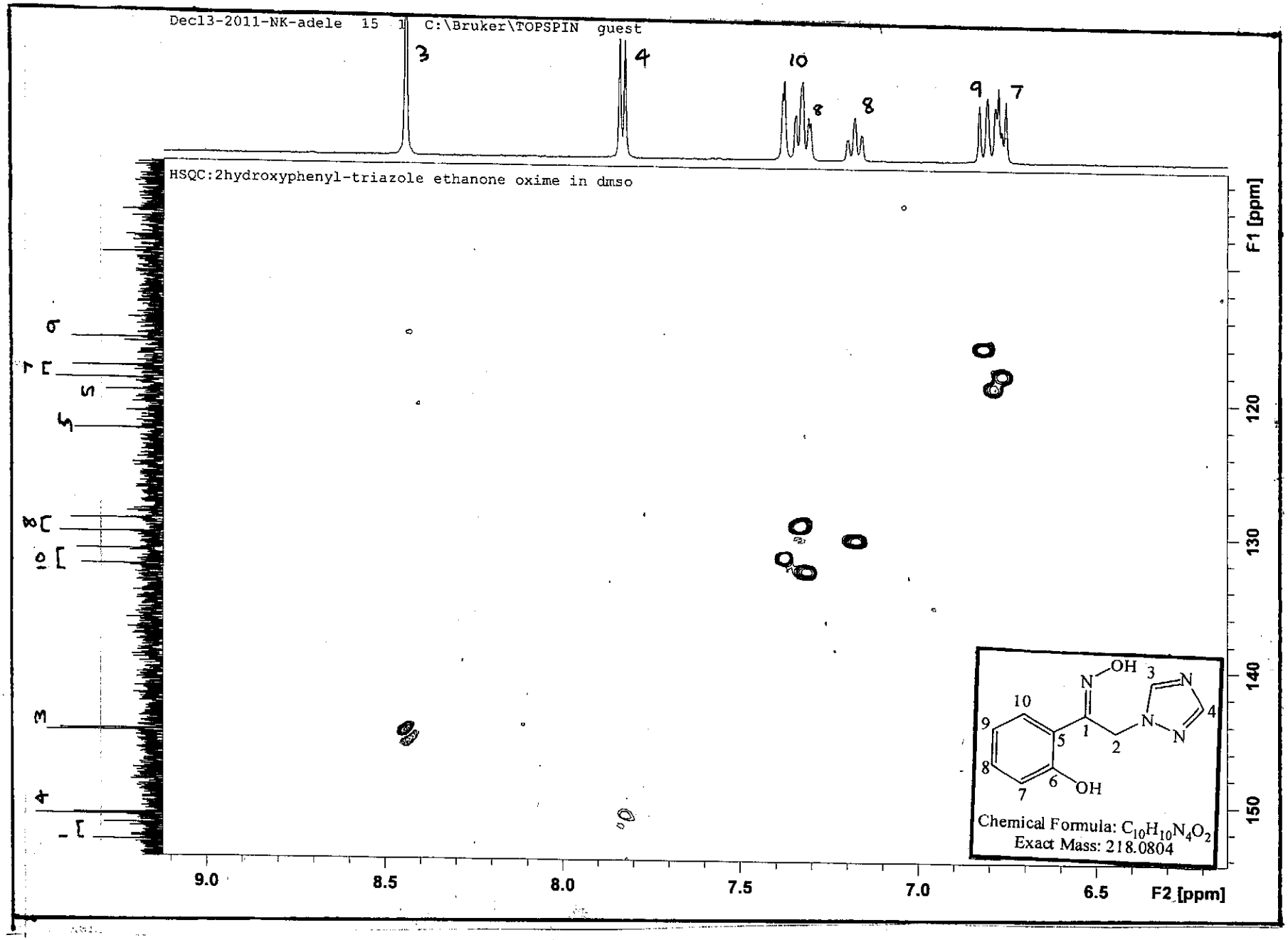

HSQC spectrum of compound 14., 1-(2-hydroxyphenyl)-2-(1 H- 1,2,4 triazol-1-yl) ethanone oxime

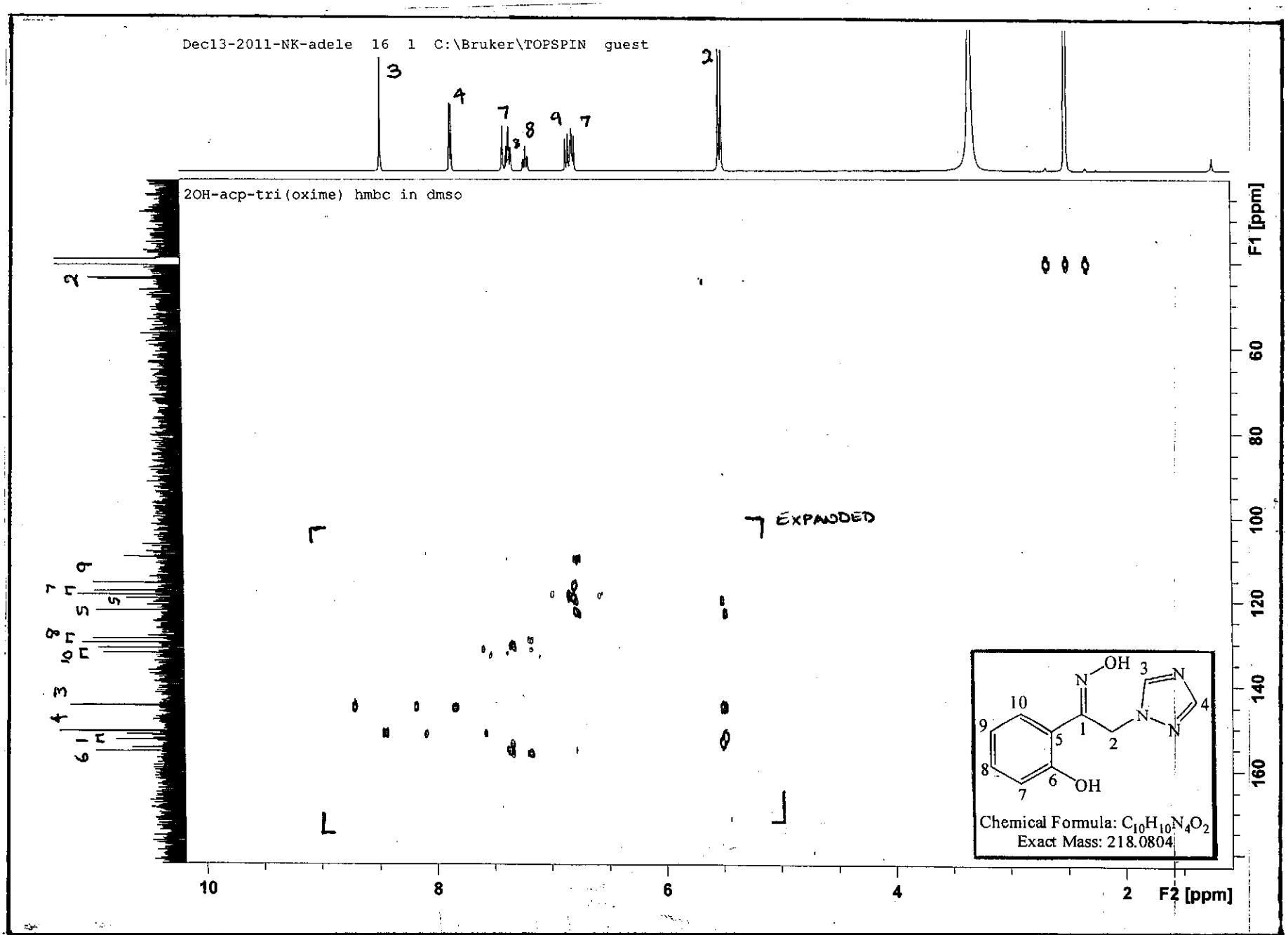

HMBC spectrum of compound 14, 1-(2-hydroxyphenyl)-2-(1 H- 1,2,4 triazol-1-yl) ethanone oxime

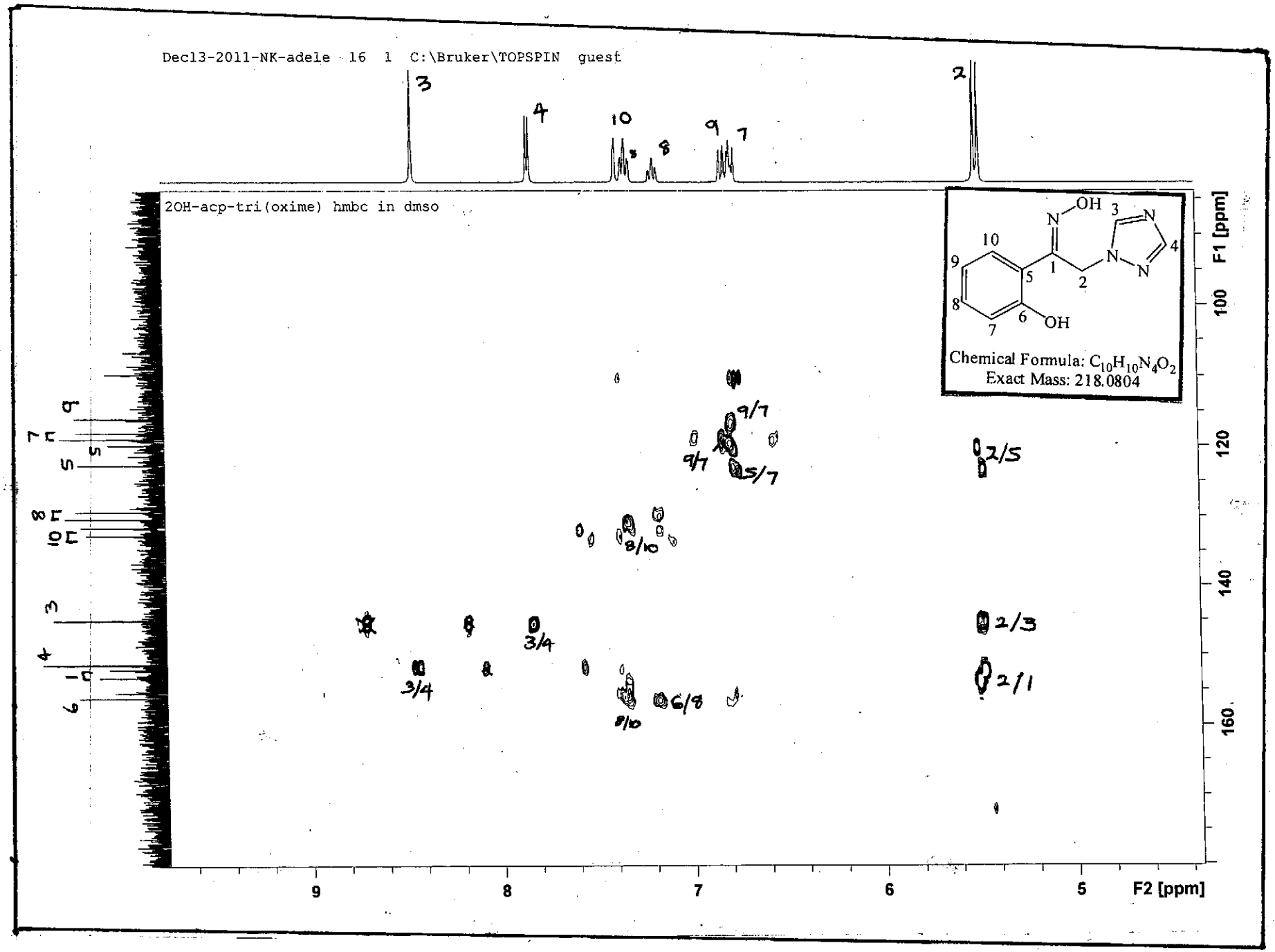

HMBC spectrum of compound 14, 1-(2-hydroxyphenyl)-2-(1 H- 1,2,4 triazol-1-yl) ethanone oxime

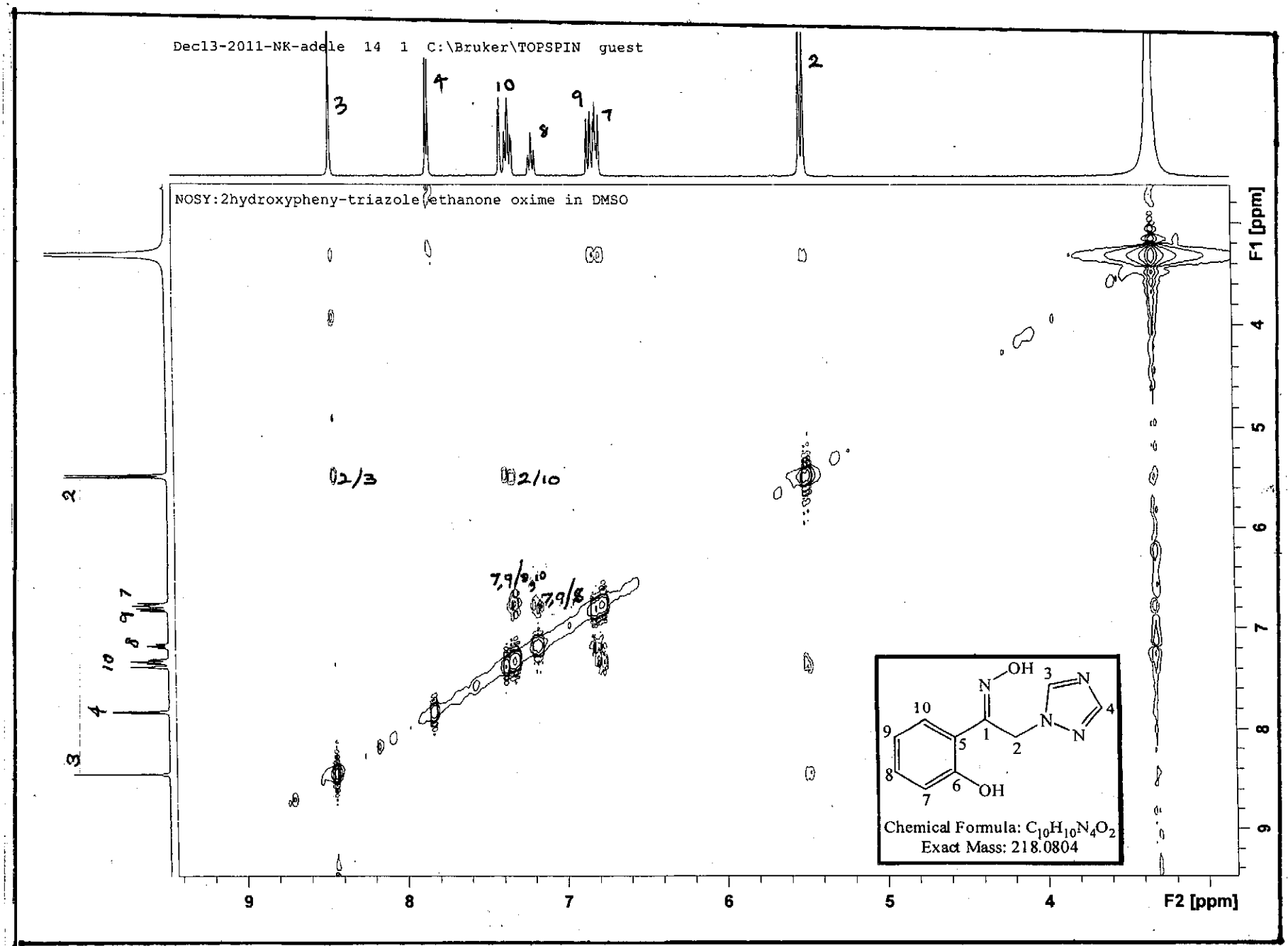

NOESY spectrum of compound 14, 1-(2-hydroxyphenyl)-2-(1 H- 1,2,4 triazol-1-yl) ethanone oxime

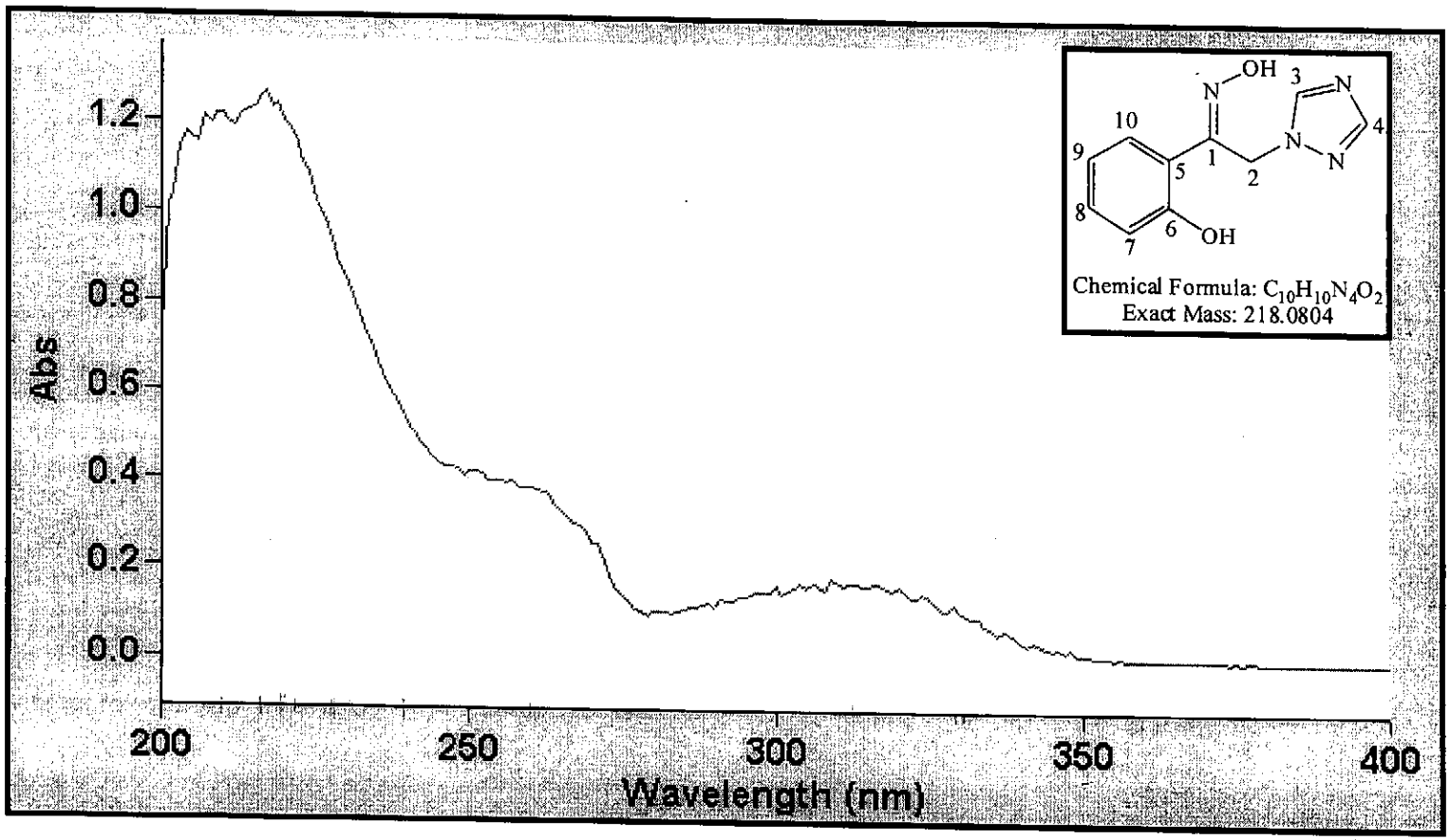

Ultra Violet spectrum of compound 14, 1-(2-hydroxyphenyl)-2-(1H-1,2,4-triazol-1-yl)ethanone oxime

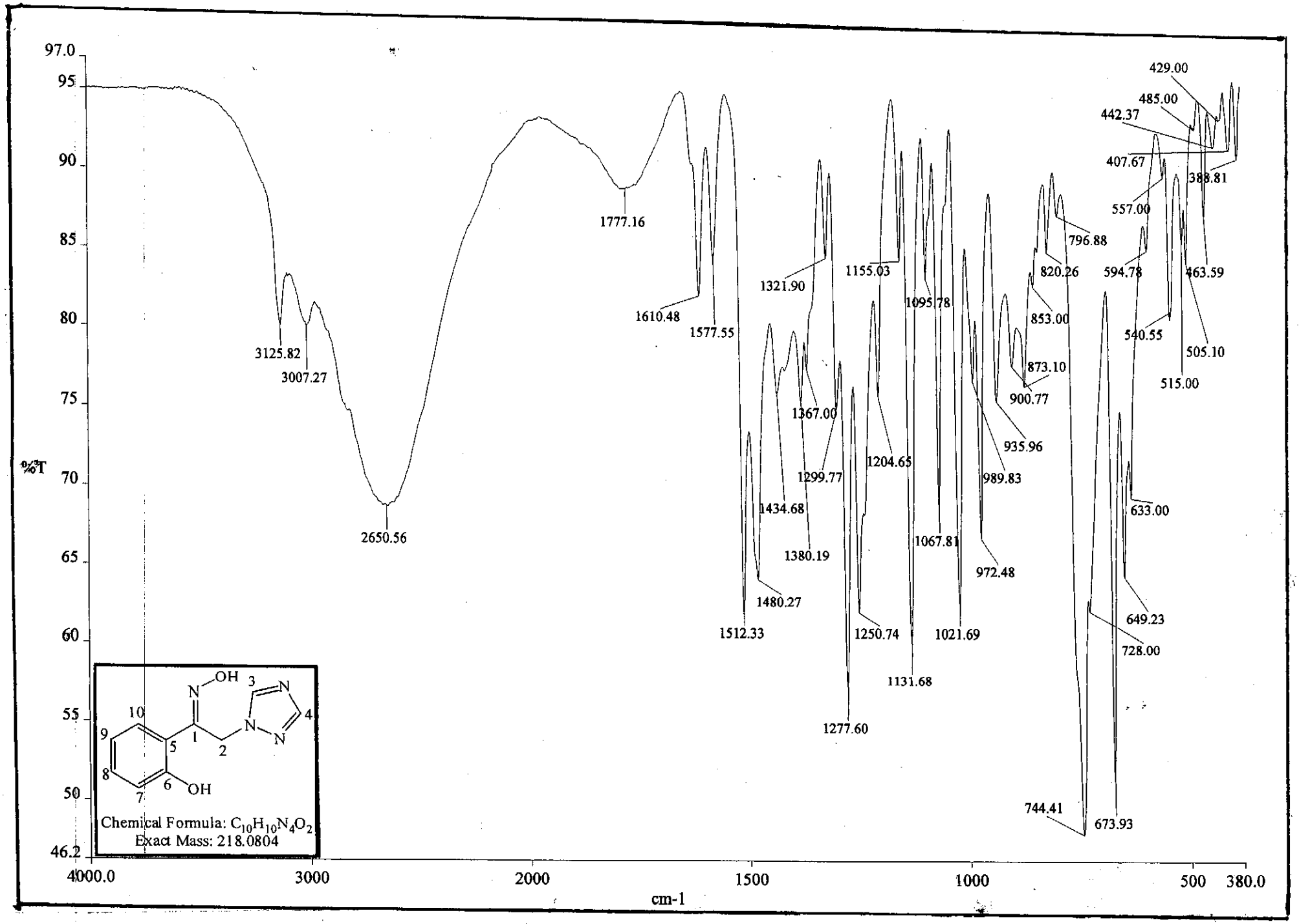

Infrared spectrum of compound 14, 1-(2-hydroxyphenyl)-2-(1 H- 1,2,4 triazol-1-yl) ethanone oxime

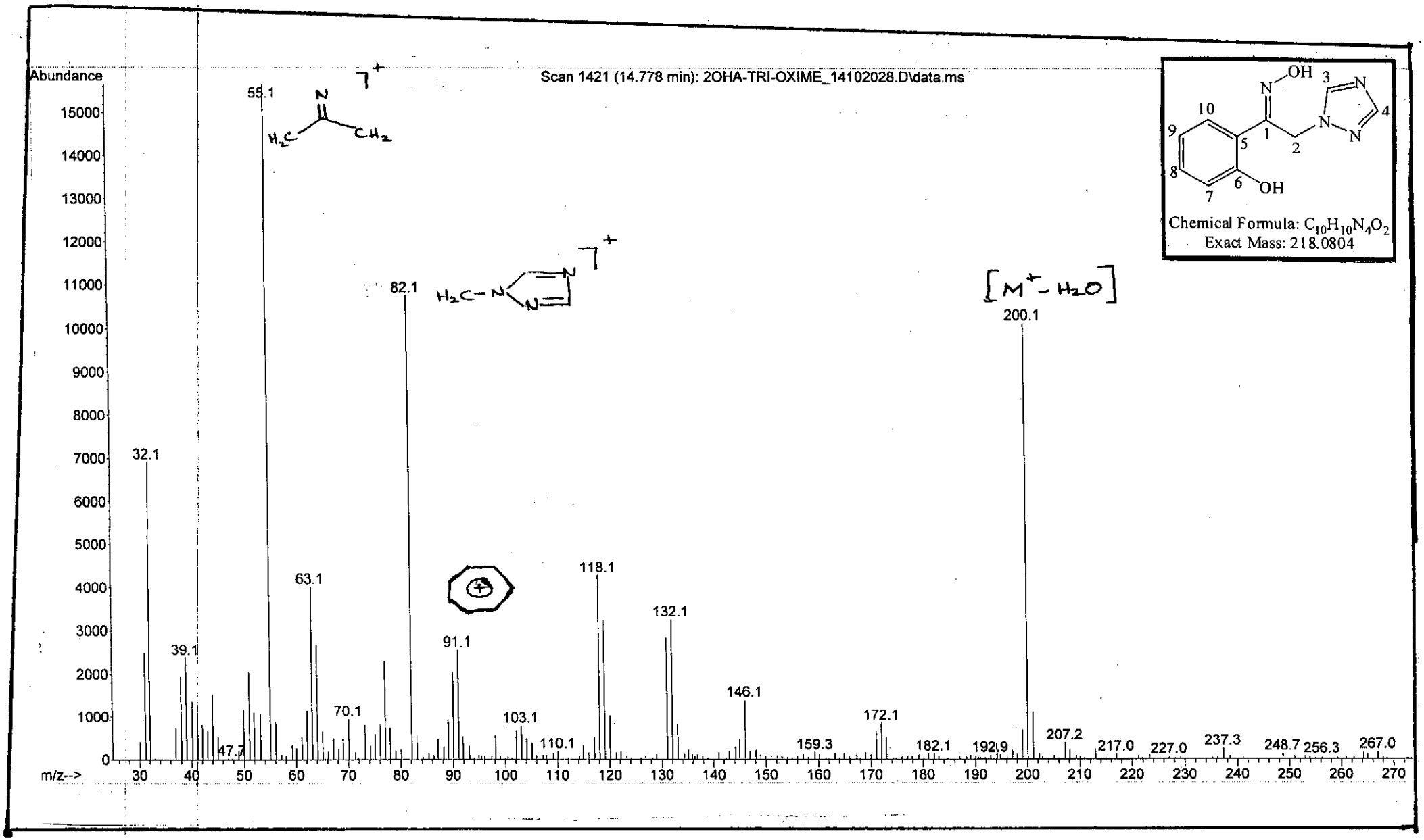

Mass spectrum of compound 14., 1-(2-hydroxyphenyl)-2-(1 H- 1,2,4 triazol-1-yl) ethanone oxime

Elemental Composition Report

Single Mass Analysis
Tolerance = 5.0 PPM / DBE: min = -1.5, max = 50.0
Element prediction: Off
Number of isotope peaks used for i-FIT = 3

Monoisotopic Mass, Even Electron Ions
22 formula(e) evaluated with 1 results within limits (up to 50 best isotopic matches for each mass)
Elements Used:
C: 10-15 H: 5-10 N: 0-5 O: 0-5
Adele 1 15 (0.239) Cm (1:31)
TOF MS ES-

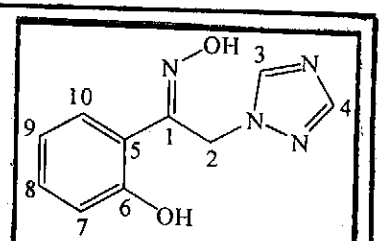

Chemical Formula: $C_{10}H_{10}N_4O_2$
Exact Mass: 218.0804

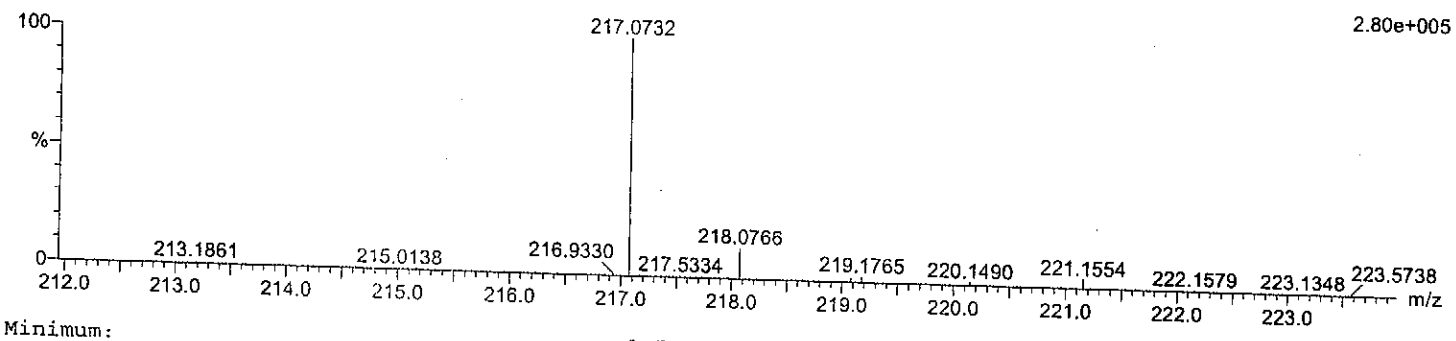

Minimum:				-1.5			
Maximum:		5.0	5.0	50.0			
Mass	Calc. Mass	mDa	PPM	DBE	i-FIT	i-FIT (Norm)	Formula
217.0732	217.0726	0.6	2.8	8.5	607.5	0.0	C10 H9 N4 O2

HRMS spectrum of compound 14, 1-(2-hydroxyphenyl)-2-(1 H- 1,2,4 triazol-1-yl) ethanone oxime